SYNTHESIS OF SMALL, CHIRAL, AND PHOTOSWITCHABLE CYCLOPARAPHENYLENES

by

PAUL JAMESON EVANS

A DISSERTATION

Presented to the Department of Chemistry and Biochemistry
and the Graduate School of the University of Oregon
in partial fulfillment of the requirements
for the degree of
Doctor of Philosophy

June 2015

DISSERTATION APPROVAL PAGE

Student: Paul Jameson Evans

Title: Synthesis of Small, Chiral, and Photoswitchable Cycloparaphenylenes

This dissertation has been accepted and approved in partial fulfillment of the requirements for the Doctor of Philosophy degree in the Department of Chemistry and Biochemistry by:

David Tyler	Chairperson
Ramesh Jasti	Advisor
Michael Haley	Core Member
Paul Wallace	Institutional Representative

and

Scott L. Pratt	Dean of the Graduate School

Original approval signatures are on file with the University of Oregon Graduate School.

Degree awarded June 2015

DISSERTATION ABSTRACT

Paul Jameson Evans

Doctor of Philosophy

Department of Chemistry and Biochemistry

June 2015

Title: Synthesis of Small, Chiral, and Photoswitchable Cycloparaphenylenes

Cycloparaphenylenes (CPPs) represent the unit-cycles of conductive armchair carbon nanotubes (CNTs). In addition to their utility for the bottom-up synthesis of CNTs with discrete diameter and chirality, these strained hydrocarbon macrocycles have attractive properties of their own for material science and organic electronics. Herein I report research focused on advancing the synthetic technology behind CPPs, culminating in the synthesis of [5]CPP, the smallest and most highly-strained member of the CPP series to date, as well as the derivitization of the CPP platform to include chiral nanohoops with a spiral carbon backbone and photoswitchable nanohoops based on azobenzene incorporation into the CPP architecture.

The synthesis and characterization of [5]CPP, 1,5-naphthyl[6]CPP, *azo*[11]CPP, and *azo*[9]CPP are reported along with advanced intermediates towards rotationally restricted 2,6-naphthyl[6]CPP and preliminary photoisomerization results for *azo*[11]CPP and *azo*[9]CPP.

This dissertation contains both previously published and unpublished co-authored material.

CURRICULUM VITAE

NAME OF AUTHOR: Paul Jameson Evans

GRADUATE AND UNDERGRADUATE SCHOOLS ATTENDED:

University of Oregon, Eugene
Boston University, Boston, Massachusetts
The College of Wooster, Wooster, Ohio

DEGREES AWARDED:

Doctor of Philosophy, Chemistry, 2015, University of Oregon
Master of Arts, Chemistry, 2014, Boston University
Bachelor of Arts, Chemistry, 2008, The College of Wooster

AREAS OF SPECIAL INTEREST:

Organic Chemistry
Organic Materials

PROFESSIONAL EXPERIENCE:

Chemist and Synthesis Specialist, Promerus LLC, Brecksville, Ohio, 2008-2009

Teaching Fellow, Department of Chemistry, Boston University, Boston Massachusetts, 2009-2014

GRANTS, AWARDS, AND HONORS:

William Bryan Ross Memorial Prize in Chemistry, The College of Wooster, 2008

PUBLICATIONS:

Evans, P. J.; Darzi, E. R.; Jasti, R., Efficient room-temperature synthesis of a highly strained carbon nanohoop fragment of buckminsterfullerene. *Nat Chem* **2014,** *6* (5), 404-408.

Evans, P.; Jasti, R., Molecular Belts. In *Polyarenes I*, Siegel, J. S.; Wu, Y.-T., Eds. Springer Berlin Heidelberg: 2014; Vol. 349, pp 249-290.

Bonvallet, P. A.; Mullen, M. R.; Evans, P. J.; Stoltz, K. L.; Story, E. N., Improved functionality and control in the isomerization of a calix[4]arene-capped azobenzene. *Tetrahedron Letters* **2011,** *52* (10), 1117-1120.

ACKNOWLEDGMENTS

I wish to express my gratitude to Professor Ramesh Jasti for his vision and dedication, for the opportunity to study under his mentorship, and trusting me to help to lay the intellectual, ethical, and scientific foundation of the Jasti lab as one of his first students. I would like to thank my loving family for teaching me about curiosity, wonder and beauty and for always encouraging me to discover more. I would also like to express my appreciation to the formative members of the Jasti lab: Dr. Elizabeth Hirst, Dr. Thomas Sisto, Dr. Xia Tian, Dr. Jianlong Xia, Eric Boon, Lanita Brandt, Evan Darzi, Matthew Golder, Penghao Li, Brittany White and Han Xiao. Special thanks to Dorothy Cacioppo, Alex Drexler, David Ganzi, and Joshua Morris for their friendship, love, and support throughout my graduate studies. Additionally, thanks to Michael Haley and the whole Department of Chemistry for welcoming me and the entire Jasti lab into our new home at the University of Oregon. This work was supported by a National Science Foundation CAREER award (CHE- 1255219), an Alfred P. Sloan Research Fellowship and a Boston University Ignition Award.

For my mother, father, and sister.

TABLE OF CONTENTS

LIST OF FIGURES

Figure Page

Figure Page

Figure Page

LIST OF TABLES

LIST OF SCHEMES

Scheme Page

Scheme Page

Scheme Page

CHAPTER I
MOLECULAR BELTS

This chapter is based on a literature review I wrote in March 2012 and was published as a chapter in *Topics in Current Chemistry: Polyarenes I* in 2014. Prof. Ramesh Jasti edited this and the original manuscript.

Chapter II is based on work published in *Nature Chemistry* in February 2014. I conceived the original project and developed the synthesis with the help of Evan Darzi whose discovery of the intramolecular homocoupling made this route very high yielding. I prepared the main text and edited the experimental, which was prepared by Darzi, for inclusion into this dissertation. Prof. Ramesh Jasti edited this chapter and the original manuscript.

Chapter III is based on unpublished work by myself and Han Xiao (where mentioned). Editing was provided by Prof. Ramesh Jasti.

Chapter IV is based on my unpublished work. Editing was provided by Prof. Ramesh Jasti.

Rigid hydrocarbon macrocycles with radially-oriented π-systems and continuous conjugation have attracted great interest in recent years. These molecular belts have novel optoelectronic properties and host-guest behavior. Certain belts may also ultimately lead to a rational synthesis of carbon nanotubes. The high strain associated with the nonplanar, conjugated backbones requires the development of new synthetic methods, and clever synthetic design. Herein we describe the synthetic history, properties, and state of the art of these structurally simple but synthetically challenging molecules at the initiation of the independent research described within this dissertation.

I.1. Radially Oriented π-Systems

Molecules with nonplanar p-orbitals have attracted great interest in recent years due to their fascinating electronics, challenging synthesis and favorable supramolecular properties.[1] Many of these, such as the calixarenes, cyclotriveratriline, and corranulenes maintain their electron rich cavities only weakly and can planarize or otherwise deform

through rotation or bowl inversion.[2] In contrast, a perplexing and synthetically challenging arrangement theorized more than 80 years ago comprises shape-persistant hydrocarbon hoops consisting of all *sp* or sp^2 hybridized carbon atoms.[3] These rigid hoops possess unique π systems that are geometrically forced into the center of the molecule (carbon nanotube-like) rather than above and below the plane of the molecule (graphene-like, Figure **I.1**).

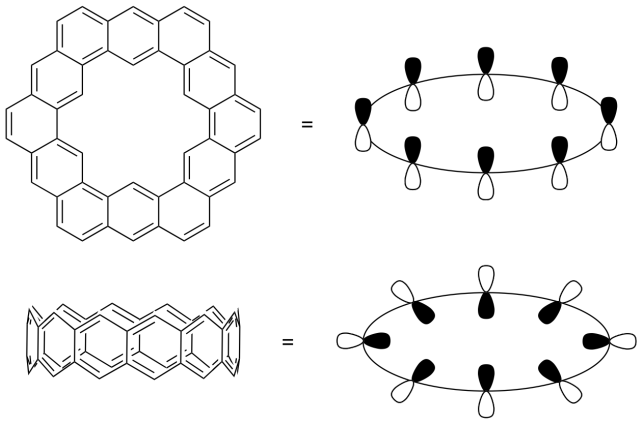

Figure I.1. PAH isomers and p-orbital orientations of $C_{48}H_{24}$: graphene-like kekulene (top) and nanotube-like $[6]_{12}$cyclacene (bottom).

The strain associated with these nonplanar belt systems renders them challenging synthetic targets. The simplest of this class are the cyclo[n]carbons, allotropes of carbon consisting of a macrocycle of all *sp*-hybridized atoms (Scheme **I.1**).

Cyclo[18]carbon was observed by Diederich and coworkers under mass spectroscopic conditions by the three-fold *retro*-Diels-Alder liberation of anthracene from the cleverly designed and stable annulene **1**. The all-carbon product, however, proved to be transient.[4-5] In spite of the reactivity of cyclocarbon, several complex hydrocarbon belts of this type have succumbed to organic synthesis and many more remain in the sights of synthetic chemists (Figure **I.2**). Herein we provide a review of the synthetic challenges, successful syntheses, and fascinating properties of this novel class of rigid hoops.

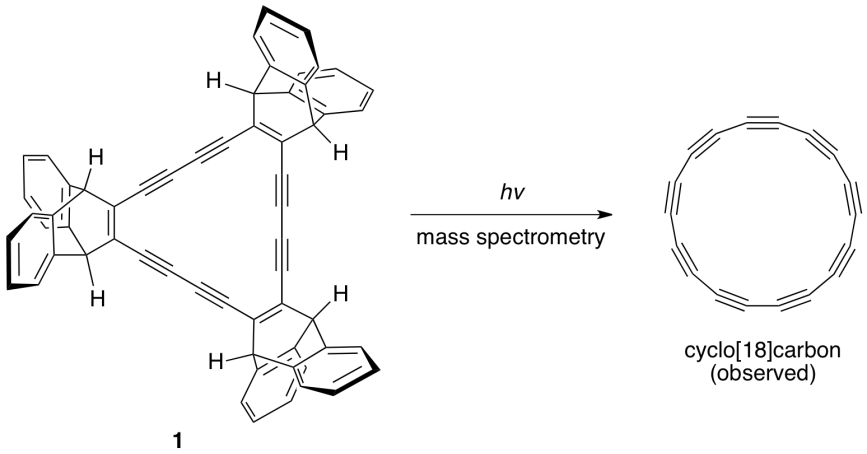

Scheme I.1. The first synthesis of a cyclo[n]carbon by Diederich et al.[4]

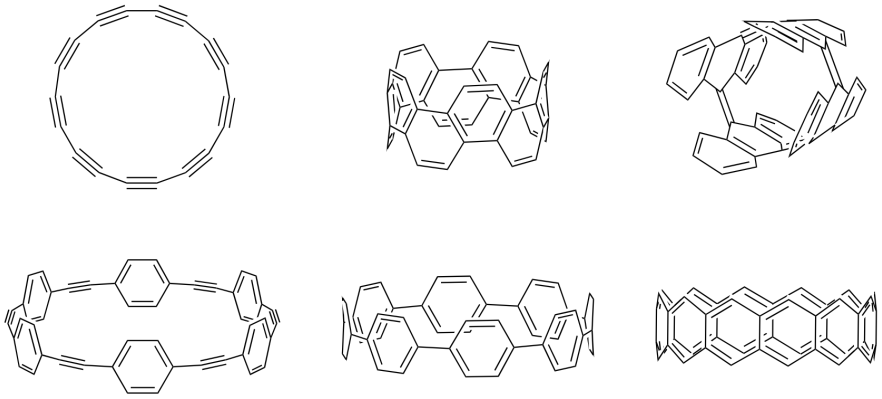

Figure I.2. Representative molecular belts (clockwise from top left, cyclocarbon, cyclophenacene, picotube, cyclacene, cycloparaphenylene, and cycloparaphenyleneacetylene).

I.2. A Hydrocarbon "Picotube"

In 1996, Herges reported the groundbreaking first bottom-up organic synthesis of a fully conjugated, aromatic hydrocarbon with a radial π-system.[6] The so-called "picotube" is a hydrocarbon with the formula $C_{56}H_{32}$ formed easily by the photoinduced ring expansion of tetradehydrodianthracene **2**.[6] Proceeding through tandem [2+2] and retro-[2+2] cycloadditions, tetraanthraceneylidene (TDDA) **3** can be obtained in 16% yield after purification (Scheme **I.2**).

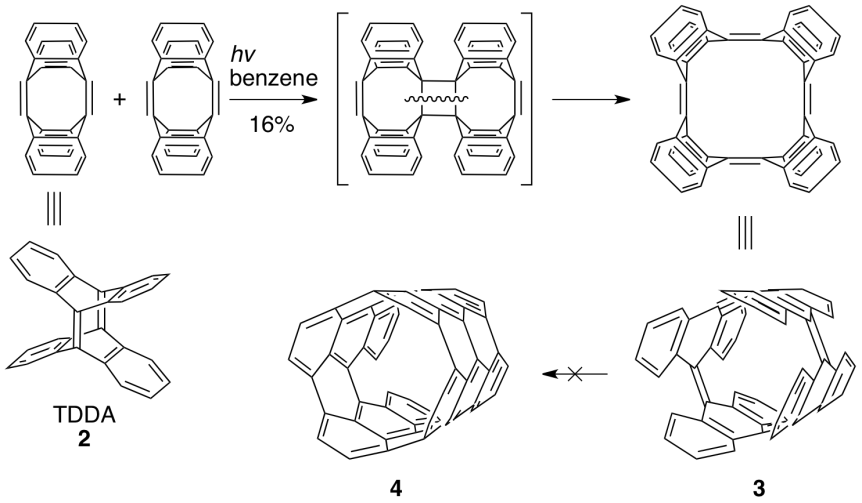

Scheme I.2. Picotube synthesis from TDDA.[6]

The resulting hydrocarbon "picotube" was found to be extremely stable to oxidation and methodology to close the remaining fjord regions to form a [4,4]carbon nanotube **4** has yet to be developed. Herges attempted this challenging closure through standard chemical cyclodehydrogenation (e.g. Schöll, etc.) which only led to polymerization. Flash vacuum pyrolysis at 800˚C however yielded 40% of the interesting rearrangement product **5** with a convoluted structure and a calculated ground state energy 52 kcal/mol more stable than that of the picotube (Scheme **I.3**).[7]

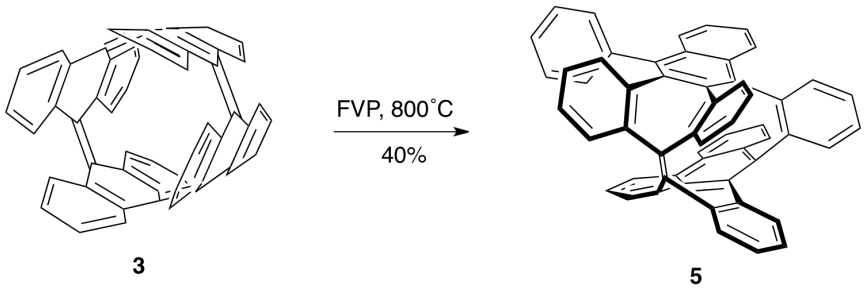

Scheme I.3. Flash vacuum pyrolysis rearrangement of **3**.[7]

The picotube did prove to be susceptible to Friedel-Crafts functionalization to prepare chiral derivatives.[8] The authors propose this as a general method for the functionalization of carbon nanotubes. The cavity of these picotubes is quite small for the encapsulation of hydrocarbons as is seen with cycloparaphenyleneacetylenes and

cycloparaphenylenes, but it has been calculated to be an appropriate guest for a (9,9) carbon nanotube (CNT), though empirical data has not yet been obtained.[9] In addition to the milestone synthesis, this picotube has attracted the interest of chemists studying its novel vibrational and spectroscopic properties.[10]

I.3. Cycloparaphenyleneacetylenes

Cycloparaphenyleneacetylenes (CPPAs) are hydrocarbon belts consisting of alkyne and phenyl moieties in differing proportions. By breaking up longer polyyne chains, responsible for the high reactivity of the cyclocarbons, with phenyl rings, one arrives at more stable hydrocarbon macrocycles. [4, 11]

I.3.1. First Synthesis by Kawase

En route to the synthetically elusive CPPA belts, Kawase reported the synthesis of strained [4]cyclometaphenyleneacetylene ([4]CMPA) in 1996 (**8**, Scheme **I.4**). This planar isomer of [4]CPPA was prepared through a McMurry coupling, bromination, and elimination sequence.[12]

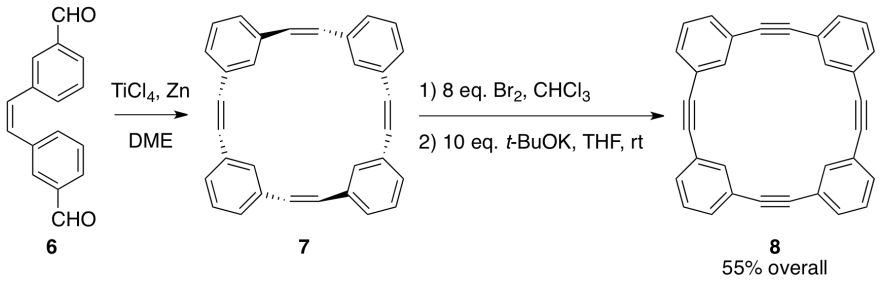

Scheme I.4. Kawase's synthesis of [4]CMPA.[12]

Having proved this synthesis tractable for the formation of bent alkynes, a similar approach was applied to synthesize [6]- and [8]CPPA (**12** and **13**, Scheme **1.5**). The "shotgun"-style macrocyclization reaction of 4,4'-diformyl-*Z*-stilbene under McMurry conditions provided moderate yields of macrocycles **9**, **10** and **11** (Scheme **I.5**). These macrocycles were then subjected as a mixture to the same bromination/elimination sequence that provided [4]CMPA.[12]

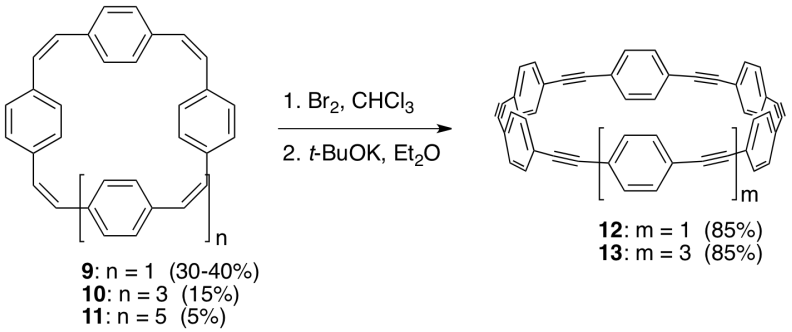

Scheme I.5. Kawase's synthesis of [6]- and [8]CPPA.[13]

Macrocycles **10** and **11** were converted efficiently to yield [6]- and [8]CPPA for the first time (17% overall yield, 4:1 **12**:**13**).[13] Owing to their strained, electron-rich nature these belts were observed to oxidize upon storage and [6]CPPA was shown to explosively decompose upon heating in air. Interestingly, the [4]CPPA precursor **9** was found to only undergo addition of *tert*-butoxide or THF (when used as solvent) at the reactive site (Scheme **I.6**).[12] This reactivity indicates that, while appropriate for the introduction of moderate strain, smaller CPPAs are unobtainable by basic elimination.[11]

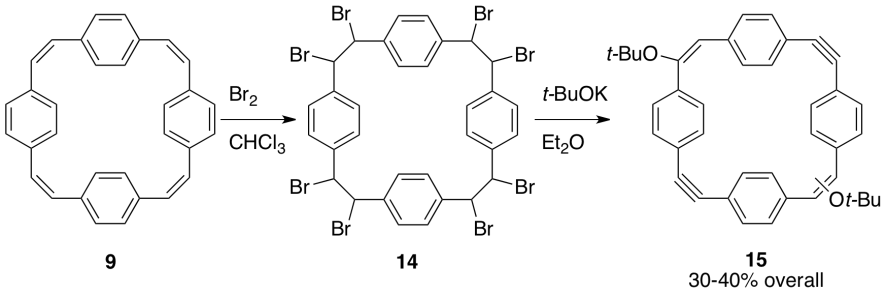

Scheme I.6. Failed conversion of **9** to [4]CPPA.[11]

I.3.2. CPPAs as Novel Host Molecules

Having overcome the challenge of [6]- and [8]CPPA with his landmark synthesis, Kawase improved upon these methods to prepare large quantities of [6]-[9]CPPA. With ample material in hand, the Kawase lab sought to exploit the unique, electron-rich cavity present in these rigid molecular belts.[13] Kawase showed for the first time that CPPAs can form all-hydrocarbon inclusion complexes with appropriate guests.[14] By co-crystallizing

[6]- and [8]CPPA with hexamethylbenzene and toluene respectively, crystal structures of a 1:1 **12**·HMB and 1:4 **13**·tol complexes were obtained (Figure **I.3**).

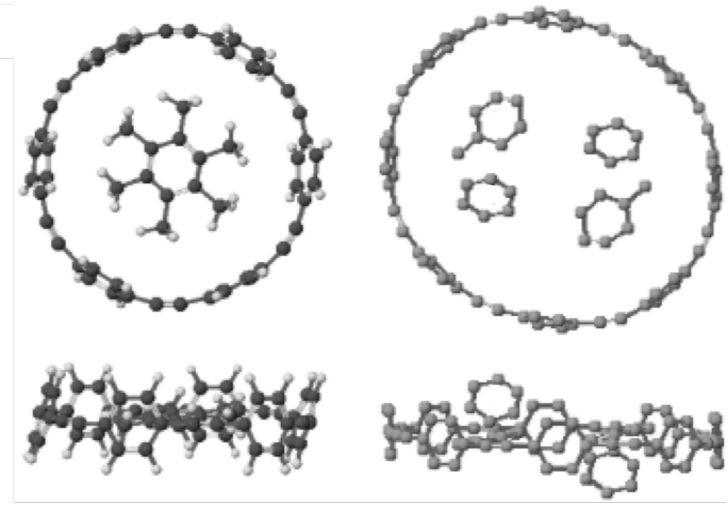

Figure I.3. Crystal structures of **12**·HMB and **13**·tol.[14]

Though the host-guest interaction in both of these complexes was quite weak, with the toluene complex efflorescing at room temperature, the improved air-stability of the complexes as compared to the CPPAs indicated a favorable electronic interaction within the CPPA cavities.[14] The authors attribute this affinity to the electron-rich nature of the molecules' interior. Furthermore, important crystallographic information about the diameters of these molecular belts was available for the rational design of stronger host-guest complexes.

With preliminary proof of the CPPAs' host activity, and in light of the then-recent discovery of fullerene@CNT peapod complexes, Kawase correctly ascertained that [6]CPPA was approximately the right size to host fullerene C_{60}. Indeed, mixtures of **12** and C_{60} yielded very strong inclusion complexes with a Gibbs activation energy for dissociation ($\Delta G^{\ddagger}$) of 9.9±0.3 kcal/mol.[15] This interaction is assumed to be stronger then the calix[8]arene-C_{60} complex that is used to purify C_{60} from carbon soot on a commercial scale.[16] The authors attribute the strength of this interaction to polar electrostatic interactions of the CPPA π-system with the electron-deficient [5:6] fusions in fullerene. Furthermore the complex of bis(ethoxycarbonyl)methanofullerene and

[6]CPPA was crystallized and X-ray crystallographic data confirmed the orientation of the CPPA phenyl rings in proximity to the [5:6] fullerene fusions (Figure **I.4**).

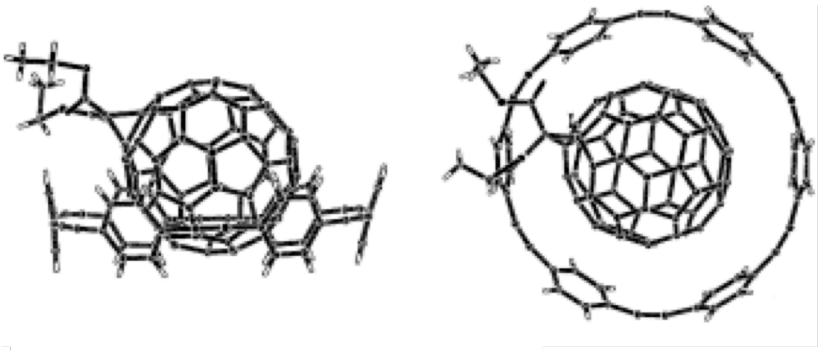

Figure I.4. Crystal structure of a [6]CPPA·fullerene complex.[17]

This structure also revealed that the fullerene is only partially encapsulated, with an average intermolecular distance of 3.4 Å, similar to the interlayer distance in multi-walled carbon nanotubes and multi-layer graphene. From this discovery, Kawase was able to further investigate the dynamics of the [6]CPPA-fullerene interaction[17] and also to synthesize naphthyl- derivatives of CPPAs with deeper cavities and stronger interactions such as **16**, **17**, and **18** (Scheme **I.7**, Figure **I.5**, and Table **I.1**).[18]

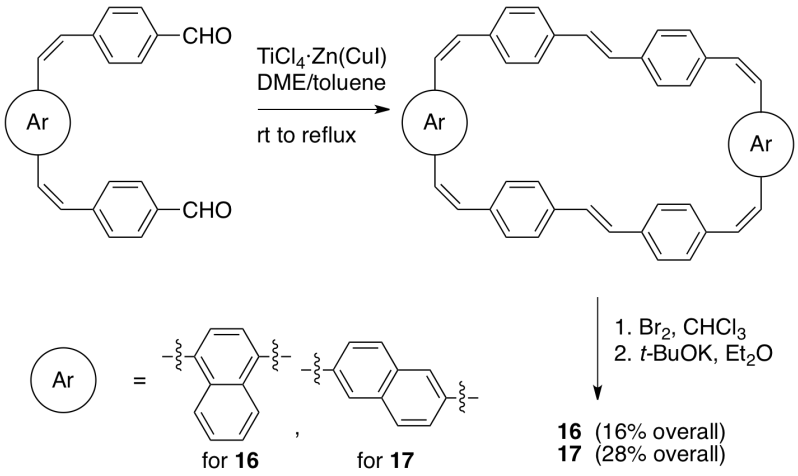

Scheme I.7. Modified CPPA synthesis for π-extended hoops.[18]

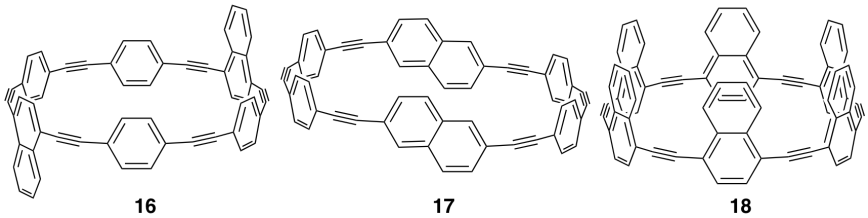

Figure I.5. Extended CPPAs synthesized by Kawase et al.[18]

Table I.1. Dissociation energy (kcal/mol) for fullerene@CPPA.

CPPA	$\Delta G^{\ddagger}$ with C_{60}	$\Delta G^{\ddagger}$ with C_{70}
[6]CPPA[a]	9.9 ± 0.2	9.6 ± 0.2
[7]CPPA[a]	<9	<9
16 [a]	10.8 ± 0.3	10.1 ± 0.2
17 [a]	<9	11.9 ± 0.8
18 [b]	14.1 ± 0.3	

a[18a] b[18b]

With experience synthesizing CPPA-fullerene complexes, Kawase went on to design and isolate an onion complex of naphthyl substituted [9]- and [6]CPPA with C_{60} (Figure **I.6**).[19]

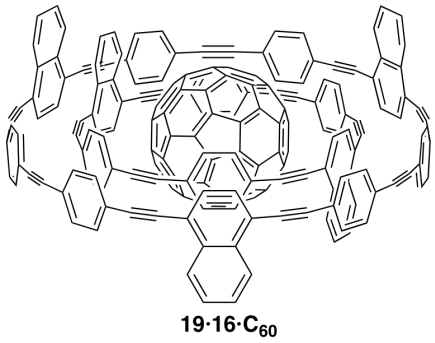

Figure I.6. A CPPA-fullerene onion complex.[19]

Similar multilayer arrangements are manufactured by "top-down" methods (multi-walled carbon nanotubes, buckyonions) but this was the first example of the assembly of such a structure from the bottom up.[20] Furthermore, at the time it represented the first double inclusion complex of three synthetically accessible organic molecules.[19] Kawase found that, like the previous CPPA-fullerene complexes, the intermolecular distance in this onion complex was 3.2 Å, closely resembling the equivalent distance in carbon materials.

This observation demonstrated further proof that discrete, small molecule belts can be accurate models of larger carbon structures.

I.3.3. The Synthesis of More Reactive CPPAs

The stability of CPPAs to oxidative and polymeric decay falls with increasing length of the polyyne segments.[21] As such, there is an inherent challenge in synthesizing nanohoops with a higher ratio of *sp* to sp^2 carbons, approximating the very reactive cyclocarbons.[4-5] These approaches have hinged upon masking either the phenyl rings[22] or one or more alkynes[23] as curved moities that can be converted to the desired functionality after macrocyclization.

Both Hopf and Tsuji attempted the synthesis of [n_2]CPPAs (having 2 alkynes per phenyl ring and n phenyl rings) using masked aromatic rings.[22] Hopf reported attempts towards [2_2]CPPA and [3_2]CPPA using syn-substituted 1,4-cyclohexadienes to install curvature (Scheme **I.8**). Structure **20** was synthesized by double addition of lithium trimethylsilylacetylide into benzoquinone followed by methylation of the resulting diol. After deprotecting the alkynes, Glaser-Ellington conditions at high dilution (4×10^{-5} M) offered low yields of macrocycles **21** and **22**.

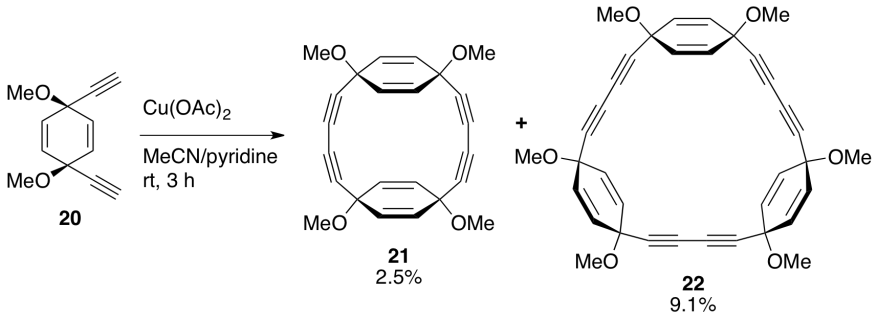

Scheme I.8. Hopf's synthesis of putative CPPA precursors **21** and **22**.[22a]

Conversion of these to the corresponding CPPAs has not been reported, presumably due to a lack of appropriate aromatization methods.[22a, 24]

Tsuji was met with success in the synthesis of [6_2]CPPA using Dewar benzenes as masked aromatic rings which can be irreversibly aromatized by irradiation in the final synthetic step (Scheme **I.9**).[22c, 25] Tsuji's approach consists of the synthesis of Dewar

benzene derivative **24** by [2+2] cycloaddition of 1,2-dichloroethylene to dimethylacetylenedicarboxylate. This adduct was then reduced and protected as the cyclohexyl ketal **26**, which is resistant to photoisomerization. Elimination afforded a mix of dichlorides **27** and **28** which were easily separated by chromatography.[22b]

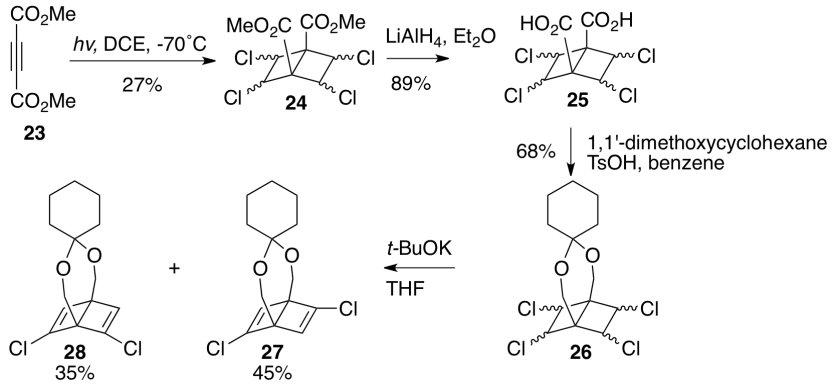

Scheme I.9. Synthesis of Dewar benzene derivatives.[22b]

Tsuji proved the usefulness of this building block in the synthesis of less strained phenylacetylene macrocycles.[22b, 25] Sonogashira alkynylation, Glasier-Ellington dimerization, and Glaser-Ellington macrocyclization afforded **31** which was quantitatively converted by photoirradiation to dodecasilyl [6_2]CPPA comprising the first synthesis of a substituted [n_2]CPPA (Scheme **I.10**).[22c]

While this remains the most unsaturated CPPA ever isolated (stable on the order of days), Tobe reported evidence of the formation of cyclocarbon-like [2_6]CPPA. [4.3.2]Propelatriene units are known to undergo photoinduced retro [2+2] addition to yield indane and the corresponding alkyne.[26] Having employed a similar strategy en route to cyclocarbon, Tobe wisely chose these as masked alkynes, providing curvature to the CPPA macrocyclic precursors **35** and **36** (Scheme **I.11**).

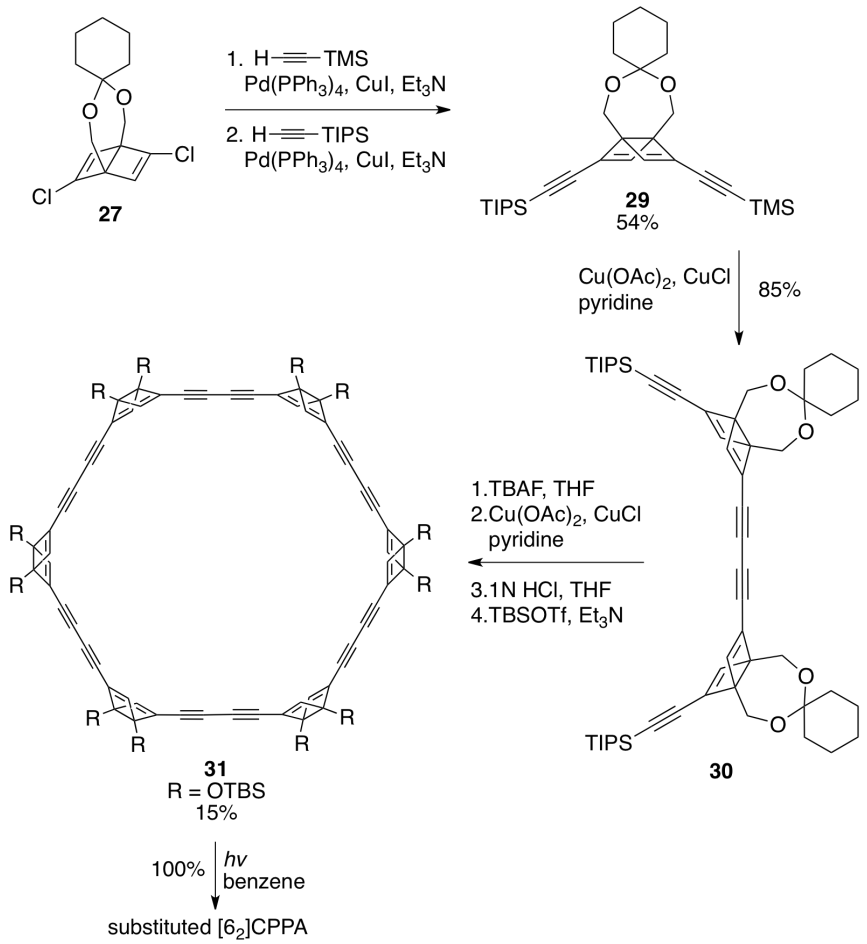

Scheme I.10. Synthesis of CPPA precursor **31** and conversion to a CPPA derivative.[22b]

Fragments **33** and **34** were synthesized by Sonogashira coupling with 1,4-diiodobenzene and 1,4-diiodo-2,3,5,6-tetrachlorobenzene respectively, followed by deprotection and dilute oxidative coupling to offer **35** and **36**. Under mass spectroscopic conditions, irradiation of the macrocycle generated the highly unstable [2_6]CPPA.[23] Interestingly, when using furan as solvent, **37** was obtained as a quickly decomposing orange solid.

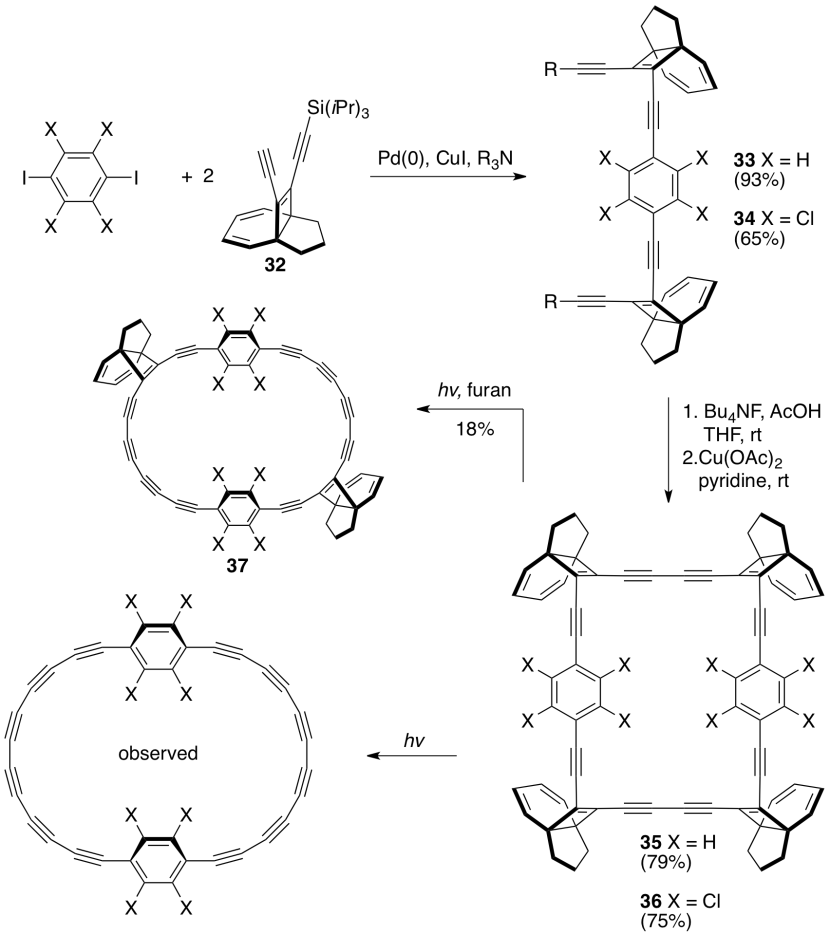

Scheme I.11. Tobe's synthesis of [2_6]CPPA.[26]

I.4. Cycloparaphenylenes

Recently, there has been an explosion of research and new syntheses surrounding the cycloparaphenylenes (CPPs).[24, 27] These conjugated macrocycles are comprised of sequential benzene rings bonded covalently at the para positions. As such, they represent the smallest unit cycle of an armchair nanotube **(**Figure **I.7**).

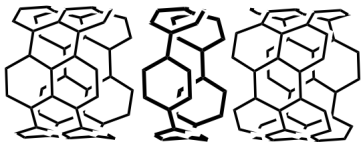

Figure I.7. [5]Cycloparaphenylene envisioned as the unit-cycle of an armchair nanotube (double bonds omitted for clarity).

These “carbon nanohoops” have been envisioned as seeds for the growth of extended nanotube structures as well as novel, porous, semiconducting and fluorescent materials in their own right.[27b, 27s, 27v, 27w]

I.4.1. Early Attempts Towards Cycloparaphenylenes

The first published attempt at the synthesis of any CPP was reported in 1934 by Parekh et al.[3] Having synthesized the parent macrocycle, *p,p*-diphenylenetetrasulfide, **38**, the thermal liberation of 4 equivalents of sulfur (as copper sulfides and sulfur oxides) upon heating with copper in air was attempted (Scheme **I.12**). Only partial desulfination was observed, however, probably owing to the extreme strain associated with the resulting [2]cycloparaphenylene.

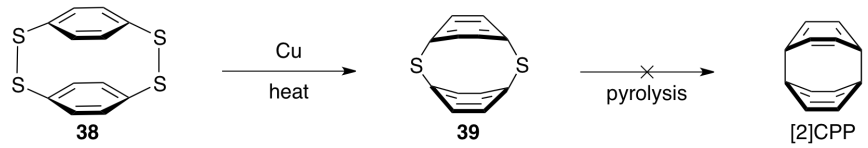

Scheme I.12. Parekh’s attempted synthesis of [2]CPP.[3]

Almost 60 years later, Vögtle and coworkers published three inspiring synthetic routes towards CPP.[28] First, in a similar fashion to the attempts towards [2]CPP by Parekh, Vögtle accessed hexaphenyl pentasulfate macrocycle **40** in 65% yield (a, Scheme **I.13**). However, thermal cleavage of the sulfide bonds again proved difficult. It is assumed that, while efficient in many cases for the buildup of strain[29], this motif is inadequate to access the highly rigid, bent aromatic backbone of the CPPs. Vögtle et al. then revised their synthesis to target the less energetic [8]- and [10]CPPs. To do so, the oligomeric phenyleneethyleneacetylene macrocycles **41** were synthesized from a tetra-Wittig reaction in dilute conditions meant to quell polymerization (b, Scheme **I.13**).

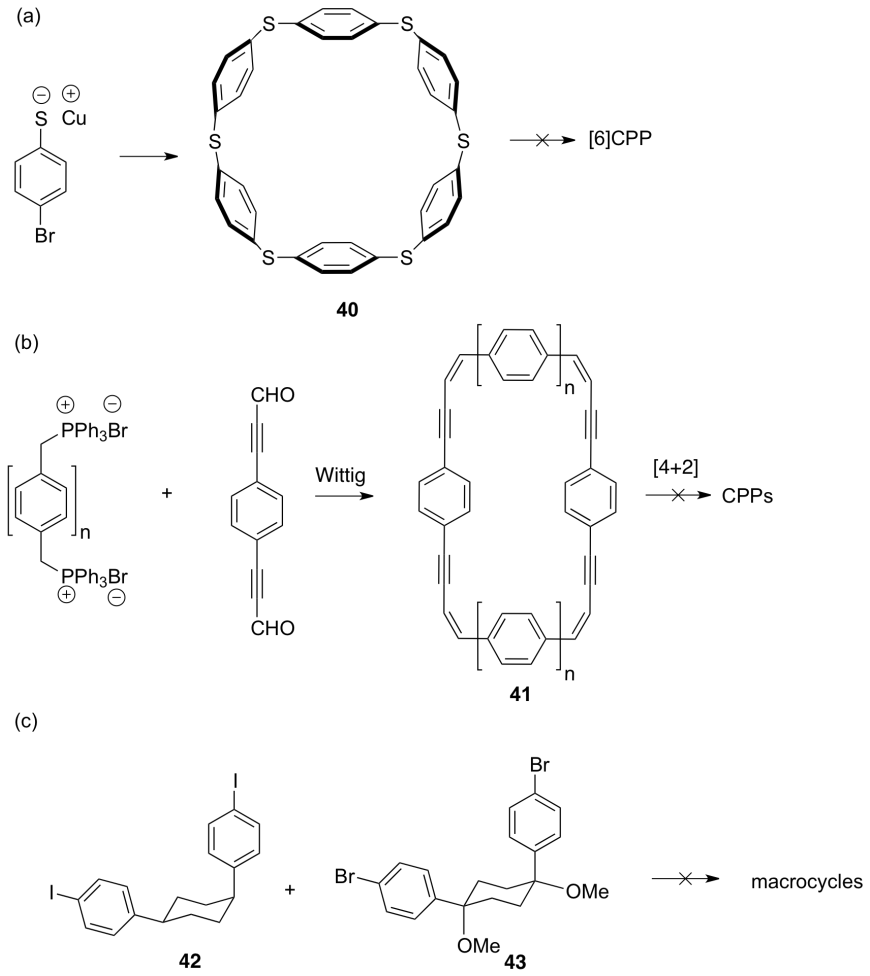

Scheme I.13. Vögtle's attempted syntheses of cycloparaphenylenes.[28]

Vögtle's vision for these macrocycles was that [4+2] cycloadditions to the ene-yne moieties would build in the final 4 phenyl rings and yield the corresponding carbon nanohoops. However, these attempts were never successful. Lastly, Vögtle prepared substituted L-shaped cyclohexanes **42** and **43** with the intent to oxidize these to phenyl rings after cyclic oligomerization, but failed to arrive at the corresponding macrocycles (c, Scheme **I.13**). This cyclohexane approach would later be employed successfully by Itami et al.[27a]

I.4.2. The First Synthesis of Cycloparaphenylene

After eluding synthesis for over 70 years, the pioneering synthesis of [9]-, [12]-, and [18]CPP was reported by Jasti and Bertozzi.[24] Using cyclohexadienes as masked aryl

rings, Jasti envisioned a final reductive aromatization from macrocycles of the type **46-48**. These aromatization reactions were expected to be highly exothermic and appropriate for building in considerable strain (Scheme **I.14**).

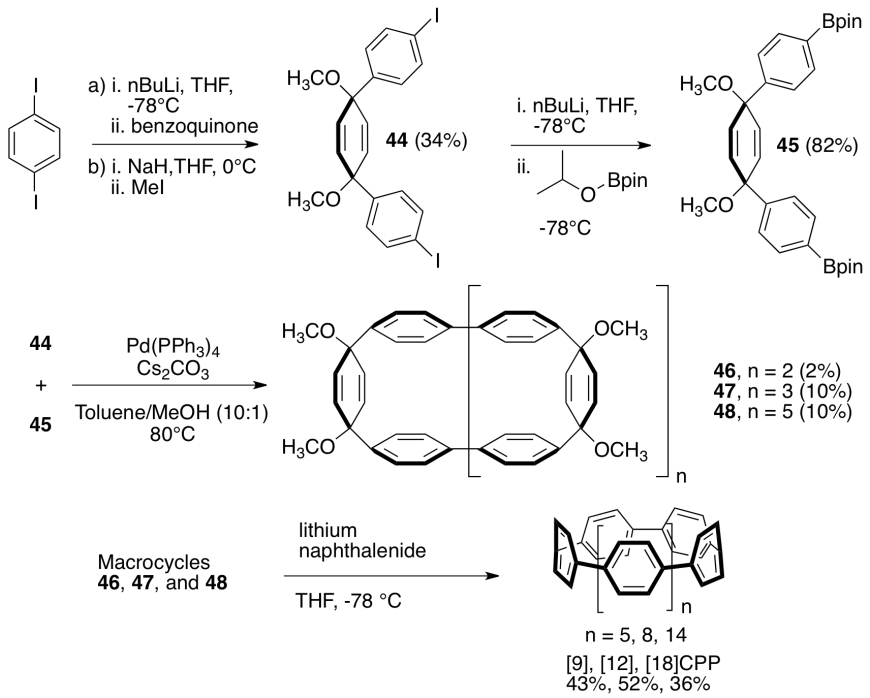

Scheme I.14. The first synthesis of [9]-, [12]-, and [18]cycloparaphenylene.[24]

To employ this method, diiodide **44** was easily synthesized on a large scale without chromatography via the addition of benzoquinone into a molar excess of lithiated diiodobenzene followed by methylation with sodium hydride and iodomethane. A portion of this diiodide was then converted to the bisboronate **45** and "shotgun" Suzuki-Miyaura cross-coupling at high dilution offered a mixture of macrocycles. These macrocycles were easily separated by standard chromatographic procedures. It is interesting to note that the 9-membered macrocycle must be the result of intramolecular homocoupling of the corresponding 9-membered bisboronate or homocoupling of **45** followed by intermolecular macrocyclization with **44**. With these macrocycles in hand, Jasti developed a reductive aromatization technique that circumvented the 1,2-phenyl shift observed under acidic or Lewis acidic conditions for similar systems (Scheme **I.15**).[30]

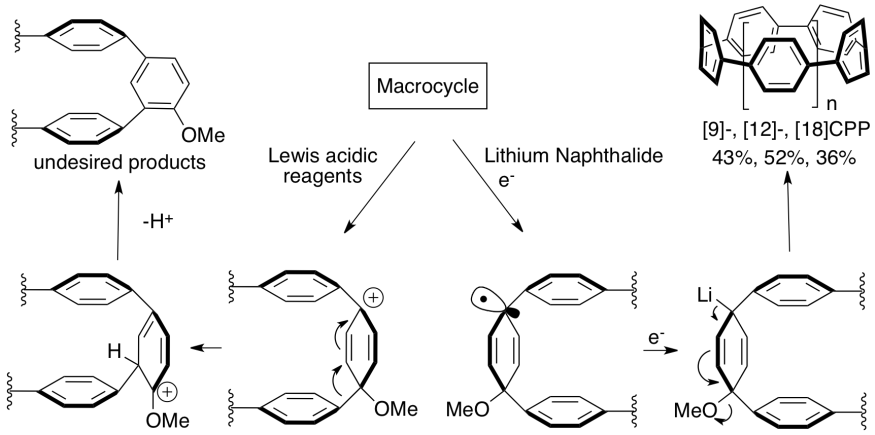

Scheme I.15. Aromatization reaction and proposed mechanism.[24]

Treating a solution of the desired macrocycle with lithium naphthalenide at –78˚C for 30 minutes offered the corresponding CPPs in moderate yield.[24] The electron-transfer mechanism of this reduction prevents rearrangement by circumventing carbocation intermediates, and builds in an amazing amount of strain at low temperatures (total calculated strain energy for [9]CPP: 69 kcal/mol). Using this procedure, Jasti synthesized 1.8, 4.2, and 1.6 mg of [9]-, [12]-, and [18]CPP for the first time.

With the elusive hydrocarbons finally in hand, Jasti obtained optical data for these highly fluorescent aromatics and observed a similar absorbance for all diameters (338-339 nm) and a fluorescence red shift with decreasing diameter. The largest absorbance-emission shift, for [9]CPP, is approximately 160 nm.[24] Oligoparaphenylenes (OPPs), the linear analogues of CPPs show a blue fluorescence shift with decreasing length, following a "particle in a box" optoelectronic model.[31] Quantum dots also exhibit blue shifted fluorescence with decreasing size. The odd trend for carbon nanohoops was attributed to the increased sp^3 character of the smaller CPPs allowing for greater relaxation in the excited state, as well as the diminished conjugation effects when considering these cyclic, infinitely conjugated molecules. As will be seen, the fluorescence of all CPPs behave in the same way and has been a current topic of interest (Figure **I.8**).[27d, 27n, 27w, 27x]

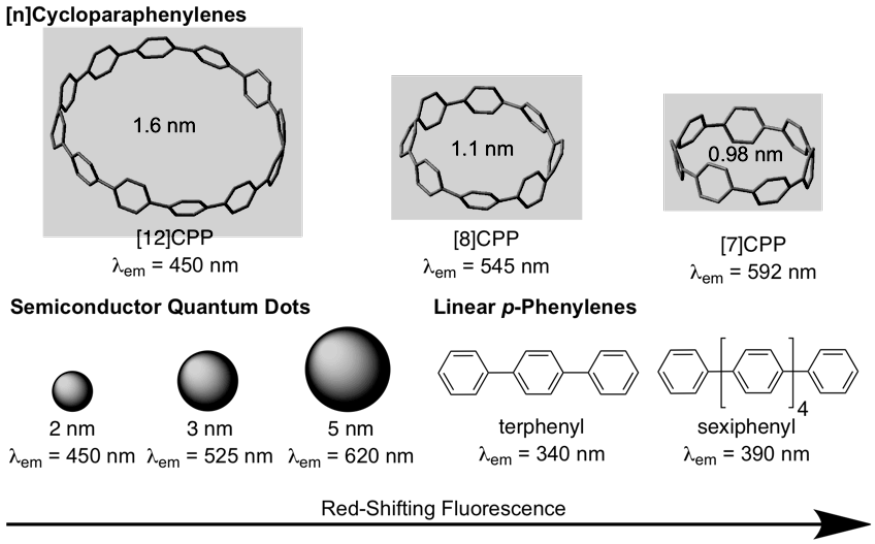

Figure I.8. Fluorescence trends in quantum dots, CPPs and OPPs.[27i]

I.4.3. Subsequent Syntheses: A New Field Emerges

In the years following the landmark synthesis by Jasti and Bertozzi, both the Itami group at Nagoya University and Yamago and coworkers at Kyoto University developed new synthetic routes to the cycloparaphenylenes.

In 2009, Itami et al. reported the selective synthesis of [12]CPP using methods inspired by Vögtle.[27a] To do so, Itami synthesized bisboronate **50** and MOM-protected **49**. This protecting group simplifies purification. Reaction of a 10-fold molar excess of **49** with **50** under appropriate palladium coupling conditions favored the formation of 9-membered diiodide **51**. Dilute coupling of **51** with bisboronate **50** yielded selectively the 12-membered macrocycle (Scheme **I.16**).

To aromatize the cyclohexane rings in this CPP precursor, Itami employed harsh-but-effective microwave conditions using stoichiometric *para*-toluenesulfonic acid at 150˚C to achieve the sequential deprotection of the alcohols, acidic elimination, and oxidation of the resulting cyclohexadienes to aryl rings.

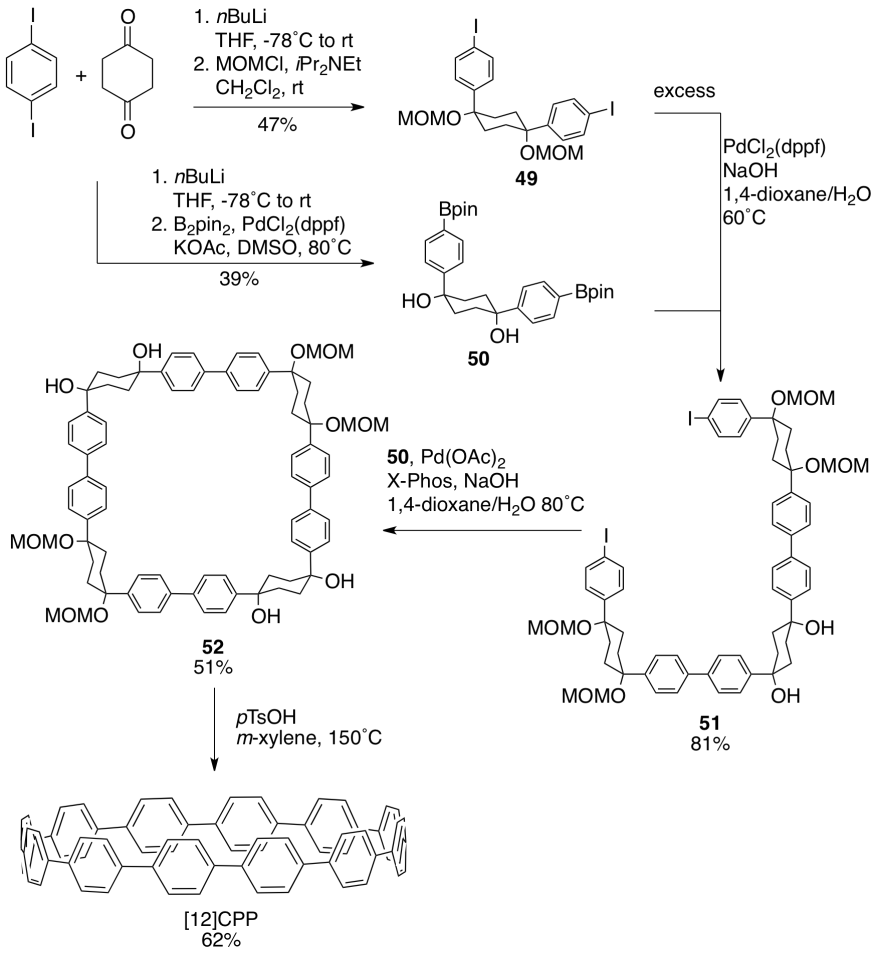

Scheme I.16. Itami's synthesis of [12]CPP.[27a]

Using this motif, Itami obtained 4.1mg of [12]CPP alone.[27a] This methodology has recently been employed by Tokyo Chemical Industry, who now offers [12]CPP of 90% purity for $1098.90 per 10mg (TCI, product number C2449). It is an incredible achievement that such a strained hydrocarbon, which was envisioned decades ago, has become commercially available so shortly after its first synthesis. It seems evident, therefore, that interest in these structures is not limited to synthetic chemists.

In 2010, Yamago et al. entered the field of carbon nanohoop synthesis, reporting the challenging synthesis of [8]CPP, the smallest and most strained CPP at the time of the publication. Unlike Itami and Jasti who relied on masked aromatic rings to relieve strain in the macrocyclic CPP precursors, Yamago employed an organometallic approach (Scheme **I.17**). By reacting 4,4'-bis(trimethyl)stannylbiphenyl **53** with

dichloro(cycloocta-1,5-diene)platinum(II), Yamago was able to generate square-shaped macrocycle **54** with very little strain energy.[32]

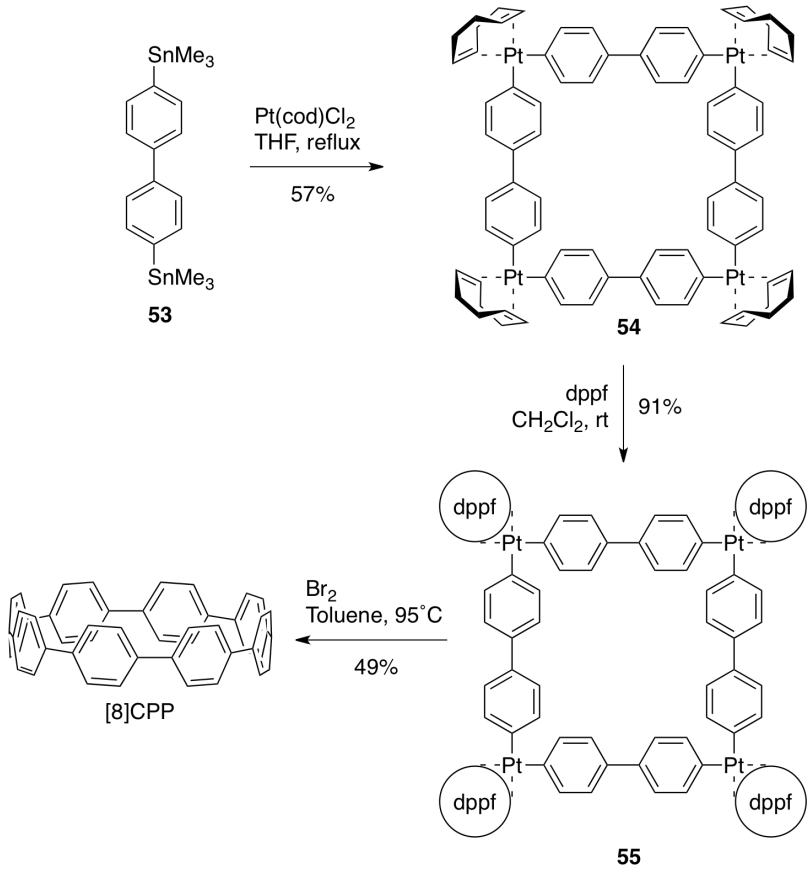

Scheme I.17. Yamago's synthesis of [8]CPP.[32]

After ligand exchange to 1,1'-bis(diphenylphosphino)ferrocene (dppf), reductive elimination with bromine led cleanly to 2.0 mg of [8]CPP in three straightforward steps. This reductive elimination builds in an incredible 74 kcal/mol of strain energy in a single reaction. Yamago observed that this new, smaller cycloparaphenylene followed the optical trend observed by Jasti having an absorption maximum at 338 nm and an even larger absorbance-emission shift of 200 nm.[32]

I.4.4. Better Synthetic Control and New CPP Sizes

With three unique synthetic strategies, each lab pushed forward to create new sizes of cycloparaphenylene and to do so selectively. In 2010, Itami reported a modified

synthesis that offered access to [14]-, [15]-, and [16]CPP selectively via U-shaped dibromide precursors with 7 or 8 rings (Scheme **I.18**).[27b] These new intermediates **57a** and **57b** were the products of palladium coupling of a molar excess of **56** with 1,4-phenylboronic acid or 4,4'-biphenylboronic acid.

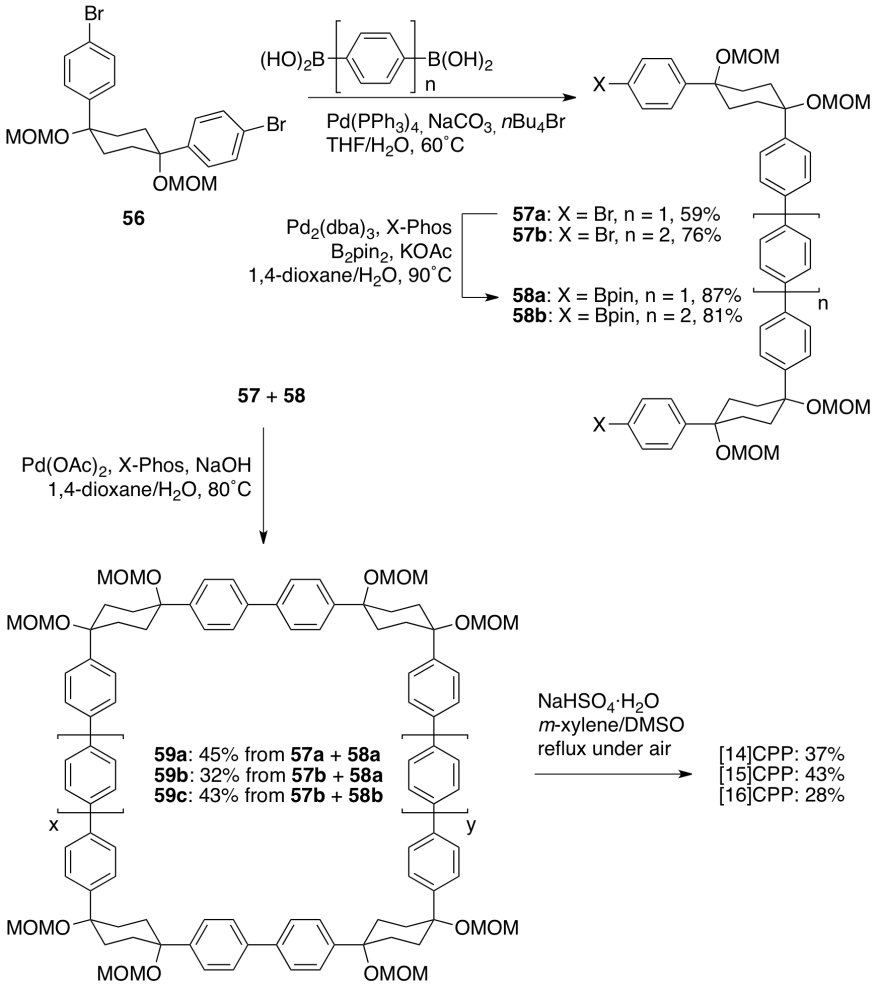

Scheme I.18. Itami's synthesis of [14]-, [15]-, and [16]CPP.[27b]

Either of these dibromides can then be converted to the corresponding bisboronates **58a** and **58b** by palladium-mediated borylation and Suzuki coupled in a 7+7, 7+8, or 8+8 fashion to offer 2.0 mg, 2.2 mg, and 2.5 mg of [14]-, [15]-, and [16]CPP respectively after acidic aromatization. The authors propose that chair-flipping accounts for increased flexibility, facilitating the 7+8 macrocyclization.[27b]

Itami went on to report a new synthesis of [12]CPP based on the "shotgun" homocoupling of dihalide **56** with bis(cyclooctadiene)nickel(0) in the presence of 2,2'-bipyridyl. This new approach circumvented the synthesis of a boronate and also the need for palladium catalysis, albeit stoichiometric nickel is required (Scheme **I.19**). With these synthetic advantages, Itami was able to synthesize **61**, the macrocyclic precursor to [12]CPP on gram-scale. In addition, the authors report that with this synthesis they were able to produce 0.5g in total of [12]CPP from combined reaction products.[27b]

At the time of publication, the "shotgun" coupling in this synthesis was reported only for the [12]CPP macrocycle. However, upon investigation of what was originally thought to be linear oligomeric byproducts, it was found that the triangular 9-membered macrocycle **60** also forms in similar yields to the [12]CPP precursor (Scheme **I.19**).[27h]

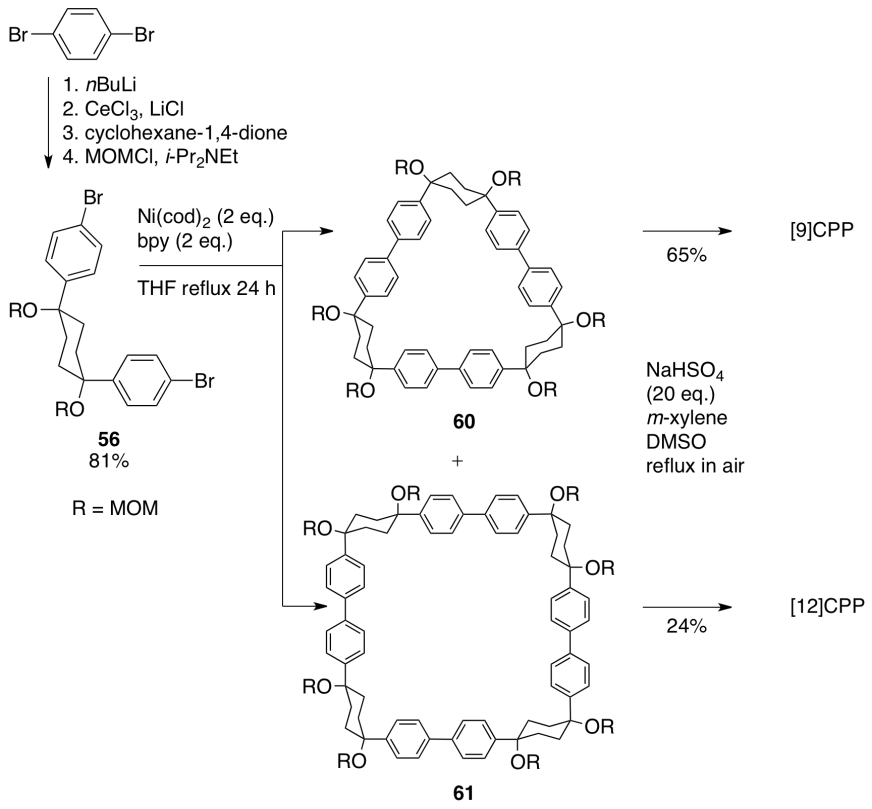

Scheme I.19. Nickel "shotgun" synthesis of [9]- and [12]CPP. [27g, 27h]

The availability of [9]- and [12]CPP on a more significant scale allowed for the analysis of their molecular structures by single crystal X-ray diffraction for the first time (Figure **I.9**). These slightly disordered structures were refined enough to confirm the

benzenoid structure of [12]CPP with *ipso*-*ipso* bond lengths of 1.481 Å and also hint at the trend towards quinoidal structures in smaller CPPs showing shortening of the *ipso*-*ipso* bond lengths of [9]CPP to 1.468 Å, still longer than the expected range for alkene bonds. In addition, it was shown that the crystal packing of [12]CPP favors a herringbone pattern with channels clearly visible from the appropriate angle, but not strictly nanotube-like.[27g, 27h]

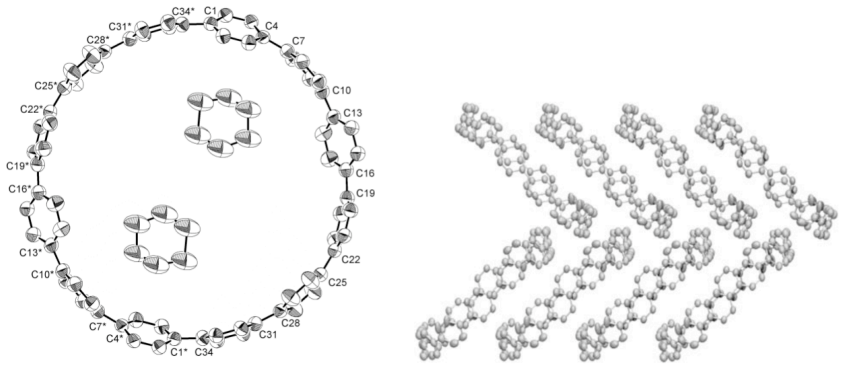

Figure I.9. Crystal structure (left) and packing orientation (right) of [12]CPP. Reproduced with permission.[27g]

Yamago also published a synthesis of new CPP sizes in 2011.[27d] By utilizing 4,4'-bis(trimethyl)stannylbiphenyl and 4,4'-bis(trimethyl)stannylterphenyl, as starting materials, Yamago showed that [8]- and [12]CPP can be selectively formed by his platinum-mediated synthesis and also that using a "shotgun" mixture of both provides a mixture of metallocycles which can be converted to the CPPs then separated by preparatory GPC to offer [8]-[13]CPP (Scheme **I.20**).

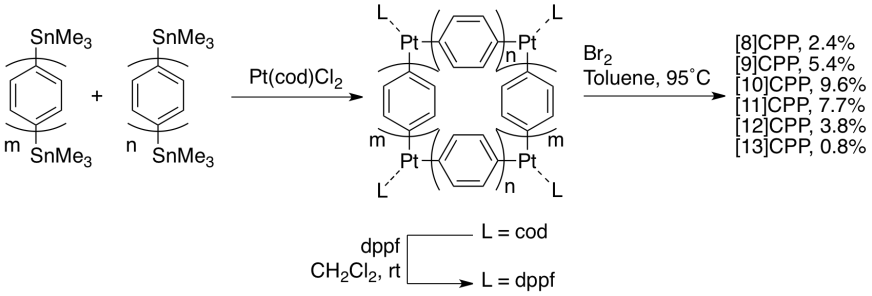

Scheme I.20. Yamago's selective and random synthesis of [8]-[13]CPP.[27d]

The formation of [13]CPP is interesting in that it implies the formation of either a 2+2+3+3+3 or a 2+2+2+2+2+3 macrocycle.

With these several sizes in hand, Yamago determined the optical characteristics by UV/Vis and fluorescence spectroscopy and the oxidation potentials of these CPPs by cyclic voltammetry. The absorbance of all the synthesized CPPs was similar, centered around 338nm, and the fluorescence followed the emission-shift trend observed by Jasti (Figure **I.10**).[24] It was theorized that the relaxation and relief of strain in the excited state geometry of these molecules accounts for the observed shift.[27w]

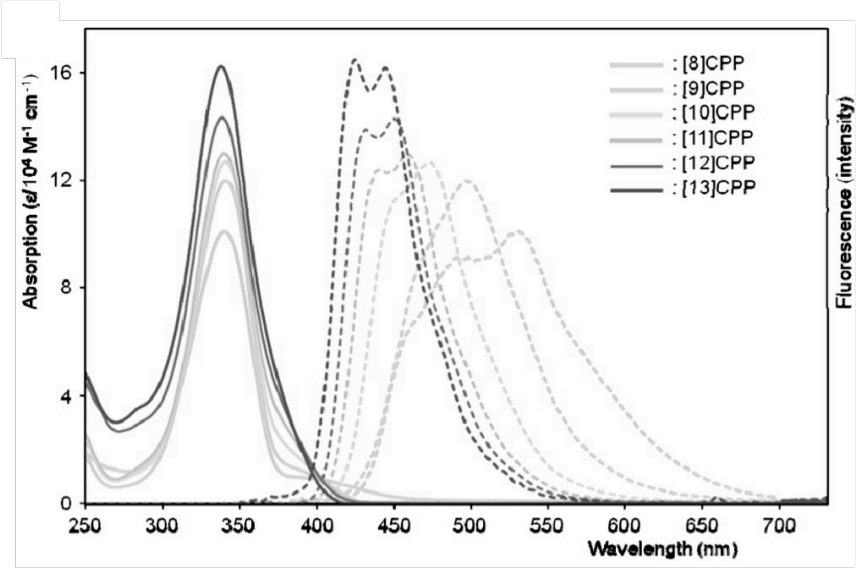

Figure I.10. Size dependent fluorescence red shift as observed by Yamago. Reproduced with permission.[27d]

The oxidation potentials were shown to lower with decreasing size. This trend is indicative of the increasing quinodimethane structure and therefore polyene character of the smaller CPPs. These CV observations also correlate well with Yamago's calculated HOMO-LUMO gap, which narrows with decreasing size (Figure **I.11**). The opposite trend is calculated for OPPs.[27d]

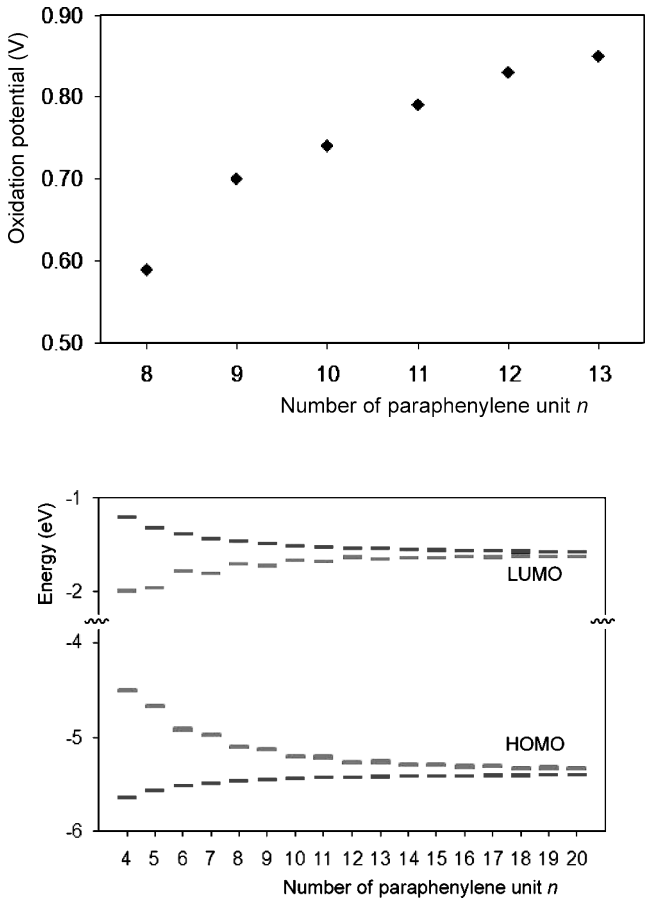

Figure I.11. Top: observed oxidation potential of [n]CPP. Bottom: calculated HOMO-LUMO gaps for [n]CPP (grey) and [n]OPP (black). Reproduced with Permission.[27d]

In an effort to probe the interesting properties of even smaller carbon nanohoops, Jasti published the first synthesis of [7]CPP.[27i] This very strained polyphenylene (83 kcal/mol) was assembled using sequential, selective Suzuki coupling reactions. Unsymmetric dihalide **64** was synthesized by the syn-selective addition of lithiated 1,4-bromochlorobenzene to **63** after deprotonation of the free alcohol (Scheme **I.21**).

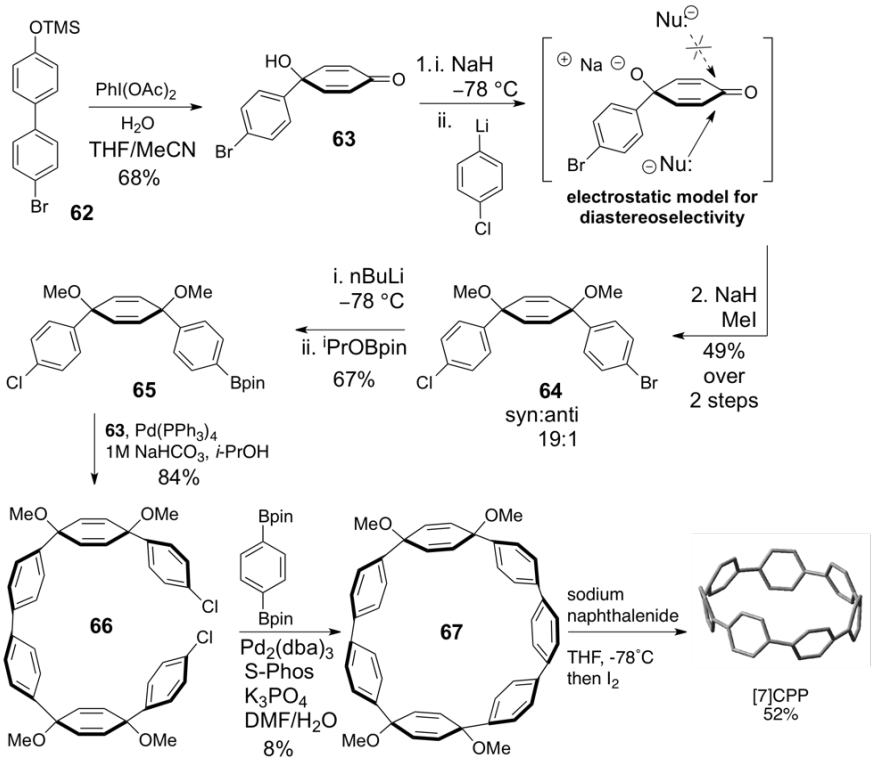

Scheme I.21. Jasti's synthesis of record-breaking [7]CPP.[27i]

The deprotonation with sodium hydride imparts diastereoselectivity consistent with an electrostatic model in which the anionic nucleophile approaches from the opposite face of the existing negative charge. A portion of this dihalide was then converted by selective lithiation to the boronate **65**. Under standard palladium coupling conditions, this boronate and **64** were coupled in a chemoselective manner to offer dichloride **66** without the need for an excess of reactants. Switching to Buchwald's S-Phos as a ligand, this dichloride was closed to macrocycle **67** by reaction of 1,4-phenylboronic acid bis(pinacol) ester at high dilution. The strained terphenyl in the resulting macrocycle explains the relatively low macrocyclization yield. Even so, this molecule was easily aromatized using sodium naphthalenide at –78˚C, yielding 1.0 mg of [7]CPP. The final step of any CPP synthesis must necessarily introduce a large amount of strain. These results highlight the reductive aromatization methodology as quite capable of generating large amounts of strain energy at low temperatures. Interestingly, [7]CPP displays an orange fluorescence, further red-shifted than [8]CPP and with a very low quantum yield, following the trends observed in larger carbon nanohoops.[27i]

A revision of the [7]CPP synthesis to incorporate more curvature in the precursors would allow for the construction of even smaller CPPs, approaching the theoretical limit of the benzenoid structure.[33] With this in mind, Jasti developed a sequential lithium addition/oxidative dearomatization strategy shown by which tightly-curved dibromide **70** can be obtained on the multigram scale (Scheme **I.22**).[27o]

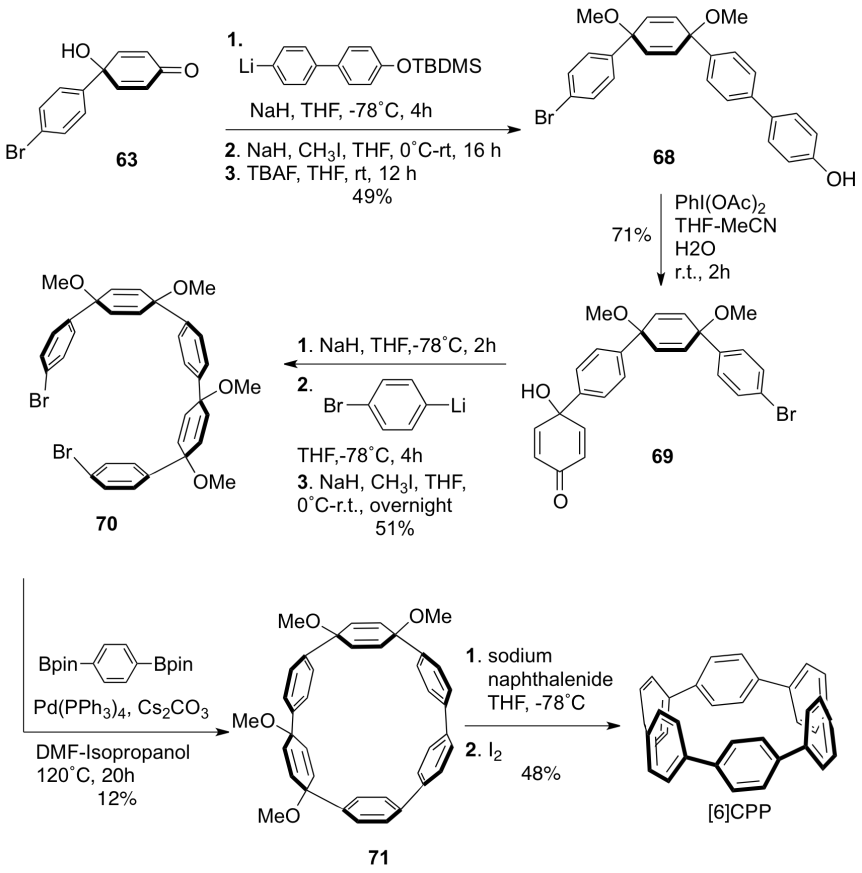

Scheme I.22. The first synthesis of [6]CPP, the smallest prior to the synthesis of [5]CPP (see Chapter II). [27o]

The addition of lithiated 4-bromo, 4'-*tert*-butyldimethylsilyl biphenyl to **63** followed by methylation and deprotection offered **68** which could be subjected to a second oxidative dearomatization to **69**. Diastereoselective addition of lithiated 1,4-dibromobenzene to **69** gives the desired dibromide **70** in a highly scalable fashion. Moreover, the increased Suzuki reactivity of bromine versus chlorine led to the application of Buchwald-ligand free palladium (0) coupling with 1,4-phenylboronic acid bis(pinacol) ester to macrocycle

71 with an incredible distorted terphenyl unit evident in the crystal structure (Figure **I.12**).[27o]

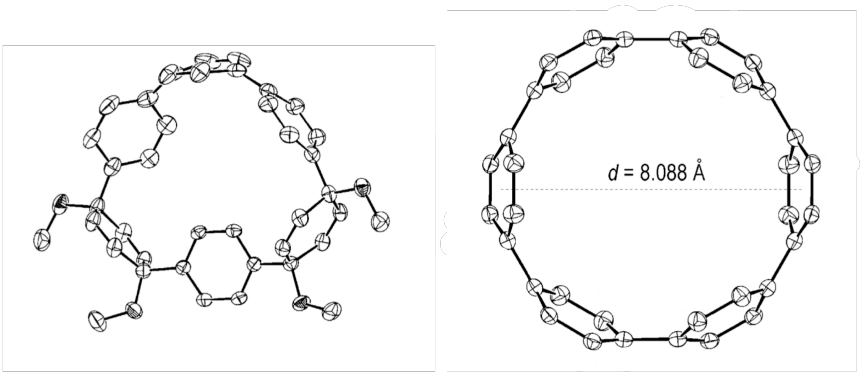

Figure I.12. Crystal structure of highly-strained **71** (left) and [6]CPP (right).[27o]

Once again, single-electron reduction was employed to aromatize the cyclohexadiene moieties in this macrocycle and [6]CPP was obtained. This is notable because it was the smallest and most synthetically challenging CPP synthesized prior to the synthesis of [5]CPP (see Chapter II), with a diameter of only 8.1 Å and 97 kcal/mol of strain energy. The optical properties followed the expected trends with no detectable fluorescence, an artifact of the unusual photophysical pathways in smaller CPPs. Most interestingly, single crystal X-ray analysis revealed that, unlike any published, larger CPP structure, [6]CPP organizes very well in the crystalline lattice into tubular nanotube-like rods (Figure **I.13**).[27o]

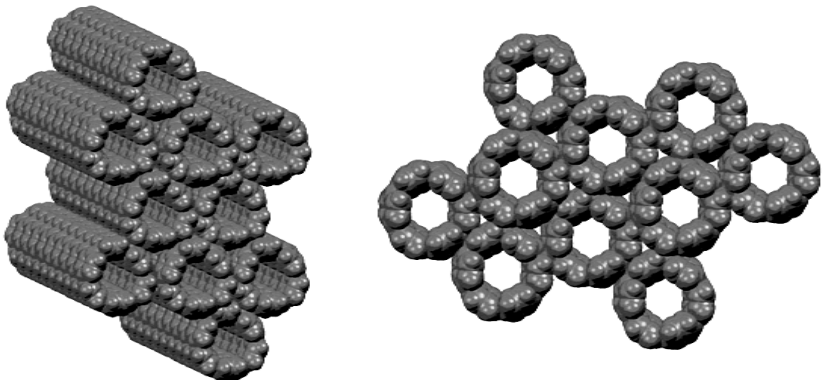

Figure I.13. Crystal packing of [6]CPP showing tubular arrangement.[27o]

This has obvious implications in the synthesis of extended nanotube structures.

More recently, Itami reported the selective syntheses of [9]-, [10]-, [11]-, and [13]CPP using modifications of previously reported methods.[27k] This is notable in that it contains the first example of intramolecular macrocyclizations to offer [9]-, [11]- and [13]CPP precursors (Scheme **I.23**).

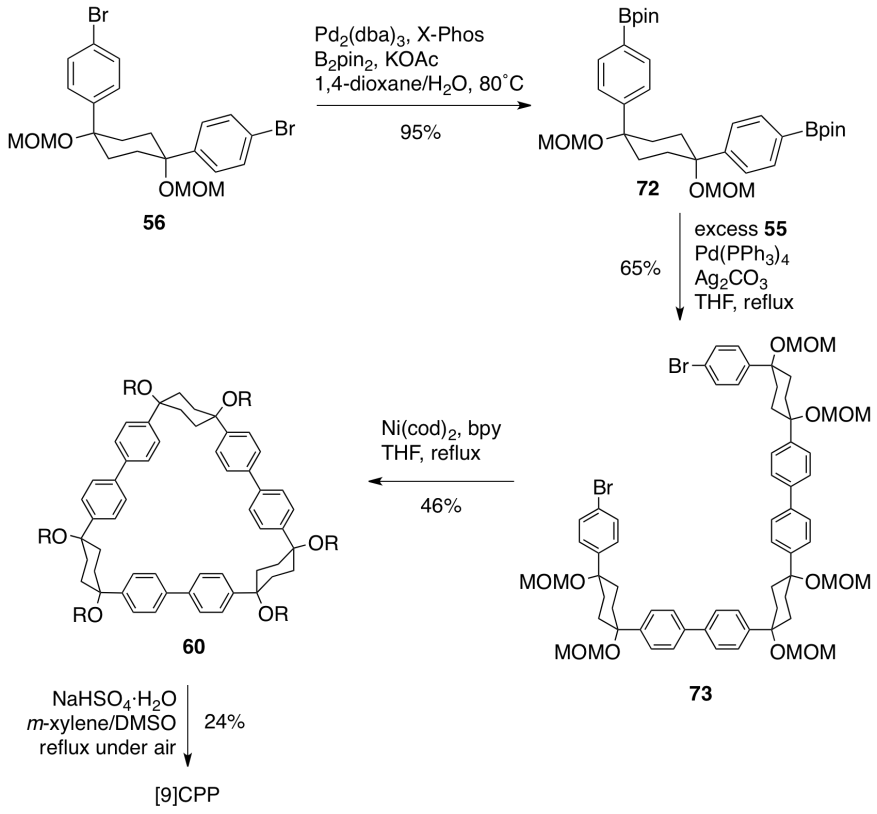

Scheme I.23. Representative intramolecular macrocyclization route to [9]CPP.[27k]

These strategies yield approximately 5 mg of the desired hydrocarbons in good to moderate yields.[27k]

I.4.5. Host-Guest Behavior of C_{60}@[10]CPP, a Fullerene Peapod

The first example of a host-guest complex with cycloparaphenylene was assembled by Yamago and coworkers.[27c] In this work, solid fullerene C_{60} was ingeniously added to an NMR sample of the product mixture from the "shotgun"

synthesis of [8-13]CPP in $CDCl_3$. The monitored proton spectrum showed the downfield shift of only the signal corresponding to [10]CPP (Figure **I.14**).

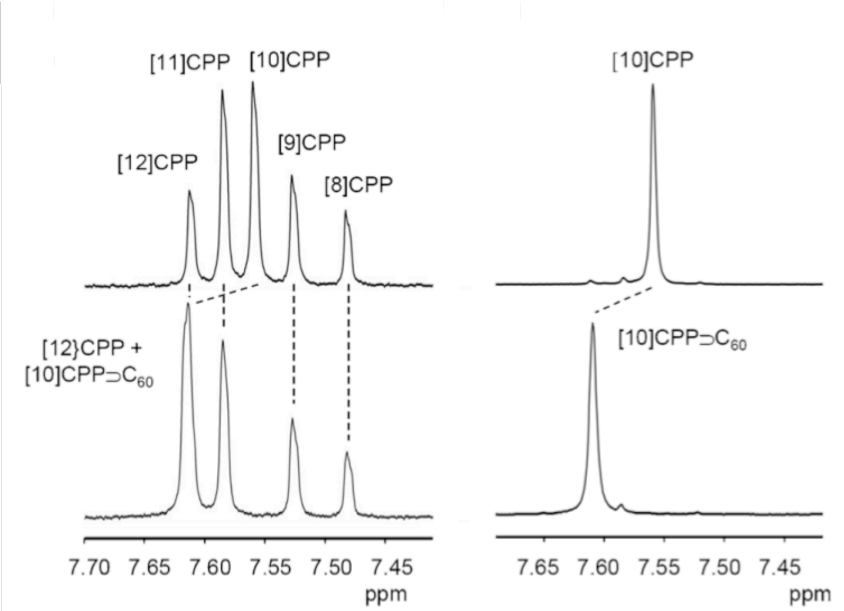

Figure I.14. Formation of C_{60}@[10]CPP observed by ^{1}H NMR. Reproduced with permission.[27c]

Yamago concluded that this shift indicated the size-selective encapsulation of the fullerene guest by [10]CPP. Similar NMR trends were seen in the CPPA·C_{60} experiments.[15, 18a] Yamago was able to confirm by optical data a 1:1 complex of [10]CPP with C_{60} with a dissociation energy of 14.1 kcal/mol, identical to Kawase's π-extended CPPA **18** with C_{60}. Moreover, computational analysis showed that the CPP-fullerene intermolecular distance was 3.35Å, which corresponds with the interlayer distance in graphene and multi-walled carbon nanotubes, as well as CNT-fullerene peapods and C_{60}@CPPA. Unlike CNTs, the discrete synthesis of single sizes of CPP made possible the application of their inward-facing π-system to offer a single length of fullerene peapod in high purity. An extension of this idea designed for photochemical control of binding affinity is presented in Chapter **IV**.

I.4.6. Functionalized Cycloparaphenylenes

In 2011, Itami et al. expanded the field of cycloparaphenylene synthesis to include a new class of macrocycle.[27f] Representing the smallest unit cycle of a [14,15] chiral carbon nanotube, naphthalene-included [13]CPPN was synthesized by modifying the selective synthesis of [12]CPP as developed by the Itami laboratory (Scheme **I.24**). It was rationalized that this new molecule racemized between the M and P isomers at room temperature via rotation of the 2,6-naphthyl moiety through the center of the CPP cavity. It is, however, possible that a smaller CPPN may have restricted isomerization, for an investigation of this see Chapter **III**. In principle, the extension of these and other arene-included CPPs could lead to a host of CNT chiralities.

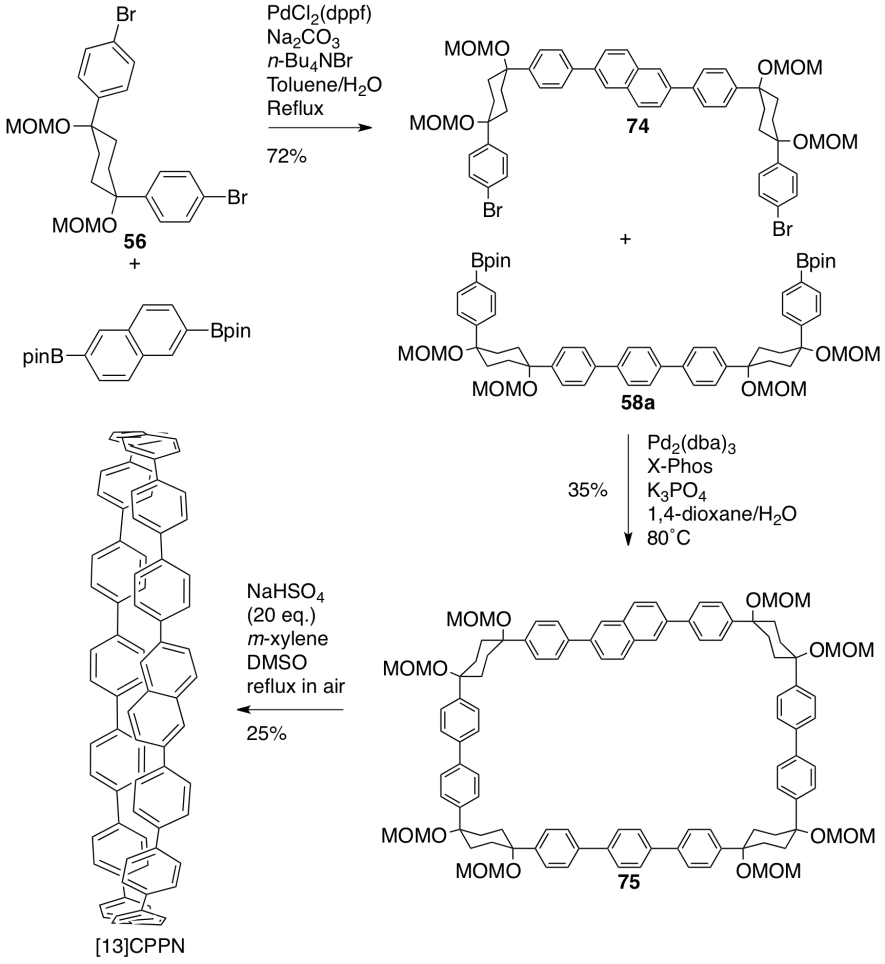

Scheme I.24. Itami's synthesis of [13]CPPN.[27f]

A much more complete model of ultrashort chiral CNTs was synthesized later that year by Isobe et al.[27e] While not, strictly speaking, a cycloparaphenylene, these cyclocrysenylenes (CC) exhibit atropisomerism, with rotation of each chrysenylene unit through the [4]CC cavity geometrically disfavored. These macrocycles were synthesized with an organometallic approach, similar to that used by Yamago (Scheme **I.25**).

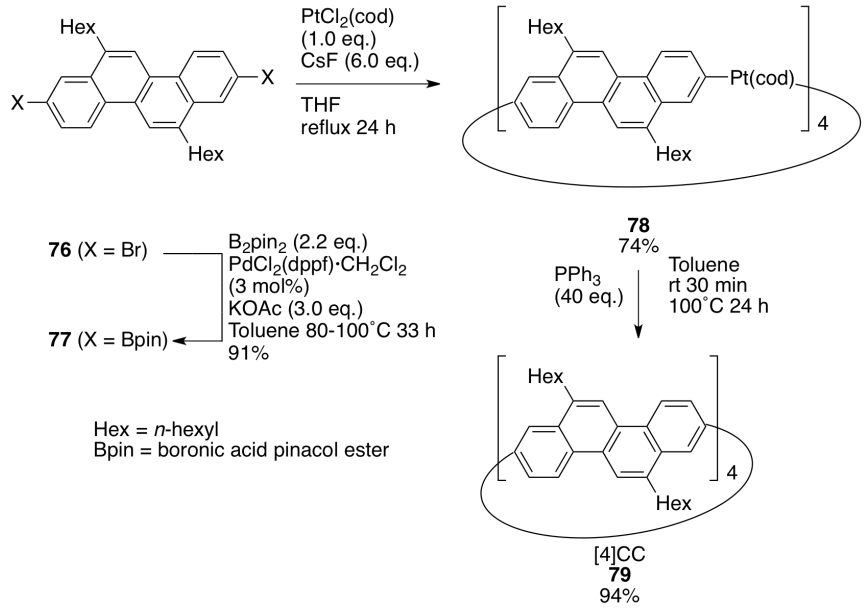

Scheme I.25. Synthesis of a chiral nanohoop with atropisomerism.[27e]

Isobe started with hexyl-functionalized dibromocrysene **76**, and accessed the metallocycle **78** via the diboronate **77** using platinum chloride and cesium fluoride. Reductive elimination with triphenylphosphine offered the hydrocarbon **79** cleanly. Given that the rotation of the aromatic domains of this macrocycle through the cavity is highly disfavored at room temperature (even in the absence of the solubilizing hexyl chains), they represent side wall portions of (10,10), (11,9), and (12,8) carbon nanotubes depending on isomerization (Figure **I.15**).[27j]

Isobe observed that above 100˚C, a single atropisomer, isolated by HPLC, will scramble to yield all 6 isomers. Models such as [4]CC with extended π-systems bring us closer to the synthesis of an ultrashort CNT. One can envision, with an appropriate extension strategy, employing Isobe's synthesis to selectively produce armchair (10,10) and chiral (11,9) and (12,8) nanotubes from a single precursor.[27j]

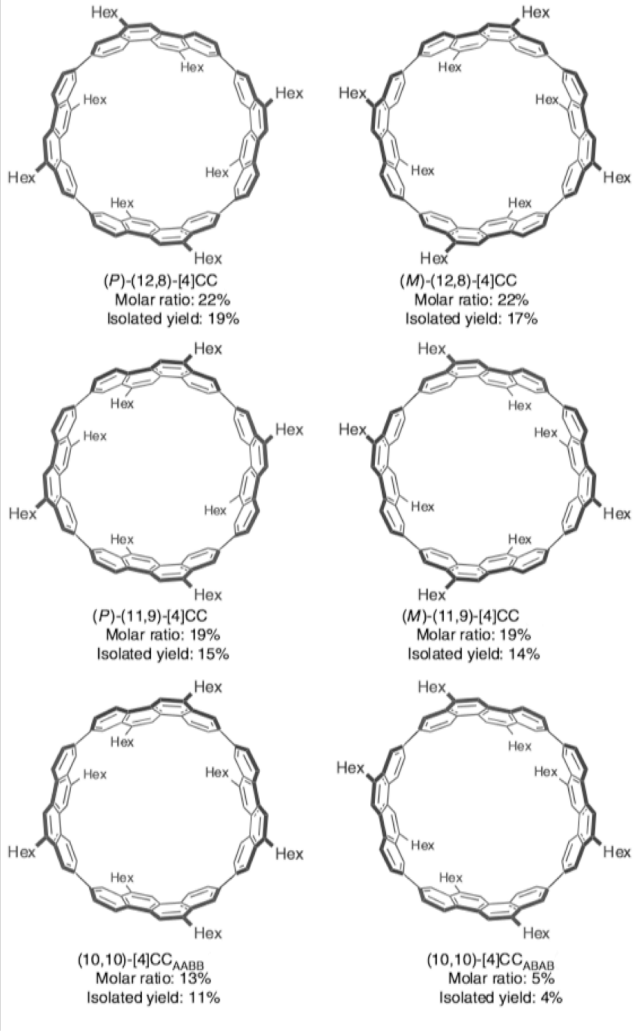

Figure I.15. Isomers of [4]CC. Reproduced with permission.[27j]

Along this route to carbon nanohoop elongation, the first π-extended cycloparaphenylene was synthesized by the Itami lab in 2012.[27m] Using the quinone addition and reductive aromatization motif developed by Jasti, dibromide **82** was synthesized by addition to naphthoquinone and macrocyclized using a nickel-catalyzed "shotgun" approach. This macrocyclization gave a poor yield (2%) of the desired 9-membered cyclic oligomer **83** which was painstakingly isolated from the reaction mixture. Single-electron reductive aromatization with granular lithium metal offered the first benzannulated CPP, [9]CN (Scheme **I.26**).

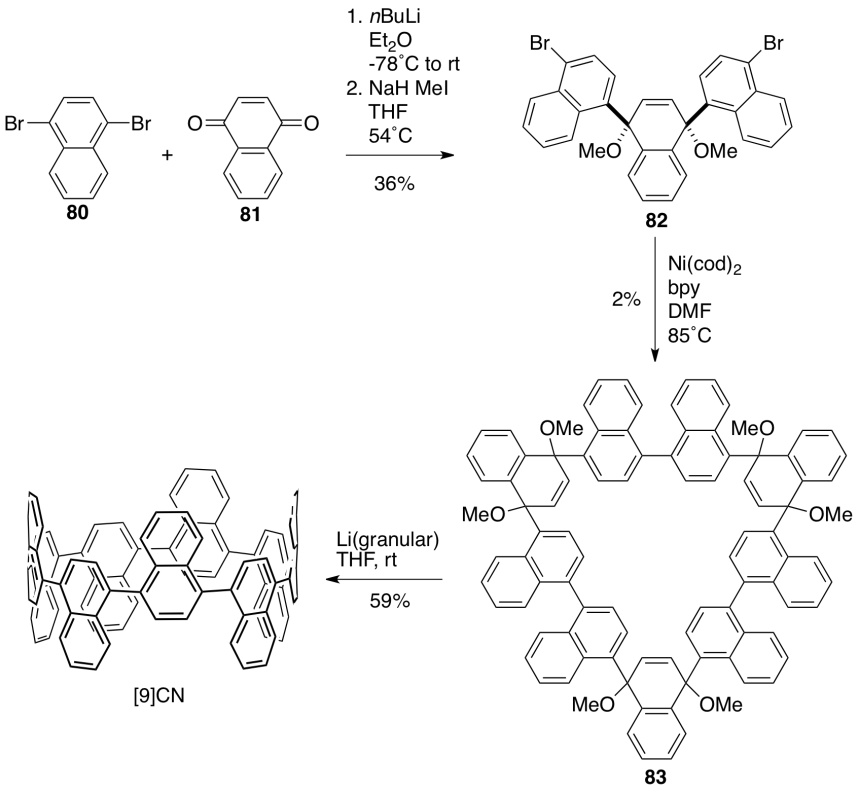

Scheme I.26. Synthesis of a benzannulated CPP, [9]CN.[27m]

Itami reported the fascinating observation that the proton NMR spectrum of this compound is highly convoluted, indicating restricted rotation of the naphthalene rings through the center of the molecule.[27m] Progress towards the closure of the fjord regions in [9]CN to offer the first example of a short CNT obtained by organic synthesis has not been reported.

Another path in which the science of cycloparaphenylenes is expanding is via the inclusion of heteroatoms into the CPP backbone. Itami reported the synthesis of [18]CPP with two 2,2'-bipyridyl units replacing 4 of the phenyl rings in the CPP structure (Scheme **I.27**).[27l] This [14,4]CPPy was synthesized using established methodology developed by the Itami group and shows a pH dependant fluorescence that can be reversibly red shifted by addition of acid. These preliminary results may open a door towards the controllable fluorescence of nitrogen-doped CPPs.

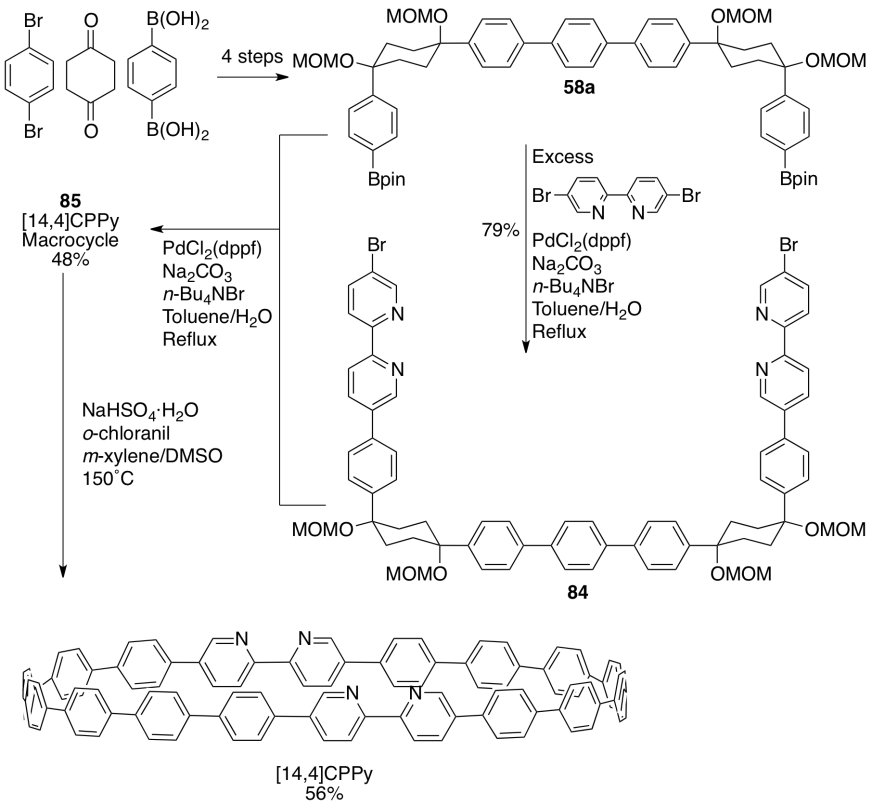

Scheme I.27. Synthesis of [14,4]CPPy.[27l]

With their fluorescent properties, high conjugation, and host capability, these nitrogen substituted CPPs are attractive materials for use as ligands and in metal-organic structures. Indeed cycloparaphenylene synthesis in general is a new and wildly exciting frontier in hydrocarbon synthesis. Material science applications of carbon nanohoops is limited, at the moment, only by the availability of large quantities of these unique molecules.

We have so far focused on single-stranded molecular belts which all display some degree of structural rotation. It is easy to envision molecular belts with two or more strands and a rotationally constrained ladder-type backbone. Discussion of these two-stranded molecular belts follows.

I.5. "Top-Down" Synthesis of [10]Cyclophenacene

One approach to the synthesis of double-stranded aromatic belts is the degradation of higher-order carbon materials with atomistic accuracy. There is only one

example of this type in the literature. Nakamura and coworkers developed controllable fullerene chemistry and were able to successfully synthesize a [10]cyclophenacene derivative by the careful selective substitution of the north and south poles of C_{60} fullerene (Scheme **I.28**).[34]

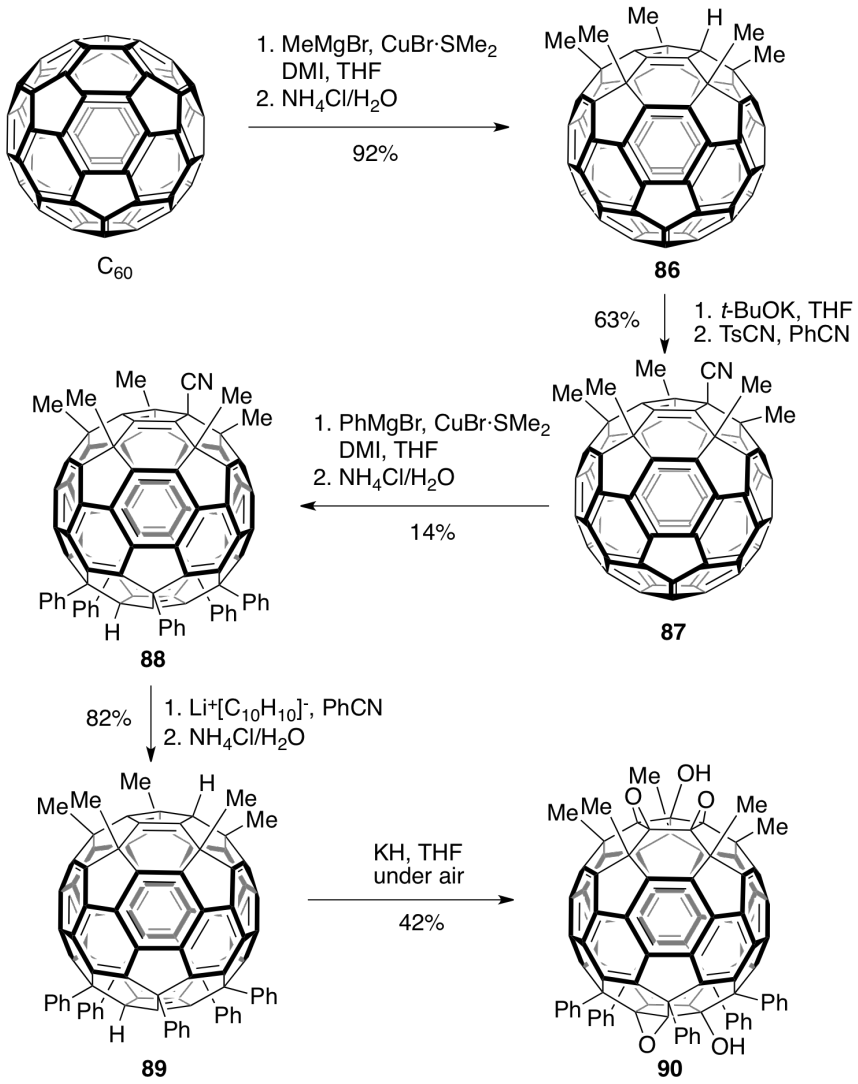

Scheme I.28. Synthesis of substituted [10]cyclophenacene by modification of C_{60} Fullerene.[34c, 34d]

The north pole of the fullerene was methylated by reaction with methyl cuprate. This methylated fullerene, **86**, was then converted to cyano-fullerene **87** to prevent formation of the cyclopentadienyl anion by deprotonation in subsequent steps. Derivative **87** was treated with a phenyl cuprate to yield phenyl-substituted **88** with an electronically

isolated [10]cyclophenacene. Removal of the cyano group and oxidation gave the penta-oxygenated derivative **90**, which could be easily crystallized for X-ray diffraction studies. Nakamura found that this molecule had remarkable bond consistency. While fullerene exhibits bond length alternation, the 20 π-electrons in the *cis*-annulene equator appeared to be fully delocalized with bond lengths of 1.40 and 1.43 Å. The outer double bonds are much shorter, conforming more to a Keukulé structure than a graphitic model and may be explained by the geometric constraint of the fullerene skeleton. NCIS calculations also confirmed the aromaticity of this novel structure.[34d] For the first time, this synthesis validated the idea that discrete, double-stranded aromatic belts can be systematically constructed with organic synthesis. These modified fullerene structures were found to be fluorescent with a quantum yield of $\phi = 0.18$ and long fluorescence lifetime of $\tau = 65\text{-}75$ ns.[34b] These cores have been functionalized and applied as chromophores.[35] Nakamura's synthesis opened the way for a host of selectively-functionalized fullerenes containing both molecular belts and corrannulene derivatives,[34b, 34c] and the properties of these have been extensively studied and employed in liquid crystal and OLED applications.[34a, 36]

I.6. Cyclacenes

Just as cycloparaphenylenes and cyclophenacenes represent the unit cycles of armchair carbon nanotubes of the type (n,n), cyclacenes are the shortest possible members of the zigzag nanotube family of (n,0) (Figure **I.16**).

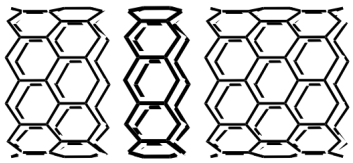

Figure I.16. Cyclacene envisioned as the unit-cycle of a zigzag nanotube (double bonds omitted for clarity).

To date there has been no synthesis of these incredibly strained, fully fused structures. There have, however, been notable attempts that provide insight to the difficult synthesis and unstable nature of these elusive hydrocarbons. Indeed, my independent research during 2009-2011 focused solely on synthetic efforts towards

[6]$_6$cyclacene. These attempts have been recorded elsewhere for posterity and will be omitted from this dissertation.

I.6.1. Towards the Synthesis of [6]$_{12}$Cyclacene

Two notable attempts at synthesizing cyclacenes have been made, the first by Stoddart towards [6]$_{12}$cyclacene in 1992 and the second by R.M. Cory towards [6]$_8$cyclacene in 1996.[37] Stoddart was able to simply build the complex macrocycle Kohnkene **93** in 17% total yield by the sequential reaction of 2 equivalents each of carefully selected but easily synthesized bisdiene **91** and dienophile **92** (Scheme **I.29**).[37a]

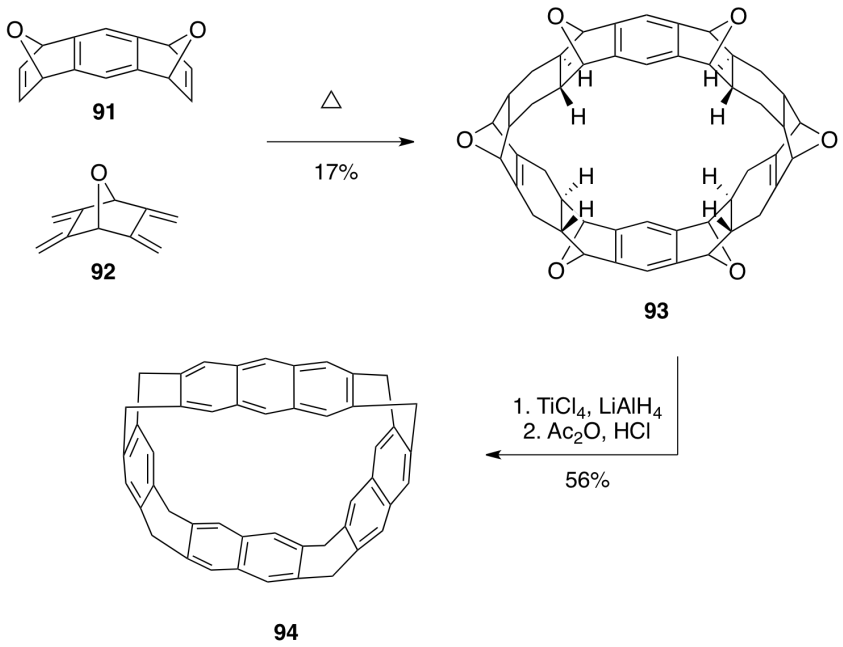

Scheme I.29. Stoddart's attempted synthesis of [6]$_{12}$cyclacene.[37a]

The electron densities favor only the Diels-Alder addition to the bottom face of the exo-diene and the top face of the bicyclic dienophile moieties, therefore yielding **93** under high temperature and pressure. Deoxygenation with low-valent titanium followed by dehydration with acetic anhydride yielded the partially-saturated cyclophane **94**. Given the propensity of linear acenes to oxidative decomposition, the late stage, harsh acidic oxidation in this synthesis likely prohibited the formation of longer acene moieties by way of spontaneous decomposition in the reaction media. Insolubility and large

energy requirements due to strain buildup may have also prevented the oxidation of eight additional carbons and conversion to $[6]_{12}$cyclacene.[37a]

I.6.2. Towards the Synthesis of $[6]_8$Cyclacene

In 1996, Cory reported attempts to access $[6]_8$cyclacene from macrocycle **97** (Scheme **I.30**). Building upon the macrocyclization work of Schlüter, this molecule was easily synthesized from the reaction of flexible bisdiene **95** with rigid and planar anthrodiquinone **96**.[38]

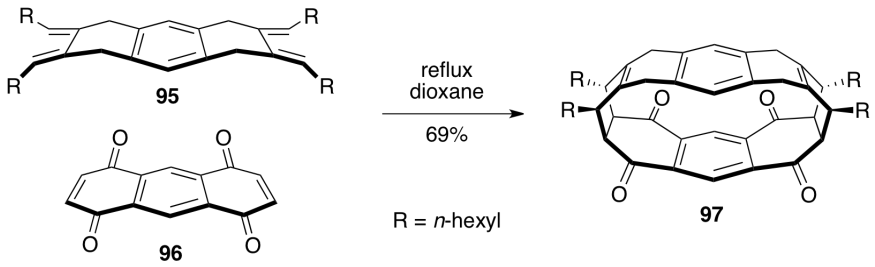

Scheme I.30. Cory's attempted synthesis of $[6]_8$cyclacene.[37b]

In this way Cory avoided issues of diastereoselectivity and was able to isolate **97** in 69% yield. Alkyl chains were used to avoid the problem of solubility encountered by Stoddart.[37b] Several attempts were made to convert unstrained **97** into $[6]_8$cyclacene including a host of oxidation and deoxygenation conditions, but formation of the cyclacene was never observed.[37b] Again, only pathways with oxidative and acidic conditions in the final steps were explored. As previously mentioned, the desired product is likely very unstable to such conditions.

Though the carbon skeleton was assembled in these two attempts, so far there is no successful synthesis of any [6]cyclacene. This enticing molecule—the shortest possible carbon nanotube, with a highly strained skeleton and double trannulene system—will surely not remain an unsolved synthetic problem indefinitely.

I.6.3. [6.8]Cyclacene

The instability of the [6]cyclacenes is due both to their highly distorted geometry and their calculated singlet-triplet gaps, which narrow with increasing size, falling to

near-degeneracy at $[6]_8$cyclacene. To circumvent these unfavorable properties, Glieter employed a moving target approach, proposing that a belt with alternating fused benzene and cyclooctatetraene rings would posses more stable electronics. The boat conformation of the cyclooctatetraene moieties should both alieviate strain and contort the π-system to increase the filled-unfilled orbital gap.[39]

This stability was confirmed by the synthesis of $[6.8]_3$cyclacene via a Wittig macrocyclization and McMurry coupling sequence (Scheme **I.31**).

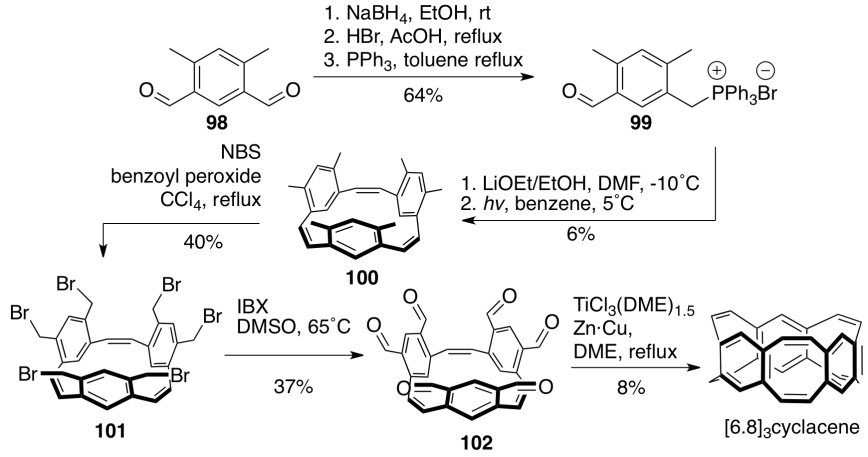

Scheme I.31. Glieter's synthesis of $[6.8]_3$cyclacene.[39]

Dialdehyde **98** was converted to the corresponding phosphine salt **99** and dilute macrocyclization followed by irradiation of the resulting *E/Z* isomer mixture coalesced into the all-*Z* **101**. Following bromination and oxidation, McMurry conditions closed down the remaining 8-membered rings to offer $[6.8]_3$cyclacene with the majority of hexaaldehyde **102** presumably oligomerizing in the reaction mixture.[39]

This cyclacene was found to have D_{3h} symmetry with boat-like cyclooctatetraenes and almost planar benzene rings (Figure **I.17**).[39]

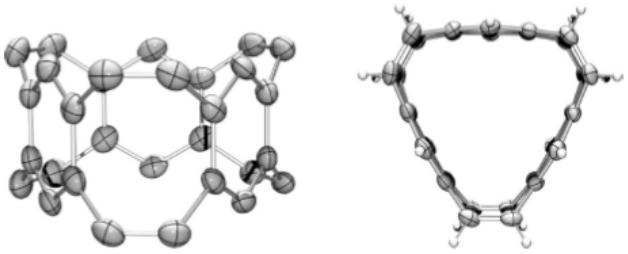

Figure I.17. Crystal structure of $[6.8]_3$cyclacene showing boat-like cyclooctatetraene moieties. Reproduced with permission.[39]

It was estimated that this bending disrupts the conjugation around the cyclacene, diminishing it to about 31%.[39] Even though this structure is electronically distinct from the highly-conjugated [6]cyclacenes, it possesses inward-facing π-orbitals and represents an important step forward in the synthesis of hydrocarbon belts as models for short carbon nanotubes.

I.6.4. Buckybelts

Over the years, the Schlüter lab has synthesized several saturated belts, including the $[6]_{18}$cyclacene framework.[40] When it became clear that [6]cyclacenes were too reactive to isolate, Schlüter proposed and found evidence for the formation of buckybelt **110** having the structure of the equator region of fullerene C_{84} (Scheme **I.32**).[41]

Reaction of hydrocarbon dienophile **103** with diene synthon **104** gave a greater than 90% yield of *endo* and *exo* adducts which were separated by benchtop chromatography. Generation of benzyne followed by trapping with furan and reaction with tetracyclone offered *syn* and *anti* products **106** and **107** from both *endo* and *exo* **105** respectively in 30% yield over 3 steps. Heating of both pure *exo* and pure *endo* **106** and **107** separately both led cleanly to the belt **108** having the framework of the target aromatic hydrocarbon. Treatment with *para*-toluenesulfonic acid installed 4 alkenes to offer **109**. Subsequent conversion of **109** to the desired belt, however, was not observed under acidic conditions, and is yet to be realized.[41a, 41c] In 2008, it was shown that upon fragmentation of tetraacetate derivative **111** in a mass spectrometer, the parent ion for **110**, m/z = 932 can be observed, confirming the production, if transient, of the desired buckybelt (Scheme **I.33**).

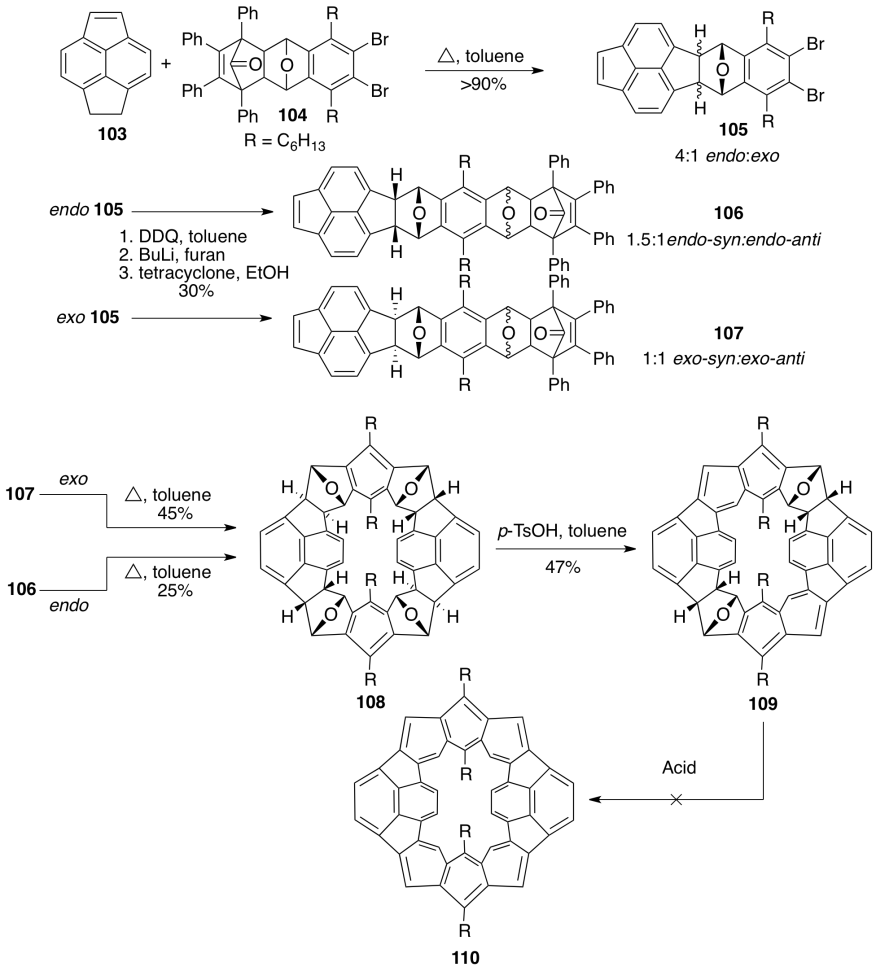

Scheme I.32. Schlüter's synthesis of a buckybelt precursor.[41a]

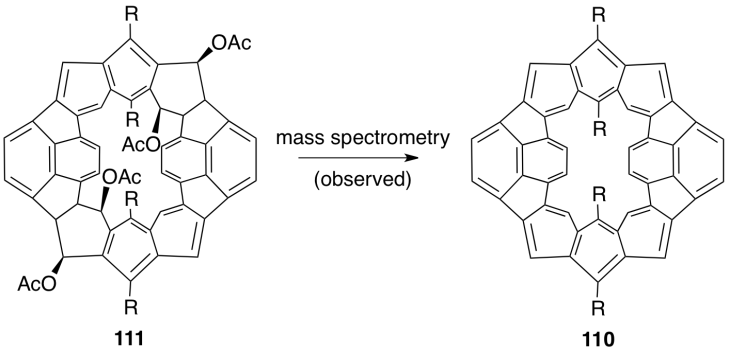

Scheme I.33. Observation of a buckybelt under mass spectrometric conditions.[41c]

As such, the synthesis of a fully aromatic, two-stranded hydrocarbon belt remains a fascinating challenge in the realm of synthetic organic chemistry.

I.7. Bridge to Chapter II

This chapter outlines a history of curved aromatic belts and includes the state of the art of cycloparaphenylene synthesis when I started the synthesis of [5]cycloparaphenylene. The remainder of this dissertation contains my efforts to explore the limits of cycloparaphenylene synthesis with a particular emphasis on new geometries. Chapter **II** details the synthesis [5]cycloparaphenylene, the smallest at the time of its publication, its characterization and observed properties.

CHAPTER II
[5]CYCLOPARAPHENYLENE

This chapter is based on work published in *Nature Chemistry* in February 2014. I conceived the original project and developed the synthesis with the help of Evan Darzi whose discovery of the intramolecular homocoupling made this route very high yielding. I prepared the main text and edited the experimental, which was originally prepared by Darzi, for inclusion into this dissertation. Prof. Ramesh Jasti edited this chapter and the original manuscript.

Warped, carbon-rich molecules have captured the imagination of scientists across many disciplines. Owing to their promising material properties and challenging synthesis, strained hydrocarbons are attractive targets that push the limits of synthetic methods and molecular design. Herein we report the synthesis and characterization of [5]cycloparaphenylene **([5]CPP**), a carbon nanohoop which can be envisioned as an open tubular fragment of C_{60}, the equator of C_{70} fullerene, and the unit-cycle of a [5,5] armchair carbon nanotube. Given its calculated 119 kcal/mol of strain energy and severely distorted benzene rings, this synthesis employing a room-temperature macrocyclization of a diboronate precursor, single-electron reduction, and elimination, is remarkably mild and high yielding (27% over 3 steps). Single crystal X-ray diffraction data was obtained to confirm its geometry and previously disputed benzenoid character. First and second pseudoreversible oxidation and reduction events were observed via cyclic voltammetry. The facile synthesis, high solubility, and narrowest optical HOMO/LUMO gap of any *para*-polyphenylene synthesized make **[5]CPP** a desirable new material for organic electronics and a significant advance in the synthesis of highly distorted aromatic molecules.

II.1. Background

Highly strained hydrocarbons have captivated synthetic and physical organic chemists for decades due to their challenging structures and unique properties. These alarming and contorted structures have bond geometries that depart from the ideal and

aromatic rings that twist out of the π plane. Just as complex natural products inform the field of the limits of synthetic technologies, imaginative geometries like cubane or paracyclophanes act as tools to push what is believed to be synthetically achievable. In many cases these limits are surpassed and synthetic breakthroughs are made in the pursuit of new high-energy geometries. Once synthesized, these new hydrocarbons are often found to have useful properties distinct from those of their unstrained analogues. The high energy present in distressed, kinetically metastable carbon frameworks requires ingenuity to overcome, frequently relying on high temperatures (cubane[1], corannulene[2]), photochemistry (quadricyclane[3], picotube[4]), or flash vacuum pyrolysis ([6]paracyclophane[5], C_{60} fullerene[6]). Of particular interest is the extreme bending of aromatic systems and reaching the geometric limit of aromaticity.[7] Cycloparaphenylenes (CPPs), hydrocarbon macrocycles consisting of distorted benzene rings linked at the *para* positions, once only the stuff of theory[8], have recently entered the realm of synthetic accessability.[9] The field of carbon nanohoops, so called because they are the smallest unit-cycles of armchair carbon nanotubes, has expanded rapidly due to their porous character[10], electronics[11], host-guest capabilities[12], synthetic challenge[13], and usefulness as carbon nanotube precursors.[14] First synthesized in 2008, carbon nanohoops have now been accessed in a variety of sizes (n = 6-16, 18)[9a-c, 10, 12b, 15] and with several functionalities incorporated.[16] The strain inherent in these distressed hydrocarbons makes synthesis, especially of the smaller [n]CPPs, very challenging. In addition to synthetic conquest, smaller and smaller CPPs are desired for their solubility and unique electronics. We observe a dramatic increase in strain, reduction of ring-to-ring dihedral angles, and narrowing of the highest occupied molecular orbital/lowest unoccupied molecular orbital (HOMO/LUMO) gap in CPPs smaller than [10]CPP (Figure **II.1**), in contrast to the widening gap in oligoparaphenylenes.[15b, 17]

Having successfully synthesized [7]CPP, an orange emitting fluorophore, and [6]CPP, which packs into tubes in the solid state, we set our sights on **[5]CPP**. This new synthetic target has 119 kcal/mol of strain energy, over 20 kcal/mol higher than [6]CPP (97 kcal/mol, all density functional theory (DFT) calculations performed with GAUSSIAN09 at the B3LYP 6-31G* level of theory. All strain energies calculated using homodesmotic reactions. See section **II.6.5** for details).[10, 15c, 18] **[5]CPP** also represents an

open tubular fragment of buckminsterfullerene, similar fragments have heretofore been synthesized by "top-down" methods, by chemically modifying fullerenes to create substituted belts, but to our knowledge, none have been synthesized from the bottom up without substitution.[19]

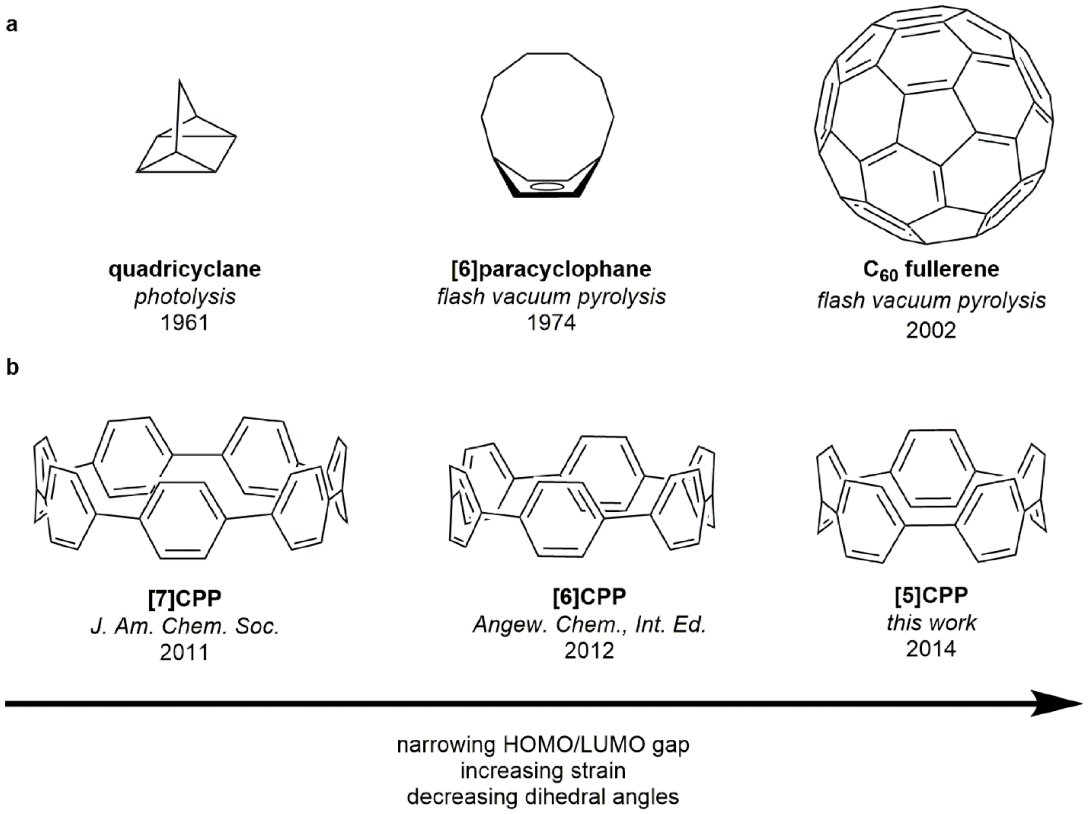

Figure II.1. Prototypical distressed hydrocarbons that have succumbed to rational organic synthesis. **a**, Classic examples of strained hydrocarbons highlighting the key techniques used to overcome the kinetic barrier during synthesis. **b**, The recently conquered small cycloparaphenylenes and trends in physical properties thereof.

II.2. Synthesis

In repeating our synthesis of [10]CPP using bisboronate **1** (Scheme **II.1**), available on the multi-gram scale,[12b] we consistently observed the formation of small amounts of a curious new compound in our macrocyclization reactions. This material appeared to have similar NMR resonances to the 1,4-dimethoxycyclohexa-2,5-diene-containing macrocyclic precursors to cycloparaphenylenes, but with an anomalous singlet in the ^{1}H NMR spectrum at δ = 6.00 ppm, further upfield than the most shielded phenyl

protons in the [6]CPP macrocycle (δ = 6.78 ppm). Mass spectrometric and unrefined single crystal X-ray diffraction data of this mysterious byproduct confirmed, to our surprise and delight, that it was not a larger macrocycle or linear oligomer, but **2**, the result of intramolecular boronate homocoupling. This structural data allowed us to assign the singlet at δ = 6.00 ppm as the four phenyl protons on the ring between two cyclohexadiene moieties. As indicated by its multiplicity, this ring spins through the center of the macrocycle bringing the protons within approximately 2.8 Å of the adjacent alkenes and the center of the nearest biphenyl ring, based on our computational investigations. The shielding cones cast by these π-systems account for the dramatic upfield shift of this phenyl signal.[20] The formation of **2** is encouraged by the rigid, curved geometry of **1** in solution. With restricted rotation allowing the boron atoms to swing into proximity, intramolecular macrocyclization at high dilution becomes competitive with intermolecular processes.

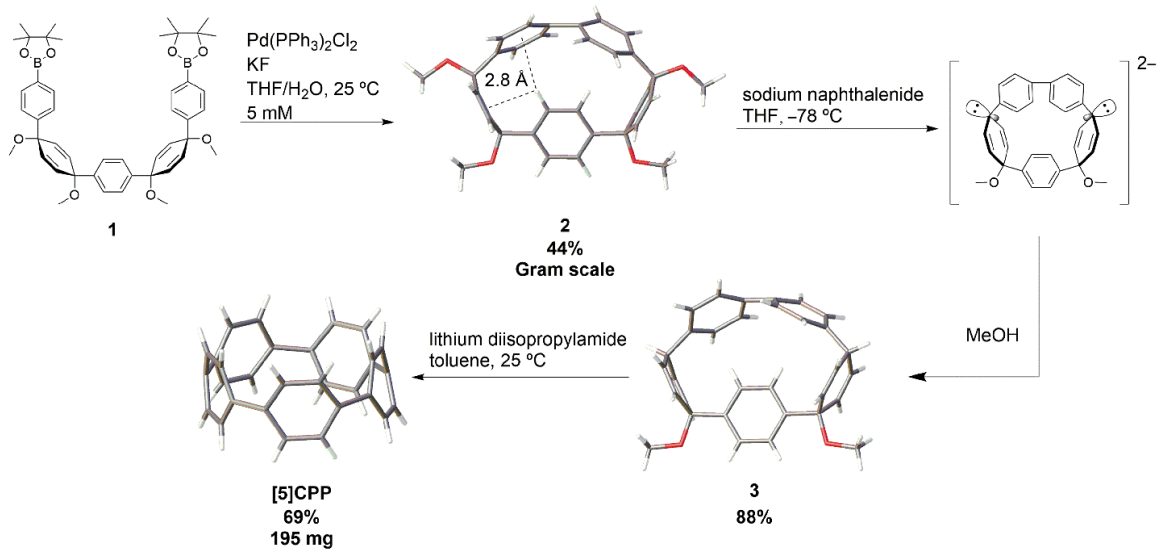

Scheme II.1. A rapid synthetic route to [5]cycloparaphenylene. Our synthesis proceeds from previously-reported diboronate **1**, which is macrocyclized to **2** (Shown here as a DFT structure with relevant π interactions highlighted) via an intramolecular boronate homocoupling open to air. Upon treatment with sodium naphthalenide, **2** forms a dianion which does not convert to **[5]CPP** at –78˚C but can be protonated by adding methanol to yield reduced macrocycle **3** (shown as a refined crystal structure, confirming the regioselectivity of reduction). Reaction with lithium diisopropylamide at room temperature effects a twofold E1cB elimination offering 195 mg (69%) of **[5]CPP**, shown as a refined crystal structure.

With this observation in mind, optimal conditions for the synthesis of **2** were developed. Using a palladium-catalyzed boronate homocoupling performed under air at room temperature,[21] macrocycle **2**, with a strain energy of 32 kcal/mol, was easily prepared. This pivotal discovery allowed for the synthesis of **2** on the gram scale at room temperature in one flask and facilitated quick determination of a synthetic route to **[5]CPP** (*vide infra*).

Reduction of **2** with 5 equivalents of sodium naphthalenide at −78 ˚C in tetrahydrofuran surprisingly did not offer the parent cycloparaphenylene, as is observed with [6]-[12] and [18]CPP.[9c, 10, 12b, 15a] Instead, the reduction stalls at a stable dianion, which is a deep royal blue in solution. We presume that this is due to unavailable energy at low temperatures to build in the 87 kcal/mol of additional strain necessary for the conversion of **2** to **[5]CPP** via elimination. Previously the most strain overcome by these conditions is 60 kcal/mol for [6]CPP and 67 kcal/mol for [7]CPP.[10, 15c] Allowing this reduction to warm past −70 ˚C results in a color change to dark brown, and precipitation of insoluble material indicating rapid decomposition. Based on solubility and MALDI-MS data the decomposed mixture appears qualitatively to contain oligophenylenes. Sodium naphthalenide reduction at a range of temperatures from −78 ˚C to room temperature does not yield more than trace (less than 1%) amounts of the desired cycloparaphenylene. However, quenching the dianion with methanol at −78 ˚C and subsequent removal of naphthalene afforded reduced macrocycle **3** in 88% yield on the half-gram scale. The regioselectivity of this reduction was confirmed by X-ray crystallography and no regioisomers were observed in the reaction mixture.

Since **3** has the same oxidation state as **[5]CPP**, we were able to probe the E1cB elimination of two equivalents of methanol to generate **[5]CPP** at higher temperatures using a non-nucleophilic, non-reducing base to avoid the decomposition seen with the sodium naphthalenide treatment of **2**. Subjecting **3** to 30 equivalents of lithium diisopropylamide in toluene at room temperature gratifyingly afforded 195 mg of **[5]CPP**, a 69% isolated yield, as a dark red solid with a deep ruby color in solution.

II.3. Characterization and Observed Properties

The structure of **[5]CPP** was confirmed by NMR, MALDI-TOF MS, and IR. Interestingly, **[5]CPP** is soluble in a wide range of common organic solvents including hydrocarbons, aromatic, polar aprotic, halogenated, and ethereal solvents. It should be noted that **[5]CPP**, unless stored under inert atmosphere, decomposes to an insoluble, bright yellow material after about 24 hours. It is possible that this is an oxidation or a nucleophilic decomposition as is seen for [6]paracyclophane.[22]

With **[5]CPP** in hand, the structure of this new carbon nanohoop was investigated. The ^{1}H NMR spectrum consists of one singlet, δ = 7.86 ppm and the ^{13}C NMR shows two signals at δ = 126.74 and 132.07 ppm. The observed isotropy suggests that at room temperature conformational changes such as phenyl ring rotation or oscillation make rotational isomers unobservable on the NMR timescale. The downfield shift of the proton signal in **[5]CPP** may be explained by the small phenyl-phenyl dihedral angles, calculated to average 16.4˚. The tendency of these rings to remain relatively in-plane with each other encourages conjugation throughout the whole molecule and induces a deshielding ring current from the extended π-system in addition to the ring currents around each phenyl ring. Wong's NICS calculations, which suggest that the aromaticity of individual benzene rings decreases with decreasing size in cycloparaphenylenes smaller than [8]CPP, may be taken as supporting evidence for the delocalization of the π-system throughout the molecule.[17] We first observed this phenomenon in the downfield shift of the ^{1}H NMR signal for [6]CPP (δ = 7.64) relative to other cycloparaphenylenes. Simple bending of a benzene ring alone does not account for such a dramatic downfield shift.[23]

The refined crystal structure of **[5]CPP** was obtained from single crystals of **[5]CPP** that were grown from the slow evaporation of a dichloromethane and hexane solution at 0˚C in the dark (Figure **II.2**). Though different levels of theory have estimated **[5]CPP** to be quinoidal or benzenoid[17, 24], we now confirm its benzenoid structure by noting the elongated phenyl-phenyl bond lengths (1.49 Å, A-A bond, Fig. **II.3**) and the shorter and nearly equivalent phenyl bonds (1.40 Å for the A-B bond and 1.38 Å for the B-B bond, Figure **II.2**). The average phenyl-phenyl dihedral angle for [5]CPP is 12.4˚, lower than the calculated 16.4˚ and much smaller than that of [6]CPP with an average

solid state dihedral angle of 26.4˚. The most striking feature of this new structure is the nonplanar phenyl rings that adopt a shallow boat conformation in the presence of considerable ring strain. The tertiary carbons in each ring are displaced out of the benzene plane by an average 15.6˚. This severe distortion is, to our knowledge, the largest of any distressed benzene isolated, with the exception of [6]- and [7]paracyclophanes.[23, 25] This includes bent benzenes found in nature and conquered by chemists, such as those in haouamine A (13.6˚)[26] and cavicularin (7.9˚),[27] and the previously most-distorted cycloparaphenylene, [6]CPP (12.7˚). This open ended structure is also splayed into steeper boats than the **[5]CPP** homologue at the equator of C_{70} fullerene (10.7˚),[28] and almost as deformed as the homologue at the rim of Scott's [5,5] carbon nanotube endcap (16.0˚)[29]. The interior of **[5]CPP** has an average diameter of 6.69 Å, measured by doubling the average distance from the centroid of each ring to the centroid of the molecule. With a size comparable to endohedral fullerenes, it is possible that very small charged guests, such as metal ions or simple organic cations may become encapsulated in **[5]CPP**'s inward-facing π system. Intriguingly, **[5]CPP** packs in a herringbone fashion, unlike the tubular packing observed for [6]CPP. The unit cells of several visually distinct crystal morphologies have been analyzed to confirm that this result is not anomalous.

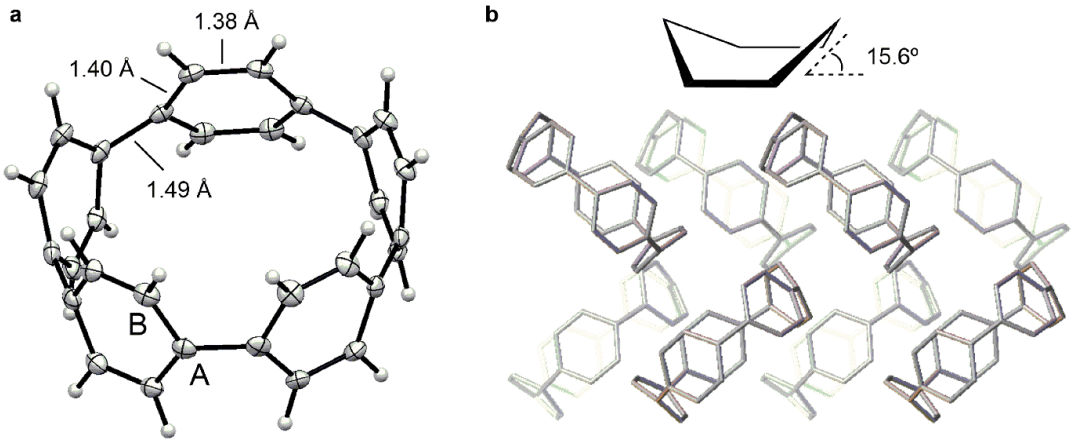

Figure II.2. Analysis of [5]CPP by X-ray diffraction crystallography. **a**, Solid state bond lengths (ORTEP ellipsoids displayed at 50% probability) confirm the benzenoid nature of the phenyl rings in **[5]CPP**, despite the extreme bending out of plane (**b**). **b**, It was determined that **[5]CPP** packs in a herringbone fashion unlike [6]CPP but similar to all other cycloparaphenylenes for which crystal data has been obtained.

[5]CPP absorbs very strongly in the UV with an extinction coefficient of 5.7×10^4 $M^{-1}cm^{-1}$ at the maximum, 335 nm (Figure **II.3**). This same absorbance is observed in all CPPs and corresponds to a combination of HOMO−2 and HOMO−1 → LUMO and HOMO → LUMO+1 and LUMO+2 transitions.[10, 15b] Additionally, apparent by its deep red color, **[5]CPP** displays a very broad second absorbance band centered around 502 nm with a maximum extinction coefficient of 4.5×10^2 $M^{-1}cm^{-1}$. This arises from a HOMO-LUMO transition which, forbidden in larger CPPs, starts to manifest in the smaller CPPs. Like [6]CPP, there is no observable fluorescence in **[5]CPP** due to the weak oscillator strength of the HOMO-LUMO transition.[30]

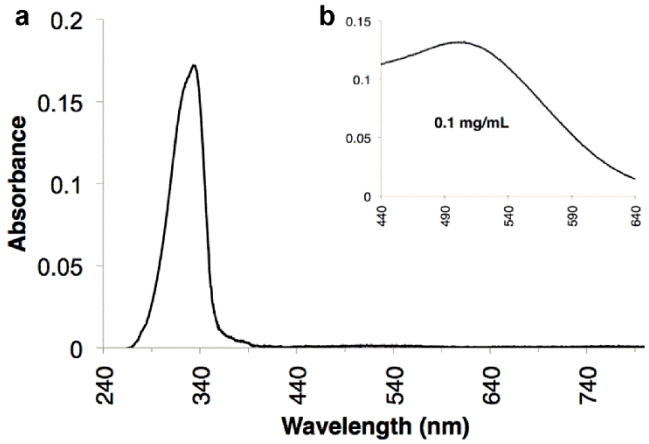

Figure II.3. UV-Vis absorbance data for [5]CPP. **a**, **[5]CPP** exhibits a major UV absorbance similar to other cycloparaphenylenes (1 μg/mL, λ_{max} = 335 nm). **b**, As apparent by its red color, a minor green absorbance from a HOMO-LUMO transition is also present (0.1 mg/mL, λ_{max} = 502 nm).

The oxidation and reduction potentials of **[5]CPP**, were obtained by cyclic voltammetry, 1 mM in tetrahydrofuran solution with 0.1 M nBu_4NPF_6 (Figure **II.4**). Interestingly, we observed two oxidation events with peak potentials of 0.25 and 0.46 V vs Fc/Fc^+ and two reductions with peak potentials of −2.27 and −2.55 V vs Fc/Fc^+. All four events appear to be pseudoreversible one-electron processes. **[5]CPP** has the lowest oxidation and least-negative reduction potential of any *para*-polyphenylene.[15b] The narrow electrochemical gap, combined with crystalline organization in the solid state make **[5]CPP** an excellent candidate as a new organic semiconductor.

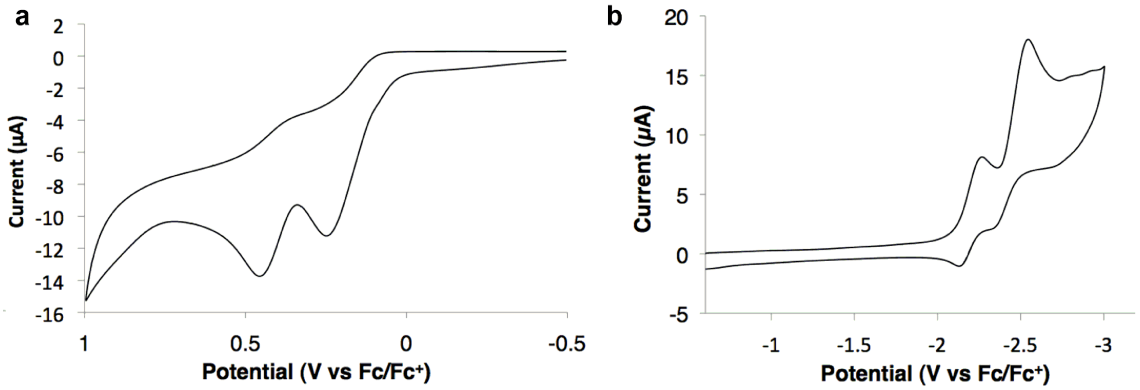

Figure II.4. Cyclic voltammetry of [5]CPP in tetrahydrofuran. Two oxidation events (**a**) and two reduction events (**b**) were observed for **[5]CPP**. All of these appeared to be pseudoreversible. **[5]CPP** has a lower oxidation potential and less negative reduction potential than any cycloparaphenylene for which CV data is available.

II.4. Conclusion

In conclusion we report the synthesis of **[5]CPP**, the smallest carbon nanohoop. Our mild and high-yielding synthesis builds in a remarkable 119 kcal/mol of strain energy in solution without heating. This work illustrates the success of rational chemical design applied to challenging carbon architectures and has offered a room-temperature synthesis of a nonplanar aromatic hydrocarbon in the same class as corannulene,[2] C_{60} fullerene,[6] or grossly warped nanographene.[31] Studies of the inclusion of **[5]CPP** in devices and host-guest complexes represent exiting next steps.

II.5. Bridge to Chapter III

The synthesis of [5]CPP established new and efficient methodology for the construction of small CPPs. Applying this to new nanohoop geometries, I focused next on the construction of a small CPP with inherent chirality: the unit-cycle of a chiral nanotube. Having established the intramolecular boronate homocoupling as a platform for macrocyclization, I attempted to apply this to the synthesis of 2,6-naphthyl-[6]cycloparaphenylene as detailed in Chapter II. This work is ongoing.

II.6. Experimental

II.6.1. General Experiment Details

Moisture and oxygen sensitive reactions were carried out under nitrogen atmosphere using standard syringe/septa technique. All the glassware was thoroughly washed, oven dried at 140°C overnight and cooled under nitrogen atmosphere before use. All reagents were obtained commercially. Tetrahydrofuran (THF) and dichloromethane (DCM) were dried by filtration through alumina according to the method descried by Grubbs.[32] Silica column chromatography was conducted with Zeochem Zeoprep n60 Eco 40-63 μm silica gel. Thin layer chromatography (TLC) was performed using Sorbent Technologies Silica Gel XHT TLC plates. Developed plates were visualized using UV light at wavelength of 254 and 365 nm. IR spectra were recorded on a Thermo Nicolet 6700. ^{1}H NMR spectra and ^{13}C NMR spectra were recorded respectively at 400 MHz and 125 MHz (or 100 MHz for compound **2**) on a Varian VNMRS. Deuterated chloroform ($CDCl_3$) was used as NMR solvent for all the compounds and all spectra were referenced to tetramethylsilane (TMS). The matrix used for MALDI-TOF was a solution of 7,7,8,8-tetracyanquinodimethane (TCNQ) in THF with 1% silver trifluoroacetate as a promoter.

II.6.2. Experimental Details

(31S,34s,51S,54s)-31,34,51,54-tetramethoxy-1,2,4(1,4)-tribenzena-3,5(1,4)-dicyclohexanacyclopentaphane-32,35,52,55-tetraene **2**

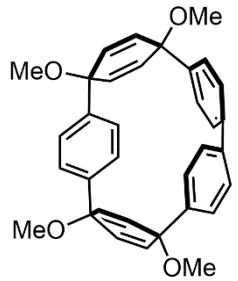

To a 2-L flask equipped with a magnetic stir bar was added diboronic bispinacol ester **1** (3.74 g, 4.90 mmol, 1.00 equiv) and tetrahydrofuran (1030 mL). The resulting solution was stirred until all the solid was in solution at which point

bis(triphylphosphine)palladium(II) dichloride (0.346 g, 0.490 mmol, 0.100 equiv) was added followed by H_2O (200 mL). To this yellow solution was added potassium fluoride (0.289 g, 4.90 mmol, 1 equiv). The solution gradually turned bright orange over two hours and was allowed to stir open to air and at room temperature for an additional ten hours at which point palladium black had coated the inside of the flask. The crude reaction mixture was filtered through a pad of Celite to remove palladium. This filter cake was washed with dichloromethane (100 mL). The solution was extracted with dichloromethane (2 × 300 mL) and the resulting organic phase was washed with brine (500 mL). The organic phase was then dried over sodium sulfate and solvent was removed at reduced pressure to give a yellow semisolid. This yellow semisolid was then washed with acetone (100 mL) to dissolve impurities while leaving the product as a white solid which was collected by vacuum filtration. This white solid (1.40 g, 52%) can be further purified on SiO_2 if necessary. The white solid was dissolved in minimal dichloromethane and loaded onto a short pad of silica. The product was eluted in 15% ethyl acetate in dichloromethane to give a pristine crystalline white solid (1.10 g, 44%). m.p: 311-312 °C. ^{1}H NMR (400 MHz, $CDCl_3$): δ(ppm) 7.46 (d, J = 9.4 Hz, 4H), 7.43 (d, J = 9.4 Hz, 4H), 6.58 (d, J = 10.2 Hz, 2H), 6.00 (s, 4H), 5.73 (d, J = 10.2 Hz, 2H), 3.46 (s, 6H), 3.26 (s, 6H); ^{13}C NMR (100 MHz, $CDCl_3$): δ(ppm) 141.67, 141.29, 140.02, 133.91, 133.73, 128.90, 127.47, 125.09, 74.96, 73.68, 52.65, 51.27; IR (neat): 3026, 2979, 2936, 2899, 2820, 1594, 1497, 1487, 1464, 1449, 1398, 1306, 1275, 1262, 1221, 1186, 1170, 1075, 1017, 988, 955, 942887, 862, 845, 823, 758, 702, 670, 617, 577, 557, 514, 467 cm^{-1}; HRMS (Q-TOF, ES+) *(m/z)*: $[M+Na]^+$ calcd. for $C_{34}H_{32}O_4$, 527.2198; found, 527.2205.

(31R,34r,51R,54r)-34,54-dimethoxy-1,2,4(1,4)-tribenzena-3,5(1,4)-dicyclohexanacyclopentaphane-32,35,52,55-tetraene **3**

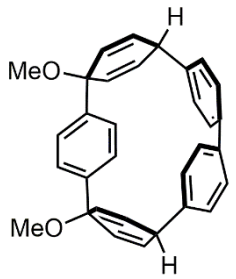

Macrocycle **2** (200 mg, 0.400 mmol, 1.00 equiv) was dissolved in dry THF (150 mL) and cooled to -78°C under N_2. 1 M sodium naphthalenide (2.00 mL, 2.00 mmol, 50.0 equiv) was added dropwise to the stirring solution to give a deep blue color. This was allowed to stir for 40 minutes at which point 1 mL of methanol was added dropwise to give a clear yellow solution. The reaction was allowed to warm to room temperature at which point water (100 mL) and DCM (100 mL) were added. The aqueous layer was then extracted with DCM (2 × 100 mL). The combined organic layers were washed with water (3 × 100 mL), brine (1 × 100 mL) and dried over sodium sulfate before being filtered and concentrated down to a solid. The crude solid was adsorbed onto silica gel and was washed with hexane (3 × 100 mL) to remove excess naphthalene. The product was eluted with a 1:1 mixture of ethyl acetate and DCM (200 mL). The solvent was then removed under vacuum to give the product as a white solid (160 mg, 91%). m.p: decomp >350°C. ^{1}H NMR (400 MHz, $CDCl_3$): δ(ppm) 7.42 (d, J = 8.6 Hz, 4H), 7.28 (d, J = 8.6 Hz, 4H), (dd, J = 10.4, 4.9 Hz, 4H), 6.05 (s, 4H), 5.63 (d, J = 10.4 Hz, 4H), 4.27 (t, *J*= 4.9 Hz, 2H), 3.21 (s, 6H); ^{13}C NMR (125 MHz, $CDCl_3$): δ(ppm) 143.04, 142.01, 138.19, 131.84, 131.60, 128.71, 127.31, 125.18, 74.85, 54.15, 36.39; IR (neat): 3052, 2990, 2930, 2898, 2873, 2820, 1722, 1703, 1665, 1592, 1512, 1487, 1467, 1454,1397, 1360, 1265, 1220, 1188, 1170, 1068, 1012, 986, 961, 920, 883, 863, 851, 834, 814, 803, 770, 734, 704, 592, 582, 541, 488, 390 cm^{-1}. HRMS (Q-TOF, ES+) *(m/z)*: $[M+Na]^+$ calcd. for $C_{12}H_{10}ClO_2$, 467.1987; found, 467.1196.

[5]Cycloparaphenylene **[5]CPP**

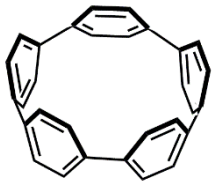

Diisopropylamine (5.00 mL, 36.0 mmol, 48.0 equiv) was added to 650 mL of dry toluene in a flame dried round bottom flask under N_2. This solution was cooled to 0 °C at

which point 2.3 M n-butyl lithium in hexanes (9.60 mL, 22.0 mmol, 30.0 equiv) was added dropwise and stirred for 20 minutes at 0 ˚C. Reduced macrocycle **3** (330 mg, 0.740 mmol, 1.00 equiv) was dissolved in dry toluene (50.0 mL) and was added dropwise to the stirring solution of lithium diisopropylamide (LDA). The reaction was warmed to room temperature and allowed to stir for 2 hours, resulting in a deep red ruby solution, at which point it was quenched with 200 mL of water. The solution was extracted with toluene (3 × 100 mL). The resulting organic phase was pooled and washed with water (3 × 200 mL), brine (1 × 200 mL) and dried over sodium sulfate before concentration under vacuum. The crude red solid was chromatographed on silica gel in pure DCM to give a solid red band that was collected and concentrated to give **[5]CPP** as brilliant red needles (195 mg, 69% yield). m.p. decomp >400°C. ^{1}H NMR (400 MHz, $CDCl_3$): δ(ppm) 7.85 (s, 20H); ^{13}C NMR (125 MHz, $CDCl_3$): δ(ppm) 131.96, 126.57; IR (neat): 3005, 2956, 2922, 2853, 1666, 1602, 1549, 1508, 1478, 1459, 1415, 1375, 1342, 1299, 1259, 1236, 1180, 1171, 1120, 1079, 1053, 1026, 956, 930, 843, 817, 767, 688, 635, 552, 463, 448, 429 cm^{-1}; MALDI-TOF *(m/z)*: $[M]^+$ calcd. for $C_{30}H_{20}$, 380.16; found 380.86.

II.6.3. Optical Characterization

Absorbance spectra were obtained in a 1-cm quartz cuvette with dichloromethane using a Varian 100 Bio UV-Vis spectrometer (Figure **II.5**) The extinction coefficient was calculated by measuring the slope of Beer-Lambert plots (absorbance: [5]CPP, 335 nm and 502 nm) and averaging over three independent trials (Figure **II.6**).

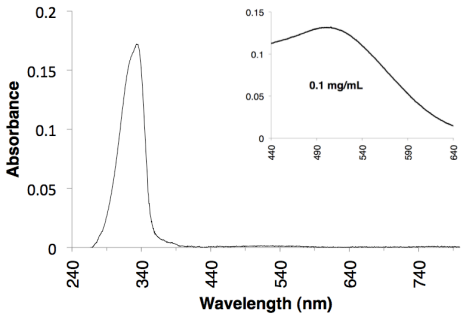

Figure II.5. UV-Vis of [5]CPP in dichloromethane, minor absorption is shown in the top right corner.

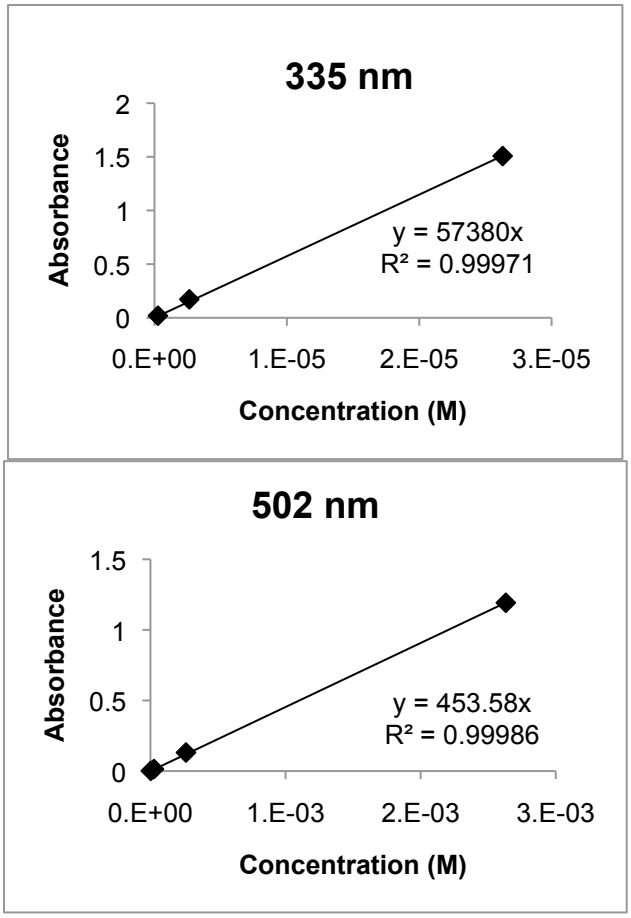

Figure II.6. Beer-Lambert plots for the determination of extinction coefficient of [5]CPP ($\varepsilon_{335nm} = 5.70 \times 10^4$ $M^{-1}cm^{-1}$, $\varepsilon_{501nm} = 4.50 \times 10^2$ $M^{-1}cm^{-1}$).

II.6.4. Electrochemical Measurements

Cyclic voltammetry experiments were performed using a CH Instruments 1200B potentiostat running CH Instruments software (Figure **II.7**). Measurements were conducted in degassed 0.1 M n-Bu_4NPF_6 in tetrahydrofuran under an N_2 atmosphere with a glassy carbon working electrode, platinum counter electrode and Ag/AgCl reference electrode. Ferrocene/ferrocenium couple was used as an internal or external reference. Supporting electrolyte tetra-*n*-butylammonium hexafluorophosphate (nBu_4PF_6) was purchased from Sigma-Aldrich and was recrystallized from methanol 3 times before use. Solvents were sparged with N_2 prior to data collection.

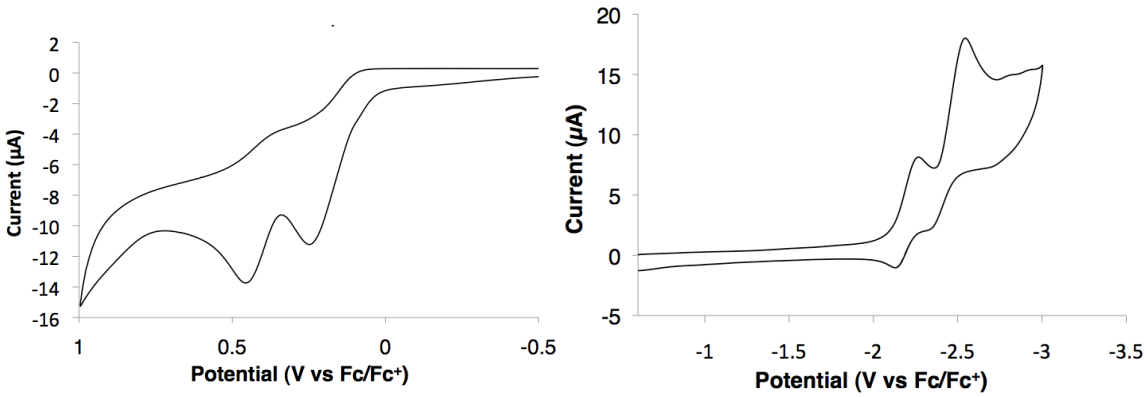

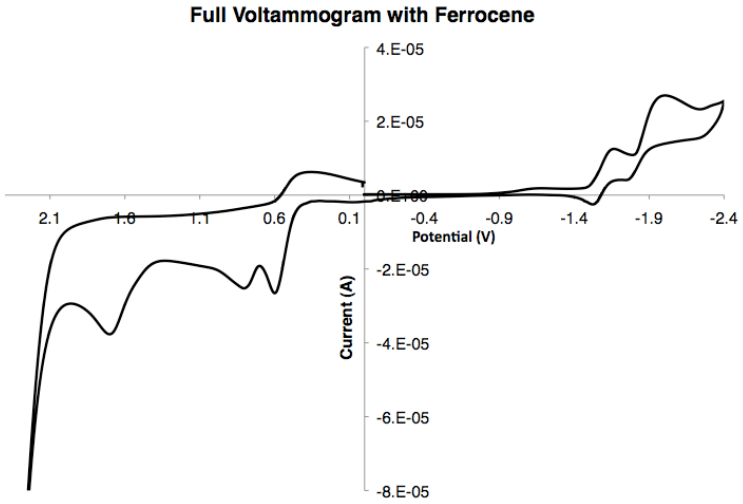

Figure II.7. Cyclic Voltammetry of [5]CPP.

II.6.5. Computational Details

All calculations were carried out with Gaussian 09 package at B3LYP/6-31g* level of theory.[18] All excited state calculations (TD-DFT) were performed on fully optimized structures. The fully optimized structures were confirmed to be true minima by vibrational analysis. Structures were minimized with no symmetry restrictions. Relevant computational data are depicted in Figures **II.8-II.10** and Tables **II.1-II.3**.

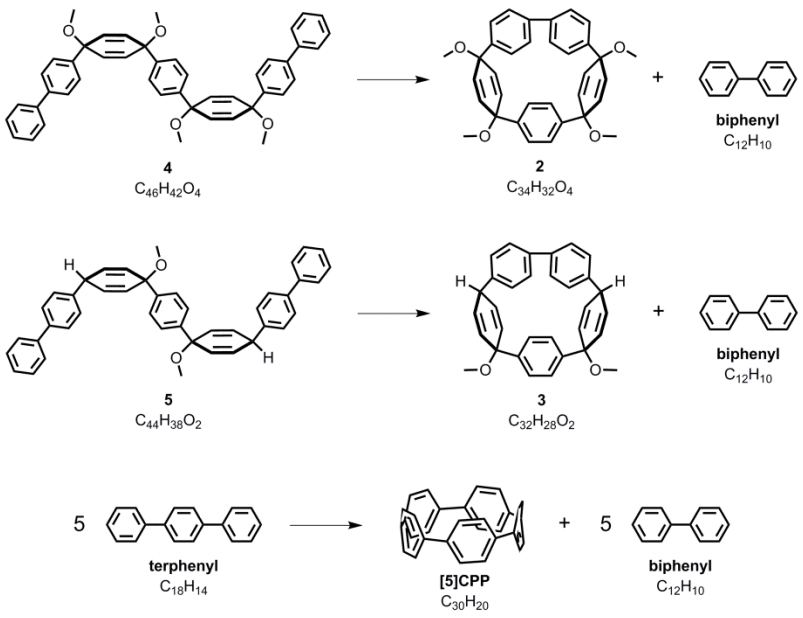

Figure II.8. Homodesmotic reactions used to calculate strain of macrocyclic compounds **2**, **3**, and **[5]CPP**.

Table II.1. Summary of homodesmotic reactions used to calculate strain of macrocyclic compounds **2**, **3**, and **[5]CPP**.

Compound	**Total Energy (Hartree)**	**Strain Energy (Hartree)**	**Strain Energy (kcal/mol)**
biphenyl	-463.30607808		
terphenyl	-694.36374497		
[5]CPP	-1155.09824925	0.19008520	119.3
2	-1615.60352147	0.05061031	31.8
3	-1386.57340782	0.05555035	34.9
4	-2078.96020986		
5	-1849.93503625		

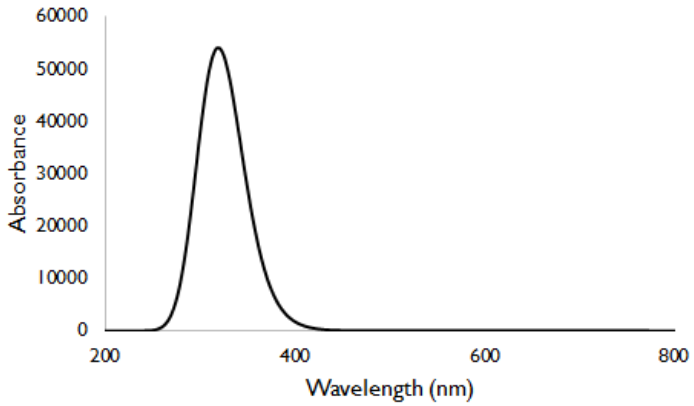

Figure II.9. Calculated UV-Vis for [5]CPP determined by TD-DFT method using B3LYP/6-31g*.

Table II.2. Major electronic transitions for [5]CPP determined by TD-DFT method using B3LYP/6-31g*.

Energy (cm^{-1})	**Wavelength (nm)**	**Osc. Strength (*f*)**	**Major contributions**
16491	606	0.0015	HOMO→LUMO (100%)
27461	364	0.0079	H-1→LUMO (28%) HOMO→L+1 (65%)
27580	363	0.0048	H-2→LUMO (37%) HOMO→L+2 (61%)
28182	355	0.0094	H-1→LUMO (20%) HOMO→L+3 (70%)
28824	347	0.0195	H-2→LUMO (11%) HOMO→L+4 (74%)
31245	320	0.6272	H-1→LUMO (49%) HOMO→L+1 (30%) HOMO→L+3 (16%)
31376	319	0.6398	H-2→LUMO (48%) HOMO→L+2 (33%) HOMO→L+4 (13%)
33154	302	0.001	H-5→LUMO (13%) H-3→LUMO (55%) HOMO→L+5 (18%)
33318	300	0.013	H-6→LUMO (34%) H-4→LUMO (10%) HOMO→L+6 (41%)
33442	299	0.0416	H-5→LUMO (26%) H-3→LUMO (31%) HOMO→L+5 (29%)
33659	297	0.0227	H-4→LUMO (75%)
35402	282	0.008	H-7→LUMO (68%) HOMO→L+8 (21%)

Table II.3. Electronic states of [5]CPP determined by B3LYP/6-31g*.

Compound	Energy (Hartrees)	ΔE of kcal/mol
[5]CPP^{-4}	-1154.443944	363.4330402
[5]CPP^{-3}	-1154.795277	142.9682012
[5]CPP^{-2}	-1155.042566	-12.20813175
[5]CPP^{-1}	-1155.12962	-66.83564457
[5]CPP Triplet Excited State	-1155.054351	-19.6033371
[5]CPP Singlet Excited State	-1155.096522	-46.06621191
[5]CPP	-1155.023111	0
[5]CPP^{+1}	-1154.88608	85.98826633
[5]CPP^{+2}	-1154.554144	294.2813002
[5]CPP^{+3}	-1154.050269	610.468052
[5]CPP^{+4}	-1153.417265	1007.684317

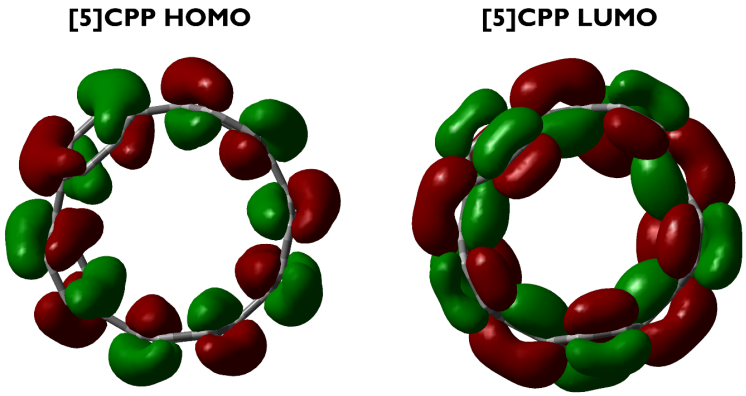

Figure II.10. Calculated HOMO and LUMO of ground state [5]CPP at B3LYP/6-31g* level of theory.

II.6.6. X-ray Crystallographic Data

General X-ray data collection: *APEX2*[33]; data reduction: *SAINT*[34]; program(s) used to refine structure: *SHELXL*[35]; molecular graphics: Olex2[36]; software used to prepare material for publication: Olex2[36]. Relevant crystallographic data are depicted in Figures **II.11** and **II.12** and Tables **II.4** and **II.5**.

X-ray crystallographic data for compound **3** (CCDC Registry #974188)

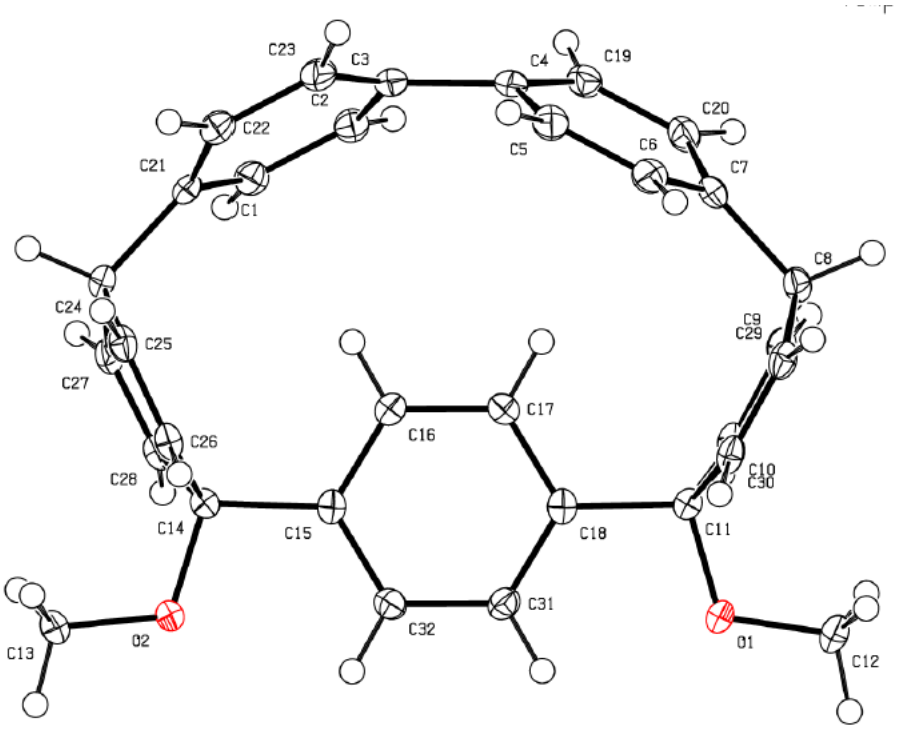

Figure II.11. ORTEP representation of X-ray crystallographic structure **3.**

Table II.4. Crystal data and structure refinement for **3**.

$C_{32}H_{28}O_2$	$F(000) = 944.0$
$M_r = 444.54$	$D_x = 1.286$ Mg m^{-3}
Monoclinic, $P2_1/c$	Cu $K\alpha$ radiation, $\lambda = 1.54178$ Å
Hall symbol: -P 2ybc	Cell parameters from 9074 reflections
$a = 17.444$ (3) Å	$\theta = 2.5–66.6°$
$b = 10.8686$ (19) Å	$\mu = 0.61$ mm^{-1}
$c = 12.1775$ (19) Å	$T = 100$ K
$\beta = 92.014$ (6)°	Fragment, colorless
$V = 2307.3$ (7) Å^3	0.11 × 0.10 × 0.06 mm
$Z = 4$	
Bruker Proteum-R diffractometer	3835 independent reflections
Radiation source: rotating anode	3548 reflections with $I > 2\sigma(I)$
multilayer	$R_{int} = 0.069$
ω & φ scans	$\theta_{max} = 66.9°$, $\theta_{min} = 2.5°$
Absorption correction: multi-scan *SADABS*[37]	$h = -20 \rightarrow 20$
$T_{min} = 0.670$, $T_{max} = 0.737$	$k = -12 \rightarrow 12$
37719 measured reflections	$l = -14 \rightarrow 14$

Table II.4. (continued).

Refinement on F^2	0 restraints
Least-squares matrix: full	Hydrogen site location: inferred from neighbouring sites
$R[F^2 > 2s(F^2)] = 0.052$	H-atom parameters constrained
$wR(F^2) = 0.098$	$w = 1/[s^2(F_o^2) + (0.0349P)^2 + 1.6425P]$ where $P = (F_o^2 + 2F_c^2)/3$
$S = 1.05$	$(D/s)_{max} = 0.001$
3835 reflections	$D\tilde{n}_{max} = 0.22$ e Å^{-3}
309 parameters	$D\tilde{n}_{min} = -0.20$ e Å^{-3}

Alert level A

PLAT029_ALERT_3_A _diffrn_measured_fraction_theta_full Low 0.932

Author Response: The rotating anode X-ray source was exhibiting frequent arcing (tripping) during the second half of the data set; the arcing resulted in low or missing intensities for some equivalent reflections, leading to an unusually high number of rejected reflections during scaling. Despite the missing data, the structural model is of high quality and meets the objectives of the crystallographic study.

X-ray crystallographic data for compound **[5]CPP** (CCDC Registry #974187)

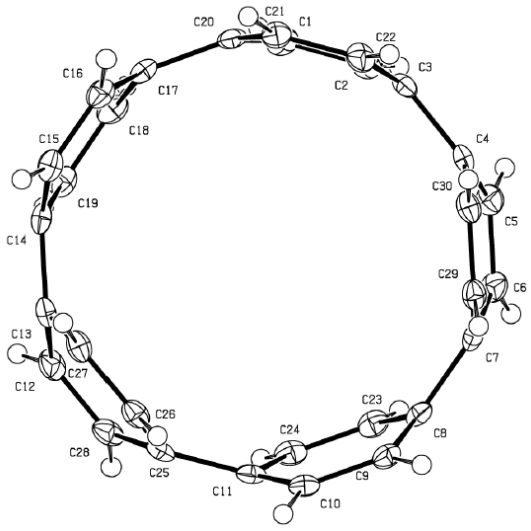

Figure II.12. ORTEP representation of X-ray crystallographic structure **[5]CPP**.

Table II.5. Crystal data and structure refinement for **[5]CPP**.

$C_{30}H_{20}$	$F(000) = 1600$
$M_r = 380.46$	$D_x = 1.243$ Mg m^{-3}
Orthorhombic, *Pbca*	Cu *K*a radiation, l = 1.54178 Å
Hall symbol: -P 2ac 2ab	Cell parameters from 9831 reflections
$a = 9.8337$ (2) Å	q = 4.5–66.6°
$b = 11.6263$ (3) Å	m = 0.53 mm^{-1}
$c = 35.5613$ (8) Å	$T = 100$ K
$V = 4065.71$ (16) Å^3	Block, dark red
$Z = 8$	0.51 × 0.44 × 0.42 mm
Bruker Proteum-R diffractometer	3543 independent reflections
Radiation source: rotating anode	3509 reflections with $I > 2s(I)$
multilayer	$R_{int} = 0.035$
w & f scans	$q_{max} = 66.6°$, $q_{min} = 2.5°$
Absorption correction: multi-scan *SADABS*[37] was used for absorption correction. wR2(int) was 0.0970 before and 0.0501 after correction. The Ratio of minimum to maximum transmission is 0.9090. The l/2 correction factor is 0.0015.	h = -11®11
$T_{min} = 0.684$, $T_{max} = 0.753$	k = -13®13
128289 measured reflections	l = -39®42
Refinement on F^2	0 restraints
Least-squares matrix: full	Hydrogen site location: inferred from neighbouring sites
$R[F^2 > 2s(F^2)] = 0.049$	H-atom parameters constrained
$wR(F^2) = 0.128$	$w = 1/[s^2(F_o^2) + (0.0643P)^2 + 3.0252P]$ where $P = (F_o^2 + 2F_c^2)/3$
$S = 1.10$	$(D/s)_{max} < 0.001$
3543 reflections	$Dñ_{max} = 0.32$ e Å^{-3}
271 parameters	$Dñ_{min} = -0.30$ e Å^{-3}

CHAPTER III
SMALL CHIRAL CYCLOPARAPHENYLENES

This chapter is based on unpublished work by myself and Han Xiao (where mentioned). Editing was provided by Prof. Ramesh Jasti.

Cycloparaphenylenes and cyclacenes represent the unit-cycles of armchair and zigzag carbon nanotubes respectively. These special cases of CNTs have benzene rings fused down the length of the tube (armchair) or around the circumference (zigzag). All other CNTs are chiral, with benzene rings fused in a handed helical twist down the length of the tube like the threads of a screw. It is therefore straightforward to imagine extending the carbon nanohoop scaffold to include a twist, creating the unit-cycle of a chiral CNT with defined helical pitch, size, and handedness. This has been achieved by the inclusion of naphthalene into the CPP backbone (*vide supra*). However, the only published example of such a nanohoop was found to isomerize rapidly at room temperature via rotation and therefore does not represent a chirally discrete unit-cycle. Herein I present strategies towards smaller chiral CPPs with long rotational half-lives and inherent chirality.

III.1. Background

Cycloparaphenylenes[1] are often envisioned as the smallest components of armchair carbon nanotubes which retain aromaticity. The as-yet-inaccessible cyclacenes[2] have an analogous relationship to zigzag CNTs. The insertion of longer acenes (such as naphthalene) into the CPP framework provides new, chiral unit cycles (Figure **III.1**). Beyond their obvious utility as templates for the synthesis of chiral CNTs, inherently chiral aromatics, such as the helicenes, display interesting properties and therefore applications (catalysis, chiral recognition, supramolecular materials, nonlinear optics, etc.) distinct from their achiral analogues[3].

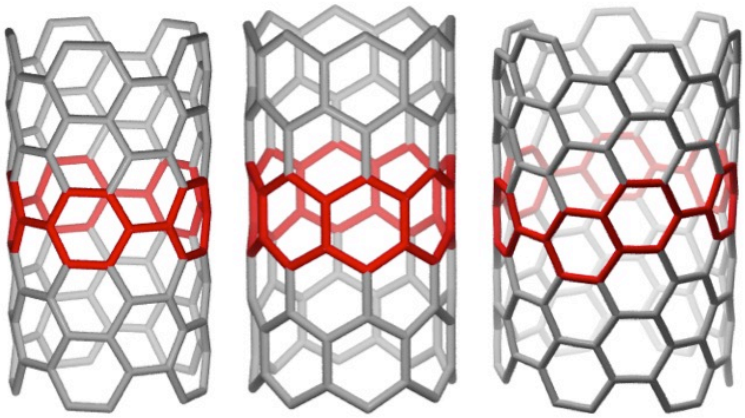

Figure III.1. Representative unit cycles of CNTs. Left: [5]CPP in an armchair (5,5)CNT. Center: $[6]_8$cyclacene in a zigzag (8,0)CNT. Right: *P*-2,6-naphthyl-[6]CPP in a chiral (7,6)CNT (double bonds omitted for clarity).

One nanohoop of this sort has been reported to date, Itami's [13]CPPN (Scheme **I.24**), herein designated 2,6-naphthyl-[14]CPP with the exact naphthalene connectivity stated and where the bracketed number refers to the total number of aromatic moieties in the nanohoop.[4] It is also worth mentioning that certain atropisomers of the molecular belts constructed by Isobe (Scheme **I.25**) are subunits of chiral CNTs, but because of the complexity of these annulated belts, they cannot be considered unit-cycles.[5] At the time of synthesis, Itami assessed the barrier to rotation of the naphthalene moiety in, and therefore racemazation between *M*- and *P*-2,6-naphthyl-[14]CPP to be 8.4 kcal/mol accounting for a half-life of 8×10^{-8} seconds at room temperature (based on the Arrhenius equation). This does not meet the requirements defined by Ōki for atropisomerism which include a half-life of 1000 seconds at 300 K, approximately a 22 kcal/mol barrier to rotation.[6] As such we set forth to synthesize a nanohoop with inherent chirality and isomers that could be observed at room temperature.

III.2. Previous Work by Han Xiao

Itami calculated that either tightening the hoop by the deletion of phenyl rings or extending the acene length will raise the barrier to inversion (Table **III.1**).[4] Because of our success in the synthesis of smaller CPPs, we chose the former approach. Han Xiao, a former student in the Jasti lab, adapted the [6]CPP synthesis[7] to a chiral target, 1,5-naphthyl-[6]CPP **4**, and the achiral constitutional isomer 1,4-naphthyl-[6]CPP **7** (Scheme

III.1). At the conception of this project, it was rationalized that the 1,5 connectivity would strain the nanohoop further than the 2,6 and thus the barrier to racimization would be higher than 29.6 kcal/mol as calculated for 2,6-naphthyl-[6]CPP by Itami.[4] This had the added advantage that naphthalene starting materials functionalized at the 1 and 5 positions are much more widely available than those with 2,6 substitution.

Table III.1. Calculated racemization barriers of CPPs with one long acene in the framework.[4] The previously reported 2,6-naphthyl-[14]CPP is shown in red. The synthetic target 2,6-naphthyl-[6]CPP is shown in blue.

Number of aromatic rings (n)	2,6-naphthyl-[n]CPP	2,6-anthracenyl-[n]CPP	2,8-tetracenyl-[n]CPP
6	29.6	45.5	No data
7	21.2	31.3	44.0
8	17.4	25.7	33.0
9	13.5	19.5	26.3
10	12.5	16.5	21.3
11	9.8	13.5	17.9
12	9.7	12.3	15.4
13	7.7	9.8	12.5
14	8.4	10.0	11.9

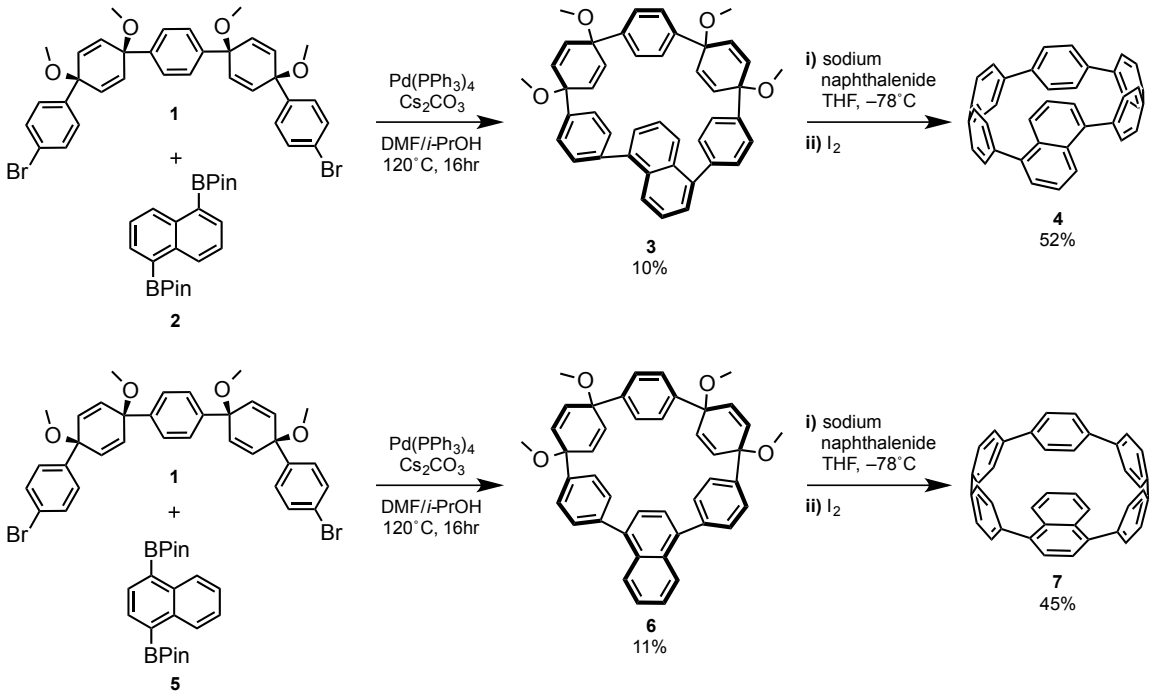

Scheme III.1. Synthesis of 1,5- and 1,4-naphthyl-[6]CPP by Xiao.

Dibromide **1** was previously reported by our lab en route to the synthesis of [6]CPP and the gram scale syntheses of [8]- and [10]CPP.[7-8] Xiao found that intermolecular macrocyclization via Suzuki coupling to either 1,5-diboronate **2** or 1,4-diboronate **3** using the conditions that furnished the [6]CPP macrocycle gave low yields of chiral CPP synthon **3** and the achiral analogue **6**. Both of these new macrocycles could be converted to the corresponding CPPs via sodium naphthalenide reduction. In this way 1,5-naphthyl-[6]CPP (**4**) and 1,4-naphthyl-[6]CPP (**7**) were prepared in a few steps from known starting material with established methodology. Xiao was able to confirm the geometry of **4** by single crystal X-ray diffraction (Figure **III.2**) and found an equimolar mixture of *M* and *P* enantiomers in the crystal lattice. Meanwhile, computational studies by Christopher D. Anderson revealed, much to our surprise, that the rotational barrier at room temperature for **4** was actually lower than it's 2,6-isomer. At 21.7 kcal/mol, this nanohoop should racemize with a half-life of 7.5 minutes at room temperature (Figure **III.2**). The ground state energies of *M*- and *P*-1,5-naphthyl-[6]CPP were calculated to be higher than the corresponding 2,6-naphthyl-[6]CPP isomers. However, the rotational transition states of both the 2,6 and 1,5 derivatives are of approximately equal energy, making the barrier to rotation smaller in **4**.

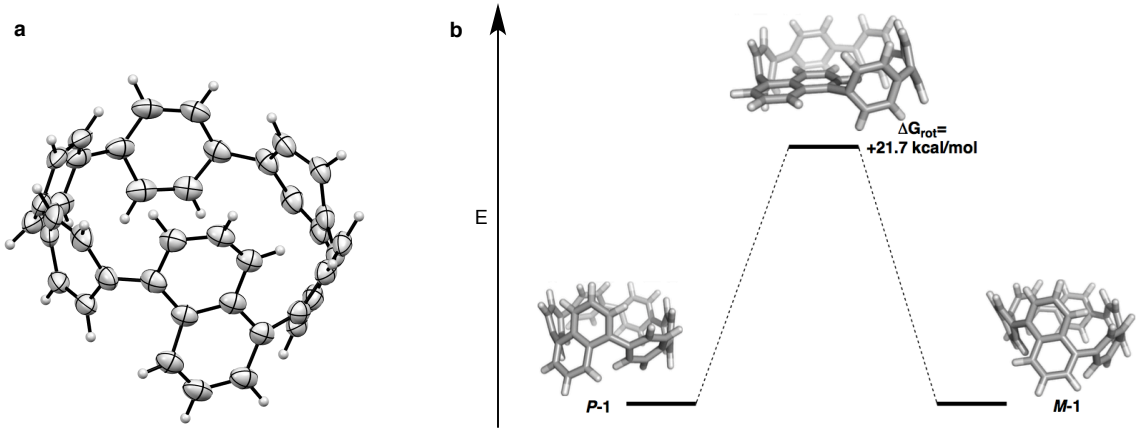

Figure III.2. Crystal structure (a) and racimization barrier (b) of 1,5-naphthyl-[6]CPP. ORTEP ellipsoid plot at 50% probability.

III.3. Synthetic Efforts Towards 2,6-naphthyl-[6]CPP

III.3.1. Motivation

Inspired by the work of Xiao and having established that **4** would racemize too quickly at room temperature to exhibit useful atropisomerism, I chose to target a third constitutional isomer in addition to those synthesized by Xiao, 2,6-naphthyl-[6]CPP. This would provide a complete set of $C_{40}H_{26}$ naphthyl-CPPs with increasing chiral character: the inherently achiral 1,4-naphthyl-[6]CPP, the chiral but quickly rotating 1,5-naphthyl-[6]CPP, and the rotationally stable 2,6-naphthyl-[6]CPP (Figure **III.3**).

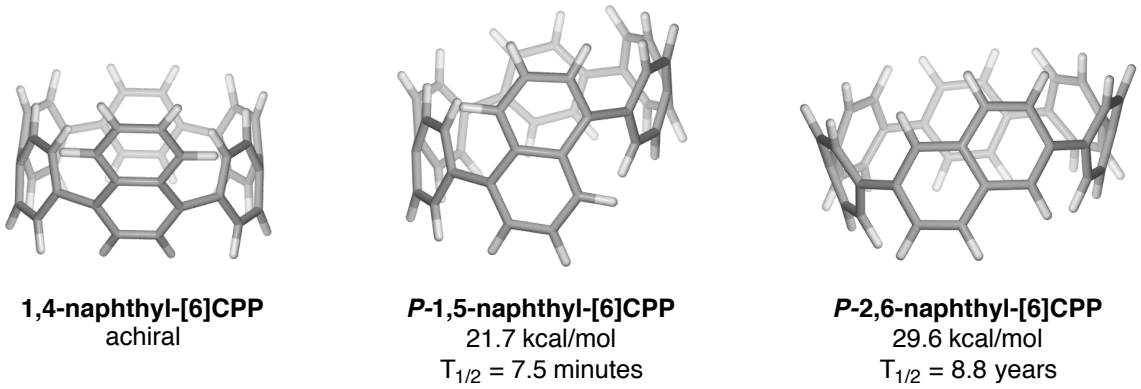

Figure III.3. Nanohoop isomers of $C_{40}H_{26}$ with increasing chiral character. Shown as B3LYP/6-31G* minimized structures with calculated racimization barriers and half-lives at room temperature.

III.3.2. Intermolecular Macrocycle Synthesis

The most straightforward approach to 2,6-naphthyl-[6]CPP is via intermolecular coupling, similar to the [6]CPP synthesis and Xiao's syntheses of **4** and **7**. To accomplish this, commercially available diol **8** was converted to ditriflate **9** with triflic anhydride in pyridine and dichloromethane (Scheme **III.2**) This pseudohalide coupling partner had the advantage of synthetic accessibility from inexpensive starting material. No such route to a 2,6-dihalo-naphthalene was tenable. The intermolecular Suzuki macrocyclization of **9** with advanced intermediate **10** (used in the [5]CPP synthesis) did not afford the desired macrocycle **11** under any conditions of varying temperature, concentration, or solvent.

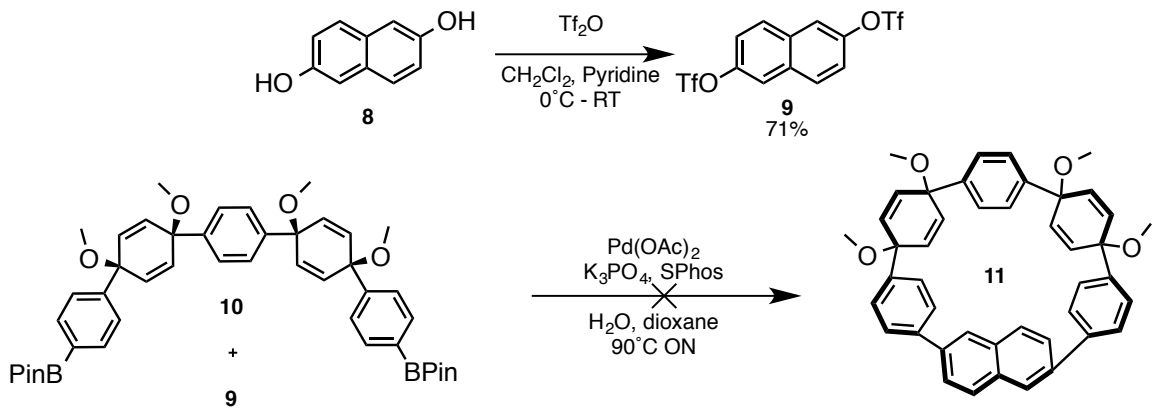

Scheme III.2. Intermolecular macrocyclization did not afford the desired macrocycle.

Upon careful examination of ^{1}H NMR signals from the major product of the macrocyclization, especially those corresponding to the alkene and aryl protons, it was determined that a higher-order macrocycle with a roughly rectangular and low-strain geometry (**12**, Scheme **III.3**) was the preferred product of this coupling. Reversing the coupling partners by using a five-ring dichloride and a borylated naphthalene produced the same result while higher dilution gave no formation of the desired 2,6-naphthyl-[6]CPP macrocycle This macrocycle was further confirmed by mass spectrometry and its conversion via sodium naphthalenide to the larger CPP **13**, with a blue fluorescence and ^{1}H NMR signals very similar to Itami's 2,6-naphthyl-[14]CPP.

Additionally, CPP macrocycles can often be identified by observed trends in their ^{1}H NMR spectra. As macrocycles become smaller, the cyclohexadiene moieties become more distorted to account for additional strain. As such, the chemical shifts of these protons become dissimilar and a "spreading out" effect is seen. The diene protons in the obtained macrocycle (Figure **III.4**, top) are separated by 15 Hz which is typical of larger macrocycles like the [10]CPP macrocycle (17 Hz, Figure **III.4**, middle) and not smaller macrocycles such as the [5]CPP macrocycle (341 Hz, Figure **III.4**, bottom).

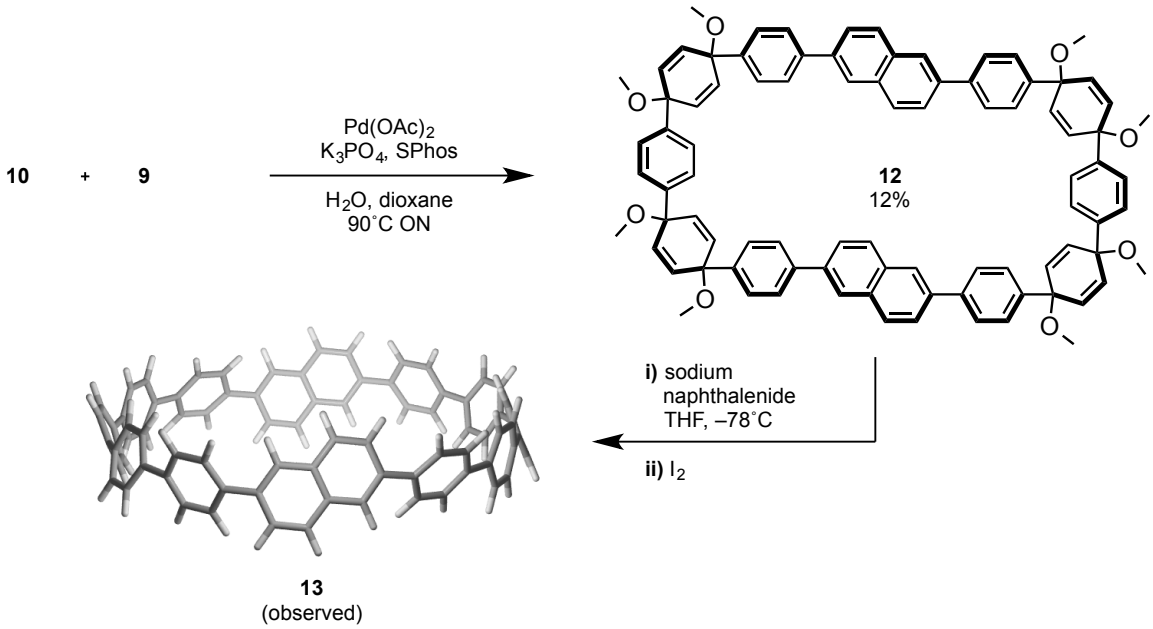

Scheme III.3. Dimeric macrocycle and observed CPP (DFT minimized) from intermolecular coupling.

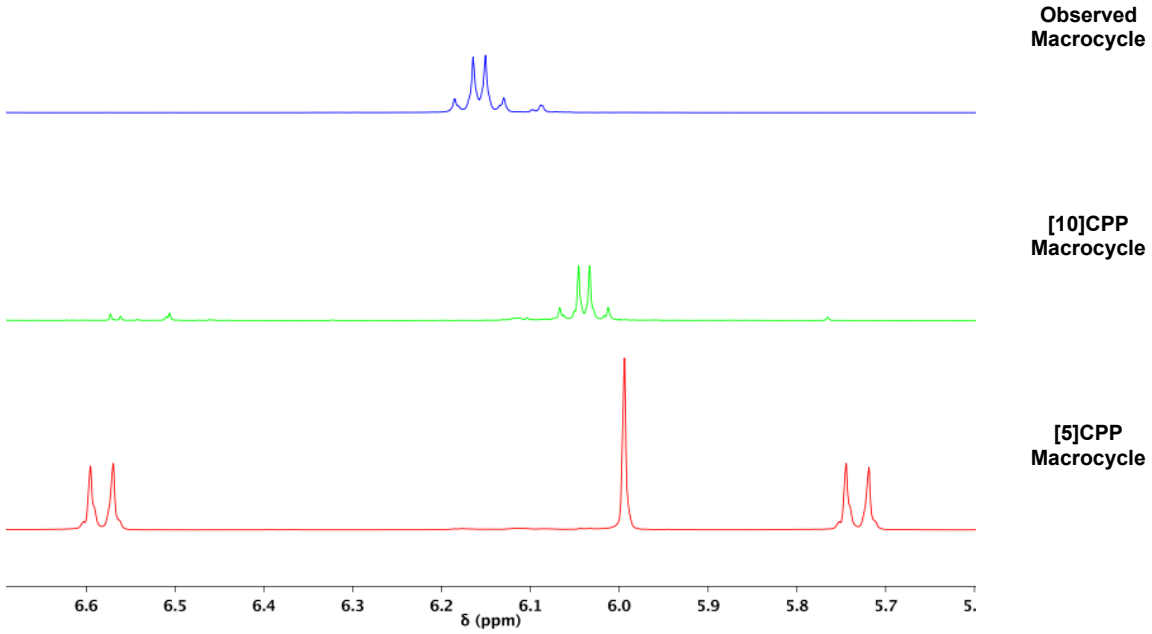

Figure III.4. Alkene ^{1}H NMR signals for **12** (top), [10]CPP macrocycle (middle), and [5]CPP macrocycle (bottom) illustrating the increasing separation of doublets with decreasing macrocycle size.

III.3.3. Intramolecular Macrocycle Synthesis

Ultimately, an intramolecular cyclization seemed more promising especially in light of the successful [5]CPP synthesis (Chapter **II**). To accomplish this, we envisioned an unsymmetrical bromo-chloro five-ring dihalide precursor with which an unsymmetrical 2,6-substituted naphthalene could be coupled to give a linear macrocycle synthon. Depending on the end-group functionality, either borylation of a trifluoromethanesulfonate (triflate) selectively and intramolecular Suzuki coupling or borylation of both ends followed by intramolecular oxidative homocoupling (as with [5]CPP) would afford the desired macrocycle (Scheme **III.4**).

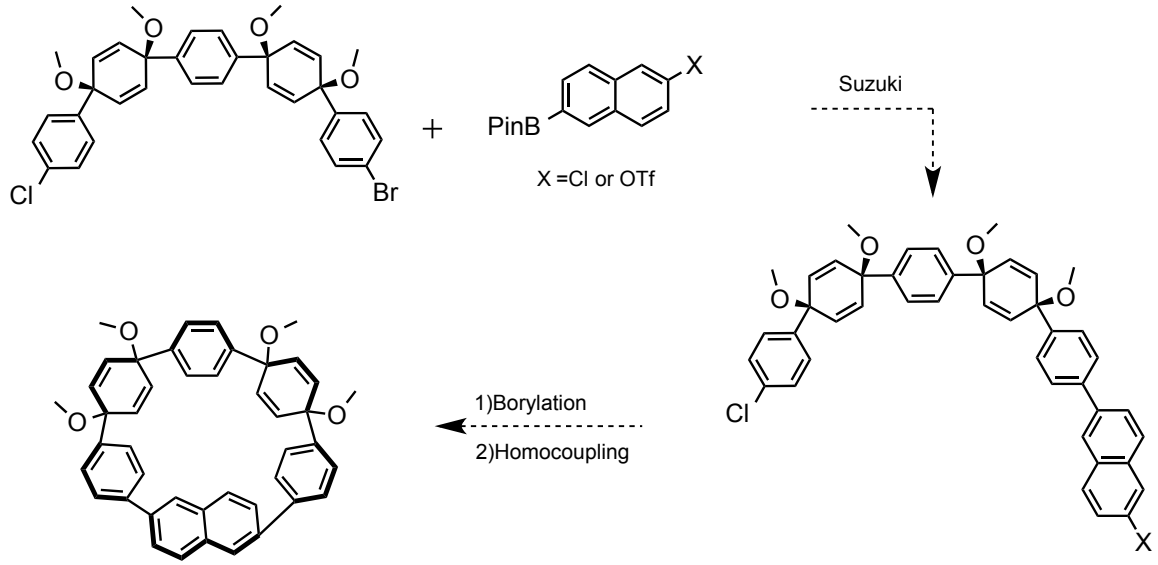

Scheme III.4. General intramolecular macrocyclization approach to a 2,6-naphthyl-[6]CPP precursor.

The unsymmetrical dihalide **15** was synthesized by the addition of (4-bromophenyl)lithium to quinol **14** (already available on multigram scale in our laboratory) followed by *in situ* methylation with methyl iodide (Scheme **III.5**). Lithium halogen exchange and borylation took place selectively at the aryl bromide on **15** to offer chloro-boronate **16**. Due to the scarcity of 2,6 disubstituted naphthalenes commercially, and in particular the chlorinated compounds such as 2-bromo-6-chloronaphthalene, triflates became an attractive alternative as a coupling partner for **16**. Commercially available 2-bromonaphthalen-2-ol was converted to the corresponding triflate **17** via literature procedure.[9] Upon subjecting **16** and **17** to Suzuki coupling conditions that favor

reactivity of the bromide in some cases[10], disappearance of starting material and a clean, roughly equimolar mixture of coupling products with a triflate or bromide terminus was obtained. Separation of these products was nontrivial.

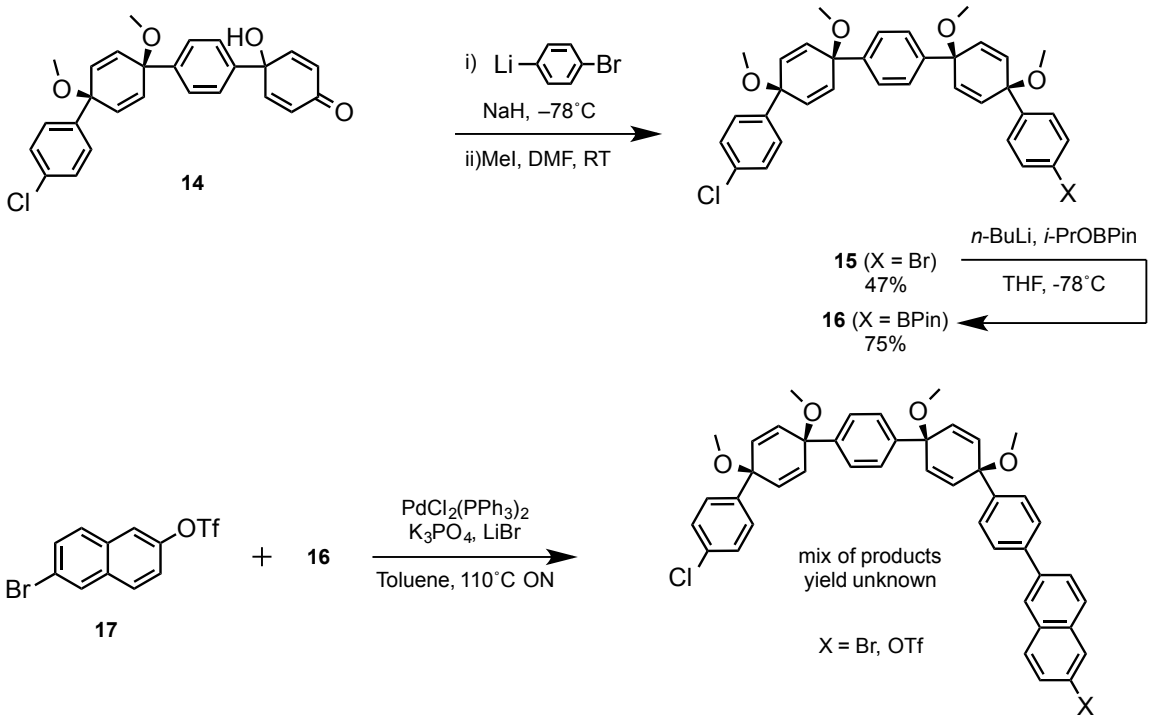

Scheme III.5. Unselective Suzuki coupling towards a macrocycle synthon.

Given the unselective nature of this coupling, an approach to couple a naphthol followed by triflation was pursued. Boronate **19** was obtained by the Miyura borylation of commercially available alcohol **18** (Scheme **III.6**). This was readily coupled under Suzuki conditions to give the chloro-alcohol **20**.

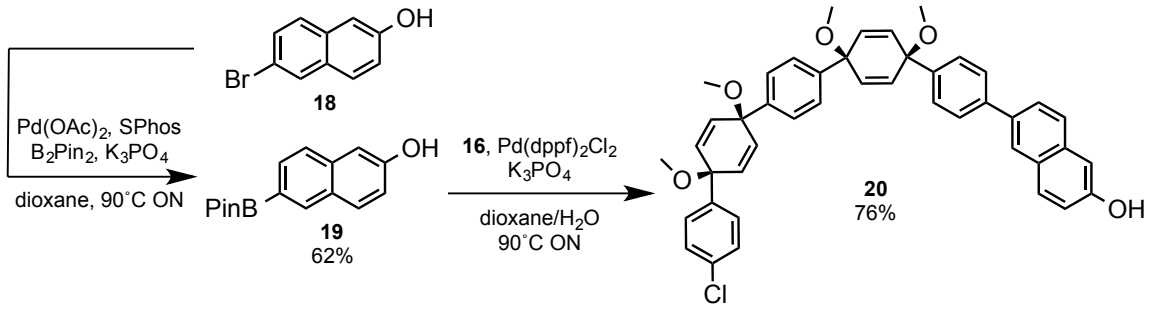

Scheme III.6. Synthesis of free alcohol **20**.

Naphthol **20** was subjected to several triflation conditions. Whether by treatment with triflic anhydride in pyridine, dichloromethane and triethylamine, or a biphasic mixture of toluene and 30% K_3PO_4 in water, and despite rigorous purification of starting material, reagents, and solvents, only a mixture of products where all cyclohexadiene moieties had quantitatively transformed into *meta*-substituted anisoles was obtained (Scheme **III.7**). This is obvious from the complete disappearance of alkene proton signals (δ = 5.0-6.5 ppm) in the ^{1}H NMR accompanied by the appearance of aryl methyl ether proton signals (ca. δ = 3.8 ppm). In the presence of acid, this is a known route of decomposition for such moieties.[11] It seems therefore that a very small amount of advantageous triflic acid may be effecting this transformation despite careful preparation and basic media. Additionally, triflic anhydride may be acting as a Lewis acid but this would certainly be a special case.

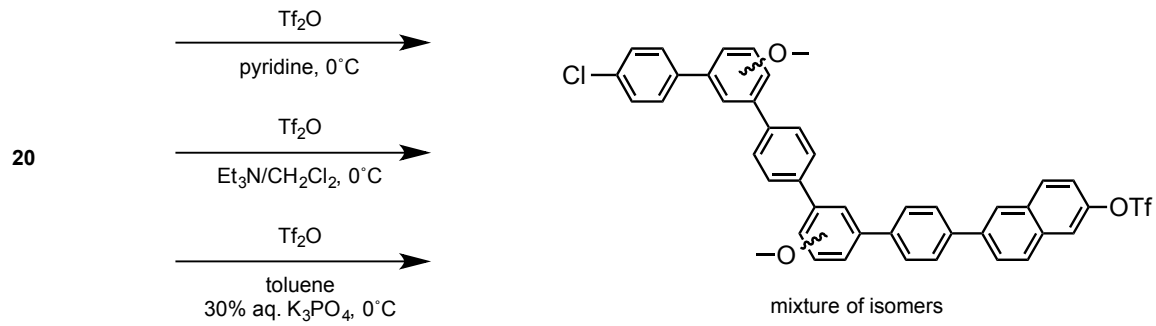

Scheme III.7. Decomposition of **20** under triflation conditions.

Switching triflating agents to *N*-phenyl-bis(trifluoromethanesulfonimide) eliminated the problem of acid-promoted rearrangement. In dry tetrahydrofuran at room temperature, **20** was cleanly converted to the desired chloro-triflate **21** (Scheme **III.8**). With halide and pseudohalide termini, **21** underwent Miyura borylation with Buchwald's SPhos to the corresponding diboronate **22**, which is ideal for intramolecular oxidative homocoupling as in the synthesis of the [5]CPP macrocycle. Additionally, we have demonstrated in our laboratory the usefulness of this type of cyclization to furnish [6]-, [7]-, and [10]CPP macrocycles.

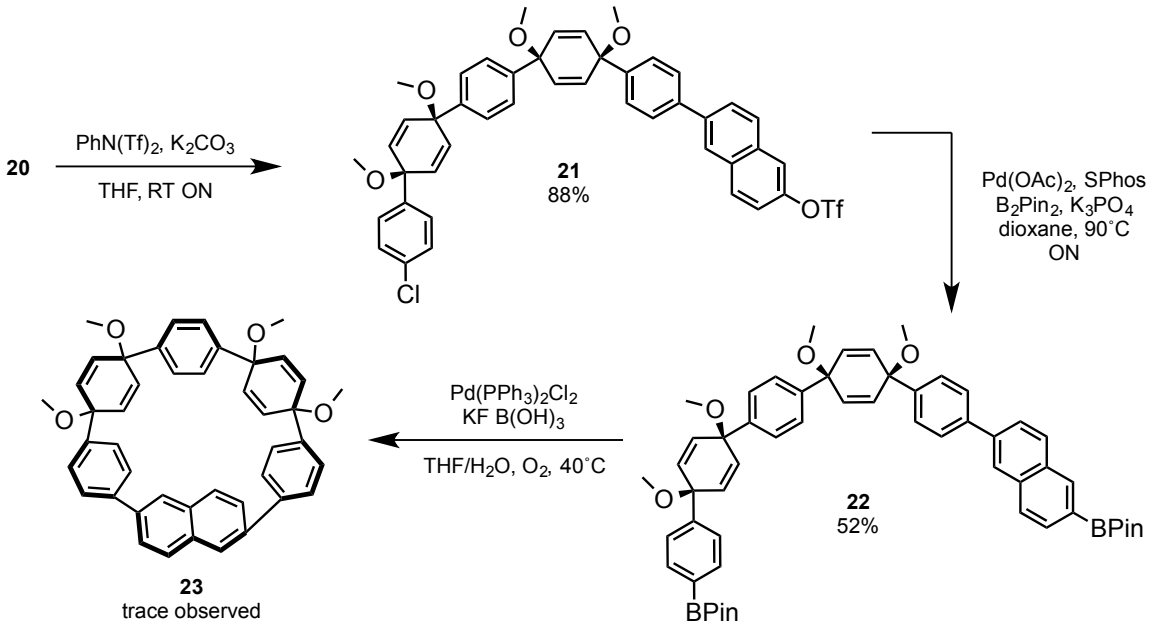

Scheme III.8. Synthesis of diboronate and troubled conversion to the desired macrocycle.

Unfortunately, under established macrocyclization conditions, a diminishingly small quantity of **23**, the pivotal 2,6-naphthyl-[6]CPP macrocycle, was formed. Evidence for the formation of **23** is not apparent in the crude reaction mixture, disappearing into the baseline of the ^{1}H NMR spectrum (Figure **III.5**). Deborylated and linear oligomers appear to be present in much larger quantities. Only after preparatory size-exclusion gel permeation chromatography (GPC) and preparatory thin-layer chromatography (pTLC) purification are signals indicative of the macrocycle present in the ^{1}H NMR spectrum. When compared to Xiao's axially-chiral 1,5-naphthyl-[6]CPP macrocycle, four diagnostic signals in the alkene region corresponding to four pairs of diasterotopic cyclohexadiene protons are expected in both spectra (Figure **III.5**). Xiao's macrocycle clearly shows these as doublets with minor coupling. In the purified product mixture, three such doublets are clearly visible. The most downfield of these signals also leans upfield, implying that the fourth expected signal is buried by the signals from the dominant products. The total mass of the sample used to obtain this spectrum was 3 mg so therefore it can be assumed that the product present represents less than 0.5 mg, corresponding to a macrocyclization yield of less than 0.3%.

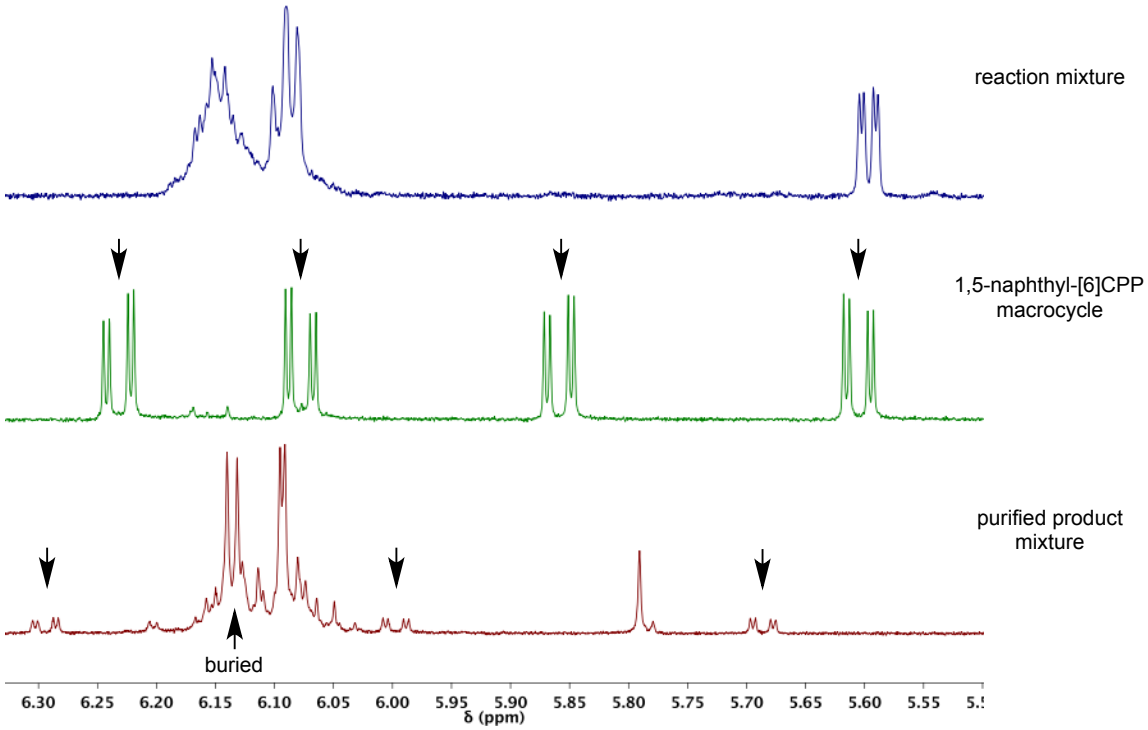

Figure III.5. ^{1}H NMR evidence of trace macrocycle formation. Reaction mixture (top) shows no sign of macrocycle. Diagnostic doublets in the chiral 1,5-naphthyl-[6]CPP macrocycle are shown with arrows (middle). Three similar doublets can be seen in the purified product mixture (bottom) with one assumed to be overwhelmed.

In light of the poor yield of intramolecular boronate homocoupling in the case of the 2,6-naphthyl-[6]CPP macrocycle, an alternate route based on an intramolecular boronate-trimethylacetate (pivalate) cross coupling was developed. Pivalate **24** is available in quantitative yield from **18** by a published procedure (Scheme **III.9**).[12] Miyura borylation of the bromide gives **25** can be coupled to dihalide **15** to obtain **26** with pivalate and chloride termini. At this point time constraints prohibited the further exploration of this route, but it is reasonable to expect the borylation of the chloride, followed by intramolecular nickel-catalyzed cross coupling of **27** with air-stable bis(tricyclohexylphosphine)nickel(II) dichloride in dry *tert*-amyl alcohol will yield the desired macrocycle, **23**, optimization notwithstanding.[13]

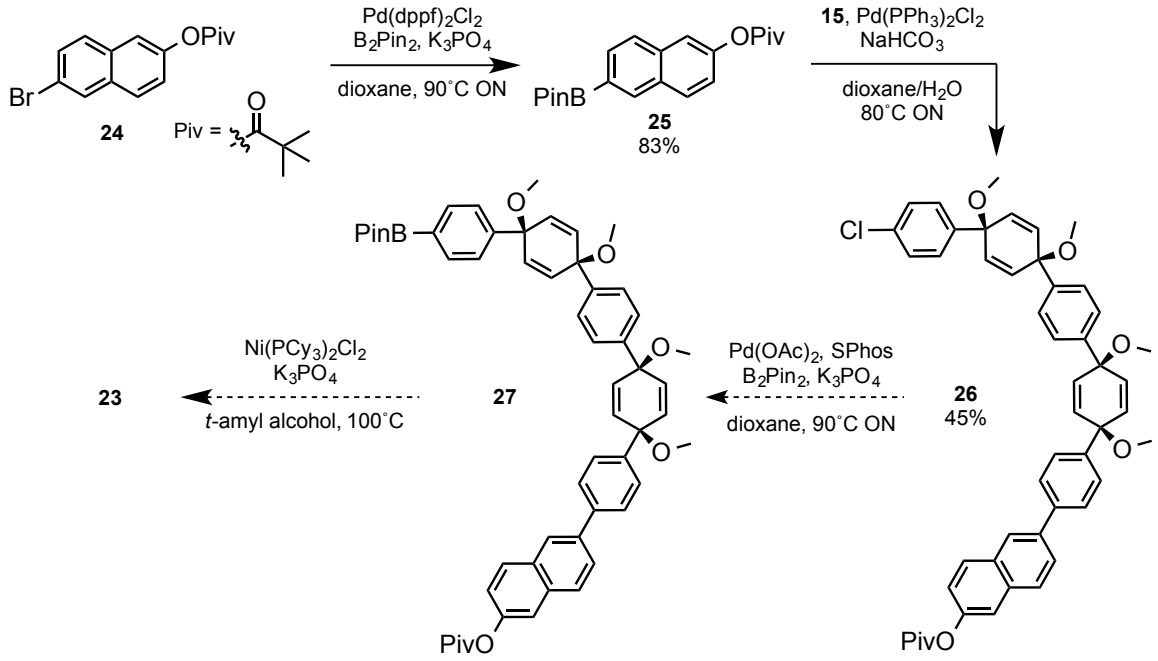

Scheme III.9. Alternate synthesis of macrocycle **22** via nickel-catalyzed intramolecular cross-coupling.

III.4. Conclusion and Future Directions

Heretofore we have reported the putative synthesis of a macrocyclic precursor to 2,6-naphthyl-[6]CPP. If a successful synthesis is developed, this will be the first chiral CNT unit-cycle with restricted rotation. Intermolecular macrocyclization attempts were found to exclusively favor the formation of a larger, dimeric macrocycle that was cleanly converted to the corresponding bis-2,6-naphthyl-[12]CPP. A straightforward synthesis of a linear diboronate **22** was developed and its conversion by intramolecular oxidative homocoupling explored. ^{1}H NMR evidence was provided for the formation of **23**, but it is in far less than 1% yield and could not be isolated from a mixture of products by silica column chromatography, GPC, or pTLC. Additionally, a route was proposed and the first key intermediates synthesized towards a new intramolecular boronate-pivalate cross coupling macrocyclization to provide **23**. Future directions for this synthesis include the further development of both macrocyclization approaches and, once optimized, the conversion to the desired CPP. Additionally, since the oxidative homocoupling conditions have never been optimized for 2,6-substituted naphthalenes, moving this moiety to the interior of the macrocyclic precursor and leaving benzene rings at the termini may lead to successful macrocyclization. Once obtained, *M*- and *P*-2,6-naphthyl-

[6]CPP may be isolable by chiral HPLC or crystallization from an enantiopure solvent mixture. The investigation of the spectroscopic, electronic, and CNT-seed properties of this new, axially chiral aromatic will then be evaluated alongside its achiral and rapidly rotating isomers. If **4** remains elusive, 2,6-anthracenyl-[7]CPP may be an attractive alternative with a similar barrier to racimization.

III.5. Bridge to Chapter IV

Chapter III detailed efforts to include a longer acene into the backbone of a CPP. This geometry modification may provide a new inherently chiral derivative. Chapter IV investigates efforts to radically distort the shape of a nanohoop by including azobenzene, a photoswitchable moiety, into the framework. This moves beyond hydrocarbon chemistry and away from thinking about CPPs as carbon nanotube precursors and into the realm of exploring the hollow CPP geometry in its own right through the design and synthesis of a nanohoop molecular container with a cavity size controlled by external stimulus.

III.6. Experimental

III.6.1. General Experiment Details

Moisture and oxygen sensitive reactions were carried out under nitrogen atmosphere using standard syringe/septa technique. All the glassware was thoroughly washed, oven dried at 140°C overnight and cooled under nitrogen atmosphere before use. All reagents were obtained commercially. Where noted as “dry”: Tetrahydrofuran (THF), toluene, dioxane, dimethylformamide (DMF) and dichloromethane (DCM) were dried by filtration through alumina according to the method descried by Grubbs.[14] For sodium naphthalenide generation and reductive aromatization solutions, THF was freshly distilled from sodium and benzophenone. Silica column chromatography was conducted with Zeochem Zeoprep n60 Eco 40-63 μm silica gel. Thin layer chromatography (TLC) was performed using Sorbent Technologies Silica Gel XHT TLC plates. Developed plates were visualized using UV light at wavelength of 254 and 365 nm or iodine vapor where appropriate. Gel permiation chromatography (GPC) was performed using a Japan

Analytical Industry LC-9101 with JAIGEL-1H and JAIGEL-2H polystyrene/divinylbenzene columns in series. IR spectra were recorded on a Thermo Nicolet 6700. ^{1}H NMR spectra were recorded at 600 (Bruker Avance III HD), 500 (Varian VNMRS) 400 (Varian VNMRS), or 300 (Varian VNMRS) MHz and ^{13}C NMR spectra were recorded at 150 (Bruker Avance III HD), 125 (Varian VNMRS), or 100 (Varian VNMRS) MHz. Deuterated chloroform ($CDCl_3$) was used as NMR solvent for all the compounds unless noted otherwise and all spectra were referenced to tetramethylsilane (TMS) due to the prevalence of compound signals overlapping with the signal from $CHCl_3$. The matricies used for MALDI-TOF were a solution of 7,7,8,8-tetracyanquinodimethane (TCNQ) in THF with 1% silver trifluoroacetate as a promoter, or trans-2-[3-(4-tert-Butylphenyl)-2-methyl-2-propenylidene]malononitrile (DCTB).

III.6.2. Experimental Details

naphthalene-2,6-diyl bis(trifluoromethanesulfonate) **9**

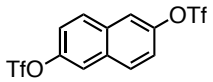

To a 250-mL flask equipped with a magnetic stir bar was added naphthalene-2,6-diol **8** (3.00 g, 18.7 mmol, 1 equiv), dry DCM (170 mL), and distilled pyridine (17 mL). The solution was cooled to 0˚C while stirring. Triflic anhydride (7.9 mL, 47 mmol, 2.5 equiv) was added dropwise via syringe. The reaction mixture was allowed to warm to room temperature then stirred an additional 1 hour. H_2O (25 mL) was added to the mixture and the solution was extracted with DCM (2 × 100 mL) and the combined organic layers were washed with 1M HCl (2 × 100 mL) and brine (100 mL) then dried over sodium sulfate and filtered. Solvent was removed under reduced pressure to yield a tan powder that was washed with methanol and dried under vacuum overnight (5.6 g, 71%). ^{1}H NMR (300 MHz, Chloroform-d) δ(ppm) 8.01 (d, J = 9.0 Hz, 1H), 7.85 (d, J = 2.4 Hz, 1H), 7.52 (dd, J = 9.0, 2.4 Hz, 1H). Matches published data.[15]

bis-2,6-naphthyl[12]cycloparaphenylene macrocycle **12**

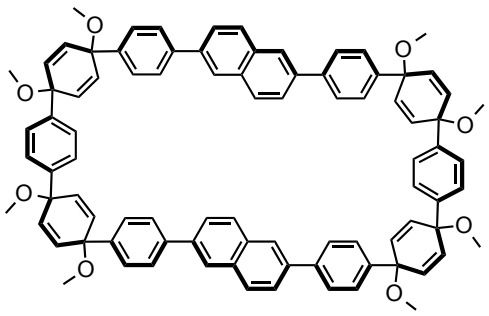

To a 500-mL flask equipped with a magnetic stir bar was added naphthalene-2,6-diyl bis(trifluoromethanesulfonate) **9** (300 mg, 0.7 mmol, 1 equiv), five-ring diboronate **10** (644 mg, 0.85 mmol, 1.2 equiv), $Pd(OAc)_2$ (74 mg, 0.11 mmol, 0.15 equiv), SPhos (123 mg, 0.3 mmol, 0.4 equiv), and ground, oven-dried K_3PO_4 (300 mg, 1.4 mmol, 2 equiv). This flask was evacuated and backfilled with dry N_2 five times to exclude moisture and air. Dry dioxane (225 mL), and N_2 sparged H_2O (25 mL) were added and the mixture was heated to 90˚C while stirring overnight. After cooling to room temperature, the solution was filtered through a pad of celite and concentrated under reduced pressure. The resulting semisolid was redissolved in 100 mL of DCM. The solution was washed with H_2O (2 × 100 mL) and brine (100 mL) then dried over sodium sulfate and filtered. Solvent was removed under reduced pressure and the crude solid was chromatographed on silica gel in an ethyl acetate/hexane gradient of increasing polarity to give a crystalline white solid (45 mg, 12%). ^{1}H NMR (500 MHz, Chloroform-d) δ(ppm) 7.67 (d, J = 8.4 Hz, 8H), 7.62 (s, 4H), 7.59 (d, J = 8.4 Hz, 8H), 7.53 (s, 8H), 7.42 (d, J = 8.5 Hz, 4H), 7.29 (d, J = 8.5 Hz, 4H), 6.20 (d, J = 10.5 Hz, 8H), 6.17 (d, J = 10.5 Hz, 8H), 3.53 (s, 12H), 3.50 (s, 12H). LRMS (FAB+) *(m/z)*: $[M]^+$ calcd. for $C_{88}H_{76}O_8$, 1260.57; found, 1261.0.

bis-2,6-naphthyl[12]cycloparaphenylene **13**

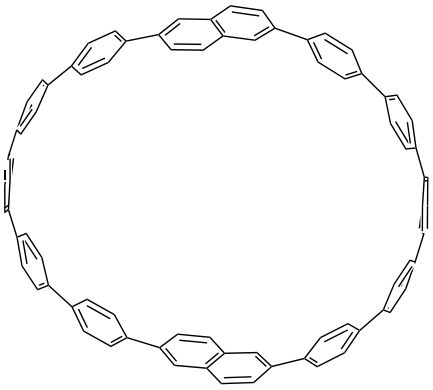

Macrocycle **2** (25 mg, 0.045 mmol, 1.00 equiv) was dissolved in freshly distilled THF (15 mL) and cooled to –78°C under N_2. 1 M sodium naphthalenide (0.3 mL, 0.30 mmol, 66.6 equiv) was added dropwise to the stirring solution to give a deep blue color. The mixture was stirred for one hour then 1 M I_2 in DCM was added (0.5 mL) followed by saturated sodium thiosulfate in H_2O (2 mL). After warming to room temperature, the solution was and concentrated under reduced pressure. The resulting solid was redissolved in 10 mL of DCM. The solution was washed with H_2O (2 × 10 mL) and brine (10 mL) then dried over sodium sulfate and filtered. Solvent was removed under reduced pressure and the crude solid was chromatographed on silica gel in an DCM/hexane gradient of increasing polarity to give a pale blue fluorescent solid (less than 1 mg). ^{1}H NMR (500 MHz, Chloroform-d) δ(ppm) 8.01 (s, 4H), 7.88 (d, J = 8.8 Hz, 4H), 7.78 (d, J = 8.8 Hz, 4H), 7.76 – 7.60 (overlap, 40H). IR (neat): 748.24, 810.54, 1021.06, 1072.24, 1123.32, 1262.56, 1461.87, 1467.46, 1484.06, 1658.8, 1665.54, 1678.15, 1691.95, 1711.6, 1725.47, 1736.61, 2853.63, 2924.57, 2956.96 cm^{-1}.

(1'S,1'''s,4's,4'''S)-4-bromo-4''''-chloro-1',1''',4',4'''-tetramethoxy-1',1''',4',4'''-tetrahydro-1,1':4',1'':4'',1''':4''',1''''-quinquephenyl **15**

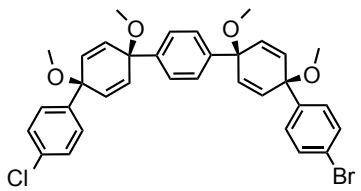

To a 1-L flask equipped with a magnetic stir bar was added quinol **14** (10.0 g, 23 mmol, 1 equiv) and dry THF (300 mL). This solution was cooled to –78˚C. Sodium hydride was added in one portion quickly (60% in mineral oil, 1.2 g, 30 mmol, 1.3 equiv) and stirred 1 hour. Meanwhile, 1,4-dibromobenzene (12 g, 51 mmol, 2.2 equiv) was added to a separate 500-mL flask, dissolved in dry THF (200 mL) and cooled to –78˚C. *n*-butyllithium (2.5 M in hexanes, 24 mL, 58 mmol, 2.5 equiv) was added to the 1,4-dibromobenzene solution dropwise and the mixture was stirred 30 minutes at –78˚C. The 4-bromophenyllithium solution was cannulated into the quinol solution and this mixture was stirred at –78˚C for 2 hours. Methyl iodide (7.2 mL, 115 mmol, 5 equiv) then dry DMF (75 mL) were added via syringe and the mixture was allowed to warm to room temperature and stirred overnight. H_2O (100 mL) was added to the mixture to quench and the solution was extracted with ethyl acetate (2 × 200 mL) and the combined organic layers were washed with H_2O (100 mL), 5% lithium chloride in H_2O (5 × 100 mL) and brine (100 mL) then dried over sodium sulfate and filtered. Solvent was removed under reduced pressure to yield a yellow solid that was recrystallized in toluene/hexane to yield bright pale yellow crystals (6.77 g, 47%). ^{1}H NMR (500 MHz, Chloroform-d) δ(ppm) 7.42 (d, J = 8.8 Hz, 2H), 7.32 – 7.31 (overlap, 6H), 7.27 (d, J = 7.3 Hz, 2H), 7.24 (d, J = 7.3 Hz, 2H), 6.10 (d, J = 10.3 Hz, 2H), 6.10 (d, J = 10.3 Hz, 2H), 6.05 (d, J = 10.3 Hz, 2H), 6.04 (d, J = 10.3 Hz, 2H), 3.42 (s, 3H), 3.42 (s, 3H), 3.42 (s, 3H), 3.41 (s, 3H). ^{13}C NMR (151 MHz, Chloroform-d) δ(ppm) 142.98, 142.92, 142.61, 142.03, 133.65, 133.48, 133.32, 133.09, 131.88, 128.72, 128.46, 127.47, 126.95, 126.57, 126.14, 126.04, 74.66, 74.64, 74.60, 74.48, 52.09, 52.01. IR (neat): 665.84, 730.52, 751.83, 764.33, 815.96, 828.78, 908.43, 951.3, 1003.08, 1014.01, 1082.18, 1174.57, 1229.68, 1404.17, 1449.55, 1482.21, 2245.89, 2822.4, 2897.65, 2938.74, 2982.55, 3027.52 cm^{-1}; LRMS (FAB+) *(m/z)*: $[M]^+$ calcd. for $C_{34}H_{32}BrClO_4$, 618.98; found, 619.7.

2-((1'S,1'''s,4's,4'''S)-4''''-chloro-1',1''',4',4'''-tetramethoxy-1',1''',4',4'''-tetrahydro-[1,1':4',1'':4'',1''':4''',1''''-quinquephenyl]-4-yl)-4,4,5,5-tetramethyl-1,3,2-dioxaborolane
16

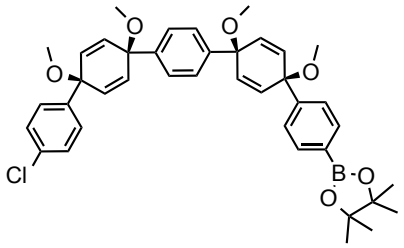

To a 50-mL flask equipped with a magnetic stir bar was added dihalide **15** (250 mg, 0.40 mmol, 1 equiv) and dry THF (25 mL). This solution was cooled to –78˚C. *n*-butyllithium (2.2 M in hexanes, 0.90 mL, 2.0 mmol, 5.0 equiv) was added to the solution dropwise and isopropoxyboronic acid pinacol ester (0.25 mL, 1.2 mmol, 3.0 equiv) was quickly injected immediately. The mixture was stirred 2 hours at –78˚C. H_2O (10 mL) was added to the mixture to quench and the solution was extracted with DCM (2 × 20 mL) and the combined organic layers were washed with H_2O (50 mL), and brine (50 mL) then dried over sodium sulfate and filtered. Solvent was removed under reduced pressure to yield a white solid that was adsorbed to a pad of silica gel washed with hexane, and the product was eluted with DCM which was removed under reduced pressure yielding a white solid (200 mg, 75%). ^{1}H NMR (500 MHz, Chloroform-*d*) δ(ppm) 7.75 (d, *J* = 8.4 Hz, 2H), 7.40 (d, *J* = 8.4 Hz, 2H), 7.35 (d, *J* = 8.8 Hz, 2H), 7.33 (d, *J* = 5.2 Hz, 2H), 7.31 (d, *J* = 5.2 Hz, 2H), 7.27 (d, *J* = 8.8 Hz, 2H), 6.11 (d, *J* = 10.3 Hz, 2H), 6.08 (s, 4H), 6.05 (d, *J* = 10.3 Hz, 2H), 3.43 (s, 3H), 3.42 (s, 3H), 3.42 (s, 3H), 3.41 (s, 3H), 1.33 (s, 12H). ^{13}C NMR (151 MHz, Chloroform-d) δ(ppm) 146.42, 142.88, 142.03, 134.91, 133.75, 133.71, 133.43, 133.37, 133.31, 133.28, 132.91, 128.51, 127.45, 126.10, 126.01, 125.29, 74.90, 74.65, 74.55, 74.46, 52.02, 51.99, 51.98, 51.97, 24.87; IR (neat): 659.32, 730.49, 829.09, 951.01, 1014.81, 1083.67, 1144.43, 1320.84, 1360.43, 1399.48, 1482.66, 1609.53, 2822.49, 2937.7, 2978.65 cm^{-1}; LRMS (FAB+) *(m/z)*: $[M]^+$ calcd. for $C_{40}H_{44}BClO_6$, 666.05; found, 669.9.

6-(4,4,5,5-tetramethyl-1,3,2-dioxaborolan-2-yl)naphthalen-2-ol **19**

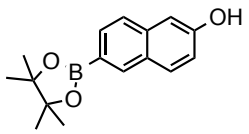

To a 250-mL flask equipped with a magnetic stir bar was added 6-bromo-naphthalen-2-ol **18** (5.00 g, 22.4 mmol, 1 equiv), bis(pinacolato)diboron (23.0 g, 89.6 mmol, 4 equiv), $Pd(OAc)_2$ (300 mg, 1.12 mmol, 0.05 equiv), SPhos (2.30 g, 5.60 mmol, 0.25 equiv), and ground, oven-dried K_3PO_4 (37.0 g, 179.2 mmol, 8 equiv). This flask was evacuated and backfilled with dry N_2 ten times to exclude moisture and air (crucial for the success of the procedure). Dry dioxane (100 mL) was added to the flask and the mixture stirred while heating to 90˚C for 4 hours. Mixture was cooled to room temperature, filtered through a pad of celite and concentrated under reduced pressure. The resulting semisolid was taken up in ethyl acetate (100 mL). This solution was washed with H_2O (2 × 100 mL) and brine (100 mL) then dried over sodium sulfate and filtered. Solvent was removed under reduced pressure and the crude solid was chromatographed on silica gel twice, each time in an ethyl acetate/hexane gradient of increasing polarity. These two identical columns were found to be more effective for the removal of bis(pinacolato)diboron than a single large column. The resulting product was a white solid (4.02 g, < 5% B_2Pin_2, 62% yield). ^{1}H NMR (500 MHz, Chloroform-d) δ(ppm) 8.29 (s, 1H), 7.80 – 7.75 (overlap, 2H), 7.64 (d, J = 8.5 Hz, 1H), 7.13 (d, J = 2.5 Hz, 1H), 7.08 (dd, J = 8.5, 2.5 Hz, 1H), 5.21 (br, 1H), 1.38 (s, 12H). Matches published data.[16]

6-((1'S,1'''s,4's,4'''S)-4''''-chloro-1',1''',4',4'''-tetramethoxy-1',1''',4',4'''-tetrahydro-[1,1':4',1'':4'',1''':4''',1''''-quinquephenyl]-4-yl)naphthalen-2-ol **20**

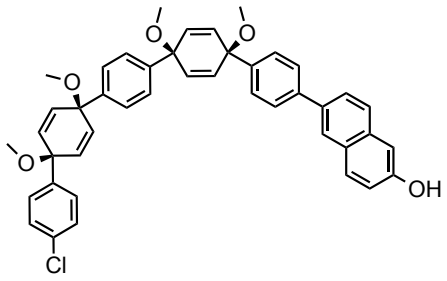

To a 50-mL flask equipped with a magnetic stir bar was added dihalide **15** (200 mg, 0.323 mmol, 1 equiv) *6-(4,4,5,5-tetramethyl-1,3,2-dioxaborolan-2-yl)naphthalen-2-ol* **19** (192 mg, 0.711 mmol, 2.2 equiv), and $Pd(dppf)_2Cl_2$ (14 mg, 0.0162 mmol, 0.05 equiv). This flask was evacuated and backfilled with dry N_2 five times to exclude moisture and air. Dry dioxane (13 mL) was added to the flask and the mixture stirred while heating to 90˚C. A sparged 0.25 M solution of K_3PO_4 in H_2O (7 mL, 1.75 mmol, 5.4 equiv) was added and the mixture was stirred at 90˚C overnight. Mixture was cooled to room temperature, filtered through a pad of celite and concentrated under reduced pressure. The resulting semisolid was taken up in ethyl acetate (20 mL). This solution was washed with H_2O (2 × 50 mL) and brine (50 mL) then dried over sodium sulfate and filtered. Solvent was removed under reduced pressure and the crude solid was chromatographed on silica gel in an ethyl acetate/DCM gradient of increasing polarity up to 1:1. The resulting product was a pale yellow solid that was washed with minimal acetone and dried under vacuum overnight (168 mg, 76%). ^{1}H NMR (500 MHz, Chloroform-d) δ(ppm) 7.94 (d, J = 1.7 Hz, 1H), 7.78 (d, J = 8.7 Hz, 1H), 7.71 (d, J = 8.5 Hz, 1H), 7.67 (dd, J = 8.6, 1.7 Hz, 1H), 7.63 (d, J = 8.4 Hz, 2H), 7.49 (d, J = 8.4 Hz, 2H), 7.40 (d, J = 8.5 Hz, 2H), 7.34 (d, J = 8.5 Hz, 2H), 7.30 (d, J = 8.7 Hz, 2H), 7.24 (d, J = 8.7 Hz, 2H), 7.11 (s, 1H), 7.09 (d, J = 8.7 Hz, 1H), 6.17 (d, J = 10.3 Hz, 2H), 6.12 (d, J = 10.3 Hz, 2H), 6.11 (d, J = 10.3 Hz, 2H), 6.03 (d, J = 10.3 Hz, 2H), 5.17 (s, 1H), 3.47 (s, 3H), 3.45 (s, 3H), 3.41 (s, 3H), 3.41 (s, 3H); ^{13}C NMR (126 MHz, Chloroform-d) δ(ppm) 153.56, 142.96, 142.52, 142.26, 141.97, 140.43, 135.89, 133.80, 133.63, 133.40, 133.35, 133.04, 130.16, 129.12, 128.47, 127.45, 127.20, 126.88, 126.48, 126.16, 126.04, 125.67, 118.20, 109.31, 74.74, 74.68, 74.62, 74.49, 52.11, 51.99.

6-((1'S,1'''s,4's,4'''S)-4''''-chloro-1',1''',4',4'''-tetramethoxy-1',1''',4',4'''-tetrahydro-[1,1':4',1'':4'',1''':4''',1''''-quinquephenyl]-4-yl)naphthalen-2-yl trifluoromethanesulfonate
21

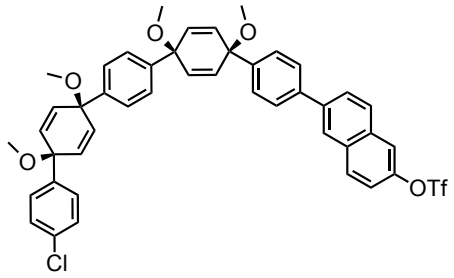

To a 100-mL flask equipped with a magnetic stir bar was added free alchohol **20** (590 mg, 0.860 mmol, 1 equiv) and ground, oven-dried K_2CO_3 (193 mg, 1.40 mmol, 1.6 equiv). Dry THF (50 mL) was added to the flask and the mixture stirred to dissolve **20**. Solid N-Phenyl-bis(trifluoromethanesulfonimide) (1.54 g, 4.32 mmol, 5 equiv) was added quickly in one portion to the reaction mixture. This mixture was stirred at room temperature overnight. Ethyl acetate (50 mL) and H_2O (50 mL) were added to the reaction mixture, the layers were separated and the aqueous layer extracted with ethyl acetate (2 × 20 mL). The combined organic aliquots were washed with H_2O (2 × 100 mL) and brine (100 mL) then dried over sodium sulfate and filtered. Solvent was removed under reduced pressure and the crude solid taken up in minimal DCM with an equivalent volume of hexanes. The DCM was removed under reduced pressure to precipitate the product as a tan solid that was filtered off and washed with hexanes and H_2O. This solid was taken up in THF (50 mL) then dried over sodium sulfate and filtered. Solvent was removed under reduced pressure yielding a white solid (617 mg, 88%). ^{1}H NMR (500 MHz, Chloroform-d) δ(ppm) 8.07 (s, 1H), 7.97 (d, J = 9.0 Hz, 1H), 7.94 (d, J = 8.6 Hz, 1H), 7.84 (dd, J = 8.6, 1.8 Hz, 1H), 7.77 (d, J = 2.5 Hz, 1H), 7.65 (d, J = 8.4 Hz, 2H), 7.53 (d, J = 8.4 Hz, 2H), 7.40 (d, J = 8.7 Hz, 2H), 7.39 (dd, J = 9.0, 2.5 Hz, 1H), 7.34 (d, J = 8.5 Hz, 2H), 7.31 (d, J = 8.7 Hz, 2H), 7.24 (d, J = 8.6 Hz, 2H), 6.16 (d, J = 11.0 Hz, 2H), 6.13 (d, J = 11.0 Hz, 2H), 6.11 (d, J = 10.3 Hz, 2H), 6.03 (d, J = 10.3 Hz, 2H), 3.48 (s, 3H), 3.45 (s, 3H), 3.41 (s, 6H); ^{19}F NMR (471 MHz, Chloroform-d) δ(ppm) –72.73; 13C NMR (151 MHz, Chloroform-d) δ(ppm) 147.09, 143.21, 142.88, 142.59, 142.02, 139.51, 133.61, 133.52, 133.31, 133.28, 133.08, 132.65, 132.45, 130.84, 128.55, 128.43,

127.44, 127.42, 127.33, 126.65, 126.12, 126.03, 125.63, 119.99, 119.03, 74.66, 74.62, 74.59, 74.45, 52.06, 52.03, 52.02, 52.00; IR (neat): 666.24, 730.56, 760.38, 793.24, 809.08, 830.1, 863.31, 921.65, 952.1, 1013.84, 1027.97, 1082.13, 1108.2, 1141.82, 1180, 1213.51, 1249.3, 1404.17, 1423.13, 1450.53, 1468.59, 1500.69, 1604.58, 2823.37, 2898.38, 2939.63, 2983.25, 3027.68 cm^{-1}; LRMS (FAB+) *(m/z)*: $[M]^+$ calcd. for $C_{45}H_{32}ClF_3O_7S$, 814.30; found, 814.0.

4,4,5,5-tetramethyl-2-(6-((1'S,1'''s,4's,4'''S)-1',1''',4',4'''-tetramethoxy-4''''-(4,4,5,5-tetramethyl-1,3,2-dioxaborolan-2-yl)-1',1''',4',4'''-tetrahydro-[1,1':4',1'':4'',1''':4''',1''''-quinquephenyl]-4-yl)naphthalen-2-yl)-1,3,2-dioxaborolane **22**

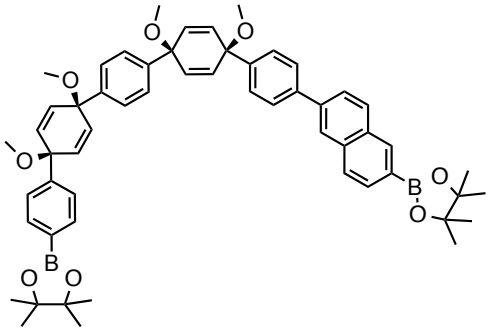

To a 25-mL flask equipped with a magnetic stir bar was added chloro-triflate **21** (50.0 mg, 0.0610 mmol, 1 equiv), bis(pinacolato)diboron (124 mg, 0.488 mmol, 8 equiv), $Pd(OAc)_2$ (2.0 mg, 0.061 mmol, 0.10 equiv), SPhos (7.0 mg, 0.15 mmol, 0.25 equiv), and ground, oven-dried K_3PO_4 (206 mg, 0.976 mmol, 16 equiv). This flask was evacuated and backfilled with dry N_2 ten times to exclude moisture and air (crucial for the success of the procedure). Dry dioxane (5 mL) was added to the flask and the mixture stirred while heating to 90˚C overnight. Mixture was cooled to room temperature, filtered through a pad of celite and concentrated under reduced pressure. The resulting semisolid was taken up in ethyl acetate (10 mL). This solution was washed with H_2O (2 × 10 mL) and brine (10 mL) then dried over sodium sulfate and filtered. Solvent was removed under reduced pressure and the crude solid was chromatographed on silica gel in an ethyl acetate/hexane gradient of increasing polarity up to 2:3. The resulting product was a white solid (28 mg, 52% yield). ^1H NMR (600 MHz, Chloroform-d) δ(ppm) 8.37 (s, 1H), 8.01 (s, 1H), 7.93

(d, J = 9.0 Hz, 1H), 7.86 (d, J = 8.2 Hz, 1H), 7.84 (d, J = 8.2 Hz, 1H), 7.75 (d, 2H), 7.72 (dd, J = 8.5, 1.8 Hz, 1H), 7.68 (d, J = 8.3 Hz, 2H), 7.51 (d, J = 8.4 Hz, 2H), 7.42 – 7.34 (overlap, 6H), 6.16 (d, J = 10.4 Hz, 2H), 6.13 (d, J = 10.4 Hz, 2H), 6.09 (d, J = 10.4 Hz, 2H), 6.07 (d, J = 10.4 Hz, 2H), 3.47 (s, 3H), 3.45 (s, 3H), 3.42 (s, 3H), 3.41 (s, 3H), 1.40 (s, 12H), 1.29 (s, 12H); ^{13}C NMR (151 MHz, Chloroform-d) δ(ppm) 146.42, 142.76, 142.73, 142.71, 140.20 139.16, 135.93, 135.25, 134.90, 133.47, 133.31, 133.25, 133.24, 131.97, 130.83, 129.12, 127.45, 127.28, 126.51, 126.09, 126.06, 125.58, 125.51, 125.29, 83.93, 83.75, 74.92, 74.71, 74.67, 74.64, 52.02 52.00, 51.96, 51.95, 24.94, 24.81.

(41S,44s,61S,64s)-41,44,61,64-tetramethoxy-1(2,6)-naphthalena-2,3,5(1,4)-tribenzena-4,6(1,4)-dicyclohexanacyclohexaphane-42,45,62,65-tetraene **23**

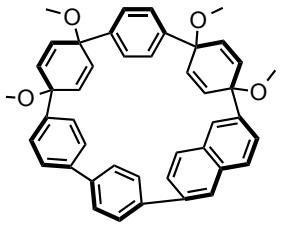

To a 250-mL flask equipped with a magnetic stir bar was added diboronate **22** (200 mg, 0.230 mmol, 1 equiv), boric acid (71.1 mg, 1.15 mmol, 5 equiv) and THF (120 mL). The resulting solution was stirred until all the solid was in solution at which point bis(triphylphosphine)palladium(II) dichloride (7.7 mg, 0.011 mmol, 0.05 equiv) was added followed by H_2O (20 mL). To this yellow solution was added potassium fluoride (22.0 mg, 0.230 mmol, 1 equiv). The solution gradually turned bright orange over two hours and was allowed to stir open to air and at room temperature for an additional ten hours at which point palladium black had coated the inside of the flask. The crude reaction mixture was filtered through a pad of Celite to remove palladium. This filter cake was washed with dichloromethane (100 mL). The solution was extracted with dichloromethane (2 × 300 mL) and the resulting organic phase was washed with brine (500 mL). The organic phase was then dried over sodium sulfate and solvent was removed at reduced pressure to give a yellow solid. This yellow solid was purified by GPC to provide the NMR evidence for trace macrocycle formation.

6-(4,4,5,5-tetramethyl-1,3,2-dioxaborolan-2-yl)naphthalen-2-yl pivalate **25**

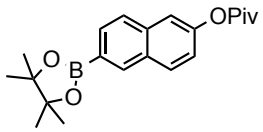

To a 100-mL flask equipped with a magnetic stir bar was added bromo-pivalate **24** (5.0 g, 16.3 mmol, 1 equiv), bis(pinacolato)diboron (6.22 g, 24.5 mmol, 1.5 equiv), $Pd(dppf)_2Cl_2$ (120 mg, 0.163 mmol, 0.01 equiv), and ground, oven-dried K_3PO_4 (7.80 g, 36.7 mmol, 2.25 equiv). This flask was evacuated and backfilled with dry N_2 ten times to exclude moisture and air (crucial for the success of the procedure). Dry dioxane (50 mL) was added to the flask and the mixture stirred while heating to 90˚C overnight. Mixture was cooled to room temperature, filtered through a pad of celite and concentrated under reduced pressure. The resulting semisolid was taken up in ethyl acetate (50 mL). This solution was washed with H_2O (2 × 50 mL) and brine (50 mL) then dried over sodium sulfate and filtered. Solvent was removed under reduced pressure and the crude solid was chromatographed on silica gel twice, each time in an ethyl acetate/hexane gradient of increasing polarity. These two identical columns were found to be more effective for the removal of bis(pinacolato)diboron than a single large column. The resulting product was a white crystalline solid (4.78 g, 83%). ^{1}H NMR (300 MHz, Chloroform-d) δ(ppm) 8.36 (s, 1H), 7.88 (d, J = 8.8 Hz, 1H), 7.84 (dd, J = 8.3, 1.2 Hz, 1H), 7.77 (d, J = 8.3 Hz, 1H), 7.52 (d, J = 2.3 Hz, 1H), 7.19 (dd, J = 8.8, 2.3 Hz, 1H), 1.40 (s, 9H), 1.39 (s, 12H); ^{13}C NMR (151 MHz, Chloroform-d) δ(ppm) 177.16, 149.73, 136.09, 135.55, 131.17, 130.80, 130.16, 126.75, 126.04 (br), 121.20, 118.31, 39.21, 27.24, 25.09, 24.99; IR (neat): 692.58, 707.18, 734.41, 820.97, 838.25, 849.74, 858.53, 903.9, 915.84, 923.93, 962.09, 1028.96, 1081.32, 1108.17, 1126.96, 1142.97, 1175.05, 1194.87, 1242.98, 1288.73, 1306.81, 1341.23, 1372.06, 1382.25, 1402.27, 1478.55, 1630.17, 1751.93, 2873.39, 2933.97, 2978.3, 3055.43 cm^{-1}; LRMS (FAB+) *(m/z)*: $[M]^+$ calcd. for $C_{21}H_{26}BO_4$, 353.20; found, 353.5.

6-((1'S,1'''s,4's,4'''S)-4''''-chloro-1',1''',4',4'''-tetramethoxy-1',1''',4',4'''-tetrahydro-[1,1':4',1'':4'',1''':4''',1''''-quinquephenyl]-4-yl)naphthalen-2-yl pivalate **20**

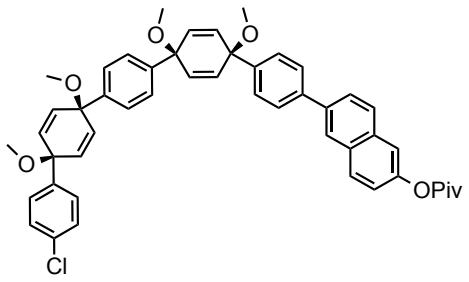

To a 250-mL flask equipped with a magnetic stir bar was added dihalide **16** (2.00 g, 3.20 mmol, 1 equiv) *6-(4,4,5,5-tetramethyl-1,3,2-dioxaborolan-2-yl)naphthalen-2-yl pivalate* **25** (1.70 g, 4.80 mmol, 1.5 equiv), $Pd(dppf)_2Cl_2$ (150 mg, 0.160 mmol, 0.05 equiv), and ground, oven-dried $NaHCO_3$ (1.34 g, 16.0 mmol, 5 equiv). This flask was evacuated and backfilled with dry N_2 five times to exclude moisture and air. Dry dioxane (100 mL) was added to the flask and the mixture stirred while heating to 90˚C. Sparged H_2O (10 mL) was added and the mixture was stirred at 90˚C overnight. Mixture was cooled to room temperature, filtered through a pad of celite and concentrated under reduced pressure. The resulting semisolid was taken up in DCM (50 mL). This solution was washed with H_2O (2 × 50 mL) and brine (50 mL) then dried over sodium sulfate and filtered. Solvent was removed under reduced pressure and the crude solid was chromatographed on silica gel in an ethyl acetate/hexanes gradient of increasing polarity up to 1:1. The resulting product was a crystalline white solid (1.08 g, 44%). ^{1}H NMR (500 MHz, Chloroform-d) δ(ppm) 8.02 (s, 1H), 7.89 (d, J = 8.8 Hz, 1H), 7.85 (d, J = 8.5 Hz, 1H), 7.74 (dd, J = 8.5, 1.8 Hz, 1H), 7.66 (d, J = 8.4 Hz, 2H), 7.54 (d, J = 2.3 Hz, 1H), 7.51 (d, J = 8.4 Hz, 2H), 7.40 (d, J = 8.5 Hz, 2H), 7.34 (d, J = 8.5 Hz, 2H), 7.31 (d, J = 8.6 Hz, 2H), 7.24 (d, J = 8.6 Hz, 2H), 7.22 (dd, J = 8.8, 2.3 Hz, 1H), 6.16 (d, J = 10.4 Hz, 2H), 6.12 (d, J = 10.4 Hz, 2H), 6.11 (d, J = 10.3 Hz, 2H), 6.03 (d, J = 10.3 Hz, 2H), 3.47 (s, 3H), 3.45 (s, 3H), 3.41 (s, 3H), 3.41 (s, 3H), 1.41 (s, 9H); 13C NMR (126 MHz, Chloroform-d) δ(ppm) 177.38, 149.01, 143.09, 142.79, 142.70, 142.14, 140.28, 138.00, 133.78, 133.52, 133.52, 133.48, 133.18, 133.12, 131.74, 129.72, 128.59, 128.23, 127.58, 127.48, 126.67, 126.34, 126.27, 126.17, 125.75, 121.74, 118.33, 74.81, 74.80, 74.72, 74.61, 52.18, 52.14, 39.31, 27.35; LRMS (FAB+) *(m/z)*: $[M]^+$ calcd. for $C_{49}H_{46}ClO_6$, 766.36; found, 766.1.

III.6.3. Computation Details

All calculations were carried out with Gaussian 09 package at B3LYP/6-31g* or M062X/6-31G* level of theory.[17] All excited state calculations (TD-DFT) were performed on fully optimized (B3LYP/6-31G*) structures. The fully optimized structures were confirmed to be true minima by vibrational analysis. Structures were minimized with no symmetry restrictions. Structures are depicted with their geometries, HOMO and LUMO orbitals followed by a summary their of total energy in Hartree unless noted. Relevant computational data are depicted in Figures **III.6-III.10**. For computational coordinates, see Appendix **I**.

2,6-naphthyl-[6]CPP

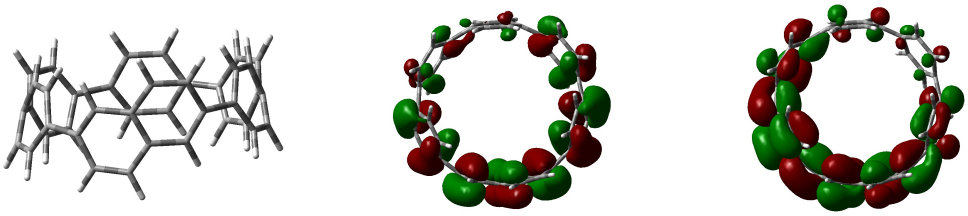

Figure III.6. DFT visualization of 2,6-naphthyl-[6]CPP. Left to right: geometry, HOMO, LUMO.

HOMO (eV) = -5.13

LUMO (eV) = -1.63

HOMO/LUMO gap (eV) = 3.50

Zero-point correction = 0.530646 (Hartree/Particle)

Thermal correction to Energy = 0.558581

Thermal correction to Enthalpy = 0.559525

Thermal correction to Gibbs Free Energy = 0.474596

Sum of electronic and zero-point Energies = -1539.312029

Sum of electronic and thermal Energies = -1539.284094

Sum of electronic and thermal Enthalpies = -1539.283149

Sum of electronic and thermal Free Energies = -1539.368079

1,4-naphthyl-[6]CPP

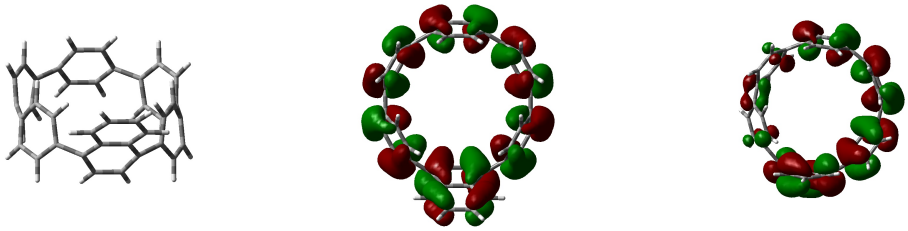

Figure III.7. DFT visualization of 1,4-naphthyl-[6]CPP. Left to right: geometry, HOMO, LUMO.

HOMO (eV) = -4.83

LUMO (eV) = -1.85

HOMO/LUMO gap (eV) = 2.98

Zero-point correction = 0.530431 (Hartree/Particle)

Thermal correction to Energy = 0.558447

Thermal correction to Enthalpy = 0.559391

Thermal correction to Gibbs Free Energy = 0.474430

Sum of electronic and zero-point Energies = -1539.301046

Sum of electronic and thermal Energies = -1539.273030

Sum of electronic and thermal Enthalpies = -1539.272086

Sum of electronic and thermal Free Energies = -1539.357047

1,5-naphthyl-[6]CPP

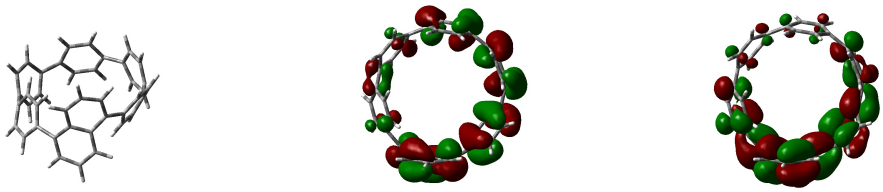

Figure III.8. DFT visualization of 1,5-naphthyl-[6]CPP. Left to right: geometry, HOMO, LUMO.

HOMO (eV) = -5.05

LUMO (eV) = -1.80

HOMO/LUMO gap (eV) = 3.25

Zero-point correction = 0.530430 (Hartree/Particle)

Thermal correction to Energy = 0.558471

Thermal correction to Enthalpy = 0.559415

Thermal correction to Gibbs Free Energy = 0.474008

Sum of electronic and zero-point Energies = -1539.291008

Sum of electronic and thermal Energies = -1539.262967

Sum of electronic and thermal Enthalpies = -1539.262023

Sum of electronic and thermal Free Energies = -1539.347430

2,6-naphthyl-[6]CPP dimer macrocycle

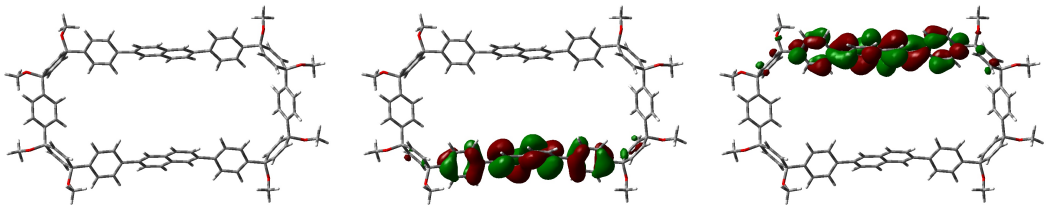

Figure III.9. DFT visualization of 2,6-naphthyl-[6]CPP dimer macrocycle. Left to right: geometry, HOMO, LUMO.

HOMO (eV) = -5.53

LUMO (eV) = -1.38

HOMO/LUMO gap (eV) = 4.15

Zero-point correction = 1.411831 (Hartree/Particle)

Thermal correction to Energy = 1.494781

Thermal correction to Enthalpy = 1.495725

Thermal correction to Gibbs Free Energy = 1.285373

Sum of electronic and zero-point Energies = -3999.263544

Sum of electronic and thermal Energies = -3999.180595

Sum of electronic and thermal Enthalpies = -3999.179650

Sum of electronic and thermal Free Energies = -3999.390003

2,6-naphthyl-[6]CPP dimer

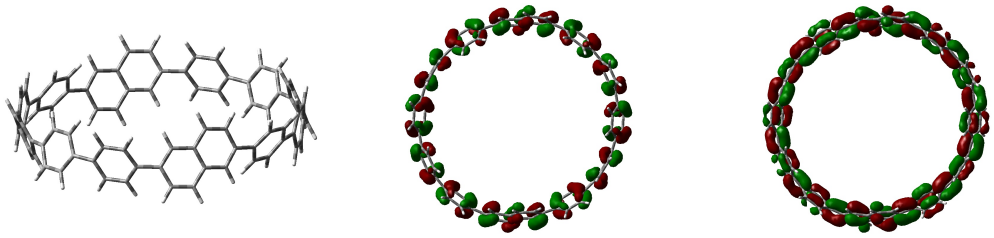

Figure III.10. DFT visualization of 2,6-naphthyl-[6]CPP dimer. Left to right: geometry, HOMO, LUMO.

HOMO (eV) = -5.21

LUMO (eV) = -1.72

HOMO/LUMO gap (eV) = 3.5

Zero-point correction = 1.064793 (Hartree/Particle)

Thermal correction to Energy = 1.123798

Thermal correction to Enthalpy = 1.124742

Thermal correction to Gibbs Free Energy = 0.968002

Sum of electronic and zero-point Energies = -3078.837502

Sum of electronic and thermal Energies = -3078.778497

Sum of electronic and thermal Enthalpies = -3078.777553

Sum of electronic and thermal Free Energies = -3078.934293

III.6.4. X-Ray Crystallographic Data

Structures are presented as an ORTEP plot of the molecule, spacefilling model of the packing, and relevant parameters. Relevant crystallographic data are depicted in Figure **III.11**.

1,5-naphthyl-[6]CPP

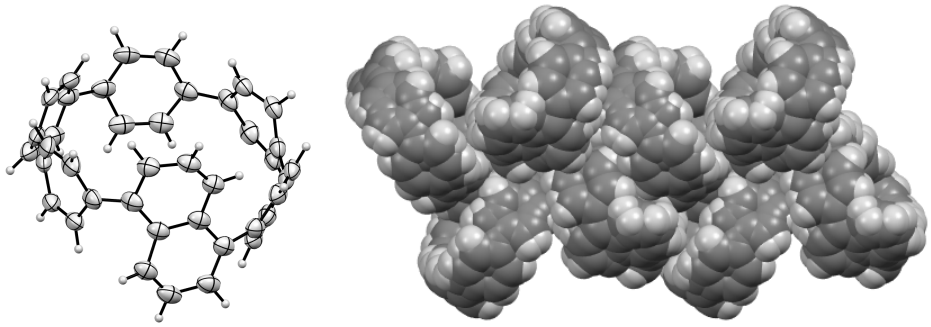

Figure III.11. X-ray structure of 1,5-naphthyl-[6]CPP. ORTEP plot at 50% probability (left) and packing (right).

Empirical formula	$C_{40}H_{26}$
Formula weight	506.61
Temperature/K	100(2)
Crystal system	N/A
Space group	$P2_1/n$
a/Å	11.8843(4)
b/Å	16.9117(5)
c/Å	15.5011(5)
α/°	90.00
β/°	105.959(2)
γ/°	90.00
Volume/Å^3	2995.39(17)
Z	4
ϱ_{calc}g/cm^3	1.123
μ/mm^{-1}	0.482
F(000)	1064.0
Crystal size/mm^3	0.147 × 0.120 × 0.041
Radiation	CuKα (λ = 1.54178)
2Θ range for data collection/°	7.9 to 132.18
Index ranges	$-14 \le h \le 9, 0 \le k \le 19, -8 \le l \le 18$
Reflections collected	5205
Independent reflections	5205 [R_{int} = 0.0296, R_{sigma} = N/A]
Data/restraints/parameters	5205/115/482
Goodness-of-fit on F^2	1.101
Final R indexes [I>=2σ (I)]	R_1 = 0.0540, wR_2 = 0.1563
Final R indexes [all data]	R_1 = 0.0601, wR_2 = 0.1618
Largest diff. peak/hole / e Å^{-3}	0.25/-0.19

CHAPTER IV
PHOTOSWITCHABLE CYCLOPARAPHENYLENES

This chapter is based on my unpublished work. Editing was provided by Prof. Ramesh Jasti.

Cycloparaphenylenes have been praised for their tunable HOMO/LUMO gap and therefore electronic and optical properties, and have generated significant interest for small-molecule electronics. Another fascinating but little explored prospect for CPPs involves exploiting their hollow geometry. With a rigid pore of tunable size and high electron density arising from the inward facing π-orbitals, CPPs are ideal for supramolecular host-guest applications. [10]CPP in particular has shown very high binding affinity for fullerene C_{60}. Our stepwise syntheses of CPPs allow for the design of a molecular container with a pore size, and therefore binding affinity, that can be controlled by external stimuli. Herein we report the synthesis of several CPPs containing photoswitchable azobenzene moieties in the conjugated framework and preliminary results evaluating their performance as reversible molecular containers.

IV.1. Background

Curved belts with inward facing π-orbitals (see Chapter **I**) have established use as molecular containers. The electron rich pore in these molecules is an ideal host for electron deficient guests.[1] The rigid, circular, electron-rich pores in cycloparaphenylacetylenes (CPPAs) and cycloparaphenylenes perfectly compliment the convex electron-poor exterior of fullerenes. [6]CPPA and [10]CPP in particular form strong host-guest complexes with buckminsterfullerene C_{60}.[1a, 2] CPPs have also shown promise for encapsulating C_{70} and metallofullerenes like Gd@C_{82} and Li@C_{60}.[3] Indeed, the world-record for binding affinity to C_{60}, a remarkable *log* K_a of 9.7 in dichloromethane, is held by a benzannulated nanohoop synthesized by Isobe.[4]

High binding affinity is only one of a set of desirable features in a molecular container. The ability to capture and release a guest has obvious usefulness for the reversible purification and separation of molecules via supramolecular interactions. One approach that has been widely applied to achieve this reversibility is the incorporation of a photoswitchable moiety into the framework of the container.[5] Though occasionally other photoresponsive moieties are used[6], taking advantage of the *cis-trans* photoisomerization of azobenzene has proved to be one of the simplest and most effective ways to open and close molecular containers (Scheme **IV.1**). The earliest examples of this approach were applied to cyclodextrins[7] and crown ethers.[8] It has since been successfully employed to control the binding affinities of more complex synthetic molecular containers including dendrimers[9], cavitands[10], cryptands[11], and calixarenes[12].

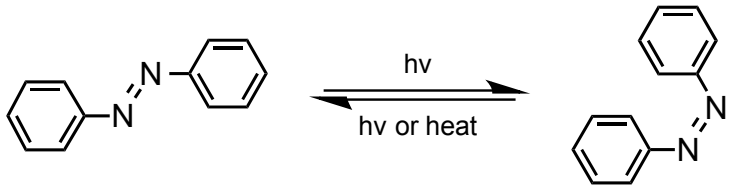

Scheme IV.1. *Cis-trans* isomerization of azobenzene, a light-activated molecular switch.

IV.2. Synthesis of azo[11]CPP

The original approach to the construction of a photoswitchable nanohoop was inspired by the selective syntheses developed in our lab and published in 2012.[13] To incorporate an azobenzene moiety into the CPP backbone, we envisioned using nine-ring dichloride **5** which was previously coupled to diboronate **3** en route to [12]CPP, **1**. By using the as-yet-unknown 4,4′-bisboronic acid pinacol ester azobenzene **4** in place of **3**, an azobenzene could replace the terphenyl in [12]CPP, resulting in *azo*[11]CPP as the nanohoop product (Scheme **IV.2**).

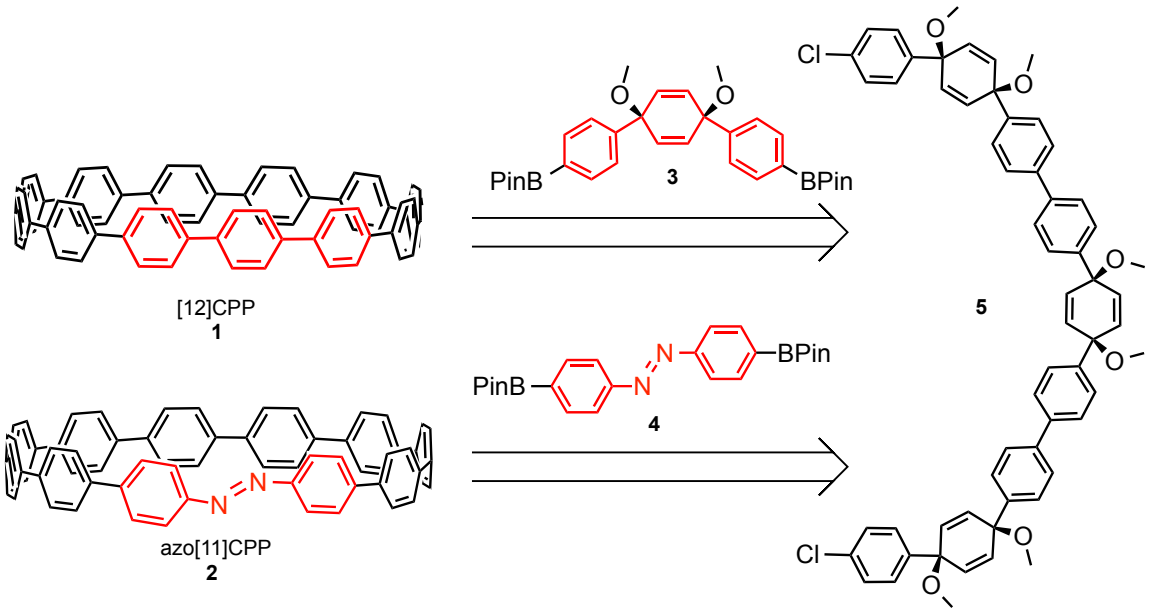

Scheme IV.2. Retrosynthetic strategies towards [12]CPP and *azo*[11]CPP from a common intermediate via Suzuki-Miyura macrocyclization followed by sodium naphthalenide reduction. Atoms which end up in the resulting CPP from **3** and **4** are highlighted in red.

This azo[11]CPP should preferentially adopt a lower-energy *cis* conformation to relieve strain. With a teardrop geometry, *cis*-azo[11]CPP (Scheme **IV.3**) has a narrower cavity than the higher-energy, circular *trans* conformation (13.0 Å at its narrowest diameter versus 15.7 Å in *trans*-azo[11]CPP based on B3LYP/6-31G* calculations). Irradiation, in principle, will allow for the control of the ratio of these "closed" and "open" hoops in solution or the solid state and therefore the capture and release of suitably sized guests. Energy calculations predict that at room temperature (298K), assuming thermal isomerization is kinetically accessible, azo[11]CPP should have a *cis* to *trans* ratio of about 3.5:1. Thus it seems that the strain added by cyclization does not contribute significantly to the instability of either isomer.

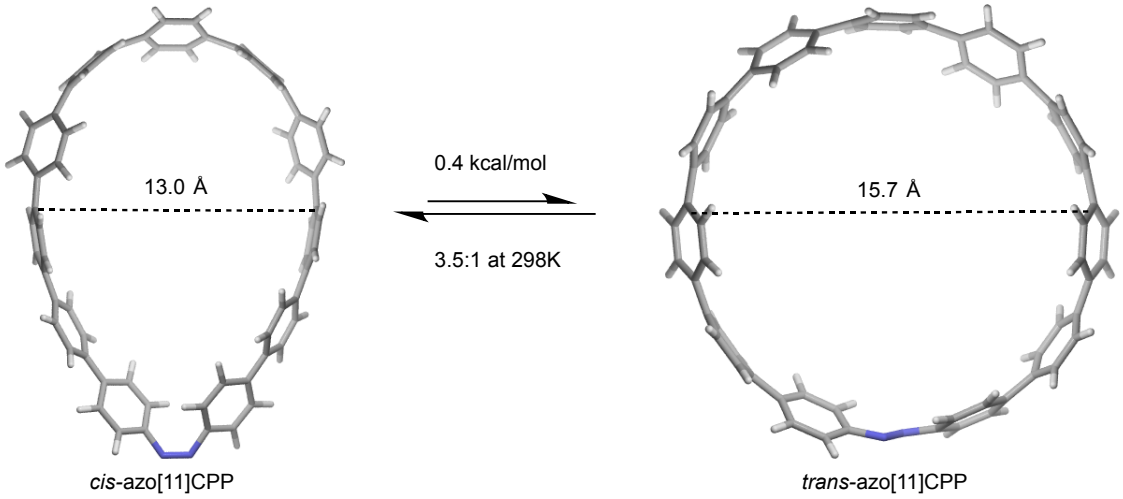

Scheme IV.3. DFT geometries (B3LYP/6-31G*), shortest cavity diameters, and room temperature ratio of azo[11]CPP isomers.

This initial synthetic plan required the synthesis of diboronate **4**, which was accessible via the palladium-catalyzed Miyura borylation of 4,4′-dibromoazobenzene, **6** (Scheme **IV.4**). Azobenzene **6** was synthesized by the oxidative coupling of 4-bromoaniline with broad precedent in the literature for the synthesis of this and other symmetric azobenzenes.[14] It should be noted that lithium-halogen exchange of **6** for conversion to **4** by addition to isopropoxyboronic acid pinacol ester failed and instead resulted in the addition of alkyllithium reagent to the azo bond.[15] This borylation suffered from low yield and tedious purification, and it was therefore decided to approach a nine-ring diboronate analogue of **5** instead. Diboronate **4**, which was unprecedented at the time, has since been reported by Rebek, et al. in the synthesis of a photoswitchable cavitand molecular contiainer.[16]

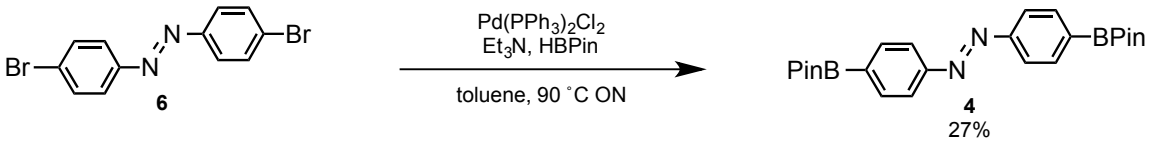

Scheme IV.4. Synthesis of diboronate azobenzene **4**.

The synthesis of a nine-ring diboronate was accomplished in five steps from commercially available alcohol **7** (Scheme **IV.5**). TMS protection of **7** to **8** followed by

PIDA oxidation afforded quinol **9** to which 4-bromophenyllithium could be added and **10**, the product of preferential *syn* addition was obtained. The differentiated halides on **10** allowed for preferential reaction of the iodide with diboronate **3** under Suzuki coupling conditions to give nine-ring dibromide **11** in 56% yield with much of the excess **10** reisolated along with the product. This new dibromide could be borylated without the need for palladium, using *n*-butyllithium and isopropoxyboronic acid pinacol ester, several hundred milligrams of diboronate **12** were synthesized for exploration of the intermolecular macrocyclization.

The desired macrocycle was formed in 13% yield from diboronate **12** and 4,4′-dibromoazobenzene, **6**. Typical sodium naphthalenide reductive aromatization proceeded cleanly to give the desired nanohoop, azo[11]CPP (**2**) as a bright orange solid with a weak fluorescence in solution.

In light of the low yield of the intermolecular macrocyclization, an attempt was made to use the oxidative azobenzene formation as an intramolecular macrocyclization from a corresponding linear dianiline. Though the oxidative coupling usually requires pressing conditions, it has precedence in macrocycle synthesis and shouldn't decompose the cyclohexadienes on the linear fragments.[17] However, attempts to couple 4-aminophenylboronic acid pinacol ester **14** to dichloride **5** resulted in consumption of starting material and isolation of an insoluble deep red tar presumed to be aromatized products. The electron-donating amine termini on the Suzuki product likely facilitates the ejection of a methyl ether and subsequent *meta*-shift of the cyclohexadienes to form the corresponding anisoles. To investigate this, a simpler system was devised. Protection of 4-bromoaniline as the dimethyl pyrrole[18] followed by lithium halogen exchange and addition into bromo-quinol **15** yielded several hundred milligrams of **16** (Scheme **IV.6**). All attempts to deprotect the pyrrole with hydroxylamine hydrochloride resulted in the observation of a yellow product which rapidly turned red at room temperature in solution. Both ^{1}H and ^{13}C NMR confirmed the absence of alkenes in the resulting decomposed product. Other protecting groups such as 1,2-bis(dimethylsilyl)ethane (STABASE) gave similar results upon deprotection. As such, the intramolecular azobenzene formation was abandoned as a macrocyclization strategy.

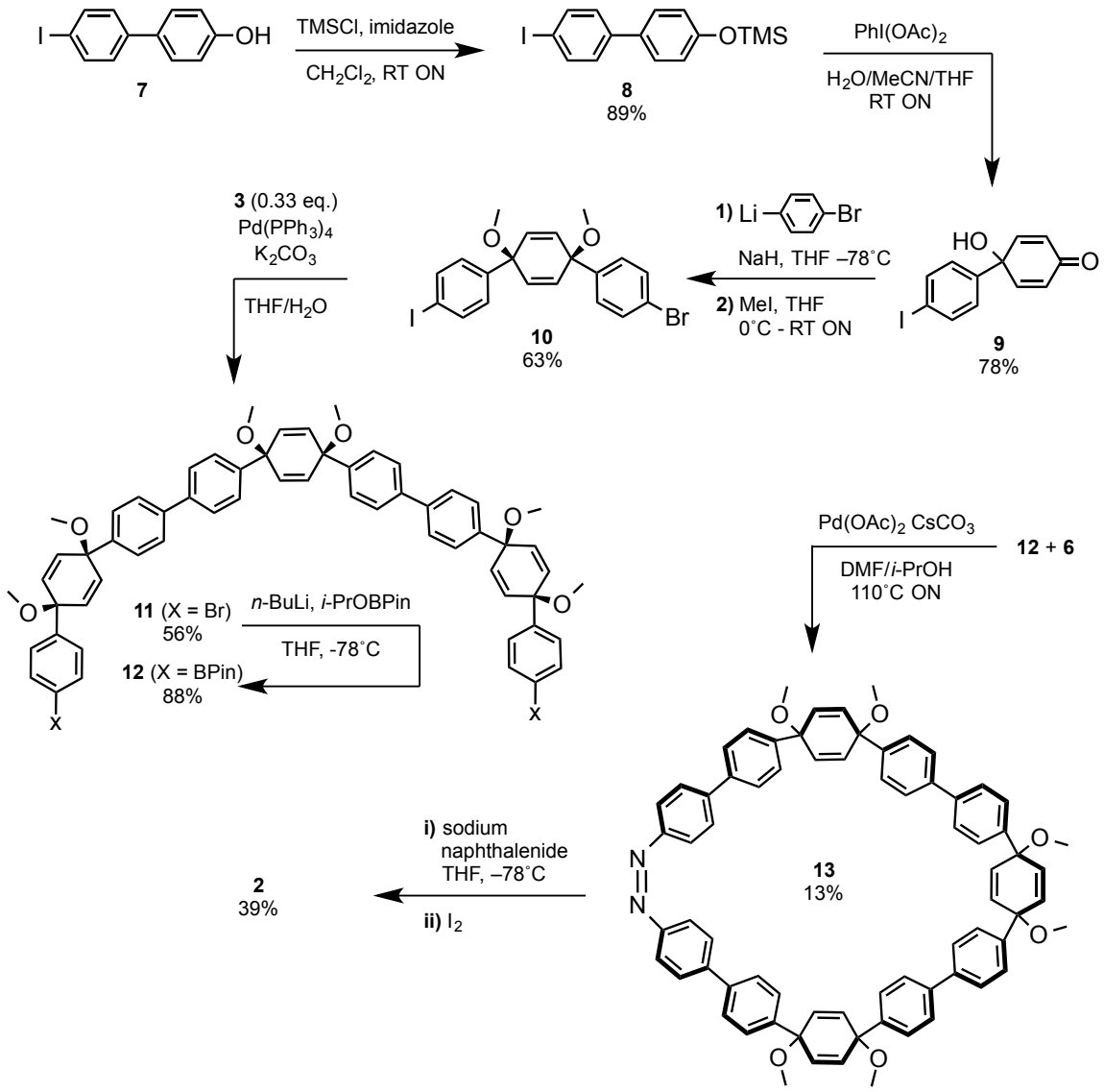

Scheme IV.5. Synthesis of azo[11]CPP.

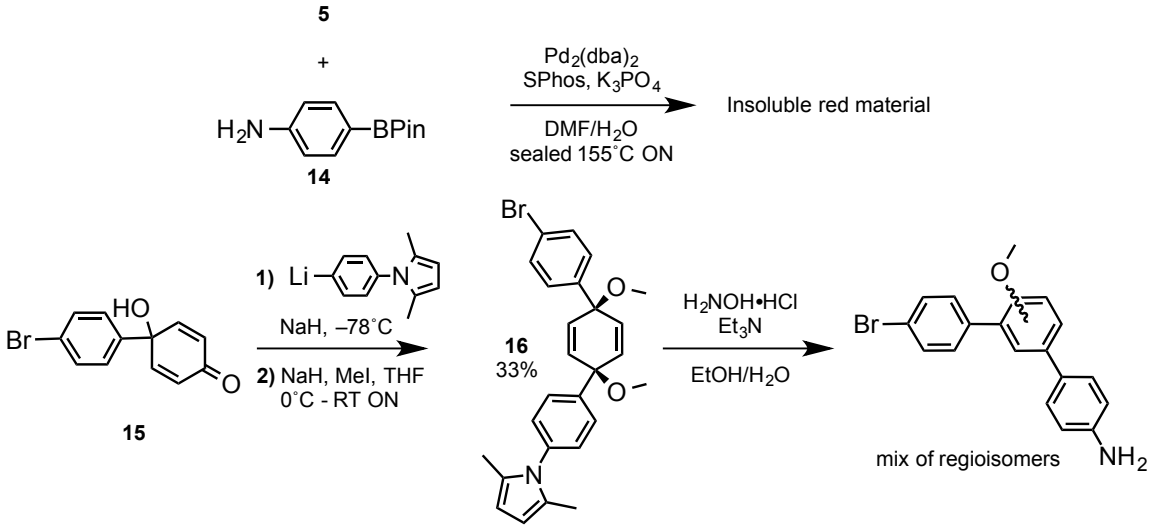

Scheme IV.6. Attempts towards an amine-terminated macrocycle precursor and investigation of cyclohexadiene stability in a three-ring model system.

IV.3. Synthetic Efforts Towards azo[7]CPP

Originally, synthesis targeted azo[11]CPP based on availability of starting materials and the state of CPP synthetic technology at the time. During the synthesis of [5]CPP (Chapter **II**) it became apparent that azo[7]CPP was now a more viable target and might be accessible on a much larger scale than azo[11]CPP. Intermolecular macrocyclization was attempted with dibromoazobenzene **6** and the same five-ring diboronate that furnished the [5]CPP macrocycle through intramolecular homocoupling, **17** (Scheme **IV.7**), using Buchwald's SPhos Pd generation 2 precatalyst.[19] However, none of the desired macrocycle **18** was isolated from this reaction.

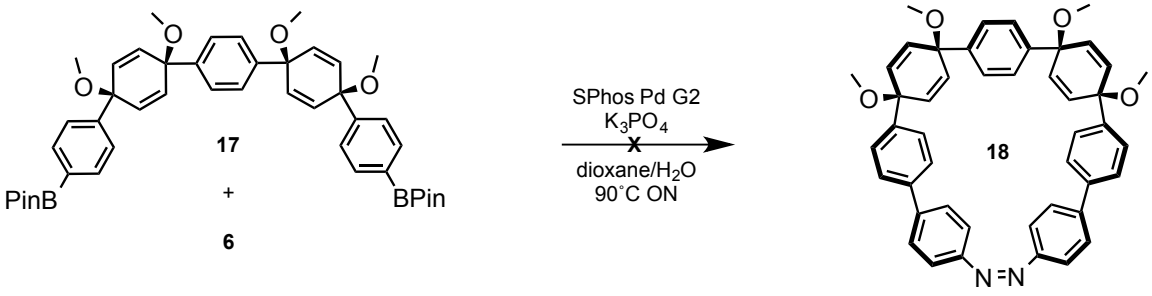

Scheme IV.7. Failed intramolecular macrocyclization towards **18**.

Upon further investigation, it was determined that the major product of this macrocyclization was the hourglass shaped all-*trans* diazobenzene macrocycle **19** arising from the coupling of two equivalents of **17** with two equivalents of **6** (Scheme **IV.8**).

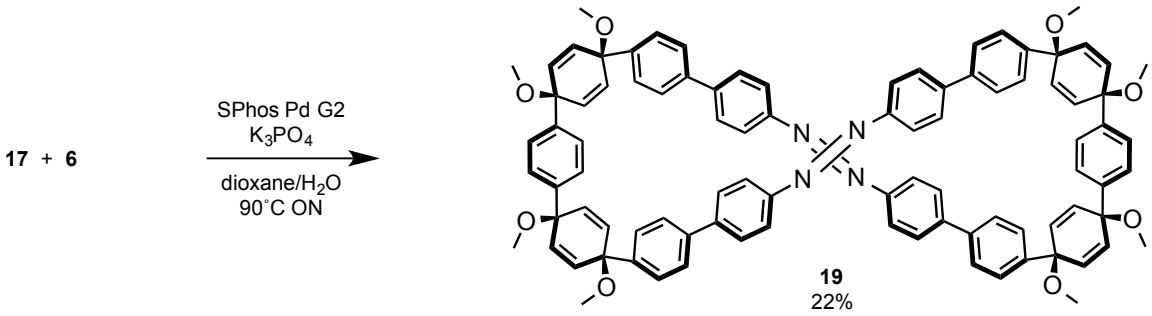

Scheme IV.8. Synthesis of dimeric novel macrocycle **19**.

X-ray Diffraction Crystallography (XRD) confirmed this structure and showed that the azobenzene nitrogen-nitrogen double bonds are in extremely close contact in the solid state (3.2 Å, Figure **IV.1**). Additionally, these molecules pack tightly into a solvent-free lattice.

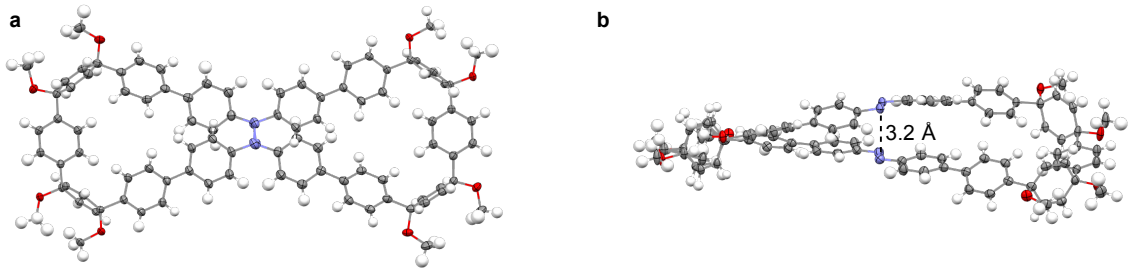

Figure IV.1. Crystal structure of macrocycle **19**. **a**, "Top" view showing hourglass structure and *trans*-azobenzene geometry. **b**, "Side" view showing proximity of nitrogen atoms. ORTEP ellipsoids at 50% probability. No solvent was present in the crystal lattice.

Owing to the high molecular weight and calculated flattened all-*cis* structure of the expected polyphenylene product (Figure **IV.2**), the treatment of **19** with sodium naphthalenide returned a fluorescent yellow-orange solid that was extremely insoluble thus uncharacterizable by NMR or XRD.

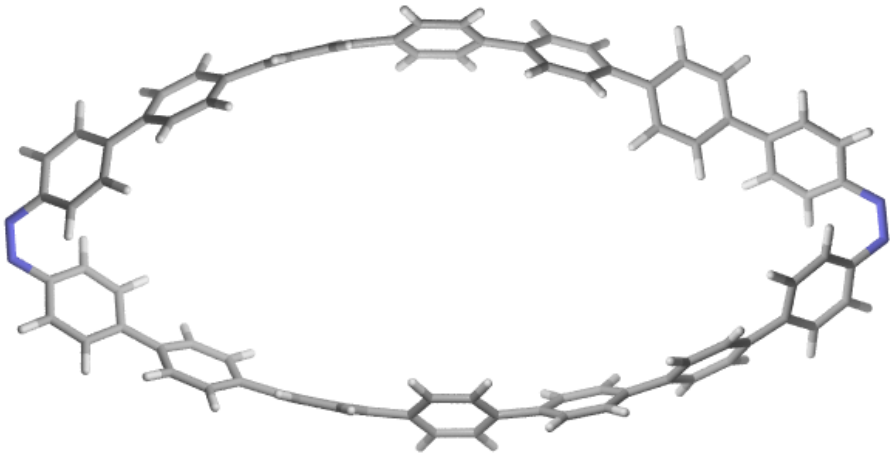

Figure IV.2. DFT minimized structure of the expected product from the aromatization of **19**. The relatively flat polyphenylene domains could be the cause of the poor solubility.

IV.4. Motivation Behind the Synthesis of azo[9]CPP

We reasoned, having seen the success of the azo[11]CPP synthesis and the dimerization of the macrocyclization en route to azo[7]CPP, that more curvature in the bent multi-ring diboronate would encourage bimolecular macrocyclization and discourage higher-order cyclic oligomers. Additionally, in computational investigations of unknown azo[n]CPPs, it came to light that one size in particular, azo[9]CPP may have an affinity for C_{60} due to its similar diameter to [10]CPP (Figure **IV.3**). When measured centroid-to-centroid [10]CPP has a diameter of 13.5 Å in the solid state and binds C_{60} with a log K_a of 6.4.[2a] The minimized geometry of *trans*-azo[9]CPP, meanwhile is just slightly smaller, with an average diameter of 13.2 Å. This is the same as Kawase's [6]cycloparaphenyleneacetylene that binds C_{60} with a log K_a of 4.2.[20] Given the enhanced π-density in the cycloparaphenylene the binding of *trans*-azo[9]CPP is expected to be intermediate between these two nanohoops.

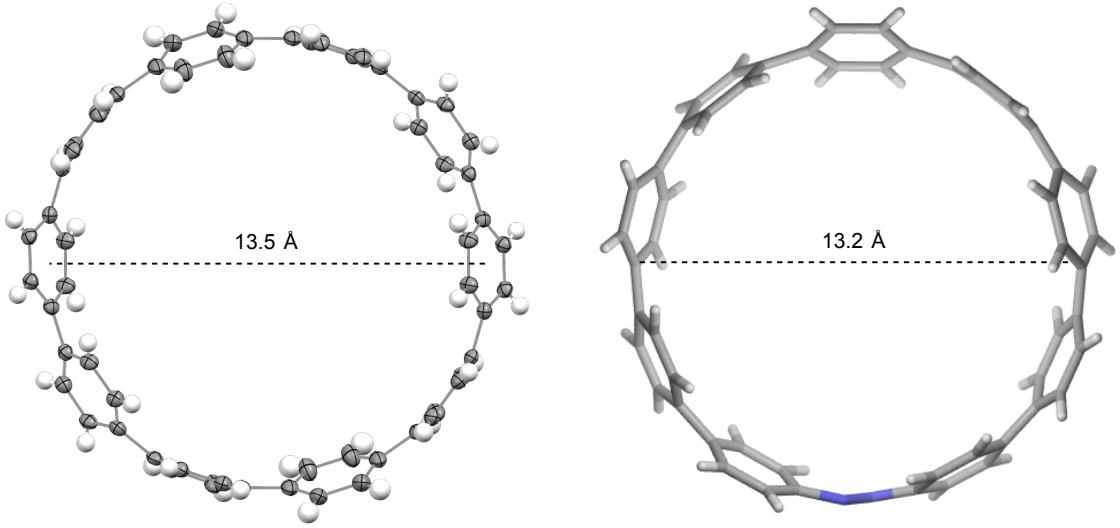

Figure IV.3. Crystal structure of [10]CPP[2b] (left) and B3LYP/6-31G* minimized geometry of *trans*-azo[9]CPP (right) showing similar diameters.

To validate the feasibility of this nanohoop as a molecular container for C_{60}, *ab initio* calculations at the M062X/6-31G* level were conducted. The ground state energy climb from *cis* to *trans* using this basis set was calculated to be 1.27 kcal/mol, slightly less than the 2.12 kcal/mol difference as calculated using B3LYP/6-31G*. However either of these differences are small compared to the 34.32 kcal/mol heat of formation of the complexation of C_{60} as a ball-in-bowl with *trans*-azo[9]CPP (Figure **IV.4**). This system assumes that these states are in equilibrium and the barriers between them are accessible under experimental conditions. The isomerization of azobenzene is known for overcoming significant strain[21] and transition state energies of over 34 kcal/mol have been reported.[22] Therefore, *trans*-azo[9]CPP should form a strong association with C_{60} in solution, and that the complex will be the major thermodynamic product. It should be noted that M062X/6-31G* is known to overestimate the energy gained in such complexations but the trends are quite reliable. For example, the heats of formation of C_{60} complexes with [10]CPP and [6]CPPA were calculated to be 41.35 kcal/mol and 28.0 kcal/mol respectively.[2a, 23] With a heat of formation intermediate between two known fullerene hosts (34.32 kcal/mol), these computational data provide a firm theoretical foundation for our choice to synthesize azo[9]CPP.

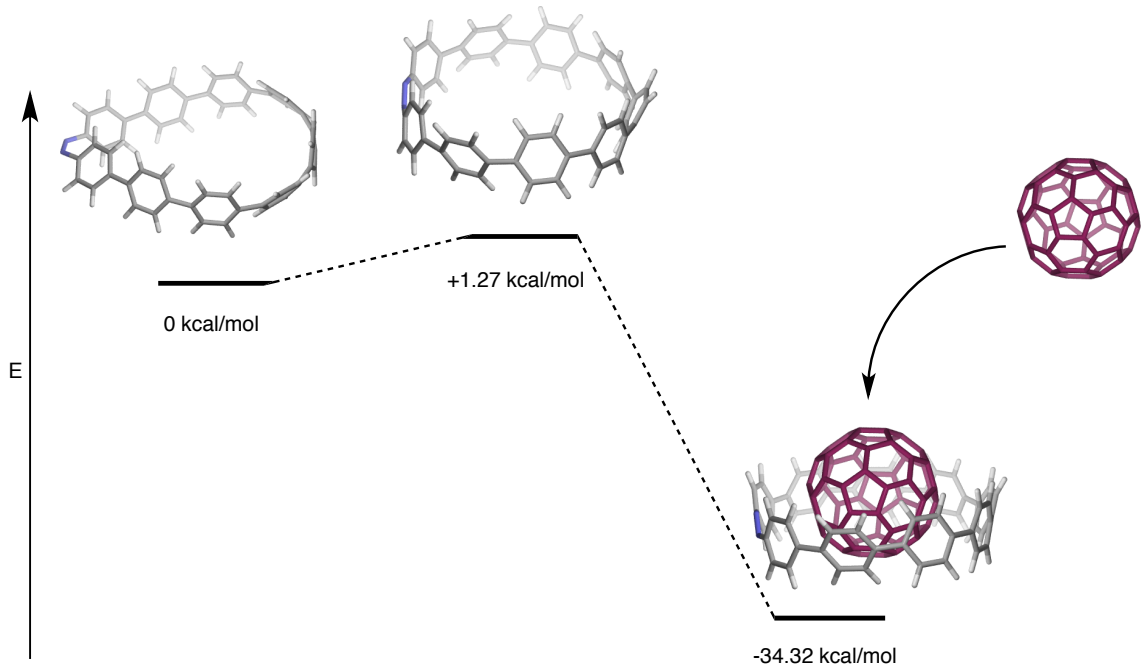

Figure IV.4. M062X/6-31G* simulation of C_{60}@*trans*-azo[9]CPP formation with relative energies shown.

IV.5. Synthesis of azo[9]CPP

To approach the synthesis of azo[9]CPP, a new diboronate was employed which was already in development in our lab based on ideas set forth by Xia in the supplementary information of the gram-scale CPP syntheses reported by our lab in 2012.[2b] In principle, continuing the dearomatization, aryllithium addition motif published en route to diboronate **17** would lead to a seven ring dihalide with alternating aryl and cyclohexadiene moieties. Instead of using this, somewhat linear, stepwise construction, a symmetric approach which extends in two directions starting from three-ring dibromide **20** was adopted (Scheme **IV.9**). Treating **20** with *n*-butyllithium in the presence of more than two equivalents of **21** yields a diketal which can be deprotected crude to yield diquinol **22**. Synthesis of **22** in this manner can be performed on multiple grams and simple precipitation yields a product that is pure enough to carry forward. Addition of excess 4-chlorophenyllithium generated *in situ* to deprotonated **22** followed by *in situ* methylation of the resulting alkoxide offers seven-ring dichloride **23** which, after precipitation, can be converted cleanly to diboronate **24** by Miyura borylation with SPhos. This rapid, synthesis builds an additional 24 carbon atoms that will remain in the

nanohoop framework in 22% yield over three steps. Using the methodology published with the synthesis of [6]CPP, synthesis of **24** would take more than ten steps.

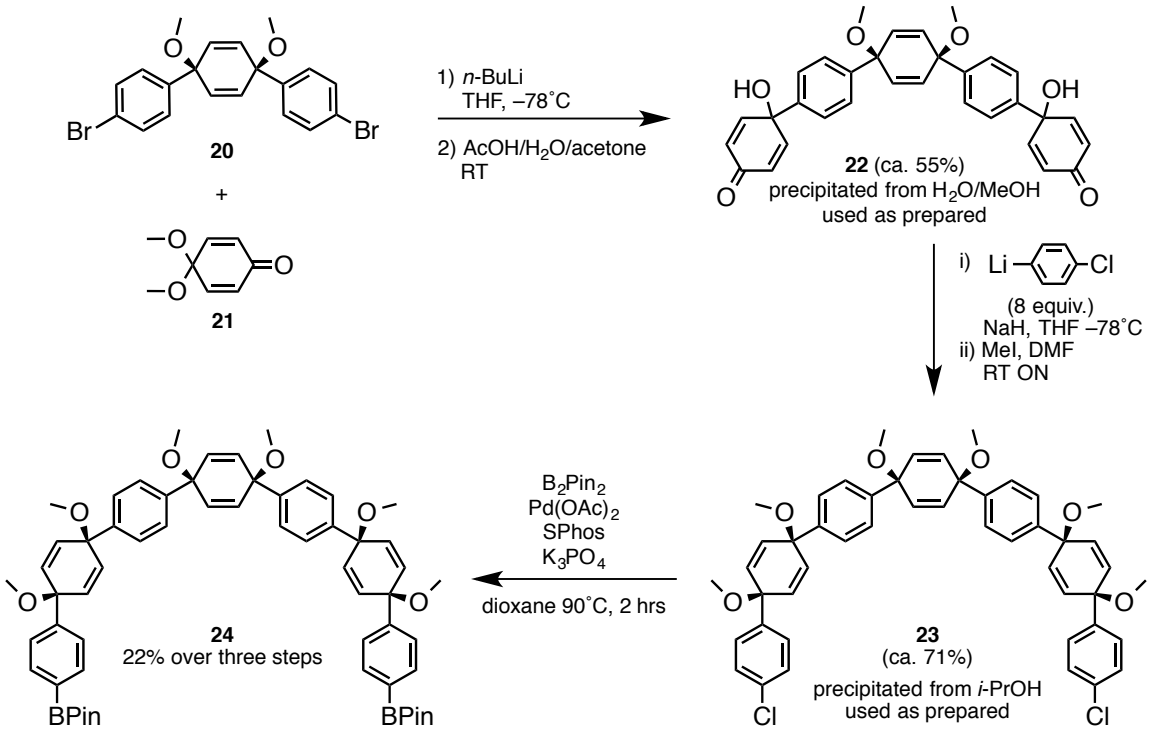

Scheme IV.9. Rapid synthesis of seven-ring diboronate **24**.

The tight curvature and few degrees of rotational freedom in diboronate **24** provide a platform for the synthesis of new CPPs via intermolecular coupling with flat coupling partners. For example, research is underway in our laboratory to couple **24** to flat polyphenyls and PAHs such as anthracene and perylene for their incorporation into CPPs.[24] It was discovered that **24** will undergo Suzuki macrocyclization with dibromoazobenzene **6**, which lies preferentially in the flat *trans* conformation in solution (Scheme **IV.10**). Silica chromatography of this reaction consistently yielded a small amount (< 5%) of a moss green solid as the only isolable macrocycle that was originally presumed to be **25**. This seemed curious since all other azobenzene macrocycles isolated (whether *cis*, like the azo[11]CPP precursor or *trans* as in **19**) absorb around 450nm and therefore have a bold orange appearance. Turning to GPC to purify the reaction mixture provided macrocycle **25** in a 22% isolated yield as orange needles.

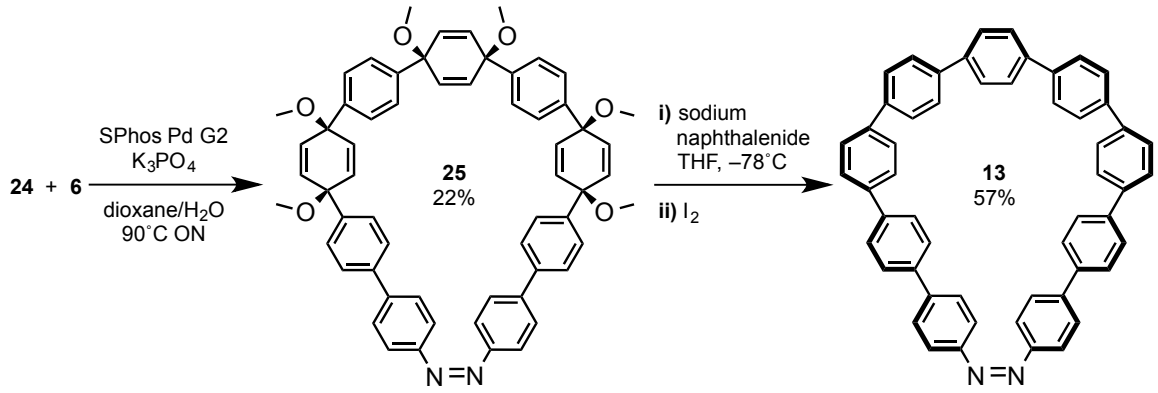

Scheme IV.10. Macrocyclization and aromatization to yield azo[9]CPP.

The ^{1}H NMR spectra of the two isolated macrocycles both show an upfield doublet corresponding to the four protons closest to the nitrogen atoms in the *cis*-azobenzene moiety and no signal for the *trans* isomer. Thermally stable *cis* azobenzenes of this type are rare, but not unknown.[21, 25] The protons responsible for the diagnostic *cis* signal lie in the shielding cone of the opposite azobenzene aryl ring, accounting for their chemical shift. The green material has a slightly more shielded doublet at δ = 6.73 ppm compared to the signal for the genuine macrocycle at δ = 6.80 ppm. The signals of all other protons in both compounds are nearly identical in chemical shift, multiplicity, and integration, ruling out the presence of a hydrazine derivative. It was therefore hypothesized that the green material was an oxidized form of the desired macrocycle (**26**, Figure **IV.5**). An azoxy derivative of this sort would display a more shielded *ortho* proton signal due to its geometry, which is calculated to push these protons further into the opposite ring via steric repulsion from the oxygen atom. The angle formed by the centroids of the azobenzene rings and the center of the nitrogen-nitrogen bond decreases from 92˚ in **25** to 90˚ upon oxidation to **26**. TD-DFT (B3LYP/6-31G*) analysis shows a broad absorption at 500 nm as expected for **25** and major absorption for the oxide at 400 nm accounting for the green appearance (Figure **IV.5**). It should be noted that TD-DFT absorbance predictions at this level of theory can slightly overestimate λ_{max} but the trends are reliable.[26]

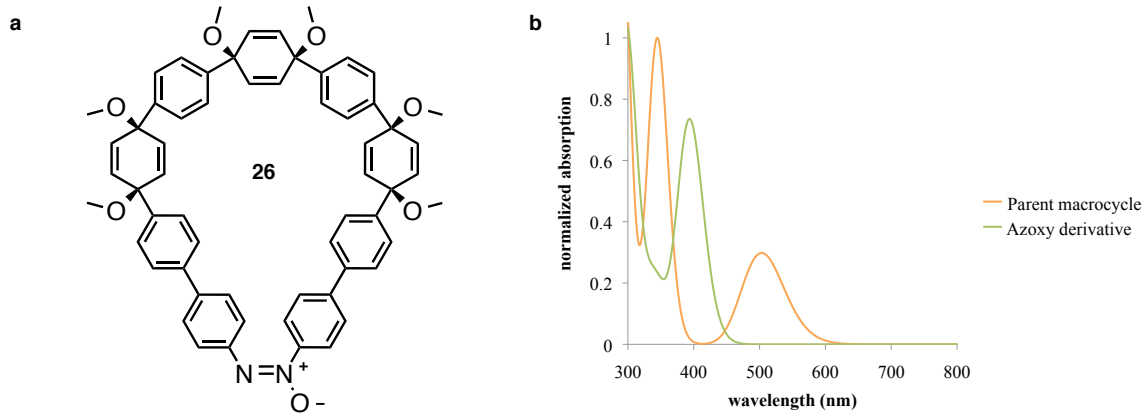

Figure IV.5. Oxidized *cis*-azo[9]CPP macrocycle **26** (a) and calculated UV-Vis absorption for **25** and **26** (b).

The identity of the desired macrocycle **25** was further confirmed by XRD (Figure **IV.6**). This molecule has a roughly triangular pore and a steep saddle shape. In the crystalline state, this curvature leads to long one-dimensional channels of nesting molecules with tetrahydrofuran disordered in the pore. The benzene rings in the azobenzene moiety are also disordered, adopting a number of conformations.

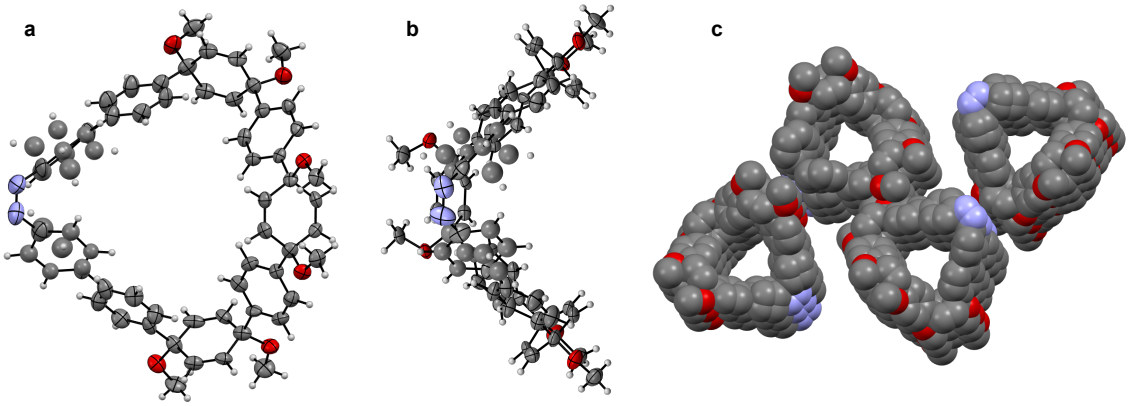

Figure IV.6. Solid state structure of **13** showing the top (a), side (b), and 1D porous packing. ORTEP ellipsoids at 50% probability. Solvent omitted for clarity.

After isolating and confirming the identity of the macrocycle, **25** was subjected to sodium naphthalenide at –78˚C and aromatized to offer azo[9]CPP (**13**, Scheme **IV.10**) in 57% yield as purified by GPC.

IV.6. UV-Vis of Photoswitchable azoCPPs

Having isolated two different sizes of azo[n]CPP, we set out to determine the feasibility of switching the pore size of these nanohoops. Larger nanohoop, azo[11]CPP was found via NMR to lie exclusively in the *cis* form in solution at room temperature, with a distinctive upfield doublet (δ = 6.83 ppm) corresponding to the 4 protons closest to the nitrogen atoms. The UV-Vis spectrum of azo[11]CPP in CH_2Cl_2 displayed a major absorption at 333 nm and though a minor absorption was apparent further in the red (qualitatively from the orange appearance of the solid and solution and also calculated by TD-DFT, Figure **IV.7**) increasing the concentration of the sample to observe this peak only resulted in the major absorbance overwhelming the region where a second absorbance was expected. However, irradiation of this sample with a 4-watt fluorescent mercury lamp at 365 nm resulted in the depression of the major absorbance and the appearance of a longer wavelength shoulder centered around 370 nm. This is likely the major absorption of the *trans* species, which should lie at a longer wavelength than the *cis* as calculated by TD-DFT (Figure **IV.7**).

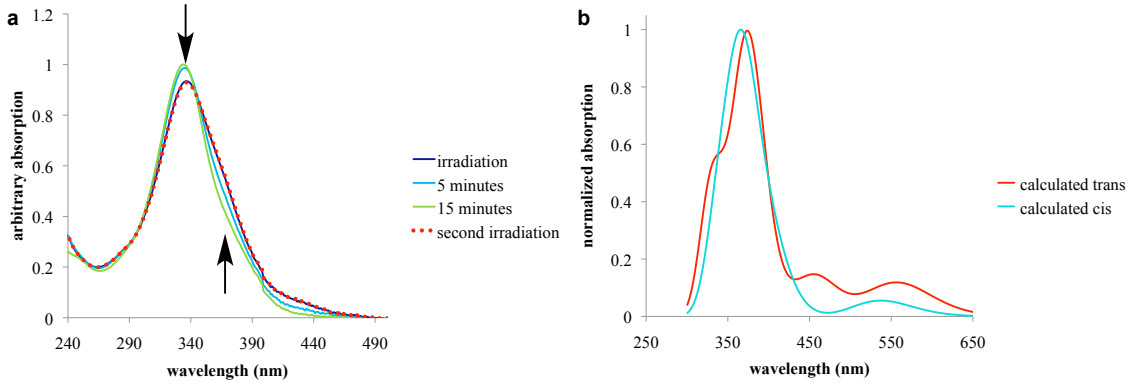

Figure IV.7. Reversible peak shape change under 365 nm irradiation in CH_2Cl_2 (a) and TD-DFT predictions (b) for azo[11]CPP.

This phenomenon was reversed over fifteen minutes at room temperature and ambient light, with a resulting spectrum identical to the starting material. This switching was found to be repeatable indefinitely.

When a shorter wavelength was used for irradiation (Fluorescent mercury lamp, 4 watts, 254 nm), the major absorption of the sample was irreversibly blue-shifted and a decrease in total absorbance was observed (Figure **IV.8**). After weeks at room temperature and under ambient light or longer wavelength irradiation (Fluorescent mercury lamp, 4 watts, 365 nm) this sample remained unchanged. In certain cases thermal azobenzene isomerizations can be very slow[27], but the original absorbance of this sample never recovered upon storage in solution.

The irreversible nature of this transformation suggests a photochemical degradation rather than an isomerization. Cyclodehydrogenation of *cis*-azobenzenes to the corresponding benzo[c]cinnolines has been observed under photochemical conditions, though typically these require the addition of a lewis acid and irradiation of higher power and longer duration than employed here.[28] Nevertheless, the resulting product was soluble and did not exhibit the bright fluorescence of an acyclic polyphenylene, so its reasonable to assume the degradation was not a ring-opening process. Furthermore, TD-DFT simulation of the benzo[c]cinnoline derivative similar to **27** (Figure **IV.9**)but with the diameter of *cis*-azo[11]CPP shows a major absorption with a smaller extinction coefficient, as was observed (Figure **IV.8**). Additionally, the broad longer wavelength absorption is predicted to disappear, accounting for the pale yellow color of the photolyzed sample. Of course, other routes of photochemical decomposition or even irreversible *cis/trans* isomerization cannot be completely ruled out by the available data. The small amount of CPP available from this synthesis precluded NMR investigation of the photoswitching or photodegridation.

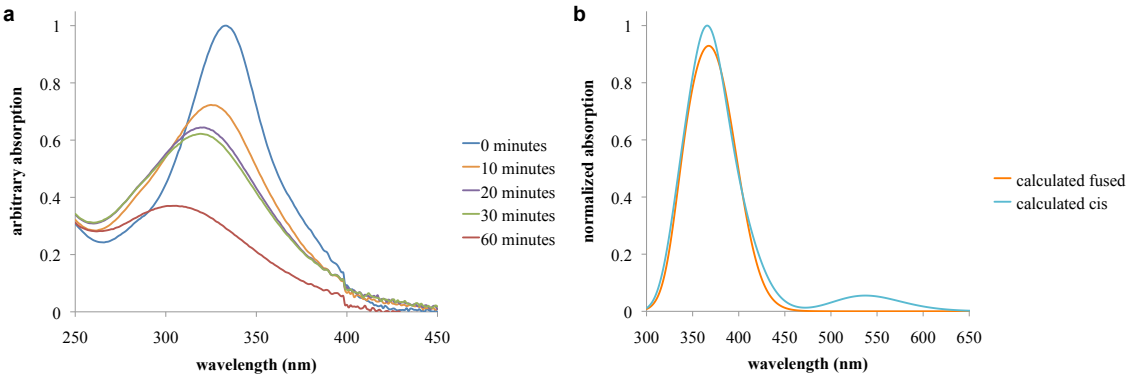

Figure IV.8. Bleaching observed with 254 nm excitation in CH_2Cl_2 over time (a) and TD-DFT (b) of the *cis* and benzo[c]cinnoline forms of azo[11]CPP.

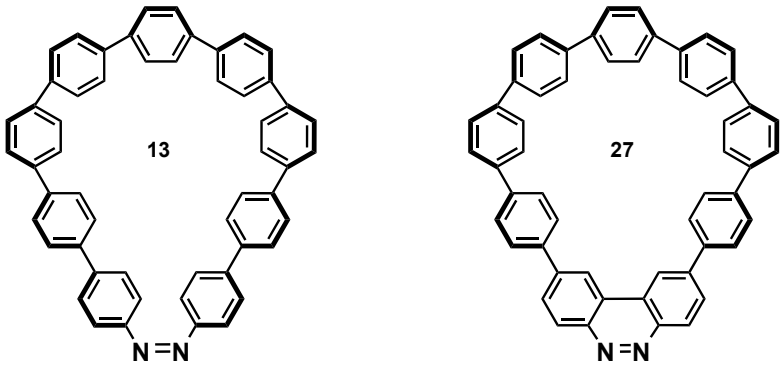

Figure IV.9. *cis*-azo[9]CPP and potential photodegradation product **27**, a benzo[c]cinnoline derivative.

The smaller azo[9]CPP also unsurprisingly lies in the *cis* conformation based on NMR data (doublet at δ = 6.80 ppm). The absorption of this nanohoop in CH_2Cl_2 was observed to be very similar to azo[11]CPP with a major absorption centered around 330 nm with two absorption shoulders at 390 nm (weak) and a 460 nm (very weak) which are both overwhelmed in solution at high concentrations by the broadened edges of the major absorption (Figure **IV.10**). This nanohoop, interestingly does not display the switching behavior as seen in the UV-Vis of azo[11]CPP. Few azobenzene derivatives have completely frozen isomerization and this usually requires high strain, as from a very small macrocycle[25], or coordination of one or more of the nitrogen atoms.[29] Multiple trials using a high-pressure mercury arc lamp (Oriel, 200-W) and longpass filters with cutoff wavelengths stepping gradually down from 550 nm to 350 nm only resulted in UV spectra identical to the original (Figure **IV.10**). Irradiation with high-intensity LED

sources (800 mW) at 365 nm and 400 nm and a fluorescent mercury lamp (4 watts) at 365 nm also produced no change despite TD-DFT predictions that the *cis-trans* isomerization of azo[9]CPP should show a larger red shift than for azo[11]CPP (Figure **IV.10**).

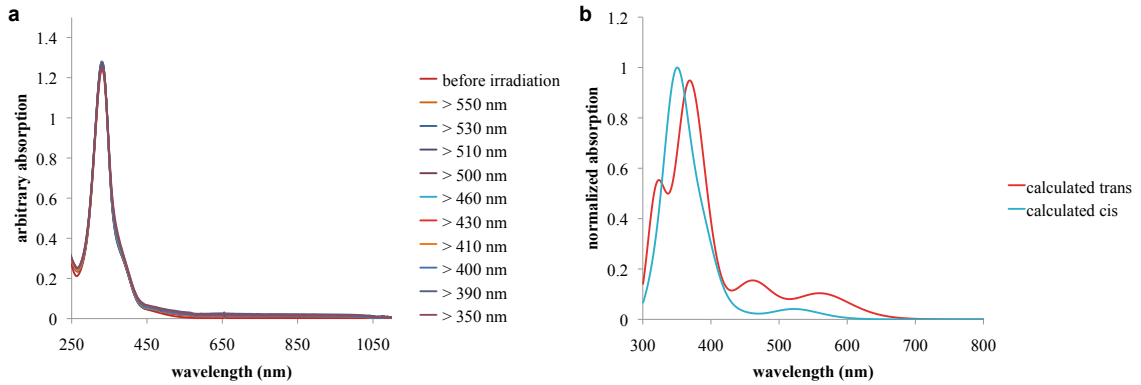

Figure IV.10. UV-Vis spectra of azo[9]CPP with high pressure UV irradiation in CH_2Cl_2 with various longpass filters (a) and TD-DFT of *cis*- and *trans*-azo[9]CPP (b).

When exposed to broadband UV irradiation from a high pressure mercury lamp (IR filter only) or 254 nm irradiation from a 4 watt florescent source, azo[9]CPP bleached in a manner similar to azo[11]CPP (Figure **IV.11**) consistent again with the predicted irreversible change in absorption upon benzo[c]cinnoline formation (Figure **IV.9**).

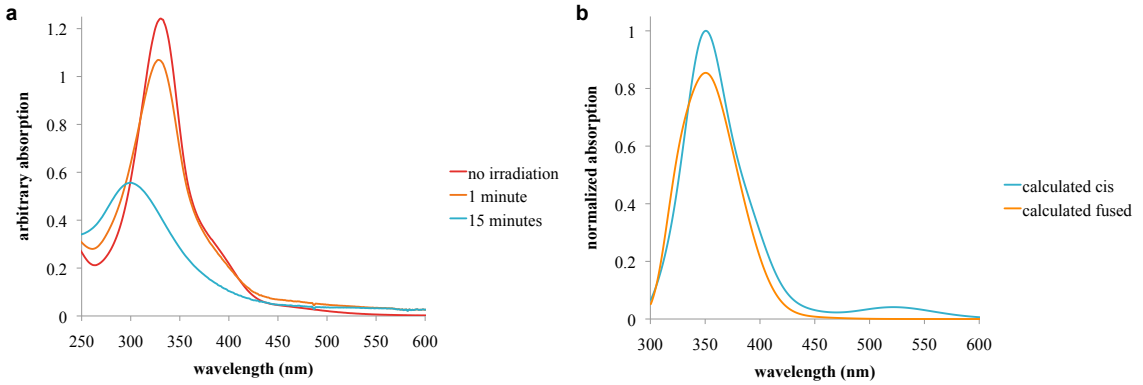

Figure IV.11. Bleaching of azo[9]CPP with high-pressure broadband UV irradiation in CH_2Cl_2 over time (a) and TD-DFT simulation of *cis*-azo[9]CPP and **27**.

IV.7. Conclusion and Future Directions

With the data available at the time of writing, the outlook for photoswitchable nanohoops is promising. Though preliminary NMR experiments did not show complexation when adding solid C_{60} to a sample of azo[9]CPP in $CDCl_3$, theoretical data shows that it should form a strong complex once the correct conditions are developed. Similarly, photoisomerization was observed in azo[11]CPP but the synthetic availability of this nanohoop was poor. With an efficient route to azo[9]CPP, photoisomerization conditions for this nanohoop will be developed with the aid of NMR spectroscopy.

The troubled isomerization of azo[9]CPP requires engineering of photoirradiation conditions suitable for high conversion of the isomers. This may include simple changes in experimental setup (source, solvent, etc.). Additionally, the excited states of geometrically-restricted azobenzenes have been probed by transient femtosecond fluorescence measurements.[30] Gathering more data about the excited state of azo[9]CPP may shed light on the prohibited isomerization pathway and lead to an appropriate solution.

For the complexation of C_{60} in azo[9]CPP, much has yet to be attempted. Solvent choice can dramatically affect binding affinity in host-guest systems. With the efficient synthesis shown, ample azo[9]CPP can be prepared to try slow crystallization of mixtures with C_{60} in a variety of solvents under irradiation and in the dark. Additionally, a screen for new guests that might bind in the cavity of this nanohoop will be useful.

IV.8. Experimental

IV.8.1. General Experiment Details

Moisture and oxygen sensitive reactions were carried out under nitrogen atmosphere using standard syringe/septa technique. All the glassware was thoroughly washed, oven dried at 140°C overnight and cooled under nitrogen atmosphere before use. All reagents were obtained commercially. Where noted as “dry”: Tetrahydrofuran (THF), toluene, dioxane, dimethylformamide (DMF) and dichloromethane (DCM) were dried by filtration through alumina according to the method descried by Grubbs.[31] For sodium naphthalenide generation and reductive aromatization solutions, THF was freshly

distilled from sodium and benzophenone. Silica column chromatography was conducted with Zeochem Zeoprep n60 Eco 40-63 μm silica gel. Thin layer chromatography (TLC) was performed using Sorbent Technologies Silica Gel XHT TLC plates. Developed plates were visualized using UV light at wavelength of 254 and 365 nm or iodine vapor where appropriate. Gel permiation chromatography (GPC) was performed using a Japan Analytical Industry LC-9101 with JAIGEL-1H and JAIGEL-2H polystyrene/divinylbenzene columns in series. UV-Vis data was obtained on a Hewlett-Packard 8453 spectrometer. Where noted, an Oriel 200-W high pressure mercury arc lamp and Corning CS filters, LED Engin LZ1-10UV00-0000 (365 nm) and LED Engin LZ1-10UA00-U7 (400 nm) LED sources, or a UVP UVGL-15 fluorescent lamp were used for UV irradiation. IR spectra were recorded on a Thermo Nicolet 6700. ^{1}H NMR spectra were recorded at 600 (Bruker Avance III HD), 500 (Varian VNMRS) 400 (Varian VNMRS), or 300 (Varian VNMRS) MHz and ^{13}C NMR spectra were recorded at 150 (Bruker Avance III HD), 125 (Varian VNMRS), or 100 (Varian VNMRS) MHz. Deuterated chloroform ($CDCl_3$) was used as NMR solvent for all the compounds unless noted otherwise and all spectra were referenced to tetramethylsilane (TMS) due to the prevalence of compound signals overlapping with the signal from $CHCl_3$. The matricies used for MALDI-TOF were a solution of 7,7,8,8-tetracyanquinodimethane (TCNQ) in THF with 1% silver trifluoroacetate as a promoter[32], or trans-2-[3-(4-tert-Butylphenyl)-2-methyl-2-propenylidene]malononitrile (DCTB).

IV.8.2. Experimental Details

(E)-1,2-bis(4-(4,4,5,5-tetramethyl-1,3,2-dioxaborolan-2-yl)phenyl)diazene **4**

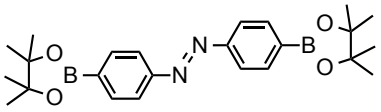

To a 100-mL flask equipped with a magnetic stir bar was added 4,4′-dibromoazobenzene **6** (1.00 g, 2.94 mmol, 1 equiv) and $Pd(PPh_3)_2Cl_2$ (300 mg, 0.430 mmol, 0.15 equiv). This flask was evacuated and backfilled with dry N_2 ten times to exclude moisture and air. Dry toluene (50 mL) was added to the flask and the mixture stirred to dissolve. 4,4,5,5-

Tetramethyl-1,3,2-dioxaborolane (6.50 mL, 44.8 mmol, 15.2 equiv) and freshly distilled triethylamine (3.00 mL, 21.34 mmol, 7.26 equiv) were added via syring and the mix was stirred while heating to 90˚C overnight. Mixture was cooled to room temperature, filtered through a pad of celite. The resulting solution was was washed with saturated sodium bicarbonate in H_2O (2 × 50 mL) and brine (50 mL) then dried over magnesium sulfate and filtered. Solvent was removed under reduced pressure and the crude solid was chromatographed on silica gel in an ethyl acetate/hexane gradient of increasing polarity. The resulting product was a brown solid (286 mg, 27%). ^{1}H NMR (500 MHz, Chloroform-d) δ(ppm) 7.67 (d, J = 8.4 Hz, 4H), 6.81 (d, J = 8.4 Hz, 4H), 1.31 (s, 24H); ^{13}C NMR (126 MHz, Chloroform-d) δ 151.10, 136.41, 111.34, 105.01, 83.38, 24.84.

((4'-iodo-[1,1'-biphenyl]-4-yl)oxy)trimethylsilane **8**

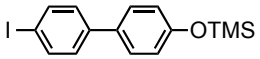

To a 100-mL flask equipped with a magnetic stir bar was added 4′-iodo-(1,1′-biphenyl)-4-ol **7** (11.3 g, 38.2 mmol, 1 equiv), imidazole (4.16 g, 61.12 mmol, 1.6 equiv), and dry DCM (50 mL). Chlorotrimethylsilane (6.30 mL, 49.6 mmol, 1.3 equiv) was added dropwise via syringe. The reaction mixture was allowed to stir at room temperature overnight. H_2O (25 mL) was added to the mixture and the solution was extracted with DCM (2 × 50 mL) and the combined organic layers were washed with saturated sodium bicarbonate in H_2O (2 × 100 mL) and brine (100 mL) then dried over sodium sulfate and filtered. Solvent was removed under reduced pressure to yield a white solid (12.4 g, 89%). ^{1}H NMR (500 MHz, Chloroform-d) δ 7.72 (d, J = 8.6 Hz, 2H), 7.42 (d, J = 8.8 Hz, 2H), 7.26 (d, J = 8.6 Hz, 2H), 6.90 (d, J = 8.8 Hz, 2H), 0.29 (s, 9H).

1-hydroxy-4'-iodo-[1,1'-biphenyl]-4(1H)-one **9**

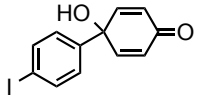

To a 100-mL flask equipped with a magnetic stir bar was added *((4'-iodo-[1,1'-biphenyl]-4-yl)oxy)trimethylsilane* **8** (12.4 g, 33.6 mmol, 1 equiv), THF (170 mL), H_2O (70 mL), and acetonitrile (45 mL). Phenyliodosodiacetate (16.2 g, 50.4 mmol, 1.5 equiv) was added to the mixture in portions over 1 hour while stirring. The reaction mixture was allowed to stir at room temperature overnight under nitrogen atmosphere. Organic solvents were removed under reduced pressure and the solution was extracted with ethyl acetate (3 × 50 mL) and the combined organic layers were washed with saturated sodium bicarbonate in H_2O (2 × 100 mL) and brine (100 mL) then dried over sodium sulfate and filtered through a pad of silica that was eluted with additional ethyl acetate. Solvent was removed under reduced pressure to yield a brown solid that was washed with methanol and used as prepared (8.18 g, 78%). ^{1}H NMR (500 MHz, Chloroform-d) δ(ppm) 7.71 (d, J = 8.7 Hz, 2H), 7.22 (d, J = 8.7 Hz, 2H), 6.85 (d, J = 10.1 Hz, 2H), 6.22 (d, J = 10.1 Hz, 2H), 2.76 (s, 1H).

(1's,4's)-4-bromo-4''-iodo-1',4'-dimethoxy-1',4'-dihydro-1,1':4',1''-terphenyl **10**

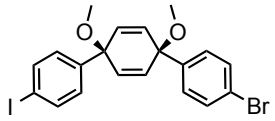

To a 100-mL flask equipped with a magnetic stir bar was added quinol **9** (1.00 g, 3.20 mmol, 1 equiv) and dry THF (30 mL). This solution was cooled to –78˚C. Sodium hydride was added in one portion quickly (60% in mineral oil, 170 mg, 4.17 mmol, 1.3 equiv) and stirred 1 hour. Meanwhile, 1,4-dibromobenzene (1.82 g, 7.70 mmol, 2.4 equiv) was added to a separate 50-mL flask, dissolved in dry THF (20 mL) and cooled to –78˚C. *n*-butyllithium (2.5 M in hexanes, 3.08 mL, 7.7 mmol, 2.4 equiv) was added to the 1,4-dibromobenzene solution dropwise and the mixture was stirred 30 minutes at –78˚C. The 4-bromophenyllithium solution was cannulated into the quinol solution and this mixture was stirred at –78˚C for 2 hours. H_2O (20 mL) was added to quench the reaction and the mixture was warmed to room temperature. The solution was extracted with ethyl ether (2 × 50 mL) and the combined organic layers were washed with brine (100 mL)

then dried over sodium sulfate and filtered. Solvent was removed under reduced pressure to yield a yellow solid that was dissolved in dry THF (75 mL) and cooled to 0˚C. Sodium hydride was added in one portion quickly (60% in mineral oil, 333 mg, 8.32 mmol, 2.6 equiv) and stirred 30 minutes. Methyl iodide (0.80 mL, 13 mmol, 4 equiv) was added via syringe and the mixture was allowed to warm to room temperature and stirred overnight. H_2O (50 mL) was added to the mixture to quench and the solution was extracted with ethyl acetate (2 × 50 mL) and the combined organic layers were washed with H_2O (100 mL), and brine (100 mL) then dried over sodium sulfate and filtered. Solvent was removed under reduced pressure and the crude solid was chromatographed on silica gel in an ethyl acetate/hexane gradient of increasing polarity up to 1:1. The resulting product was a white solid (1.0 g, 63%). ^{1}H NMR (500 MHz, Chloroform-d) δ(ppm) 7.64 (d, J = 8.6 Hz, 2H), 7.43 (d, J = 8.8 Hz, 2H), 7.24 (d, J = 8.8 Hz, 2H), 7.11 (d, J = 8.6 Hz, 2H), 6.06 (s, 4H), 3.41 (s, 3H), 3.41 (s, 3H). ^{13}C NMR (126 MHz, Chloroform-d) δ(ppm) 143.00, 142.28, 137.46, 133.30, 133.27, 131.49, 127.96, 127.73, 121.70, 104.97, 93.41, 74.48, 74.41, 52.00.

nine-ring dibromide **11**

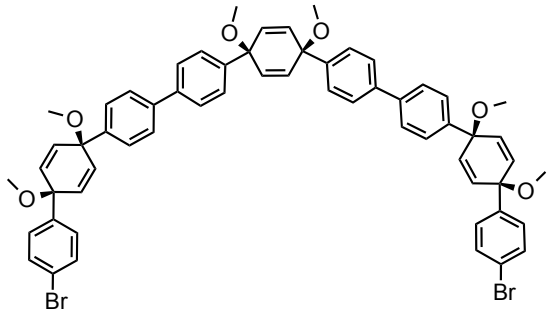

To a 100-mL flask equipped with a magnetic stir bar was added dihalide **10** (230 mg, 0.460 mmol, 3 equiv), diboronate **3** (80 mg, 0.147 mmol, 1 equiv), and $Pd(PPh_3)_4$ (5.0 mg, 0.004 mmol, 0.03 equiv). This flask was evacuated and backfilled with dry N_2 five times to exclude moisture and air. Dry THF (50 mL) was added to the flask and then a sparged 2.00 M solution of K_3CO_3 in H_2O (12.0 mL, 24.0 mmol, 52.2 equiv) was added and the mixture was stirred at reflux overnight. The mixture was cooled to room

temperature, filtered through a pad of celite and concentrated under reduced pressure. The resulting semisolid was taken up in ethyl ether (20 mL). This solution was washed with H_2O (2 × 50 mL) and brine (50 mL) then dried over sodium sulfate and filtered. Solvent was removed under reduced pressure and the crude solid was chromatographed on silica gel in an ethyl acetate/hexanes gradient of increasing polarity up to 1:1. The resulting product was a white solid (85.0 mg, 56%). ^{1}H NMR (500 MHz, Chloroform-d) δ(ppm) 7.54 (d, J = 8.6 Hz, 4H), 7.53 (d, J = 8.6 Hz, 4H), 7.49 (d, J = 8.6 Hz, 4H), 7.43 (d, J = 8.6 Hz, 4H), 7.42 (d, J = 8.6 Hz, 4H), 7.28 (d, J = 8.6 Hz, 4H), 6.17 (s, 4H), 6.16 (d, J = 10.1 Hz, 4H), 6.07 (d, J = 10.1 Hz, 4H), 3.47 (s, 6H), 3.44 (s, 6H), 3.43 (s, 6H); ^{13}C NMR (126 MHz, Chloroform-d) δ(ppm) 142.56, 142.52, 142.24, 140.09, 139.90, 133.69, 133.37, 132.97, 131.43, 127.82, 127.12, 127.07, 126.44, 126.35, 121.59, 74.71, 74.59, 74.53, 52.01.

nine-ring diboronate **12**

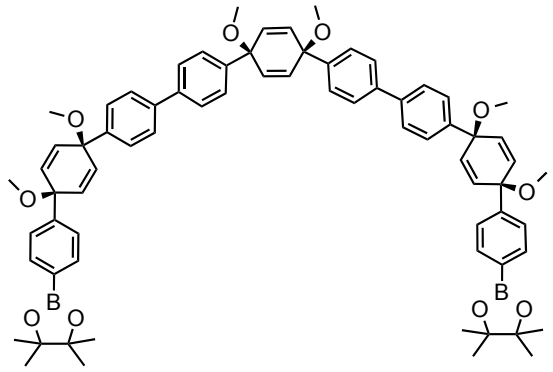

To a 25-mL flask equipped with a magnetic stir bar was added dibromide **11** (100 mg, 0.103 mmol, 1 equiv) and dry THF (10 mL). This solution was cooled to –78˚C. *n*-butyllithium (2.5 M in hexanes, 0.080 mL, 0.21 mmol, 2.1 equiv) was added to the solution dropwise and isopropoxyboronic acid pinacol ester (0.080 mL, 0.40 mmol, 4 equiv) was quickly injected immediately. The mixture was stirred 2 hours at –78˚C. H_2O (10 mL) was added to the mixture to quench and the solution was extracted with DCM (2 × 20 mL) and the combined organic layers were washed with H_2O (50 mL), and brine (50 mL) then dried over sodium sulfate and filtered. Solvent was removed under reduced

pressure to yield a white solid that was adsorbed to a pad of silica gel washed with hexane, and the product was eluted with DCM which was removed under reduced pressure yielding a white solid (98 mg, 88%). ^{1}H NMR (500 MHz, Chloroform-d) δ(ppm) 7.75 (d, J = 8.4 Hz, 4H), 7.55 (d, J = 8.7 Hz, 4H), 7.52 (d, J = 8.7 Hz, 4H), 7.50 (d, J = 8.7 Hz, 4H), 7.44 (d, J = 8.7 Hz, 4H), 7.42 (d, J = 8.4 Hz, 4H), 6.17 (s, 4H), 6.13 (d, J = 9.6 Hz, 4H), 6.10 (d, J = 9.6 Hz, 4H), 3.48 (s, 6H), 3.44 (s, 6H), 3.44 (s, 6H), 1.31 (s, 24H).

azo[11]cycloparaphenylene macrocycle **12**

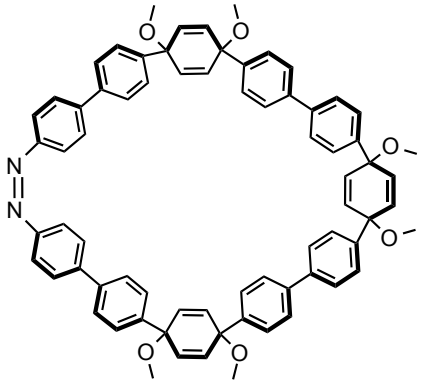

To a 100-mL flask equipped with a magnetic stir bar was added diboronate **12** (297 mg, 0.264 mmol, 1 equiv), 4,4′-dibromoazobenzene **6** (90.0 mg, 0.264 mmol, 1 equiv), $Pd(OAc)_2$ (27 mg, 0.040 mmol, 0.15 equiv), and ground, oven-dried Cs_2CO_3 (430 mg, 1.32 mmol, 5 equiv). This flask was evacuated and backfilled with dry N_2 five times to exclude moisture and air. Dry DMF (50 mL), and N_2 sparged isopropyl alcohol (5 mL) were added and the mixture was heated to 110˚C while stirring overnight. After cooling to room temperature, the solution was filtered through a pad of celite and concentrated under reduced pressure. The resulting semisolid was redissolved in 50 mL of DCM. The solution was washed with H_2O (2 × 50 mL) and brine (50 mL) then dried over sodium sulfate and filtered. Solvent was removed under reduced pressure and the crude solid was chromatographed on silica gel in an ethyl acetate/hexane gradient of increasing polarity to give an orange solid (35 mg, 13%). ^{1}H NMR (500 MHz, Chloroform-d) δ 7.56 (d, J = 8.7 Hz, 4H), 7.53 (d, J = 3.7 Hz, 4H), 7.51 (d, J = 3.7 Hz, 4H), 7.47 (d, J = 8.1 Hz, 4H),

7.45 (d, J = 8.1 Hz, 4H), 7.42 (d, J = 4.1 Hz, 4H), 7.40 (d, J = 4.1 Hz, 4H), 6.82 (d, J = 8.7 Hz, 4H), 6.16 (s, 4H), 6.17 – 6.12 (overlap, 8H), 3.47 (s, 6H), 3.45 (s, 6H), 3.45 (s, 6H). ^{13}C NMR (126 MHz, Chloroform-d) δ(ppm) 147.56, 142.87, 142.64, 141.50, 140.00, 139.96, 139.94, 133.11, 132.15, 127.89, 127.13, 127.05, 126.50, 126.46, 126.43, 126.41, 126.29, 126.27, 112.81, 74.88, 74.70, 74.13, 52.04, 51.96, 51.92; IR (neat): 3020.0, 2998.8, 2933.2, 2927.5, 2841.4, 1737.6, 1587.2, 1486.9, 1436.7, 1376.9, 1172.9, 1118.5, 1074.2, 1018.2, 948.8, 823.5, 754.0, 723.2, 694.3, 663.4 cm^{-1}

azo[11]cycloparaphenylene **2**

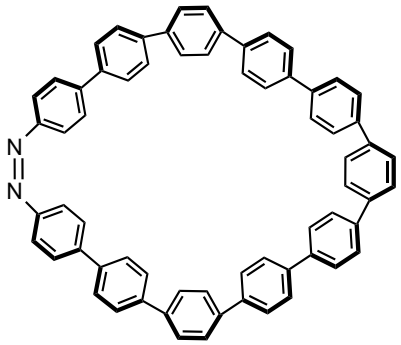

Macrocycle **12** (19 mg, 0.018 mmol, 1.00 equiv) was dissolved in freshly distilled THF (5 mL) and cooled to –78°C under N_2. 1 M sodium naphthalenide (0.40 mL, 0.40 mmol, 20 equiv) was added dropwise to the stirring solution to give a deep blue color. The mixture was stirred for one hour then 1 M I_2 in DCM was added (1.0 mL) followed by saturated sodium thiosulfate in H_2O (2 mL). After warming to room temperature, the solution was and concentrated under reduced pressure. The resulting solid was redissolved in 10 mL of DCM. The solution was washed with H_2O (2 × 10 mL) and brine (10 mL) then dried over sodium sulfate and filtered. Solvent was removed under reduced pressure and the crude solid was chromatographed on basic alumina in an THF/petroleum ether gradient of increasing polarity up to 1:5 to give a bold orange solid (6 mg, 39%). ^{1}H NMR (500 MHz, Chloroform-d) δ(ppm) 7.62 – 7.52 (overlap, 36H), 7.47 (d, J = 8.6 Hz, 4H), 6.90 (d, J = 8.6 Hz, 4H). IR (neat) 2851.29, 2940.96, 2921.68, 2851.29, 1714.44, 1659.47, 1589.08, 1482.05, 1454.09, 1376.95, 1375.98, 1259.35, 1259.31, 1071.28, 809.97 cm^{-1}.

1-((1's,4's)-4''-bromo-1',4'-dimethoxy-1',4'-dihydro-[1,1':4',1''-terphenyl]-4-yl)-2,5-dimethyl-1H-pyrrole **16**

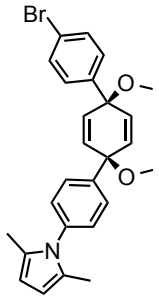

To a 100-mL flask equipped with a magnetic stir bar was added quinol **15** (220 mg, 0.83 mmol, 1 equiv) and dry THF (30 mL). This solution was cooled to –78˚C. Sodium hydride was added in one portion quickly (60% in mineral oil, 43.2 mg, 1.08 mmol, 1.3 equiv) and stirred 1 hour. Meanwhile, 1-(4-Bromophenyl)-2,5-dimethylpyrrole (500 mg, 1.99 mmol, 2.4 equiv) was added to a separate 50-mL flask, dissolved in dry THF (20 mL) and cooled to –78˚C. *n*-butyllithium (2.5 M in hexanes, 0.80 mL, 1.99 mmol, 2.4 equiv) was added to the pyrrole solution dropwise and the mixture was stirred 30 minutes at –78˚C. The lithiated solution was cannulated into the quinol solution and this mixture was stirred at –78˚C for 2 hours. H_2O (20 mL) was added to quench the reaction and the mixture was warmed to room temperature. The solution was extracted with ethyl ether (2 × 50 mL) and the combined organic layers were washed with brine (100 mL) then dried over sodium sulfate and filtered. Solvent was removed under reduced pressure to yield a yellow solid that was dissolved in dry THF (50 mL) and cooled to 0˚C. Sodium hydride was added in one portion quickly (60% in mineral oil, 450 mg, 11.2 mmol, 13.5 equiv) and stirred 30 minutes. Methyl iodide (1.10 mL, 17.3 mmol, 20.8 equiv) was added via syringe and the mixture was allowed to warm to room temperature and stirred overnight. H_2O (50 mL) was added to the mixture to quench and the solution was extracted with ethyl acetate (2 × 50 mL) and the combined organic layers were washed with H_2O (100 mL), and brine (100 mL) then dried over sodium sulfate and filtered. Solvent was removed under reduced pressure and the crude solid was chromatographed on silica gel in an ethyl acetate/hexane gradient of increasing polarity

up to 1:1. The resulting product was a tan solid (303 mg, 33%). ^{1}H NMR (500 MHz, Chloroform-d) δ(ppm) 7.46 (d, J = 8.7 Hz, 2H), 7.42 (d, J = 8.6 Hz, 2H), 7.28 (d, J = 8.7 Hz, 2H), 7.16 (d, J = 8.6 Hz, 2H), 6.17 (d, J = 10.3 Hz, 2H), 6.12 (d, J = 10.3 Hz, 2H), 5.89 (s, 2H), 3.46 (s, 3H), 3.44 (s, 3H), 2.02 (s, 6H).

bis-azo[11]cycloparaphenylene macrocycle **19**

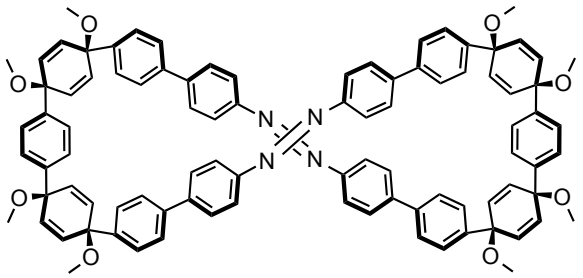

To a 1-L flask equipped with a magnetic stir bar was added 4,4′-dibromoazobenzene **6** (408 mg, 1.20 mmol, 1 equiv), five-ring diboronate **10** (1.00 g, 1.32 mmol, 1.1 equiv), and SPhos Pd G2 (87.0 mg, 0.120 mmol, 0.05 equiv). This flask was evacuated and backfilled with dry N_2 five times to exclude moisture and air. Dry dioxane (600 mL) was added and the mixture was heated to 90˚C while stirring. Ground, oven-dried K_3PO_4 (300 mg, 1.4 mmol, 2 equiv) in N_2 sparged H_2O (25 mL) was added via syringe and the mixture stirred at 90˚C overnight. After cooling to room temperature, the solution was filtered through a pad of celite and concentrated under reduced pressure. The resulting semisolid was redissolved in 150 mL of DCM. The solution was washed with H_2O (2 × 150 mL) and brine (150 mL) then dried over sodium sulfate and filtered. Solvent was removed under reduced pressure and the crude solid was chromatographed on silica gel in an ethyl acetate/hexane gradient of increasing polarity to give a bright orange solid (181 mg, 22%). ^{1}H NMR (300 MHz, Chloroform-d) δ(ppm) 7.79 (d, J = 8.6 Hz, 8H), 7.70 – 7.42 (overlap, 32H), 6.19 (d, J = 11.0 Hz, 8H), 6.14 (d, J = 11.0 Hz, 8H), 3.52 (s, 12H), 3.48 (s, 12H); ^{13}C NMR (151 MHz, Chloroform-d) δ(ppm) 151.34, 143.43, 142.47, 139.49, 133.46, 133.20, 127.15, 126.95, 126.55, 126.16, 123.45, 74.72, 52.08, 52.01; IR (neat): 731.76, 825.06, 907.55, 949.95, 1004.14, 1016.93, 1082.51, 1174.73, 1226.57,

1360.53, 1398.57, 1461.6, 1487.2, 1598.91, 2245.82, 2822.81, 2898.27, 2936.68, 2980.41, 3029.73 cm^{-1}.

(1''s,4''s)-1,1''''-dihydroxy-1'',4''-dimethoxy-1'',4''-dihydro-[1,1':4',1'':4'',1''':4''',1''''-quinquephenyl]-4,4''''(1H,1''''H)-dione **12**

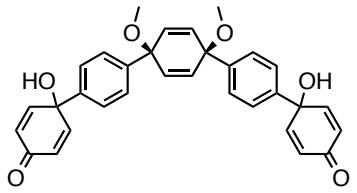

To a 500-mL flask equipped with a magnetic stir bar was added dibromide **20** (12.8 g, 28.4 mmol, 1 equiv) and dry THF (300 mL). This solution was cooled to –78˚C. *n*-butyllithium (2.5 M in hexanes, 25.0 mL, 57.5 mmol, 2.1 equiv) was added to the solution dropwise and ketal **21** (9.60 g, 62.5 mmol, 2.2 equiv) was quickly injected immediately. The mixture was allowed to warm to RT and stired overnight. H_2O (20 mL) was added to the mixture to quench and the solution was extracted with DCM (2 × 100 mL) and the combined organic layers were washed with H_2O (150 mL), and brine (150 mL) then dried over sodium sulfate and filtered. Solvent was removed under reduced pressure to yield a white semisolid that was redissolved in acetone (200 mL) and water (75 mL). Acetic acid (5 mL) was added to the mixture and stirring continued 30 minutes at room temperature. Saturated sodium bicarbonate (50 mL) was added to neutralize the solution, forming a pale yellow precipitate that was filtered off. The solid was washed with H_2O on the filter, air dried, and redissolved in THF (100 mL). This solution was dried over sodium sulfate and filtered. Solvent was removed under reduced pressure and the resulting solid was washed with minimal methanol and dried under high vacuum to give a tan solid that was used as prepared. (7.8 g, 55%). ^{1}H NMR (500 MHz, Chloroform-d) δ(ppm) 7.41 (s, 8H), 6.87 (d, J = 9.8 Hz, 4H), 6.23 (d, J = 9.8 Hz, 4H), 6.09 (s, 4H), 3.42 (s, 6H), 2.42 (s, 2H); ^{13}C NMR (151 MHz, DMSO-d6) δ(ppm) 185.50, 152.51, 142.99, 139.57, 133.03, 126.12, 125.55, 125.38, 73.86, 69.91, 51.49; IR (neat): 665.96, 700.79, 735.09, 764.23, 833.02, 859.16, 948.54, 1015.94, 1027.5, 1078.34,

1171.62, 1227.79, 1266.22, 1395.25, 1448.72, 1461.42, 1500.16, 1621.32, 1665.36, 2823.69, 2936.05, 3400.15, cm^{-1}.

seven-ring dichloride **23**

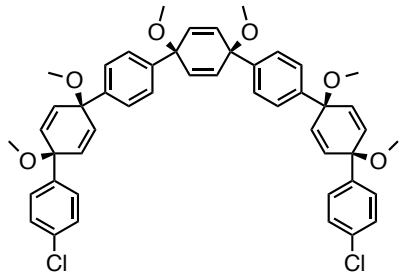

To a 250-mL flask equipped with a magnetic stir bar was added diketone **22** (2.00 g, 3.94 mmol, 1 equiv), 1-bromo-4-chlorobenzene (6.00 g, 31.3 mmol, 8 equiv) and dry THF (50 mL). This solution was cooled to –78˚C. Sodium hydride was added in one portion quickly (60% in mineral oil, 800 mg, 20 mmol, 5 equiv) and stirred 30 minutes. *n*-butyllithium (2.5 M in hexanes, 16 mL, 40 mmol, 10 equiv) was added to the mixture dropwise and the mixture was stirred 2 hours at –78˚C. Methyl iodide (26.0 mL, 417 mmol, 105 equiv) then dry DMF (10 mL) were added via syringe and the mixture was allowed to warm to room temperature and stirred overnight. H_2O (100 mL) was added to the mixture to quench and the solution was extracted with ethyl acetate (2 × 50 mL) and the combined organic layers were washed with H_2O (100 mL), 5% lithium chloride in H_2O (5 × 100 mL) and brine (100 mL) then dried over sodium sulfate and filtered. Solvent was removed under reduced pressure to yield a yellow solid that was dissolved in DCM (20 mL) to which was added isopropyl alcohol (100 mL). the DCM in this mixture was removed under reduced pressure resulting in a pale yellow precipitate in the remaining alcohol which was filtered off as a yellow powder. This powder was again dissolved in DCM (50 mL) dried over sodium sulfate, filtered, and concentrated under reduced pressure to afford a pale yellow powder that was used as prepared (2.2 g, 71%). ^{1}H NMR (500 MHz, Chloroform-d) δ(ppm) 7.43 – 7.28 (overlap, 16H), 6.14 (d, J = 10.3 Hz, 4H), 6.10 (s, 4H), 6.07 (d, J = 10.3 Hz, 4H), 3.45 (s, 6H), 3.45 (s, 6H), 3.44 (s, 6H); ^{13}C NMR (151 MHz, Chloroform-d) δ(ppm) 142.55, 142.94, 142.06, 133.72, 133.35,

133.34, 133.00, 128.48, 127.47, 126.08, 125.99, 74.58, 74.57, 74.45, 52.03, 52.02, 52.01; IR (neat): 665.9, 730.37, 758.97, 829.17, 909.48, 950.98, 1013.52, 1028.56, 1081.52, 1174.31, 1228.6, 1404.47, 1450.18, 1461.89, 1483.15, 1501.11, 2246.1, 2822.61, 2898.72, 2937.52, 2982.16, 3026.95 cm^{-1}.

seven-ring diboronate **24**

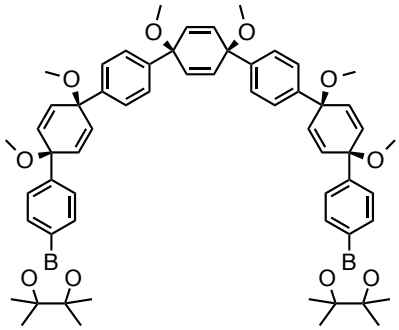

To a 100-mL flask equipped with a magnetic stir bar was added dichloride **23** (1.93 g, 2.44 mmol, 1 equiv), bis(pinacolato)diboron (4.96 g, 19.55 mmol, 8 equiv), $Pd(OAc)_2$ (65.6 mg, 0.240 mmol, 0.10 equiv), SPhos (250 mg, 0.61 mmol, 0.25 equiv), and ground, oven-dried K_3PO_4 (4.14 g, 19.5 mmol, 8 equiv). This flask was evacuated and backfilled with dry N_2 ten times to exclude moisture and air (crucial for the success of the procedure). Dry dioxane (25 mL) was added to the flask and the mixture stirred while heating to 90˚C overnight. Mixture was cooled to room temperature, filtered through a pad of celite and concentrated under reduced pressure. The resulting semisolid was taken up in ethyl acetate (100 mL). This solution was washed with H_2O (2 × 100 mL) and brine (100 mL) then dried over sodium sulfate and filtered. Solvent was removed under reduced pressure and the crude solid dissolved in DCM (20 mL) to which was added isopropyl alcohol (100 mL). the DCM in this mixture was removed under reduced pressure resulting in a pale yellow precipitate in the remaining alcohol which was filtered off as a yellow powder. This powder was again dissolved in DCM (50 mL) dried over sodium sulfate, filtered, and concentrated under reduced pressure to afford a white powder that was very pure (1.52 g, 64%, 22% over three steps from **20**). ^1H NMR (500 MHz, Chloroform-d) δ(ppm) 7.76 (d, J = 8.2 Hz, 4H), 7.40 (d, J = 8.2 Hz, 4H), 7.34 (s,

8H), 6.00 – 6.10 (overlap, 12H), 3.42 (s, 12H), 3.41 (s, 6H); ^{13}C NMR (151 MHz, Chloroform-d) δ(ppm) 146.60, 142.90, 142.76, 135.06, 133.51, 133.42, 133.25, 126.17, 125.42, 83.88, 75.01, 74.76, 74.71, 52.08, 52.06, 51.99, 24.99; IR (neat): 659.37, 733.04, 757.38, 832.15, 859.02, 910.39, 950.76, 1016.74, 1085.7, 1144.71, 1173.71, 1228.74, 1272.8, 1320.51, 1361.06, 1398.69, 1462.59, 1502.09, 1609.72, 2245.8, 2822.7, 2899.12, 2936.83, 2978.78 cm^{-1}; LRMS (FAB+) *(m/z)*: [M–pinacol]$^{+}$ calcd. for $C_{54}H_{58}B_2O_8$, 856.83; found, 857.9.

azo[9]cycloparaphenylene macrocycle **25**

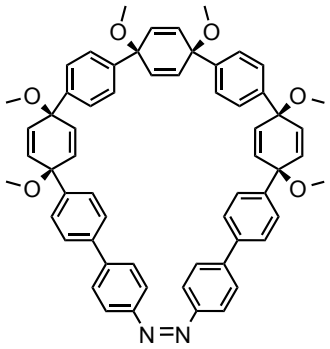

To a 1-L flask equipped with a magnetic stir bar was added 4,4′-dibromoazobenzene **6** (175 mg, 0.514 mmol, 1 equiv), seven-ring diboronate **24** (500 mg, 0.514 mmol, 1 equiv), and SPhos Pd G2 (37.0 mg, 0.0514 mmol, 0.1 equiv). This flask was evacuated and backfilled with dry N_2 five times to exclude moisture and air. Dry dioxane (500 mL) was added and the mixture was heated to 90˚C while stirring. 2M K_3PO_4 in N_2 sparged H_2O (13 mL, 26 mmol, 50 equiv) was added via syringe and the mixture stirred at 90˚C overnight. After cooling to room temperature, the solution was filtered through a pad of celite and concentrated under reduced pressure. The resulting semisolid was redissolved in 150 mL of DCM. The solution was washed with H_2O (2 × 150 mL) and brine (150 mL) then dried over sodium sulfate and filtered. Solvent was removed under reduced pressure and the crude solid was purified by GPC to give a bright orange crystalline solid (85 mg, 22%). When silica gel chromatography is used, azoxy derivative **26** is obtained but this is not observed with GPC. ^{1}H NMR (600 MHz, Chloroform-d) δ(ppm) 7.42 (d, J = 8.7 Hz, 4H), 7.40 (d, J = 8.7 Hz, 4H), 7.37 (d, J = 8.7 Hz, 4H), 7.34 (d, J = 4.8 Hz, 4H),

7.32 (d, J = 4.8 Hz, 4H), 6.80 (d, J = 8.7 Hz, 4H), 6.14 (s, 4H), 6.08 (d, J = 10.2 Hz, 4H), 6.00 (d, J = 10.2 Hz, 4H), 3.43 (s, 6H), 3.42 (s, 6H), 3.36 (s, 6H); ^{13}C NMR (151 MHz, Chloroform-d) δ(ppm) 153.72, 143.05, 142.99, 142.79, 139.28, 138.71, 130.85, 127.67, 126.81, 126.77, 126.29, 126.25, 126.06, 120.94, 104.16, 74.44, 52.05, 52.01, 51.93; IR (neat): 665.79, 730.71, 756.16, 774.32, 811.49, 828.32, 908.23, 950.28, 1016.15, 1079.73, 1111.83, 1175.55, 1230.26, 1247.31, 1402.92, 1431.92, 1450.22, 1470.18, 1486.2, 1494.24, 1589.03, 1605.35, 2244.81, 2822.44, 2898.61, 2936.15, 2980.76, 3029.34, 3452.37 cm^{-1}.

azo[9]cycloparaphenylene **13**

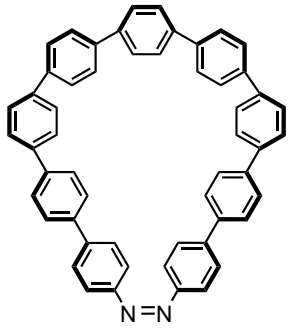

Macrocycle **25** (40 mg, 0.054 mmol, 1 equiv) was dissolved in freshly distilled THF (20 mL) and cooled to –78°C under N_2. 0.25 M sodium naphthalenide (3.21 mL, 0.803 mmol, 15 equiv) was added dropwise to the stirring solution to give a deep blue color. The mixture was stirred for one hour then 1 M I_2 in DCM was added (2.0 mL) followed by saturated sodium thiosulfate in H_2O (5 mL). After warming to room temperature, the solution was and concentrated under reduced pressure. The resulting solid was redissolved in 10 mL of DCM. The solution was washed with H_2O (2 × 10 mL) and brine (10 mL) then dried over sodium sulfate and filtered. Solvent was removed under reduced pressure and the crude solid was chromatographed on silica gel in an DCM/hexanes gradient of increasing polarity up to 1:1 then further purified by GPC to give a crystalline orange solid (22 mg, 57%). ^{1}H NMR (600 MHz, Chloroform-d) δ 7.61 (s, 4H), 7.57 (d, J = 8.8 Hz, 4H), 7.53 (d, J = 2.5 Hz, 4H), 7.51 (d, J = 2.5 Hz, 4H), 7.50 (d, J = 8.6 Hz, 4H), 7.47 (d, J = 8.6 Hz, 4H), 7.45 (d, J = 8.3 Hz, 4H), 7.41 (d, J = 8.8 Hz, 4H), 6.84 (d, J = 8.3 Hz, 4H); ^{13}C NMR (151 MHz, Chloroform-d) δ(ppm) 153.14, 139.24, 138.91,

138.04, 137.84, 127.69, 127.66, 127.59, 127.55, 127.23, 127.03, 127.01, 126.94, 120.86; LRMS (FAB+) *(m/z)*: $[M]^+$ calcd. for $C_{54}H_{36}N_2$, 712.90; found, 714.4.

IV.8.3. Computation Details

All calculations were carried out with Gaussian 09 package at B3LYP/6-31g* or M062X/6-31G* (where noted) level of theory.[33] All excited state calculations (TD-DFT) were performed on fully optimized (B3LYP/6-31G*) structures. The fully optimized structures were confirmed to be true minima by vibrational analysis. Structures were minimized with no symmetry restrictions. Structures are depicted with their geometries, HOMO and LUMO orbitals followed by a summary their of total energy in Hartree unless noted. Relevant computational data are depicted in Figures **IV.12-IV.25** and Tables **IV.1-IV.8**. For computational coordinates, see Appendix **I**.

cis-azo[11]CPP

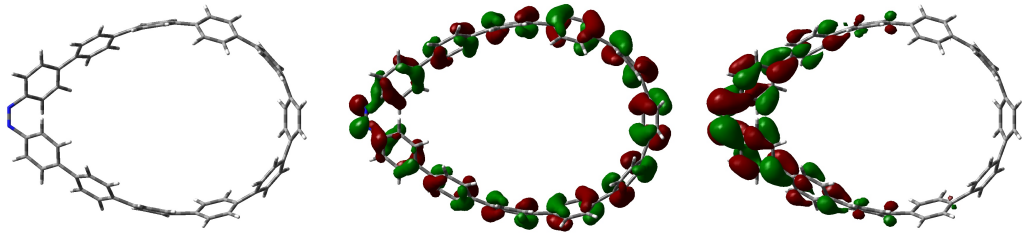

Figure IV.12. DFT visualization of *cis*-azo[11]CPP. Left to right: geometry, HOMO, LUMO.

HOMO (eV) = -5.23
LUMO (eV) = -2.22
HOMO/LUMO gap (eV) = 3.01
Zero-point correction = 0.899563 (Hartree/Particle)
Thermal correction to Energy = 0.950353
Thermal correction to Enthalpy = 0.951297
Thermal correction to Gibbs Free Energy = 0.812418
Sum of electronic and zero-point Energies = -2650.102162
Sum of electronic and thermal Energies = -2650.051372
Sum of electronic and thermal Enthalpies = -2650.050428

Sum of electronic and thermal Free Energies = -2650.189307

Table IV.1. Major electronic transitions for *cis*-azo[11]CPP determined by TD-DFT method using B3LYP/6-31g*.

Energy (cm^{-1})	Wavelength (nm)	Osc. Strength	Major contribs
18622.66384	536.9801058	0.1295	H-3->LUMO (11%), H-1->LUMO (40%), HOMO->LUMO (37%)
22730.47392	439.9380336	0.0034	H-3->LUMO (10%), H-1->LUMO (22%), HOMO->LUMO (57%)
24637.98832	405.8772928	0.4242	H-2->LUMO (87%)
25509.87968	392.0049849	0.1231	H-1->LUMO (10%), HOMO->L+1 (63%)
26493.88288	377.4456181	0.676	H-3->LUMO (46%), H-1->LUMO (18%), HOMO->L+1 (20%)
27398.03664	364.9896572	1.3643	HOMO->L+2 (95%)
28625.62096	349.3374	0.1186	H-1->L+1 (78%)
28769.18864	347.5940919	0.2177	H-2->L+1 (46%), H-1->L+2 (38%)
29362.8168	340.566781	0.4705	H-4->LUMO (45%), H-2->L+1 (37%)
29804.00512	335.5253752	0.1983	H-2->L+2 (55%), H-1->L+2 (15%)
30311.33136	329.9096262	0.0134	H-4->LUMO (30%), H-2->L+2 (20%), H-1->L+2 (34%)
30954.15968	323.058358	0.1069	H-5->LUMO (21%), HOMO->L+3 (46%)

trans-azo[11]CPP

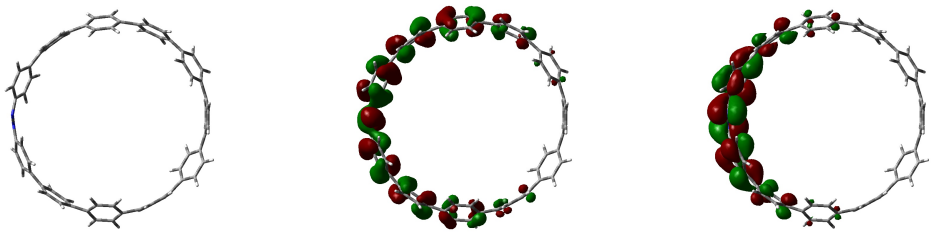

Figure IV.13. DFT visualization of *trans*-azo[11]CPP. Left to right: geometry, HOMO, LUMO.

HOMO (eV) = -5.27

LUMO (eV) = -2.39

HOMO/LUMO gap (eV) = 2.88

Zero-point correction = 0.899507 (Hartree/Particle)

Thermal correction to Energy = 0.950231

Thermal correction to Enthalpy = 0.951175

Thermal correction to Gibbs Free Energy = 0.812860

Sum of electronic and zero-point Energies = -2650.104358

Sum of electronic and thermal Energies = -2650.053634

Sum of electronic and thermal Enthalpies = -2650.052690

Sum of electronic and thermal Free Energies = -2650.191005

Table IV.2. Major electronic transitions for *trans*-azo[11]CPP determined by TD-DFT method using B3LYP/6-31g*.

Energy (cm^{-1})	Wavelength (nm)	Osc. Strength	Major contribs
17946.76656	557.2034364	0.2757	H-4->LUMO (18%), H-2->LUMO (15%), HOMO->LUMO (60%)
21663.39504	461.6081635	0.1374	H-1->LUMO (99%)
22104.58336	452.3948648	0.2044	H-4->LUMO (25%), H-2->LUMO (31%), HOMO->LUMO (35%)
25641.34896	389.9950824	0.1318	H-3->LUMO (90%)
25813.14624	387.3995021	0.344	H-2->LUMO (18%), H-1->L+1 (67%)
26720.52624	374.2441264	1.1344	H-4->LUMO (38%), H-2->LUMO (30%), H-1->L+1 (22%)
27045.56992	369.7463218	0.8069	HOMO->L+1 (93%)
29544.2928	338.4748475	0.4411	H-1->L+2 (25%), HOMO->L+2 (59%)
29713.6704	336.5454306	0.3395	H-1->L+2 (59%), HOMO->L+2 (26%)
30469.41712	328.1979422	0.0534	H-5->LUMO (44%), H-2->L+1 (12%), HOMO->L+3 (29%)
30790.428	324.7762584	0.2529	H-2->L+1 (63%), H-1->L+3 (17%), HOMO->L+3 (10%)
30963.03184	322.9657887	0.2517	H-3->L+1 (11%), H-2->L+1 (17%), H-1->L+3 (59%)

azo[7]CPP dimer macrocycle

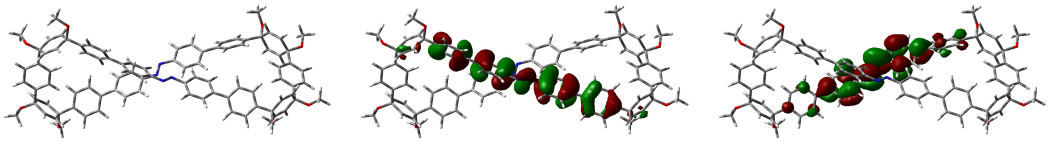

Figure IV.14. DFT visualization of azo[7]CPP dimer macrocycle. Left to right: geometry, HOMO, LUMO.

HOMO (eV) = -5.66

LUMO (eV) = -2.34

HOMO/LUMO gap (eV) = 3.32

Zero-point correction = 1.498859 (Hartree/Particle)

Thermal correction to Energy = 1.589797

Thermal correction to Enthalpy = 1.590741

Thermal correction to Gibbs Free Energy = 1.359221

Sum of electronic and zero-point Energies = -4372.932481

Sum of electronic and thermal Energies = -4372.841543

Sum of electronic and thermal Enthalpies = -4372.840599

Sum of electronic and thermal Free Energies = -4373.072119

azo[7]CPP dimer CPP

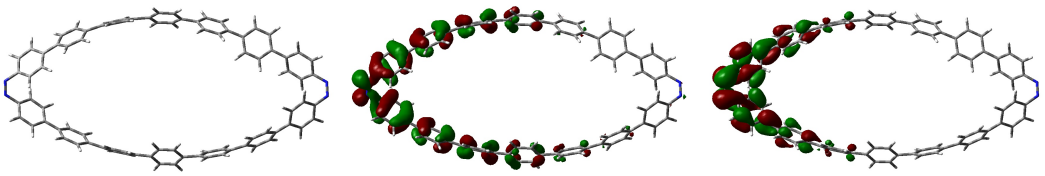

Figure IV.15. DFT visualization of azo[7]CPP dimer CPP. Left to right: geometry, HOMO, LUMO.

HOMO (eV) = -5.38

LUMO (eV) = -2.20

HOMO/LUMO gap (eV) = 3.18

Zero-point correction = 1.151574 (Hartree/Particle)

Thermal correction to Energy = 1.218703

Thermal correction to Enthalpy = 1.219648

Thermal correction to Gibbs Free Energy = 1.040724

Sum of electronic and zero-point Energies = -3452.495348

Sum of electronic and thermal Energies = -3452.428219

Sum of electronic and thermal Enthalpies = -3452.427274

Sum of electronic and thermal Free Energies = -3452.606198

trans-azo[9]CPP

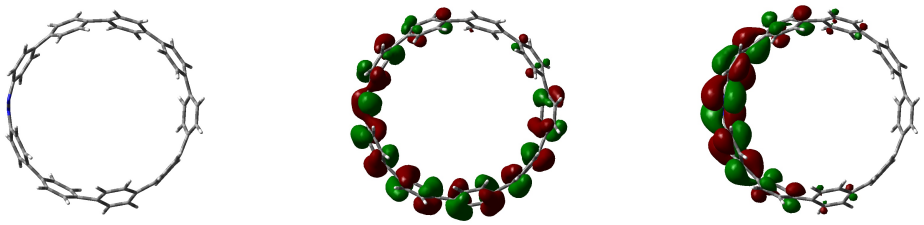

Figure IV.16. DFT visualization of *trans*-azo[9]CPP dimer CPP. Left to right: geometry, HOMO, LUMO.

HOMO (eV) = -5.27

LUMO (eV) = -2.38

HOMO/LUMO gap (eV) = 2.89

Zero-point correction = 0.736986 (Hartree/Particle)

Thermal correction to Energy = 0.778305

Thermal correction to Enthalpy = 0.779250

Thermal correction to Gibbs Free Energy = 0.662740

Sum of electronic and zero-point Energies = -2188.137512

Sum of electronic and thermal Energies = -2188.096192

Sum of electronic and thermal Enthalpies = -2188.095248

Sum of electronic and thermal Free Energies = -2188.211758

Table IV.3. Major electronic transitions for *trans*-azo[9]CPP determined by TD-DFT method using B3LYP/6-31g*.

Energy (cm^{-1})	Wavelength (nm)	Osc. Strength	Major contribs
17804.812	561.6459191	0.1775	H-4->LUMO (16%), H-2->LUMO (19%), H-1->LUMO (18%), HOMO->LUMO (43%)
21343.19072	468.5335071	0.1388	H-1->LUMO (56%), HOMO->LUMO (40%)
22033.60608	453.8521731	0.1375	H-4->LUMO (17%), H-2->LUMO (37%), H-1->LUMO (23%), HOMO->LUMO (12%)
25967.1992	385.1012165	0.5728	H-2->LUMO (11%), H-1->L+1 (46%), HOMO->L+1 (33%)
26676.16544	374.8664711	0.1537	H-3->LUMO (22%), H-1->L+1 (24%), HOMO->L+1 (50%)
27360.93488	365.4845876	0.5845	H-3->LUMO (53%), H-1->L+1 (20%)
27733.5656	360.5739033	0.6101	H-4->LUMO (48%), H-3->LUMO (18%), H-2->LUMO (20%)
30407.312	328.8682669	0.0599	HOMO->L+2 (87%)
30565.39776	327.1673439	0.3981	H-1->L+2 (82%)
31441.32192	318.052785	0.0262	H-9->LUMO (14%), H-8->LUMO (24%), H-7->LUMO (12%)
31510.68608	317.3526585	0.02	H-13->LUMO (12%), H-11->LUMO (10%), H-10->LUMO (18%), H-8->LUMO (20%)
31546.17472	316.9956449	0.5034	H-2->L+1 (81%)

trans-azo[9]CPP (M062X)

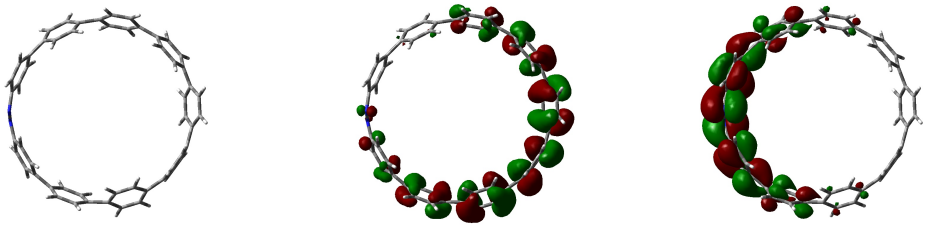

Figure IV.17. DFT visualization of *trans*-azo[9]CPP (M062X). Left to right: geometry, HOMO, LUMO.

HOMO (eV) = -6.53

LUMO (eV) = -1.50

HOMO/LUMO gap (eV) = 5.03

Zero-point correction = 0.744485 (Hartree/Particle)

Thermal correction to Energy = 0.785460

Thermal correction to Enthalpy = 0.786404

Thermal correction to Gibbs Free Energy = 0.670729

Sum of electronic and zero-point Energies = -2187.226232

Sum of electronic and thermal Energies = -2187.185256

Sum of electronic and thermal Enthalpies = -2187.184312

Sum of electronic and thermal Free Energies = -2187.299988

cis-azo[9]CPP

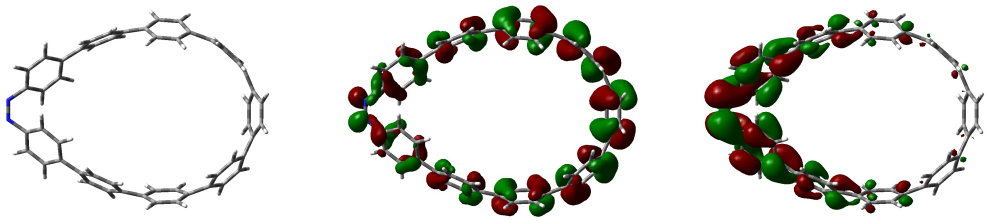

Figure IV.18. DFT visualization of *cis*-azo[9]CPP. Left to right: geometry, HOMO, LUMO.

HOMO (eV) = -5.21

LUMO (eV) = -2.15

HOMO/LUMO gap (eV) = 3.06

Zero-point correction = 0.737050 (Hartree/Particle)

Thermal correction to Energy = 0.778382

Thermal correction to Enthalpy = 0.779327

Thermal correction to Gibbs Free Energy = 0.662677

Sum of electronic and zero-point Energies = -2188.140824

Sum of electronic and thermal Energies = -2188.099492

Sum of electronic and thermal Enthalpies = -2188.098548

Sum of electronic and thermal Free Energies = -2188.215197

Table IV.4. Major electronic transitions for *cis*-azo[9]CPP determined by TD-DFT method using B3LYP/6-31g*.

Energy (cm^{-1})	Wavelength (nm)	Osc. Strength	Major contribs
19143.7016	522.3650164	0.0712	H-1->LUMO (44%), HOMO->LUMO (40%)
22750.63792	439.5481144	0.0415	H-1->LUMO (26%), HOMO->LUMO (54%)
25570.37168	391.0776161	0.1835	H-2->LUMO (13%), HOMO->L+1 (69%)
25917.19248	385.8442618	0.3793	H-2->LUMO (78%), HOMO->L+1 (15%)
28070.70768	356.2432452	0.4985	H-3->LUMO (57%), H-1->LUMO (19%)
28353.81024	352.686285	0.7861	HOMO->L+2 (93%)
29275.70832	341.5801213	0.0493	H-1->L+1 (84%)
29695.11952	336.7556744	0.5745	H-2->L+1 (70%), H-1->L+2 (21%)
30975.13024	322.8396434	0.0956	H-4->LUMO (36%), H-2->L+1 (22%), H-1->L+2 (33%)
31692.16208	315.5354303	0.1342	H-4->LUMO (15%), H-2->L+2 (56%), H-1->L+2 (13%)
32113.1864	311.3985599	0.01	H-4->LUMO (30%), H-2->L+2 (31%), H-1->L+2 (25%)
32361.60688	309.0081416	0.0318	H-6->LUMO (24%), HOMO->L+3 (24%)

cis-azo[9]CPP (M062X)

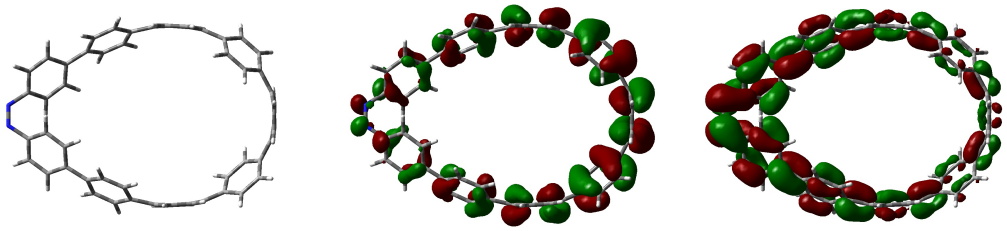

Figure IV.19. DFT visualization of *cis*-azo[9]CPP (M062X). Left to right: geometry, HOMO, LUMO.

HOMO (eV) = -6.41

LUMO (eV) = -1.29

HOMO/LUMO gap (eV) = 5.12

Zero-point correction = 0.744967 (Hartree/Particle)

Thermal correction to Energy = 0.785906

Thermal correction to Enthalpy = 0.786850

Thermal correction to Gibbs Free Energy = 0.670974

Sum of electronic and zero-point Energies = -2187.227778

Sum of electronic and thermal Energies = -2187.186839

Sum of electronic and thermal Enthalpies = -2187.185895

Sum of electronic and thermal Free Energies = -2187.301771

fullerene C_{60} (M062X)

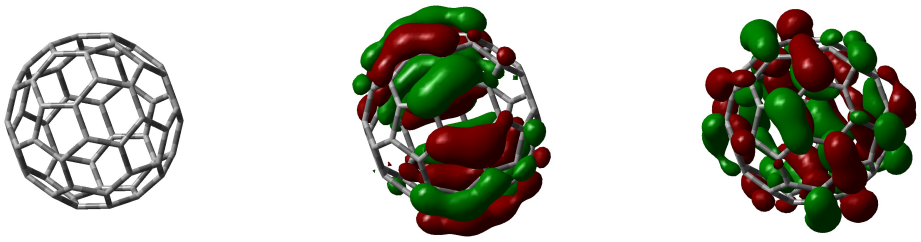

Figure IV.20. DFT visualization of fullerene C_{60} (M062X). Left to right: geometry, HOMO, LUMO.

HOMO (eV) = -5.99

LUMO (eV) = -3.23

HOMO/LUMO gap (eV) = 2.76

Zero-point correction= 0.382079 (Hartree/Particle)

Thermal correction to Energy= 0.402489

Thermal correction to Enthalpy= 0.403433

Thermal correction to Gibbs Free Energy= 0.339169

Sum of electronic and zero-point Energies= -2285.074430

Sum of electronic and thermal Energies= -2285.054020

Sum of electronic and thermal Enthalpies= -2285.053076

Sum of electronic and thermal Free Energies= -2285.117341

fullerene C_{60} @ trans-azo[9]CPP (M062X)

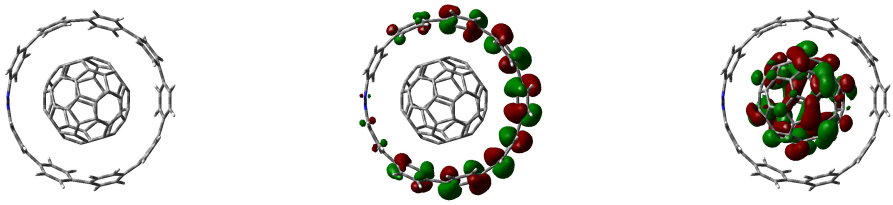

Figure IV.21. DFT visualization of fullerene C_{60}@*trans*-azo[9]CPP (M062X). Left to right: geometry, HOMO, LUMO.

HOMO (eV) = -6.54

LUMO (eV) = -2.42

HOMO/LUMO gap (eV) = 4.12

Zero-point correction = 1.128308 (Hartree/Particle)

Thermal correction to Energy = 1.190615

Thermal correction to Enthalpy = 1.191559

Thermal correction to Gibbs Free Energy = 1.041639

Sum of electronic and zero-point Energies = -4472.353617

Sum of electronic and thermal Energies = -4472.291309

Sum of electronic and thermal Enthalpies = -4472.290365

Sum of electronic and thermal Free Energies = -4472.440286

fused azo[11]CPP

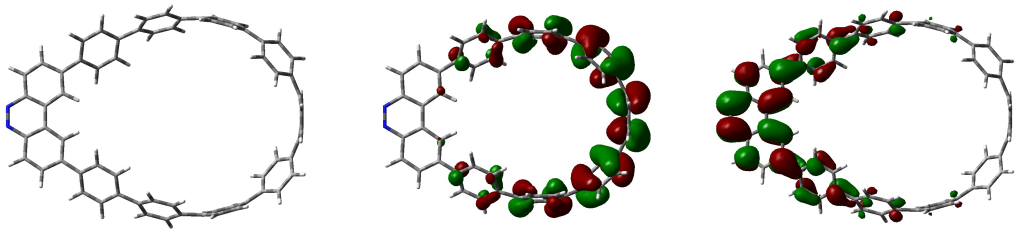

Figure IV.22. DFT visualization of fused azo[11]CPP. Left to right: geometry, HOMO, LUMO.

HOMO (eV) = -5.27

LUMO (eV) = -2.16

HOMO/LUMO gap (eV) = 3.11

Zero-point correction = 0.878905 (Hartree/Particle)

Thermal correction to Energy = 0.928248

Thermal correction to Enthalpy = 0.929192

Thermal correction to Gibbs Free Energy = 0.794784

Sum of electronic and zero-point Energies = -2648.964807

Sum of electronic and thermal Energies = -2648.915464

Sum of electronic and thermal Enthalpies = -2648.914519

Sum of electronic and thermal Free Energies = -2649.048927

Table IV.5. Major electronic transitions for fused azo[11]CPP determined by TD-DFT method using B3LYP/6-31g*.

Energy (cm^{-1})	Wavelength (nm)	Osc. Strength	Major contribs
22438.4992	445.6626047	0.0017	H-3->LUMO (84%)
22590.13248	442.6711534	0.0003	HOMO->LUMO (80%)
25549.40112	391.3986067	0.2746	HOMO->LUMO (11%), HOMO->L+1 (79%)
25655.86704	389.7743929	0.5992	H-1->LUMO (99%)
26860.06112	372.2999719	0.7768	H-2->LUMO (86%)
27677.1064	361.3094467	0.7827	HOMO->L+2 (97%)
29141.0128	343.1589722	0.9206	H-1->L+1 (93%)
29425.72848	339.8386554	0.0287	H-6->LUMO (52%), H-2->L+3 (13%), HOMO->L+3 (20%)
30101.62576	332.2079704	0.0105	H-1->L+2 (82%)

Table IV.5 (continued).

30976.74336	322.8228314	0	H-6->LUMO (12%), H-3->L+3 (30%), HOMO->L+3 (50%)
31049.33376	322.0681022	0	H-3->L+3 (53%), HOMO->L+3 (29%)
31208.22608	320.4283375	0.0595	H-2->L+1 (80%)

fused azo[9]CPP

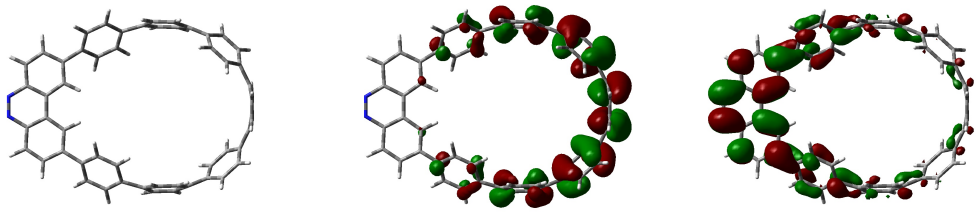

Figure IV.23. DFT visualization of fused azo[9]CPP. Left to right: geometry, HOMO, LUMO.

HOMO (eV) = -5.28

LUMO (eV) = -2.13

HOMO/LUMO gap (eV) = 3.15

Zero-point correction = 0.716315 (Hartree/Particle)

Thermal correction to Energy = 0.756286

Thermal correction to Enthalpy = 0.757230

Thermal correction to Gibbs Free Energy = 0.644318

Sum of electronic and zero-point Energies = -2187.000657

Sum of electronic and thermal Energies = -2186.960686

Sum of electronic and thermal Enthalpies = -2186.959742

Sum of electronic and thermal Free Energies = -2187.072654

Table IV.6. Major electronic transitions for fused azo[9]CPP determined by TD-DFT method using B3LYP/6-31g*.

Energy (cm^{-1})	Wavelength (nm)	Osc. Strength	Major contribs
22404.62368	446.3364412	0.0056	H-2->LUMO (10%), HOMO->LUMO (73%)
22561.09632	443.2408717	0.0038	H-3->LUMO (61%), H-2->LUMO (13%), HOMO->LUMO (17%)
25908.32032	385.976392	0.3027	HOMO->L+1 (87%)
27091.54384	369.1188682	0.4053	H-1->LUMO (98%)
28348.97088	352.746491	0.5837	H-3->LUMO (21%), H-2->LUMO (70%)
28767.57552	347.613583	0.4731	HOMO->L+2 (91%)
29553.16496	338.3732339	0.0033	H-4->LUMO (47%), HOMO->L+3 (37%)
30616.21104	326.624349	0.6765	H-1->L+1 (73%)
30927.5432	323.3363845	0.1052	H-4->LUMO (20%), H-3->L+3 (12%), H-1->L+1 (14%), HOMO->L+3 (47%)
31128.37664	321.2502893	0.0039	H-3->L+2 (12%), H-3->L+3 (47%), H-2->L+3 (20%)
32151.09472	311.0313999	0.0008	H-2->L+1 (52%), H-1->L+2 (33%)
32818.11984	304.7097167	0	H-7->L+1 (11%), HOMO->L+4 (12%), HOMO->L+6 (52%)

azoxy[9]CPP macrocycle

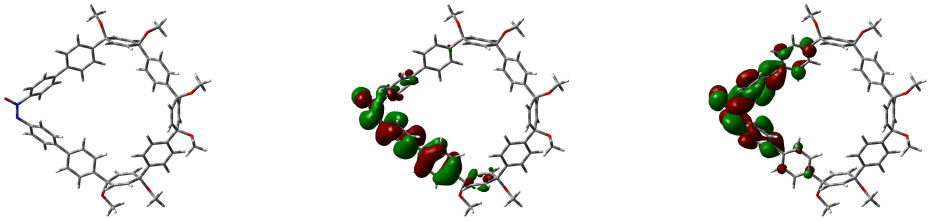

Figure IV.24. DFT visualization of fused azoxy[9]CPP macrocycle. Left to right: geometry, HOMO, LUMO.

HOMO (eV) = -5.69

LUMO (eV) = -2.01

HOMO/LUMO gap (eV) = 3.68

Zero-point correction = 1.002240 (Hartree/Particle)

Thermal correction to Energy = 1.062586

Thermal correction to Enthalpy = 1.063530

Thermal correction to Gibbs Free Energy = 0.904131

Sum of electronic and zero-point Energies = -2953.662845

Sum of electronic and thermal Energies = -2953.602500

Sum of electronic and thermal Enthalpies = -2953.601555

Sum of electronic and thermal Free Energies = -2953.760954

Table IV.7. Major electronic transitions for azoxy[9]CPP macrocycle determined by TD-DFT method using B3LYP/6-31g*.

Energy (cm^{-1})	Wavelength (nm)	Osc. Strength	Major contribs
25419.54496	393.3980729	0.2598	HOMO->LUMO (91%)
29328.94128	340.9601426	0.0749	H-1->LUMO (43%)
32326.11824	309.3473805	0.1484	H-15->LUMO (11%), H-11->LUMO (10%), H-1->LUMO (43%)
33648.07008	297.1938651	0.129	H-8->LUMO (20%), HOMO->L+1 (59%)
33859.3888	295.3390582	0.0072	H-4->LUMO (15%), H-2->LUMO (68%)
34132.81264	292.9732192	0.0969	H-8->LUMO (31%), H-3->LUMO (26%), HOMO->L+1 (18%)
34743.37856	287.8246277	0.0511	H-8->LUMO (24%), H-3->LUMO (36%)
35028.09424	285.4851289	0.0021	H-5->LUMO (15%), H-4->LUMO (57%), H-3->LUMO (19%)
35357.97728	282.8216083	0.0036	H-5->LUMO (74%)
35635.43392	280.619566	0.0748	HOMO->L+3 (23%), HOMO->L+4 (60%)
36379.8888	274.8771459	0.0083	HOMO->L+2 (85%)
36783.1688	271.8634725	0.0179	H-13->LUMO (35%), H-12->LUMO (11%), H-11->LUMO (20%)

azo[9]CPP macrocycle

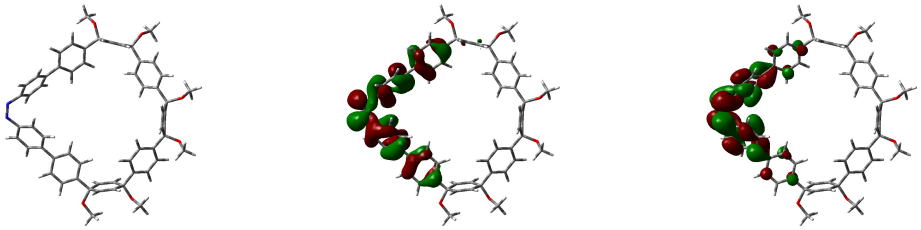

Figure IV.25. DFT visualization of fused azo[9]CPP macrocycle. Left to right: geometry, HOMO, LUMO.

HOMO (eV) = -5.51

LUMO (eV) = -2.04

HOMO/LUMO gap (eV) = 3.68

Zero-point correction = 0.997458 (Hartree/Particle)

Thermal correction to Energy = 1.056763

Thermal correction to Enthalpy = 1.057707

Thermal correction to Gibbs Free Energy = 0.901530

Sum of electronic and zero-point Energies = -2878.483116

Sum of electronic and thermal Energies = -2878.423811

Sum of electronic and thermal Enthalpies = -2878.422866

Sum of electronic and thermal Free Energies = -2878.579043

Table IV.8. Major electronic transitions for azo[9]CPP macrocycle determined by TD-DFT method using B3LYP/6-31g*.

Energy (cm^{-1})	Wavelength (nm)	Osc. Strength	Major contribs
19887.34992	502.8322044	0.1056	HOMO->LUMO (86%)
28907.1104	345.9356491	0.258	H-3->LUMO (25%), H-2->LUMO (52%), HOMO->LUMO (13%)
29404.75792	340.0810177	0.1014	H-1->LUMO (88%)
33163.32752	301.5378959	0.0019	H-9->LUMO (51%), H-2->LUMO (12%), HOMO->L+5 (10%)
33589.99776	297.7076709	0.0295	H-3->LUMO (51%), H-2->LUMO (21%)
33915.848	294.8474117	0.1962	H-4->LUMO (35%), HOMO->L+1 (34%)

Table IV.8 (continued).

34280.41312	291.7117704	0.1223	H-4->LUMO (42%), HOMO->L+1 (29%)
34705.47024	288.1390147	0.0226	H-15->LUMO (26%), H-5->LUMO (28%), H-4->LUMO (17%)
34819.1952	287.1979074	0.0342	H-15->LUMO (16%), H-5->LUMO (61%)
35413.62992	282.3771532	0.0898	HOMO->L+1 (11%), HOMO->L+2 (18%), HOMO->L+3 (25%), HOMO->L+4 (22%)
35481.38096	281.8379592	0.0684	HOMO->L+2 (61%), HOMO->L+4 (10%)
35574.13536	281.1031076	0.0091	H-8->LUMO (78%)

IV.8.4. X-Ray Crystallographic Data

Structures are presented as an ORTEP plot of the molecule, spacefilling model of the packing, and relevant parameters. Relevant crystallographic data are depicted in Figures **IV.26-IV.27**.

azo[7]CPP dimer macrocycle

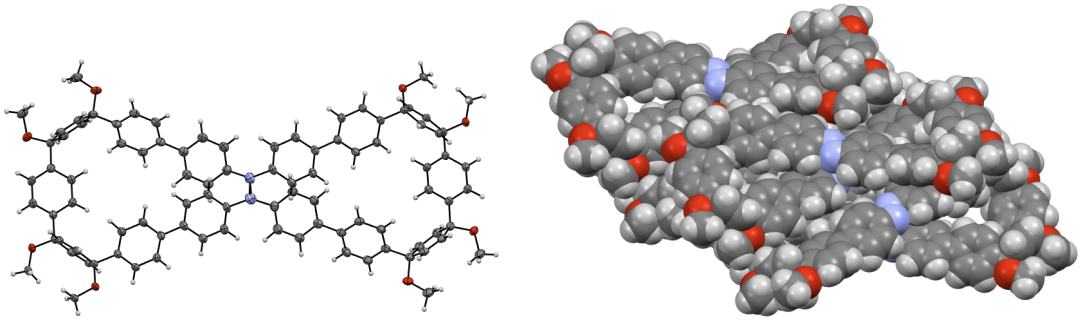

Figure IV.26. X-ray structure of azo[7]CPP dimer macrocycle. ORTEP plot at 50% probability (left) and packing (right). No solvent detected in crystal lattice.

Empirical formula	$C_{92}H_{80}N_4O_8$
Formula weight	1369.60
Temperature/K	173(2)
Crystal system	N/A
Space group	P-1

a/Å	10.5600(3)
b/Å	13.1564(3)
c/Å	26.5177(7)
α/°	99.5092(13)
β/°	101.2355(14)
γ/°	90.8824(14)
Volume/Å^3	3559.57(16)
Z	2
ϱ_{calc}g/cm^3	1.278
μ/mm^{-1}	0.643
F(000)	1448.0
Crystal size/mm^3	0.13 × 0.12 × 0.08
Radiation	CuKα (λ = 1.54178)
2Θ range for data collection/°	6.82 to 133.3
Index ranges	-12 ≤ h ≤ 12, -15 ≤ k ≤ 15, -31 ≤ l ≤ 31
Reflections collected	35840
Independent reflections	12338 [R_{int} = 0.0597, R_{sigma} = N/A]
Data/restraints/parameters	12338/0/1257
Goodness-of-fit on F^2	1.011
Final R indexes [I>=2σ (I)]	R_1 = 0.0482, wR_2 = 0.1086
Final R indexes [all data]	R_1 = 0.0698, wR_2 = 0.1187
Largest diff. peak/hole / e Å^{-3}	0.18/-0.24

azo[9]CPP macrocycle

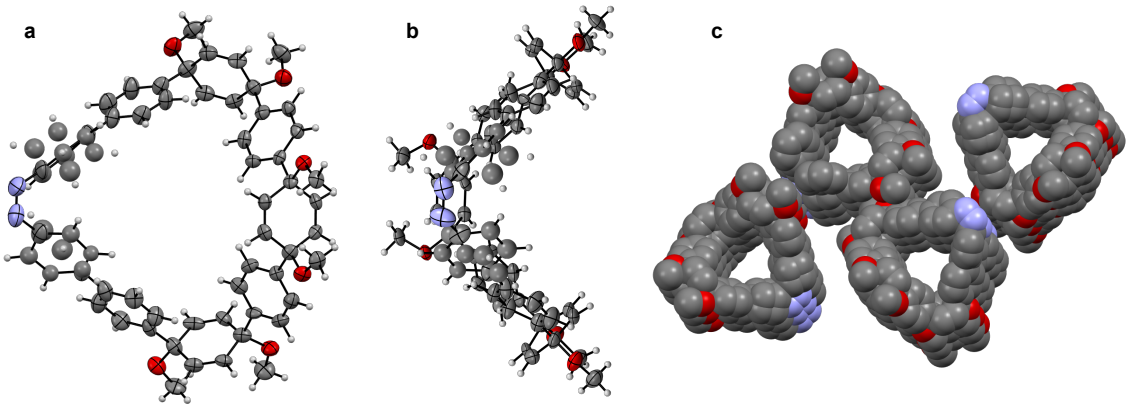

Figure IV.27. X-ray structure of azo[9]CPP macrocycle. ORTEP plot at 50% probability (a, b) and packing (c). Solvent omitted for clarity.

Empirical formula	$C_{71}H_{75}Cl_3N_2O_7$
Formula weight	1174.68

Temperature/K	173(2)
Crystal system	monoclinic
Space group	$P2_1/n$
a/Å	6.4870(5)
b/Å	38.319(3)
c/Å	25.818(2)
α/°	90
β/°	93.552(6)
γ/°	90
Volume/Å^3	6405.3(9)
Z	4
ϱ_{calc}g/cm^3	1.218
μ/mm^{-1}	1.725
F(000)	2488.0
Crystal size/mm^3	0.150 × 0.050 × 0.040
Radiation	CuKα (λ = 1.54178)
2Θ range for data collection/°	4.132 to 99.65
Index ranges	$-6 \le h \le 5$, $-37 \le k \le 23$, $-25 \le l \le 25$
Reflections collected	16773
Independent reflections	6410 [R_{int} = 0.0916, R_{sigma} = 0.1438]
Data/restraints/parameters	6410/17/758
Goodness-of-fit on F^2	1.001
Final R indexes [I>=2σ (I)]	R_1 = 0.0986, wR_2 = 0.2557
Final R indexes [all data]	R_1 = 0.1915, wR_2 = 0.3151
Largest diff. peak/hole / e Å^{-3}	0.54/-0.45

APPENDIX

CARTESIAN COORDINATES OF ALL CALCULATED STRUCTURES

All data calculated at the B3LYP/6-31G* level of theory unless noted.

Chapter II

Cartesian coordinates (in Å) of Macrocycle **2**:

C	-0.00287	-2.15455	0.94975
C	1.00735	-2.6536	1.64454
C	2.15923	-2.05156	1.64655
C	2.35105	-0.95233	0.92169
C	1.29157	-0.21789	0.38343
C	0.03908	-0.85687	0.39971
H	0.88004	-3.56362	2.19237
H	2.96855	-2.45974	2.21495
H	1.42822	0.75702	-0.03494
H	-0.83463	-0.38939	-0.00453
C	4.44531	-1.731	1.39713
C	5.68923	-1.99882	1.13241
C	6.35443	-1.26618	0.25379
C	5.84758	-0.04414	-0.23389
C	4.49531	0.2317	0.03526
C	3.81375	-0.74719	0.76234
H	3.91663	-2.32579	2.11248
H	6.1716	-2.82374	1.6137
H	6.45612	0.63075	-0.79898
H	4.01458	1.12168	-0.3141
C	6.6125	-4.73586	-0.10952
C	7.50116	-4.14804	1.0315
C	7.99983	-2.86965	1.00599
C	7.64417	-1.91308	-0.14089
C	7.41089	-2.70387	-1.44145
C	6.94967	-3.9879	-1.42464
H	7.74578	-4.77494	1.86368
H	8.6364	-2.53359	1.79753
H	7.61414	-2.23461	-2.38126
H	6.82439	-4.50131	-2.35511
C	3.10229	-5.99058	1.0281
C	4.50083	-5.79591	0.87241
C	5.0496	-4.68511	0.197
C	4.16251	-3.64444	-0.1799
C	2.61145	-3.85967	-0.00714
C	2.1406	-5.08934	0.52072
H	5.16743	-6.53104	1.27249

H	4.54119	-2.73106	-0.5891
H	1.92254	-3.09455	-0.29662
C	-0.17929	-4.98561	-0.63542
C	0.62123	-5.57023	0.55683
C	-0.1301	-5.20862	1.8775
C	-0.95232	-4.11591	1.99387
C	-1.12256	-3.1378	0.82268
C	-0.96548	-3.87703	-0.51829
H	-0.12047	-5.47574	-1.58467
H	-0.0113	-5.85094	2.72486
H	-1.47282	-3.93961	2.91204
H	-1.48431	-3.51104	-1.37976
O	8.67912	-0.94882	-0.34956
O	6.94391	-6.11944	-0.26277
O	-2.40018	-2.49721	0.86382
C	8.33357	-6.24755	-0.57426
H	8.91723	-5.83147	0.22006
H	8.57907	-7.28256	-0.69255
H	8.54427	-5.72491	-1.48365
C	-2.50529	-1.57838	-0.22737
H	-2.40355	-2.10846	-1.15157
H	-3.45956	-1.09548	-0.19674
H	-1.73116	-0.84408	-0.1506
C	9.89006	-1.61984	-0.70748
H	10.17493	-2.28578	0.08001
H	9.73622	-2.17726	-1.60789
H	10.66504	-0.89859	-0.86268
O	0.65231	-6.99492	0.44206
H	2.76302	-6.86644	1.54046
C	-0.68563	-7.49821	0.43651
H	-1.21935	-7.08029	-0.3914
H	-0.66582	-8.56403	0.34678
H	-1.17328	-7.22638	1.34951

Cartesian coordinates (in Å) of Macrocycle **3**:

C	-0.00287	-2.15455	0.94975
C	1.00735	-2.6536	1.64454
C	2.15923	-2.05156	1.64655
C	2.35105	-0.95233	0.92169
C	1.29157	-0.21789	0.38343
C	0.03908	-0.85687	0.39971
H	0.88004	-3.56362	2.19237
H	2.96855	-2.45974	2.21495
H	1.42822	0.75702	-0.03494
H	-0.83463	-0.38939	-0.00453
C	4.44531	-1.731	1.39713

C	5.68923	-1.99882	1.13241
C	6.35443	-1.26618	0.25379
C	5.84758	-0.04414	-0.23389
C	4.49531	0.2317	0.03526
C	3.81375	-0.74719	0.76234
H	3.91663	-2.32579	2.11248
H	6.1716	-2.82374	1.6137
H	6.45612	0.63075	-0.79898
H	4.01458	1.12168	-0.3141
C	6.6125	-4.73586	-0.10952
C	7.50116	-4.14804	1.0315
C	7.99983	-2.86965	1.00599
C	7.64417	-1.91308	-0.14089
C	7.41089	-2.70387	-1.44145
C	6.94967	-3.9879	-1.42464
H	7.74578	-4.77494	1.86368
H	8.6364	-2.53359	1.79753
H	7.61414	-2.23461	-2.38126
H	6.82439	-4.50131	-2.35511
C	3.10229	-5.99058	1.0281
C	4.50083	-5.79591	0.87241
C	5.0496	-4.68511	0.197
C	4.16251	-3.64444	-0.1799
C	2.61145	-3.85967	-0.00714
C	2.1406	-5.08934	0.52072
H	5.16743	-6.53104	1.27249
H	4.54119	-2.73106	-0.5891
H	1.92254	-3.09455	-0.29662
C	-0.17929	-4.98561	-0.63542
C	0.62123	-5.57023	0.55683
C	-0.1301	-5.20862	1.8775
C	-0.95232	-4.11591	1.99387
C	-1.12256	-3.1378	0.82268
C	-0.96548	-3.87703	-0.51829
H	-0.12047	-5.47574	-1.58467
H	-0.0113	-5.85094	2.72486
H	-1.47282	-3.93961	2.91204
H	-1.48431	-3.51104	-1.37976
O	6.94391	-6.11944	-0.26277
C	8.33357	-6.24755	-0.57426
H	8.91723	-5.83147	0.22006
H	8.57907	-7.28256	-0.69255
H	8.54427	-5.72491	-1.48365
O	0.65231	-6.99492	0.44206
H	2.76302	-6.86644	1.54046
C	-0.68563	-7.49821	0.43651

H	-1.21935	-7.08029	-0.3914
H	-0.66582	-8.56403	0.34678
H	-1.17328	-7.22638	1.34951
H	-2.07867	-2.65841	0.85347
H	8.41866	-1.19149	-0.29704

Cartesian coordinates (in Å) of **[5]CPP**:

C	-1.94207	-0.81005	-1.73001
C	-0.55981	-0.59243	-1.80113
C	-0.1535	0.74847	-1.80697
C	-0.88363	1.70256	-1.08548
C	-2.26658	1.4851	-1.01444
C	-2.73837	0.34164	-1.6736
H	-2.3631	-1.79264	-1.77412
H	0.1356	-1.39927	-1.90244
H	-0.4249	2.57253	-0.66401
H	-2.92489	2.17971	-0.53579
C	-4.44624	-0.69031	-3.25557
C	-4.05251	0.40445	-2.47402
C	-4.77264	1.60484	-2.54062
C	-5.32622	1.91528	-3.79017
C	-5.08776	0.98498	-4.81063
C	-4.99988	-0.37979	-4.50498
H	-4.28287	-1.70104	-2.94451
H	-4.84794	2.27149	-1.70697
H	-5.84827	2.83273	-3.96579
H	-5.28345	-1.13962	-5.20293
C	-4.75833	1.47442	-6.23306
C	-4.37282	0.55279	-7.2156
C	-3.33231	0.9623	-8.06014
C	-2.81328	2.24019	-7.81202
C	-3.65661	3.25803	-7.34665
C	-4.69737	2.84836	-6.50199
H	-4.80458	-0.42402	-7.28183
H	-2.92352	0.31608	-8.80853
H	-3.4846	4.28935	-7.57376
H	-5.36611	3.54882	-6.047
C	0.75902	1.35894	-7.48165
C	0.94308	2.37076	-6.52956
C	0.43675	3.65549	-6.76934
C	-0.75958	3.71329	-7.49754
C	-1.29389	2.47887	-7.89093
C	-0.43703	1.41689	-8.20982
H	1.45911	0.55943	-7.60613
H	0.90135	4.5344	-6.37362
H	-1.26102	4.63887	-7.68966

H	-0.70261	0.66441	-8.92267
C	0.98994	1.19756	-2.73551
C	1.61501	0.26268	-3.57145
C	1.91552	0.70716	-4.86591
C	1.55178	2.02894	-5.15639
C	1.60131	3.00372	-4.15011
C	1.30076	2.55879	-2.85511
H	1.79984	-0.74483	-3.26206
H	2.34308	0.05853	-5.60191
H	1.79927	4.03353	-4.36295
H	1.25616	3.22904	-2.0222

Cartesian coordinates (in Å) of biphenyl:

C	-2.5406	0.29002	0.
C	-1.14544	0.29002	0.
C	-0.44791	1.49777	0.
C	-1.14556	2.70628	-0.0012
C	-2.54038	2.70621	-0.00168
C	-3.23799	1.498	-0.00068
H	-3.09036	-0.66229	0.00045
H	-0.59594	-0.66249	0.00132
H	-0.59536	3.65843	-0.00126
H	-3.09051	3.65849	-0.00263
H	-4.33759	1.49818	-0.00086
C	1.09209	1.49789	0.00089
C	1.78953	2.70621	0.00089
C	1.78969	0.29003	0.0018
C	3.18424	2.70659	0.00112
H	1.23927	3.65829	-0.00061
C	3.18482	0.29024	0.00303
H	1.24016	-0.66241	0.00198
C	3.88216	1.49824	0.00255
H	3.73403	3.65897	0.00049
H	3.73458	-0.66225	0.00417
H	4.98184	1.49879	0.0028

Cartesian coordinates (in Å) of terphenyl:

C	-4.21114	-0.0348	0.
C	-2.81598	-0.0348	0.
C	-2.11844	1.17295	0.
C	-2.81609	2.38146	-0.0012
C	-4.21092	2.38138	-0.00168
C	-4.90852	1.17317	-0.00068
H	-4.7609	-0.98712	0.00045
H	-2.26647	-0.98732	0.00132
H	-2.26589	3.3336	-0.00126

H	-4.76104	3.33366	-0.00263
H	-6.00812	1.17336	-0.00086
C	-0.57844	1.17306	0.00089
C	0.11899	2.38139	0.00089
C	0.11915	-0.03479	0.0018
C	1.51371	2.38177	0.00112
H	-0.43127	3.33347	-0.00061
C	1.51429	-0.03459	0.00303
H	-0.43037	-0.98724	0.00198
C	2.21163	1.17341	0.00255
H	2.0635	3.33415	0.00049
H	2.06404	-0.98708	0.00417
C	3.75162	1.17418	0.00289
C	4.44975	-0.03375	0.00433
C	4.44853	2.38243	0.00166
C	5.84446	-0.03333	0.00521
H	3.90003	-0.98614	0.00608
C	5.84367	2.38302	0.00154
H	3.89846	3.33456	0.00035
C	6.54169	1.17542	0.00345
H	6.3948	-0.98539	0.00697
H	6.39288	3.33583	0.00015
H	7.64137	1.1755	0.00409

Cartesian coordinates (in Å) of open macrocycle **4**:

C	1.33985	-6.12655	2.98364
C	2.51154	-6.17337	3.75157
C	2.45903	-6.12711	5.14137
C	1.23352	-6.02422	5.82167
C	0.06358	-5.97323	5.04707
C	0.1156	-6.02626	3.65479
H	3.46874	-6.26514	3.24775
H	3.38199	-6.19856	5.71026
H	-0.90002	-5.8683	5.53794
H	-0.80857	-5.97859	3.08575
C	-5.29765	-1.38575	-5.03747
C	-5.59636	-1.2309	-3.68543
C	-6.3448	-0.13645	-3.23528
C	-6.79276	0.7953	-4.18005
C	-6.49636	0.6359	-5.53162
C	-5.73878	-0.45378	-5.99047
H	-4.73628	-2.2578	-5.36151
H	-5.25136	-1.97669	-2.97593
H	-7.37844	1.64545	-3.85057
H	-6.83666	1.38523	-6.24137
C	-4.80669	-0.96811	0.4719

C	-6.04667	-1.68221	-0.03333
C	-6.83364	-1.2265	-1.01073
C	-6.61448	0.08246	-1.7369
C	-5.44835	0.85231	-1.14487
C	-4.64604	0.3852	-0.18551
H	-6.25717	-2.63361	0.45188
H	-7.69997	-1.79756	-1.33963
H	-5.28114	1.8364	-1.57921
H	-3.81199	0.98039	0.18167
C	-2.03566	-3.58253	0.97934
C	-3.11296	-2.72738	1.219
C	-3.58271	-1.86654	0.22178
C	-2.9465	-1.88594	-1.02658
C	-1.87697	-2.74483	-1.26813
C	-1.40618	-3.6056	-0.26819
H	-3.58713	-2.71859	2.19324
H	-3.2863	-1.22479	-1.81786
H	-1.40745	-2.74831	-2.24804
C	-0.54428	-5.93535	-0.09464
C	-0.21302	-4.53091	-0.55399
C	1.03217	-4.00749	0.12629
C	1.76255	-4.70628	0.99467
C	1.43841	-6.11588	1.44644
C	0.17385	-6.62896	0.7904
H	-1.43521	-6.36811	-0.54575
H	1.32643	-3.00055	-0.16197
H	2.66487	-4.28343	1.43016
H	-0.14878	-7.62734	1.07818
O	-7.81777	0.87843	-1.69082
O	-4.86677	-0.81219	1.90522
O	2.59384	-6.87859	1.02027
C	-5.96081	-0.07004	2.41693
H	-6.92698	-0.53368	2.17586
H	-5.83224	-0.0591	3.50248
H	-5.96807	0.96422	2.04739
C	2.53235	-8.28579	1.20294
H	1.8358	-8.76235	0.49986
H	3.53985	-8.66024	1.00245
H	2.24986	-8.56087	2.22827
C	-8.25989	1.2834	-0.40611
H	-8.49718	0.42622	0.23808
H	-7.52148	1.91304	0.10869
H	-9.16984	1.86574	-0.5733
O	-0.03157	-4.50991	-1.98281
H	-1.68187	-4.24016	1.76387
C	1.00653	-5.33431	-2.49428

H	0.80669	-6.40085	-2.3266
H	1.03749	-5.13939	-3.56931
H	1.98128	-5.09251	-2.05242
C	0.14217	-6.6019	8.01433
C	0.09429	-6.55685	9.40691
C	1.08645	-5.88619	10.124
C	2.12681	-5.25992	9.43437
C	2.17172	-5.30194	8.041
C	1.18059	-5.97466	7.30492
H	-0.62059	-7.15106	7.46942
H	-0.71585	-7.05485	9.93308
H	1.0502	-5.85263	11.20942
H	2.90405	-4.73238	9.98144
H	2.97207	-4.78923	7.51474
C	-3.837	-1.19894	-9.19256
C	-4.14771	-1.06252	-7.8402
C	-5.41387	-0.61088	-7.43079
C	-6.36078	-0.30305	-8.42245
C	-6.05251	-0.44147	-9.77498
C	-4.78902	-0.88897	-10.16569
H	-2.84473	-1.53301	-9.48365
H	-3.39068	-1.28086	-7.09195
H	-7.35428	0.02339	-8.12745
H	-6.80366	-0.20569	-10.5246
H	-4.54787	-0.99387	-11.22026

Cartesian coordinates (in Å) of open macrocycle **5**:

C	1.33985	-6.12655	2.98364
C	2.51154	-6.17337	3.75157
C	2.45903	-6.12711	5.14137
C	1.23352	-6.02422	5.82167
C	0.06358	-5.97323	5.04707
C	0.1156	-6.02626	3.65479
H	3.46874	-6.26514	3.24775
H	3.38199	-6.19856	5.71026
H	-0.90002	-5.8683	5.53794
H	-0.80857	-5.97859	3.08575
C	-5.29765	-1.38575	-5.03747
C	-5.59636	-1.2309	-3.68543
C	-6.3448	-0.13645	-3.23528
C	-6.79276	0.7953	-4.18005
C	-6.49636	0.6359	-5.53162
C	-5.73878	-0.45378	-5.99047
H	-4.73628	-2.2578	-5.36151
H	-5.25136	-1.97669	-2.97593
H	-7.37844	1.64545	-3.85057

H	-6.83666	1.38523	-6.24137
C	-4.80669	-0.96811	0.4719
C	-6.04667	-1.68221	-0.03333
C	-6.83364	-1.2265	-1.01073
C	-6.61448	0.08246	-1.7369
C	-5.44835	0.85231	-1.14487
C	-4.64604	0.3852	-0.18551
H	-6.25717	-2.63361	0.45188
H	-7.69997	-1.79756	-1.33963
H	-5.28114	1.8364	-1.57921
H	-3.81199	0.98039	0.18167
C	-2.03566	-3.58253	0.97934
C	-3.11296	-2.72738	1.219
C	-3.58271	-1.86654	0.22178
C	-2.9465	-1.88594	-1.02658
C	-1.87697	-2.74483	-1.26813
C	-1.40618	-3.6056	-0.26819
H	-3.58713	-2.71859	2.19324
H	-3.2863	-1.22479	-1.81786
H	-1.40745	-2.74831	-2.24804
C	-0.54428	-5.93535	-0.09464
C	-0.21302	-4.53091	-0.55399
C	1.03217	-4.00749	0.12629
C	1.76255	-4.70628	0.99467
C	1.43841	-6.11588	1.44644
C	0.17385	-6.62896	0.7904
H	-1.43521	-6.36811	-0.54575
H	1.32643	-3.00055	-0.16197
H	2.66487	-4.28343	1.43016
H	-0.14878	-7.62734	1.07818
O	-4.86677	-0.81219	1.90522
C	-5.96081	-0.07004	2.41693
H	-6.92698	-0.53368	2.17586
H	-5.83224	-0.0591	3.50248
H	-5.96807	0.96422	2.04739
O	-0.03157	-4.50991	-1.98281
H	-1.68187	-4.24016	1.76387
C	1.00653	-5.33431	-2.49428
H	0.80669	-6.40085	-2.3266
H	1.03749	-5.13939	-3.56931
H	1.98128	-5.09251	-2.05242
C	0.14217	-6.6019	8.01433
C	0.09429	-6.55685	9.40691
C	1.08645	-5.88619	10.124
C	2.12681	-5.25992	9.43437
C	2.17172	-5.30194	8.041

C	1.18059	-5.97466	7.30492
H	-0.62059	-7.15106	7.46942
H	-0.71585	-7.05485	9.93308
H	1.0502	-5.85263	11.20942
H	2.90405	-4.73238	9.98144
H	2.97207	-4.78923	7.51474
C	-3.837	-1.19894	-9.19256
C	-4.14771	-1.06252	-7.8402
C	-5.41387	-0.61088	-7.43079
C	-6.36078	-0.30305	-8.42245
C	-6.05251	-0.44147	-9.77498
C	-4.78902	-0.88897	-10.16569
H	-2.84473	-1.53301	-9.48365
H	-3.39068	-1.28086	-7.09195
H	-7.35428	0.02339	-8.12745
H	-6.80366	-0.20569	-10.5246
H	-4.54787	-0.99387	-11.22026
H	-7.50644	0.67249	-1.70274
H	2.29188	-6.67926	1.13164

Cartesian coordinates (in Å) of **[5]CPP^{+4}**:

C	-2.88209	-1.96002	-1.21329
C	-3.41488	-0.69595	-1.21345
C	-3.46115	0.06808	-0.00008
C	-3.4147	-0.69575	1.21343
C	-2.88198	-1.95986	1.21349
C	-2.36713	-2.5262	0.00014
H	-2.73757	-2.46671	-2.16095
H	-3.67645	-0.23848	-2.16115
H	-3.67614	-0.23804	2.16105
H	-2.73727	-2.46628	2.16127
C	-3.13376	1.47035	-0.00019
C	-2.75482	2.13522	1.21321
C	-2.75448	2.13492	-1.21359
C	-1.71724	3.03263	1.21332
H	-3.19207	1.84102	2.16084
C	-1.71681	3.03226	-1.21354
H	-3.19143	1.84059	-2.16132
C	-1.00481	3.31259	-0.00004
H	-1.36313	3.42286	2.161
H	-1.36239	3.42225	-2.16119
C	1.17961	3.27962	-1.21323
C	2.3537	2.57017	-1.21324
C	2.83982	1.97898	0.00016
C	2.35332	2.56955	1.21364
C	1.17922	3.27909	1.21363

C	0.43003	3.43461	0.00016
H	0.7649	3.60454	-2.16093
H	2.83446	2.3541	-2.16087
H	2.83381	2.35313	2.16132
H	0.76434	3.60366	2.16137
C	-0.39352	-3.46222	-1.2133
C	0.97334	-3.34641	-1.2134
C	1.67107	-3.03155	-0.00003
C	0.97342	-3.34597	1.21349
C	-0.39345	-3.46188	1.21363
C	-1.13434	-3.2704	0.00019
H	-0.90953	-3.56947	-2.16094
H	1.4998	-3.36552	-2.16115
H	1.49999	-3.36484	2.16118
H	-0.90933	-3.56899	2.16137
C	2.75995	-2.08924	-0.00023
C	3.17201	-1.44428	1.21315
C	3.17135	-1.44404	-1.21365
C	3.48439	-0.10855	1.21322
H	3.11493	-1.96832	2.16071
C	3.4837	-0.10827	-1.21353
H	3.11396	-1.96789	-2.1613
C	3.40001	0.65247	-0.00007
H	3.66578	0.38611	2.1609
H	3.66464	0.3866	-2.1612

Cartesian coordinates (in Å) of **[5]CPP^{+3}**:

C	-2.78108	-1.71521	-1.20575
C	-3.45161	-0.67932	-1.28584
C	-3.49785	0.08471	-0.07247
C	-3.47438	-0.62465	1.14104
C	-2.89578	-1.99772	1.14111
C	-2.40391	-2.5096	-0.07225
H	-2.52201	-2.03212	-2.2098
H	-3.71315	-0.22184	-2.23354
H	-3.7358	-0.16693	2.08865
H	-2.75109	-2.50415	2.08889
C	-3.17042	1.48697	-0.07258
C	-2.63314	1.99779	1.19825
C	-2.79112	2.15153	-1.28598
C	-1.75385	3.04921	1.14093
H	-3.05996	1.72448	2.15683
C	-1.75342	3.04884	-1.28592
H	-3.22808	1.85721	-2.23371
C	-1.04141	3.32915	-0.07243
H	-1.51003	3.57778	2.05577

H	-1.39899	3.43882	-2.23358
C	1.14301	3.29612	-1.28562
C	2.31708	2.58663	-1.28563
C	2.80317	1.99543	-0.07223
C	2.31669	2.58601	1.14125
C	1.14262	3.29558	1.14124
C	0.39339	3.21897	-0.12582
H	0.7283	3.62105	-2.23332
H	2.79782	2.37055	-2.23326
H	2.87058	2.33652	2.23371
H	0.72774	3.62017	2.08898
C	-0.43032	-3.44568	-1.28569
C	0.93654	-3.3299	-1.28579
C	1.63428	-3.01506	-0.07242
C	0.93662	-3.32946	1.1411
C	-0.29249	-3.21715	1.06123
C	-1.17114	-3.25383	-0.0722
H	-0.94634	-3.55291	-2.23333
H	1.463	-3.34903	-2.23354
H	1.46319	-3.34836	2.08879
H	-0.6938	-3.13447	2.06519
C	2.72319	-2.07278	-0.07262
C	3.13527	-1.42784	1.14076
C	3.1346	-1.4276	-1.28603
C	3.44768	-0.09212	1.14084
H	3.07817	-1.95188	2.08832
C	3.447	-0.09183	-1.28592
H	3.07721	-1.95144	-2.23369
C	3.36333	0.6689	-0.07246
H	3.62909	0.40254	2.08851
H	3.62795	0.40303	-2.23359

Cartesian coordinates (in Å) of **[5]CPP^{+2}**:

C	3.30494	-1.12941	1.23592
C	3.49852	0.24571	1.15125
C	3.40515	0.92232	-0.08302
C	3.51865	0.09772	-1.22267
C	3.29495	-1.27313	-1.13835
C	2.9771	-1.88797	0.0916
H	3.23461	-1.56959	2.22583
H	3.53942	0.80698	2.07968
H	3.60536	0.53701	-2.21188
H	3.19427	-1.82521	-2.06777
C	2.70599	2.24136	-0.15409
C	1.99007	2.56702	-1.32411
C	2.30045	2.93345	1.00874

C	0.74703	3.18579	-1.25732
H	2.29168	2.1563	-2.2817
C	1.05851	3.56146	1.0751
H	2.88229	2.85531	1.92297
C	0.1664	3.5202	-0.01803
H	0.14572	3.20976	-2.1606
H	0.72662	3.94851	2.03512
C	-1.70836	2.62599	1.33708
C	-2.68616	1.63763	1.31381
C	-3.29534	1.24827	0.10502
C	-3.15733	2.15483	-0.96803
C	-2.17821	3.14653	-0.94404
C	-1.29652	3.26766	0.1524
H	-1.1182	2.73045	2.2417
H	-2.80578	1.02239	2.20002
H	-3.71243	1.99535	-1.88921
H	-2.00656	3.72629	-1.84746
C	1.13917	-3.06353	1.31873
C	-0.23141	-3.28517	1.24902
C	-0.88699	-3.41075	0.00822
C	-0.0473	-3.69542	-1.09009
C	1.32428	-3.46249	-1.02133
C	1.9188	-2.94229	0.14986
H	1.5502	-2.78231	2.28229
H	-0.81105	-3.14803	2.15636
H	-0.47816	-3.95054	-2.05474
H	1.90079	-3.54277	-1.93848
C	-2.21011	-2.73626	-0.1538
C	-2.4243	-2.00269	-1.33761
C	-3.00808	-2.35815	0.94825
C	-3.06529	-0.76886	-1.31048
H	-1.90065	-2.27853	-2.24712
C	-3.65015	-1.12123	0.97601
H	-3.00884	-2.96124	1.85265
C	-3.52092	-0.21516	-0.09817
H	-3.00536	-0.14683	-2.19804
H	-4.12511	-0.80381	1.90107

Cartesian coordinates (in Å) of **[5]CPP^{+1}**:

C	3.30494	-1.12941	1.23592
C	3.49852	0.24571	1.15125
C	3.40515	0.92232	-0.08302
C	3.51865	0.09772	-1.22267
C	3.29495	-1.27313	-1.13835
C	2.9771	-1.88797	0.0916
H	3.23461	-1.56959	2.22583

H	3.53942	0.80698	2.07968
H	3.60536	0.53701	-2.21188
H	3.19427	-1.82521	-2.06777
C	2.70599	2.24136	-0.15409
C	1.99007	2.56702	-1.32411
C	2.30045	2.93345	1.00874
C	0.74703	3.18579	-1.25732
H	2.29168	2.1563	-2.2817
C	1.05851	3.56146	1.0751
H	2.88229	2.85531	1.92297
C	0.1664	3.5202	-0.01803
H	0.14572	3.20976	-2.1606
H	0.72662	3.94851	2.03512
C	-1.70836	2.62599	1.33708
C	-2.68616	1.63763	1.31381
C	-3.29534	1.24827	0.10502
C	-3.15733	2.15483	-0.96803
C	-2.17821	3.14653	-0.94404
C	-1.29652	3.26766	0.1524
H	-1.1182	2.73045	2.2417
H	-2.80578	1.02239	2.20002
H	-3.71243	1.99535	-1.88921
H	-2.00656	3.72629	-1.84746
C	1.13917	-3.06353	1.31873
C	-0.23141	-3.28517	1.24902
C	-0.88699	-3.41075	0.00822
C	-0.0473	-3.69542	-1.09009
C	1.32428	-3.46249	-1.02133
C	1.9188	-2.94229	0.14986
H	1.5502	-2.78231	2.28229
H	-0.81105	-3.14803	2.15636
H	-0.47816	-3.95054	-2.05474
H	1.90079	-3.54277	-1.93848
C	-2.21011	-2.73626	-0.1538
C	-2.4243	-2.00269	-1.33761
C	-3.00808	-2.35815	0.94825
C	-3.06529	-0.76886	-1.31048
H	-1.90065	-2.27853	-2.24712
C	-3.65015	-1.12123	0.97601
H	-3.00884	-2.96124	1.85265
C	-3.52092	-0.21516	-0.09817
H	-3.00536	-0.14683	-2.19804
H	-4.12511	-0.80381	1.90107

Cartesian coordinates (in Å) of **[5]CPP** *Triplet Excited State*:

C	2.11264	3.16836	0.95683

C	3.10732	2.19263	0.99128
C	3.27937	1.29632	-0.08577
C	2.68747	1.68736	-1.30241
C	1.69484	2.66044	-1.33614
C	1.24883	3.28495	-0.15474
H	1.91647	3.73735	1.86196
H	3.64743	2.03515	1.92165
H	2.83364	1.08276	-2.19198
H	1.12327	2.76365	-2.25272
C	-0.81587	3.22484	1.23636
C	-0.21948	3.51826	-0.00616
C	-1.097	3.50474	-1.11195
C	-2.32755	2.85643	-1.04014
C	-2.74075	2.20275	0.14207
C	-2.05071	2.59041	1.30927
H	-0.23274	3.29923	2.14889
H	-0.75901	3.85995	-2.08186
H	-2.88939	2.72974	-1.9611
H	-2.36657	2.2243	2.28035
C	-3.41642	0.86936	0.10145
C	-3.46047	0.05282	1.25163
C	-3.21792	-1.31432	1.16882
C	-2.94932	-1.9353	-0.06891
C	-3.34131	-1.19341	-1.20397
C	-3.55614	0.17902	-1.12186
H	-3.50027	0.49802	2.24079
H	-3.05446	-1.85368	2.09669
H	-3.31264	-1.64472	-2.19138
H	-3.66001	0.72946	-2.05197
C	0.10444	-3.73019	1.05993
C	0.93682	-3.39731	-0.03061
C	0.27875	-3.24036	-1.26616
C	-1.09499	-3.03643	-1.32696
C	-1.8745	-2.97065	-0.15436
C	-1.27159	-3.51996	0.9993
H	0.54268	-4.00918	2.01482
H	0.85621	-3.0599	-2.16737
H	-1.51077	-2.71956	-2.27746
H	-1.84835	-3.64373	1.91177
C	3.52142	-0.16494	0.11216
C	3.06287	-0.73114	1.31737
C	2.44057	-1.97475	1.33324
C	2.24973	-2.70588	0.14458
C	3.05118	-2.31095	-0.94915
C	3.67414	-1.06412	-0.96556
H	2.98356	-0.11427	2.20696

H	1.91017	-2.26212	2.23547
H	3.06878	-2.9106	-1.85576
H	4.15383	-0.73557	-1.88427

Cartesian coordinates (in Å) of **[5]CPP** *Singlet Excited State*:

C	-0.65812	-3.43717	-1.20535
C	0.71495	-3.42566	-1.20527
C	1.44972	-3.16983	-0.00007
C	0.71482	-3.42649	1.20484
C	-0.65827	-3.43803	1.20474
C	-1.39716	-3.19348	-0.00025
H	-1.17514	-3.48828	-2.15866
H	1.23294	-3.46803	-2.15849
H	1.23267	-3.4696	2.15811
H	-1.1754	-3.48991	2.15795
C	-3.04225	-1.73945	-1.20489
C	-2.56955	-2.35808	-0.00007
C	-3.04171	-1.73951	1.20501
C	-3.47757	-0.43734	1.2051
C	-3.4734	0.34127	0.00022
C	-3.47813	-0.43726	-1.2047
H	-2.92318	-2.24514	-2.15821
H	-2.92214	-2.24524	2.15824
H	-3.68699	0.03793	2.1585
H	-3.68803	0.03804	-2.15798
C	-3.03877	1.71389	0.00019
C	-2.5944	2.35273	-1.20479
C	-1.48961	3.16842	-1.20488
C	-0.74814	3.40498	-0.00009
C	-1.4893	3.1684	1.20488
C	-2.5941	2.35272	1.20508
H	-3.03777	2.08257	-2.15828
H	-1.10112	3.51289	-2.15837
H	-1.10054	3.51284	2.15828
H	-3.03726	2.08258	2.15867
C	2.55482	2.39486	-1.20516
C	3.00977	1.76359	-0.00007
C	2.55514	2.39554	1.20476
C	1.43712	3.19291	1.20461
C	0.69185	3.41708	-0.00024
C	1.43681	3.19223	-1.20518
H	3.00249	2.13189	-2.15863
H	3.00309	2.13316	2.15828
H	1.04304	3.53135	2.15799
H	1.04247	3.5301	-2.15864
C	2.60824	-2.31547	0.00019

C	3.07095	-1.68926	-1.2047
C	3.48492	-0.38002	-1.20468
C	3.46704	0.39853	0.00018
C	3.48401	-0.37974	1.20528
C	3.07005	-1.68895	1.2053
H	2.9607	-2.19704	-2.15796
H	3.6872	0.0987	-2.15793
H	3.6855	0.09927	2.15855
H	2.95901	-2.19649	2.1586

Cartesian coordinates (in Å) of **[5]CPP^{-1}**:

C	3.30494	-1.12941	1.23592
C	3.49852	0.24571	1.15125
C	3.40515	0.92232	-0.08302
C	3.51865	0.09772	-1.22267
C	3.29495	-1.27313	-1.13835
C	2.9771	-1.88797	0.0916
H	3.23461	-1.56959	2.22583
H	3.53942	0.80698	2.07968
H	3.60536	0.53701	-2.21188
H	3.19427	-1.82521	-2.06777
C	2.70599	2.24136	-0.15409
C	1.99007	2.56702	-1.32411
C	2.30045	2.93345	1.00874
C	0.74703	3.18579	-1.25732
H	2.29168	2.1563	-2.2817
C	1.05851	3.56146	1.0751
H	2.88229	2.85531	1.92297
C	0.1664	3.5202	-0.01803
H	0.14572	3.20976	-2.1606
H	0.72662	3.94851	2.03512
C	-1.70836	2.62599	1.33708
C	-2.68616	1.63763	1.31381
C	-3.29534	1.24827	0.10502
C	-3.15733	2.15483	-0.96803
C	-2.17821	3.14653	-0.94404
C	-1.29652	3.26766	0.1524
H	-1.1182	2.73045	2.2417
H	-2.80578	1.02239	2.20002
H	-3.71243	1.99535	-1.88921
H	-2.00656	3.72629	-1.84746
C	1.13917	-3.06353	1.31873
C	-0.23141	-3.28517	1.24902
C	-0.88699	-3.41075	0.00822
C	-0.0473	-3.69542	-1.09009
C	1.32428	-3.46249	-1.02133

C	1.9188	-2.94229	0.14986
H	1.5502	-2.78231	2.28229
H	-0.81105	-3.14803	2.15636
H	-0.47816	-3.95054	-2.05474
H	1.90079	-3.54277	-1.93848
C	-2.21011	-2.73626	-0.1538
C	-2.4243	-2.00269	-1.33761
C	-3.00808	-2.35815	0.94825
C	-3.06529	-0.76886	-1.31048
H	-1.90065	-2.27853	-2.24712
C	-3.65015	-1.12123	0.97601
H	-3.00884	-2.96124	1.85265
C	-3.52092	-0.21516	-0.09817
H	-3.00536	-0.14683	-2.19804
H	-4.12511	-0.80381	1.90107

Cartesian coordinates (in Å) of **[5]CPP^{-2}**:

C	3.30494	-1.12941	1.23592
C	3.49852	0.24571	1.15125
C	3.40515	0.92232	-0.08302
C	3.51865	0.09772	-1.22267
C	3.29495	-1.27313	-1.13835
C	2.9771	-1.88797	0.0916
H	3.23461	-1.56959	2.22583
H	3.53942	0.80698	2.07968
H	3.60536	0.53701	-2.21188
H	3.19427	-1.82521	-2.06777
C	2.70599	2.24136	-0.15409
C	1.99007	2.56702	-1.32411
C	2.30045	2.93345	1.00874
C	0.74703	3.18579	-1.25732
H	2.29168	2.1563	-2.2817
C	1.05851	3.56146	1.0751
H	2.88229	2.85531	1.92297
C	0.1664	3.5202	-0.01803
H	0.14572	3.20976	-2.1606
H	0.72662	3.94851	2.03512
C	-1.70836	2.62599	1.33708
C	-2.68616	1.63763	1.31381
C	-3.29534	1.24827	0.10502
C	-3.15733	2.15483	-0.96803
C	-2.17821	3.14653	-0.94404
C	-1.29652	3.26766	0.1524
H	-1.1182	2.73045	2.2417
H	-2.80578	1.02239	2.20002
H	-3.71243	1.99535	-1.88921

H	-2.00656	3.72629	-1.84746
C	1.13917	-3.06353	1.31873
C	-0.23141	-3.28517	1.24902
C	-0.88699	-3.41075	0.00822
C	-0.0473	-3.69542	-1.09009
C	1.32428	-3.46249	-1.02133
C	1.9188	-2.94229	0.14986
H	1.5502	-2.78231	2.28229
H	-0.81105	-3.14803	2.15636
H	-0.47816	-3.95054	-2.05474
H	1.90079	-3.54277	-1.93848
C	-2.21011	-2.73626	-0.1538
C	-2.4243	-2.00269	-1.33761
C	-3.00808	-2.35815	0.94825
C	-3.06529	-0.76886	-1.31048
H	-1.90065	-2.27853	-2.24712
C	-3.65015	-1.12123	0.97601
H	-3.00884	-2.96124	1.85265
C	-3.52092	-0.21516	-0.09817
H	-3.00536	-0.14683	-2.19804
H	-4.12511	-0.80381	1.90107

Cartesian coordinates (in Å) of **[5]CPP^{-3}**:

C	-0.07178	3.53887	1.19513
C	-1.41838	3.24401	1.19505
C	-2.10335	2.83251	-0.00005
C	-1.41832	3.244	-1.19512
C	-0.07173	3.53887	-1.19508
C	0.72242	3.4523	0.00004
H	0.41775	3.68242	2.15797
H	-1.92293	3.16967	2.15796
H	-1.92283	3.16969	-2.15804
H	0.41785	3.68236	-2.15791
C	-3.06103	1.75411	-0.00005
C	-3.38889	1.02547	-1.19514
C	-3.38904	1.02552	1.19502
C	-3.52427	-0.34638	-1.19509
H	-3.37471	1.53545	-2.15798
C	-3.52441	-0.34632	1.19504
H	-3.37494	1.53552	2.15785
C	-3.34451	-1.12498	0.00001
H	-3.60977	-0.84907	-2.15802
H	-3.61003	-0.84892	2.15801
C	-2.02275	-2.90556	1.1952
C	-0.75948	-3.45735	1.19518
C	0.03638	-3.5266	0.00002

C	-0.75956	-3.4575	-1.19506
C	-2.02283	-2.90573	-1.19506
C	-2.61461	-2.36888	0.00004
H	-2.50332	-2.73437	2.15805
H	-0.30737	-3.69366	2.15801
H	-0.30756	-3.69389	-2.15792
H	-2.50339	-2.73465	-2.15793
C	2.64735	2.35106	1.19519
C	3.34483	1.16207	1.19518
C	3.50803	0.37997	0.
C	3.34495	1.16219	-1.19511
C	2.64749	2.35117	-1.19506
C	2.04418	2.87504	0.00005
H	2.42052	2.8079	2.15807
H	3.63301	0.74094	2.15799
H	3.63321	0.74116	-2.15794
H	2.42075	2.80807	-2.15794
C	3.36665	-1.05532	-0.00004
C	3.05467	-1.79091	-1.19512
C	3.05484	-1.79105	1.19498
C	2.13886	-2.82124	-1.19512
H	3.41945	-1.43437	-2.15798
C	2.13902	-2.82135	1.195
H	3.4197	-1.43464	2.15785
C	1.44517	-3.21776	-0.00002
H	1.82755	-3.22544	-2.15795
H	1.82785	-3.22558	2.15786

Cartesian coordinates (in Å) of **[5]CPP^{-4}**:

C	-0.07178	3.53887	1.19513
C	-1.41838	3.24401	1.19505
C	-2.10335	2.83251	-0.00005
C	-1.41832	3.244	-1.19512
C	-0.07173	3.53887	-1.19508
C	0.72242	3.4523	0.00004
H	0.41775	3.68242	2.15797
H	-1.92293	3.16967	2.15796
H	-1.92283	3.16969	-2.15804
H	0.41785	3.68236	-2.15791
C	-3.06103	1.75411	-0.00005
C	-3.38889	1.02547	-1.19514
C	-3.38904	1.02552	1.19502
C	-3.52427	-0.34638	-1.19509
H	-3.37471	1.53545	-2.15798
C	-3.52441	-0.34632	1.19504
H	-3.37494	1.53552	2.15785

C	-3.34451	-1.12498	0.00001
H	-3.60977	-0.84907	-2.15802
H	-3.61003	-0.84892	2.15801
C	-2.02275	-2.90556	1.1952
C	-0.75948	-3.45735	1.19518
C	0.03638	-3.5266	0.00002
C	-0.75956	-3.4575	-1.19506
C	-2.02283	-2.90573	-1.19506
C	-2.61461	-2.36888	0.00004
H	-2.50332	-2.73437	2.15805
H	-0.30737	-3.69366	2.15801
H	-0.30756	-3.69389	-2.15792
H	-2.50339	-2.73465	-2.15793
C	2.64735	2.35106	1.19519
C	3.34483	1.16207	1.19518
C	3.50803	0.37997	0.
C	3.34495	1.16219	-1.19511
C	2.64749	2.35117	-1.19506
C	2.04418	2.87504	0.00005
H	2.42052	2.8079	2.15807
H	3.63301	0.74094	2.15799
H	3.63321	0.74116	-2.15794
H	2.42075	2.80807	-2.15794
C	3.36665	-1.05532	-0.00004
C	3.05467	-1.79091	-1.19512
C	3.05484	-1.79105	1.19498
C	2.13886	-2.82124	-1.19512
H	3.41945	-1.43437	-2.15798
C	2.13902	-2.82135	1.195
H	3.4197	-1.43464	2.15785
C	1.44517	-3.21776	-0.00002
H	1.82755	-3.22544	-2.15795
H	1.82785	-3.22558	2.15786

Chapter III

2,6-naphthyl[6]CPP **4**

C	4.5971	5.4859	8.8642
C	3.3587	5.444	9.778
C	2.6307	6.6318	10.015
C	1.2511	6.5962	10.2358
C	2.6689	4.1986	9.976
C	1.2601	4.1761	10.165
C	0.5515	5.3739	10.2287
C	-0.8568	5.3746	10.1477
C	0.54	2.9582	10.1374

C	-0.8767	2.9525	10.0163
C	-1.6052	4.1677	9.9423
C	-3.0269	4.2278	9.3084
C	-3.4306	5.4595	8.756
C	-4.284	5.5291	7.6746
C	-3.7921	3.0756	8.9294
C	-4.6713	3.1543	7.8083
C	-4.7603	4.365	7.0756
C	-4.6997	4.3965	5.5529
C	-4.8213	5.6107	4.8251
C	-4.1295	5.8027	3.6077
C	-4.012	3.3343	4.9383
C	-3.3346	3.5219	3.7314
C	-3.3112	4.7807	3.0805
C	-2.1079	5.0744	2.1954
C	-1.4908	6.3394	2.3265
C	-0.0927	6.4304	2.3123
C	-1.3358	3.9958	1.7183
C	0.0542	4.0834	1.7333
C	0.6844	5.2633	2.1603
C	2.0364	5.2084	2.8251
C	2.8393	6.3468	3.0041
C	3.8791	6.3554	3.9529
C	2.3508	4.0496	3.5699
C	3.3707	4.0587	4.5226
C	4.13	5.2256	4.7696
C	4.8548	5.3413	6.099
C	4.8876	6.5967	6.7301
C	4.7883	6.6785	8.1173
C	5.097	4.1939	6.8854
C	5.0056	4.2738	8.2766
H	3.0645	7.6108	9.8844
H	0.7147	7.5349	10.2777
H	3.1515	3.2574	9.79
H	-1.3179	6.3372	10.1042
H	1.0811	2.0208	10.0917
H	-1.3626	1.9979	9.8576
H	-2.9448	6.3809	8.9721
H	-4.3145	6.4815	7.1745
H	-3.6014	2.0938	9.3442
H	-5.0983	2.2378	7.408
H	-5.3024	6.4715	5.2658
H	-4.1192	6.7957	3.1805
H	-3.8055	2.4167	5.4744
H	-2.6699	2.7231	3.4394
H	-2.0273	7.2067	2.6834

H	0.3473	7.3594	2.6494
H	-1.7701	3.021	1.5536
H	0.62	3.1746	1.5803
H	2.6059	7.2643	2.4847
H	4.3967	7.2854	4.1142
H	1.7122	3.1741	3.5395
H	3.4406	3.1879	5.1607
H	4.7285	7.5177	6.1907
H	4.5568	7.6582	8.4949
H	5.1387	3.2068	6.4517
H	4.9659	3.335	8.8051

1,5-naphthyl[6]CPP

C	4.637	10.921	1.0956
C	5.3157	10.4885	2.2479
C	6.712	10.2711	2.2183
C	7.4187	10.8772	1.152
C	6.7341	11.3692	0.0194
C	5.3274	11.2195	-0.1095
C	8.8196	7.3538	3.0775
C	7.8535	6.5787	3.7681
C	6.829	7.2963	4.4335
C	6.5508	8.6294	4.0762
C	7.2977	9.2749	3.0595
C	8.5458	8.6927	2.7287
C	6.1061	3.3718	3.2339
C	6.7441	3.0154	2.0209
C	8.0935	3.4214	1.8753
C	8.5898	4.4969	2.6379
C	7.7424	5.1684	3.554
C	6.6024	4.4489	3.9949
C	4.3697	3.3443	-1.301
C	3.7614	2.8277	-0.1319
C	4.5662	2.4573	0.9664
C	5.9767	2.5905	0.8918
C	6.5362	2.6363	-0.409
C	5.7366	3.0327	-1.4975
C	1.8798	5.9892	-2.1956
C	2.3571	4.695	-1.8925
C	3.7226	4.3649	-2.0614
C	4.5065	5.282	-2.7977
C	4.0484	6.59	-3.034
C	2.7583	7.0214	-2.6237
C	3.4812	10.4749	-1.6079
C	3.3724	9.4499	-2.5894
C	4.1959	9.5184	-3.7365

C	5.2098	10.493	-3.756
C	5.5222	11.2285	-2.601
C	4.7436	11.116	-1.423
C	2.3345	10.8298	-0.8626
C	1.199	10.0105	-0.9843
C	1.2602	8.7899	-1.6767
C	2.417	8.4043	-2.3998
H	3.5711	10.8374	1.1703
H	4.6915	10.1302	3.0487
H	8.4952	10.8512	1.1025
H	7.3562	11.6694	-0.8068
H	9.6893	6.9114	2.6214
H	6.1079	6.8152	5.0723
H	5.6513	9.0614	4.4831
H	9.2216	9.1524	2.0265
H	5.1222	3.0185	3.4936
H	8.706	3.0941	1.0519
H	9.5403	4.901	2.3319
H	5.9567	4.8155	4.7751
H	2.7062	2.9361	0.0595
H	4.0579	2.2955	1.9028
H	7.599	2.6161	-0.5849
H	6.2431	3.2635	-2.4211
H	0.857	6.1881	-1.9252
H	1.6746	4.0132	-1.4105
H	5.5524	5.1139	-2.9936
H	4.8183	7.2576	-3.3715
H	4.0421	8.8655	-4.5835
H	5.8442	10.5806	-4.6263
H	6.4369	11.7993	-2.6198
H	2.3125	11.7117	-0.2375
H	0.3058	10.2625	-0.4308
H	0.4204	8.1277	-1.551

1,4-naphthyl-[6]CPP

C	-0.4373	-5.1291	0.5645
C	-0.5952	-5.5053	1.9139
C	0.5155	-5.964	2.6636
C	1.7974	-5.6495	2.1492
C	1.9534	-5.2959	0.7951
C	0.8294	-5.21	-0.0655
C	-0.9297	-8.9085	4.3673
C	0.2687	-9.6334	4.586
C	1.4443	-8.8648	4.7696
C	1.4934	-7.5279	4.3271
C	0.3675	-6.9379	3.7013

C	-0.8808	-7.5684	3.9315
C	-0.5913	-12.8097	2.9163
C	0.716	-13.1628	2.5004
C	1.7767	-12.769	3.3523
C	1.5909	-11.7086	4.2614
C	0.3431	-11.0393	4.3293
C	-0.7763	-11.7485	3.8256
C	1.4379	-12.8115	-1.5223
C	0.1558	-13.2736	-1.134
C	-0.0774	-13.656	0.2032
C	0.9702	-13.5779	1.1554
C	2.2893	-13.5859	0.6384
C	2.5222	-13.1958	-0.6953
C	2.741	-9.6745	-3.0026
C	2.771	-11.0167	-2.5764
C	1.5787	-11.7781	-2.5016
C	0.4631	-11.2741	-3.2151
C	0.4405	-9.9369	-3.6619
C	1.5276	-9.0626	-3.4085
C	2.168	-5.6401	-2.1419
C	2.3647	-6.7192	-3.0559
C	3.5896	-6.8549	-3.7514
C	4.6029	-5.9129	-3.5
C	4.408	-4.8519	-2.6042
C	3.1921	-4.6889	-1.9181
C	0.9205	-5.5152	-1.4645
C	-0.1823	-6.0732	-2.1528
C	0.0104	-7.1366	-3.0491
C	1.3081	-7.6501	-3.2812
H	-1.3366	-4.9498	-0.0025
H	-1.6052	-5.594	2.2782
H	2.7055	-5.8864	2.6774
H	2.964	-5.3407	0.4269
H	-1.8923	-9.3894	4.3198
H	2.3854	-9.3088	5.0476
H	2.4642	-7.0605	4.315
H	-1.8102	-7.15	3.5826
H	-1.4723	-13.159	2.4045
H	2.793	-13.088	3.1917
H	2.4822	-11.3123	4.7188
H	-1.7835	-11.3819	3.9309
H	-0.7178	-13.1324	-1.7477
H	-1.1077	-13.779	0.4933
H	3.1574	-13.658	1.2728
H	3.5478	-13.016	-0.9727
H	3.6273	-9.105	-2.7787

H	3.6861	-11.3368	-2.1081
H	-0.459	-11.8256	-3.2963
H	-0.4923	-9.5715	-4.0604
H	3.7443	-7.639	-4.4783
H	5.5447	-5.999	-4.0222
H	5.2018	-4.1354	-2.4502
H	3.0477	-3.8447	-1.2588
H	-1.1949	-5.9392	-1.8086
H	-0.8754	-7.6977	-3.2957

2,6-naphthyl-[6]CPP dimer macrocycle **12**

C	10.0548	-3.7486	-0.1015
C	9.4074	-4.281	1.1758
C	8.3473	-5.0977	1.203
C	7.6307	-5.613	-0.0294
C	8.2415	-5.0322	-1.3047
C	9.3039	-4.2172	-1.3318
C	10.1078	-2.2107	-0.1553
C	10.8006	-1.5942	-1.2132
C	10.9344	-0.209	-1.2715
C	10.3778	0.6146	-0.2759
C	9.6629	0.0029	0.7773
C	9.5312	-1.3894	0.8373
C	10.6163	2.1348	-0.3512
C	10.059	2.8858	0.8567
C	9.1654	3.8784	0.7806
C	8.5738	4.406	-0.5253
C	9.0954	3.6258	-1.7161
C	9.9892	2.6308	-1.6398
C	7.0357	4.3295	-0.5645
C	6.2719	3.7581	0.4707
C	4.8733	3.7683	0.4193
C	4.1816	4.352	-0.6712
C	4.9645	4.9035	-1.7137
C	6.357	4.8909	-1.6568
O	11.3736	-4.2791	-0.2324
O	12.0135	2.3956	-0.4825
C	12.7799	2.0443	0.6567
O	8.9939	5.7536	-0.7377
C	8.6412	6.6439	0.307
C	6.1364	-5.2762	0.1351
O	7.8074	-7.0293	-0.0093
C	7.2444	-7.7009	-1.1231
C	12.2289	-3.9869	0.8594
C	5.4317	-4.4558	-0.7664
C	4.0582	-4.2324	-0.6087

C	3.3359	-4.8213	0.4587
C	4.0631	-5.6261	1.3673
C	5.4291	-5.8464	1.2047
C	1.8324	-4.6402	0.6043
C	1.0565	-4.0388	-0.4208
C	-0.342	-3.9394	-0.3083
C	-0.9916	-4.4302	0.8356
C	-0.2383	-4.9976	1.8654
C	1.1474	-5.1051	1.7552
C	-1.1016	-3.3732	-1.3379
C	-2.4957	-3.314	-1.2443
C	-3.1763	-3.8226	-0.1101
C	-2.3895	-4.3689	0.9345
C	-10.5965	4.0335	0.5615
C	-9.9159	4.5779	1.816
C	-8.8317	5.3613	1.8059
C	-8.1166	5.8252	0.5383
C	-8.7737	5.2501	-0.7014
C	-9.8599	4.4658	-0.6913
C	-10.6733	2.4952	0.5402
C	-11.375	1.8642	-0.4999
C	-11.5212	0.479	-0.5325
C	-10.978	-0.3409	0.4808
C	-10.2409	0.2969	1.5105
C	-10.0971	1.6882	1.5413
C	-11.1966	-1.8825	0.4397
C	-10.7162	-2.4213	-0.9053
C	-9.7879	-3.3751	-1.0506
C	-9.0792	-4.074	0.1074
C	-9.5382	-3.5182	1.4396
C	-10.462	-2.5597	1.5834
C	-7.5462	-3.93	0.053
C	-6.7672	-4.6154	0.9981
C	-5.375	-4.5646	0.9603
C	-4.6947	-3.8231	-0.0343
C	-5.4852	-3.1198	-0.9756
C	-6.8835	-3.1719	-0.9316
O	-11.9081	4.5839	0.4435
O	-12.5572	-2.2485	0.6924
C	-13.5351	-1.7761	-0.2093
O	-9.4332	-5.4566	0.1284
C	-9.1262	-6.1531	-1.0671
C	-6.6311	5.417	0.5031
O	-8.2302	7.2421	0.4082
C	-7.7107	7.97	1.5077
C	-12.7485	4.3259	1.5551

C	-6.0288	4.637	1.5092
C	-4.661	4.3439	1.4664
C	-3.8412	4.8183	0.4138
C	-4.4642	5.5831	-0.6007
C	-5.8266	5.8744	-0.5521
C	-2.3434	4.559	0.3923
C	-1.5597	4.8736	-0.7461
C	-0.1677	4.6976	-0.7412
C	0.4764	4.1954	0.4005
C	-0.2851	3.8556	1.5239
C	-1.6718	4.033	1.5239
C	0.5888	5.039	-1.8641
C	1.9775	4.9104	-1.851
C	2.6614	4.4276	-0.7064
C	1.8755	4.0577	0.4165
H	9.8459	-4.0006	2.1296
H	8.001	-5.4309	2.1771
H	7.8042	-5.3139	-2.2586
H	9.6619	-3.8965	-2.306
H	11.2659	-2.1939	-1.9851
H	11.4998	0.2237	-2.0869
H	9.2169	0.5902	1.567
H	8.9894	-1.8145	1.6702
H	10.4195	2.6129	1.8447
H	8.8581	4.3466	1.7117
H	8.7467	3.9064	-2.7059
H	10.3041	2.1731	-2.5732
H	6.7458	3.311	1.3331
H	4.3569	3.3212	1.2498
H	4.5274	5.378	-2.5727
H	6.9124	5.3497	-2.4653
H	13.8331	1.9093	0.3363
H	12.4734	1.0806	1.1167
H	12.7608	2.8648	1.4045
H	8.6415	7.6746	-0.1024
H	9.3972	6.6064	1.1193
H	7.6193	6.4732	0.7082
H	7.0772	-8.76	-0.8397
H	7.9518	-7.6913	-1.9789
H	6.2518	-7.3033	-1.4247
H	13.2777	-4.0745	0.5098
H	12.0845	-4.7282	1.6733
H	12.1189	-2.9502	1.2434
H	5.9301	-3.9921	-1.6058
H	3.5823	-3.6013	-1.3386
H	3.5951	-6.1247	2.1962

H	5.9362	-6.4933	1.9097
H	1.5104	-3.6733	-1.326
H	-0.726	-5.3771	2.756
H	1.6587	-5.5615	2.5831
H	-0.6167	-2.9914	-2.2289
H	-3.0216	-2.8931	-2.0834
H	-2.8392	-4.7619	1.8296
H	-10.3429	4.3282	2.7834
H	-8.449	5.6971	2.7658
H	-8.357	5.5102	-1.6703
H	-10.2496	4.1433	-1.6527
H	-11.8314	2.4523	-1.286
H	-12.0718	0.055	-1.3576
H	-9.7827	-0.2629	2.311
H	-9.541	2.1233	2.3594
H	-11.1493	-2.0208	-1.815
H	-9.5391	-3.6792	-2.0637
H	-9.1137	-3.9401	2.3461
H	-10.7303	-2.2724	2.5971
H	-7.2427	-5.2186	1.7613
H	-4.8551	-5.1421	1.7031
H	-5.0443	-2.5264	-1.7577
H	-7.4367	-2.6243	-1.6813
H	-14.4601	-2.3629	-0.0365
H	-13.2809	-1.9541	-1.2719
H	-13.7994	-0.7213	0.0088
H	-9.0573	-7.2341	-0.8292
H	-8.1444	-5.8717	-1.5042
H	-9.9418	-6.0254	-1.8097
H	-7.4807	8.9988	1.1633
H	-6.7571	7.5576	1.9012
H	-8.4707	8.0492	2.3133
H	-13.8017	4.4271	1.2229
H	-12.5761	5.078	2.3536
H	-12.6505	3.2939	1.9545
H	-6.6036	4.2582	2.3423
H	-4.2659	3.7485	2.271
H	-3.9153	5.9972	-1.427
H	-6.2534	6.4873	-1.3361
H	-2.0054	5.2656	-1.6438
H	0.1964	3.4685	2.4144
H	-2.1934	3.7795	2.4301
H	0.1048	5.4249	-2.754
H	2.492	5.2033	-2.7476
H	2.3272	3.6915	1.3219

2,6-naphthyl-[6]CPP dimer **13**

C	-9.6239	-0.7938	-0.0898
C	-9.662	-0.1055	-1.3238
C	-9.5854	1.2895	-1.3753
C	-9.468	2.0577	-0.1956
C	-9.5957	1.3782	1.0353
C	-9.6718	-0.0139	1.0872
C	-8.9548	3.4921	-0.2316
C	-9.273	-2.2772	-0.0221
C	-8.7615	4.2342	0.9552
C	-7.9468	5.3707	0.9718
C	-7.2901	5.8157	-0.1975
C	-7.6079	5.1616	-1.4076
C	-8.4204	4.0273	-1.4245
C	-6.1139	6.7823	-0.1295
C	-5.4317	7.1982	-1.2949
C	-4.1698	7.7978	-1.2208
C	-3.5305	8.0092	0.022
C	-4.2712	7.7105	1.1872
C	-5.5306	7.1124	1.1132
C	-2.0436	8.3395	0.1097
C	-1.2207	8.2821	-1.0454
C	0.1801	8.2774	-0.936
C	0.7897	8.3679	0.3245
C	-0.0067	8.5396	1.4615
C	-1.4009	8.5183	1.3613
C	0.9722	8.0898	-2.0718
C	2.3489	7.8943	-1.9519
C	2.9827	7.8935	-0.6834
C	2.1805	8.1962	0.4494
C	4.4122	7.3822	-0.5336
C	5.2011	7.0581	-1.6601
C	6.3772	6.3119	-1.533
C	6.8217	5.8518	-0.2725
C	6.0996	6.2867	0.8622
C	4.9255	7.0327	0.7345
C	-9.0905	-2.9298	1.2178
C	-8.4111	-4.148	1.3017
C	-7.8814	-4.7724	0.15
C	-8.1989	-4.1947	-1.0999
C	-8.8781	-2.9771	-1.1839
C	-6.8254	-5.8693	0.2665
C	-6.1005	-6.302	-0.8672

C	-4.9265	-7.0478	-0.738
C	-4.4161	-7.3993	0.5309
C	-5.2077	-7.0773	1.6559
C	-6.3838	-6.3313	1.5274
C	-2.9869	-7.9102	0.6827
C	-2.1835	-8.2149	-0.4483
C	-0.7928	-8.3864	-0.322
C	-0.1846	-8.2934	0.9396
C	-0.9781	-8.1037	2.0737
C	-2.3546	-7.9085	1.9522
C	0.0048	-8.5603	-1.4572
C	1.3989	-8.5388	-1.3559
C	2.0403	-8.3574	-0.1036
C	1.216	-8.2979	1.0501
C	3.5271	-8.027	-0.0153
C	4.2694	-7.7318	-1.1802
C	5.5287	-7.1335	-1.1065
C	6.1103	-6.7996	0.1362
C	5.4265	-7.2119	1.3017
C	4.1647	-7.8118	1.2279
C	7.2864	-5.8328	0.2027
C	7.8776	4.7548	-0.1567
C	9.62	0.7763	0.084
C	9.6616	0.0895	1.3187
C	9.585	-1.3055	1.3721
C	9.4642	-2.075	0.1936
C	9.5882	-1.3971	-1.0384
C	9.6643	-0.005	-1.0923
C	8.951	-3.5092	0.2326
C	9.2692	2.2596	0.0153
C	8.759	-4.2543	-0.9527
C	7.9443	-5.3909	-0.9671
C	7.6029	-5.1755	1.4114
C	8.4155	-4.0411	1.4262
C	9.0849	2.9111	-1.2249
C	8.4055	4.1294	-1.3088
C	8.1969	4.1781	1.0931
C	8.876	2.9605	1.1771
H	-9.6386	-0.6188	-2.2681
H	-9.5119	1.7294	-2.3542
H	-9.5095	1.8814	1.9813
H	-9.6408	-0.4495	2.0688
H	-9.1428	3.9037	1.9052
H	-7.7711	5.8221	1.9325
H	-7.1463	5.427	-2.3415
H	-8.5073	3.5234	-2.37

H	-5.8103	6.9944	-2.281
H	-3.6835	8.008	-2.1567
H	-3.8607	7.8284	2.1734
H	-5.9724	6.8209	2.0491
H	-1.6356	8.1295	-2.0258
H	0.448	8.6134	2.4424
H	-1.9489	8.5775	2.2846
H	0.5155	8.015	-3.052
H	2.876	7.6628	-2.8595
H	2.5936	8.2123	1.4429
H	4.8907	7.2959	-2.6618
H	6.8654	6.0342	-2.4494
H	6.3584	5.9825	1.8594
H	4.3887	7.2306	1.6444
H	-9.3665	-2.4752	2.1519
H	-8.2227	-4.5172	2.2931
H	-7.8444	-4.6031	-2.0283
H	-8.9739	-2.5571	-2.1684
H	-6.3568	-5.9961	-1.8645
H	-4.3872	-7.2439	-1.6468
H	-4.8994	-7.317	2.658
H	-6.8743	-6.0554	2.4429
H	-2.5958	-8.2331	-1.4424
H	-0.5224	-8.0268	3.0544
H	-2.8828	-7.675	2.8585
H	-0.4489	-8.6361	-2.4388
H	1.9478	-8.5998	-2.2783
H	1.6298	-8.1434	2.0309
H	3.8603	-7.8528	-2.1667
H	5.9718	-6.8449	-2.0426
H	5.8037	-7.0051	2.2878
H	3.6772	-8.019	2.1637
H	9.6412	0.604	2.2625
H	9.5144	-1.7446	2.3516
H	9.4989	-1.9015	-1.9835
H	9.6302	0.4294	-2.0742
H	9.1416	-3.9261	-1.903
H	7.7697	-5.8448	-1.9268
H	7.1403	-5.4383	2.3456
H	8.5012	-3.5345	2.3703
H	9.3596	2.4557	-2.1589
H	8.2158	4.4977	-2.3003
H	7.8438	4.5873	2.0217
H	8.9731	2.5413	2.1618

Chapter IV

cis-azo[11]CPP

C	-5.4209	-4.9981	-0.619
C	-4.1982	-5.66	-0.6371
C	-3.2544	-5.4913	0.3924
C	-3.6488	-4.6975	1.4855
C	-4.8812	-4.0565	1.5157
C	-5.785	-4.1485	0.442
H	-6.0816	-5.1085	-1.4735
H	-3.9663	-6.2982	-1.4844
H	-2.9603	-4.531	2.3078
H	-5.1316	-3.4554	2.3845
C	-1.8647	-6.0015	0.2851
C	-1.0323	-6.1398	1.4107
C	-1.2734	-6.2372	-0.9699
C	0.3349	-6.3599	1.2807
H	-1.4483	-6.0306	2.4078
C	0.0884	-6.4827	-1.0983
H	-1.8715	-6.1608	-1.8725
C	0.9439	-6.4788	0.0183
H	0.9485	-6.3644	2.1766
H	0.4989	-6.6327	-2.0924
C	2.419	-6.4008	-0.1279
C	2.9729	-5.7964	-1.2705
C	3.3096	-6.7371	0.9094
C	4.3106	-5.4274	-1.3185
H	2.328	-5.508	-2.0942
C	4.6492	-6.3574	0.8667
H	2.9437	-7.2714	1.7818
C	5.166	-5.6323	-0.2219
H	4.6681	-4.8632	-2.1746
H	5.2939	-6.5932	1.7095
C	6.4373	-4.8683	-0.1673
C	6.7844	-4.1896	1.0132
C	7.175	-4.5596	-1.3256
C	7.6712	-3.1177	0.9908
H	6.2485	-4.408	1.9326
C	8.0646	-3.4903	-1.3471
H	6.9995	-5.1223	-2.2388
C	8.2511	-2.6782	-0.2125
H	7.7989	-2.5263	1.8927

H	8.5663	-3.2376	-2.2776
C	8.2946	0.866	-1.3908
C	8.6449	1.5748	-0.2272
C	9.2382	0.8288	0.8107
C	9.2712	-0.563	0.7728
C	8.7248	-1.2744	-0.3115
C	8.3368	-0.5211	-1.4334
H	7.844	1.3899	-2.2273
H	9.6144	1.3361	1.6948
H	9.6651	-1.1052	1.6287
H	7.9197	-1.0267	-2.2989
C	8.1058	2.9457	-0.0302
C	7.717	3.3673	1.2553
C	7.6793	3.7431	-1.1091
C	6.7883	4.3857	1.4321
H	8.0525	2.8164	2.1285
C	6.7289	4.7444	-0.9347
H	8.0196	3.519	-2.1159
C	6.1805	5.0172	0.3317
H	6.4643	4.6291	2.4399
H	6.3266	5.2404	-1.8135
C	4.8673	5.6966	0.4617
C	4.3668	6.621	-0.4741
C	3.9701	5.2354	1.4422
C	3.016	6.9648	-0.5012
H	5.034	7.0529	-1.2155
C	2.6268	5.5793	1.4167
H	4.3025	4.5051	2.1726
C	2.0999	6.4045	0.4081
H	2.6642	7.6583	-1.2605
H	1.9572	5.11	2.1306
C	-2.1625	5.9885	-0.11
C	-1.5913	6.0833	1.1724
C	-0.2364	6.3364	1.3462
C	0.6276	6.4863	0.2468
C	0.0364	6.5149	-1.0288
C	-1.3246	6.2807	-1.2016
H	-2.1981	5.8828	2.0499
H	0.1668	6.3673	2.3542
H	0.6625	6.6442	-1.9071
H	-1.7307	6.2807	-2.209
C	-3.5352	5.4531	-0.2873
C	-3.8821	4.7297	-1.4432
C	-4.5001	5.5152	0.7343
C	-5.0878	4.0449	-1.5399
H	-3.1735	4.6506	-2.2617

C	-5.6959	4.8112	0.6473
H	-4.3032	6.099	1.6285
C	-6.0077	4.024	-0.4764
H	-5.3031	3.4961	-2.4518
H	-6.374	4.8331	1.495
C	-7.1964	3.1373	-0.488
C	-8.3312	3.402	0.3017
C	-7.2011	1.9488	-1.2461
C	-9.3863	2.4994	0.374
H	-8.4	4.335	0.8528
C	-8.2416	1.0322	-1.1657
H	-6.3483	1.7082	-1.8729
C	-9.3261	1.2762	-0.3089
H	-10.2645	2.717	0.9745
H	-8.2013	0.1173	-1.7467
C	-8.1878	-1.252	0.9588
C	-9.2381	-1.5847	0.0886
C	-9.2125	-2.8318	-0.5523
C	-8.1134	-3.6733	-0.4228
C	-7.0143	-3.3209	0.3832
C	-7.1018	-2.1066	1.0947
H	-8.2103	-0.3188	1.5105
H	-10.063	-3.1181	-1.1637
H	-6.2799	-1.7966	1.7319
H	-8.1208	-4.6275	-0.9404
N	-10.4744	0.4312	-0.1871
N	-10.4335	-0.8181	-0.0897

trans-azo[11]CPP

C	1.16005	7.88359	1.083
C	2.50425	7.54438	1.1789
C	3.24635	7.16198	0.0462
C	2.62005	7.32868	-1.2029
C	1.28195	7.69349	-1.3008
C	0.48815	7.8871	-0.1542
H	0.60615	8.0578	2.
H	2.96375	7.51028	2.1622
H	3.15725	7.07798	-2.1126
H	0.83375	7.76149	-2.2874
C	4.51654	6.40257	0.1649
C	5.43324	6.26676	-0.8953
C	4.73604	5.60167	1.3003
C	6.41884	5.28236	-0.8797
H	5.35155	6.91266	-1.7652
C	5.72463	4.62696	1.3203
H	4.05204	5.65937	2.1407

C	6.54343	4.39216	0.2023
H	7.07704	5.17935	-1.7385
H	5.78253	3.95826	2.1738
C	7.29692	3.11545	0.1282
C	7.82172	2.49235	1.2756
C	7.28422	2.36585	-1.0606
C	8.14941	1.14045	1.2739
H	7.92352	3.06155	2.1958
C	7.61281	1.01345	-1.0626
H	6.89092	2.81215	-1.9695
C	7.9683	0.34955	0.1244
H	8.50031	0.67814	2.1929
H	7.4675	0.43855	-1.9728
C	7.87719	-1.13055	0.1923
C	8.18049	-1.97516	-0.8906
C	7.23469	-1.71455	1.2976
C	7.73228	-3.29365	-0.9246
H	8.73769	-1.58346	-1.7378
C	6.77768	-3.02525	1.2579
H	6.97829	-1.09715	2.1533
C	6.94668	-3.82755	0.115
H	7.95728	-3.90095	-1.7971
H	6.17508	-3.38654	2.085
C	4.47646	-6.57653	0.9186
C	3.88886	-6.80883	-0.3381
C	4.56506	-6.29173	-1.4582
C	5.64227	-5.42494	-1.315
C	6.11697	-5.04924	-0.0448
C	5.57036	-5.72854	1.0599
H	4.01206	-6.98253	1.8126
H	4.19696	-6.50813	-2.457
H	6.05277	-4.95584	-2.2041
H	5.95437	-5.53454	2.0571
C	2.50685	-7.34042	-0.4436
C	1.65896	-6.82691	-1.4411
C	1.91605	-8.17141	0.527
C	0.28586	-7.0206	-1.3962
H	2.06296	-6.16802	-2.2028
C	0.53615	-8.3635	0.5741
H	2.53834	-8.64572	1.2813
C	-0.32095	-7.7373	-0.3496
H	-0.33414	-6.5074	-2.1243
H	0.11684	-8.981	1.3643
C	-1.78645	-7.60469	-0.1556
C	-2.33135	-7.47069	1.1341
C	-2.65005	-7.36168	-1.2388

C	-3.60905	-6.95448	1.3287
H	-1.71175	-7.67719	2.0023
C	-3.91844	-6.82737	-1.0444
H	-2.29765	-7.52199	-2.2538
C	-4.39774	-6.52797	0.2443
H	-3.96664	-6.81298	2.3447
H	-4.50294	-6.54587	-1.915
C	-7.20872	-3.27905	0.4272
C	-7.32813	-4.25995	-0.5738
C	-6.51663	-5.39146	-0.5745
C	-5.53554	-5.58867	0.4159
C	-5.52813	-4.68327	1.4924
C	-6.34722	-3.56086	1.5011
H	-8.03493	-4.11395	-1.3866
H	-6.61534	-6.10716	-1.3861
H	-4.78823	-4.78927	2.2793
H	-6.22572	-2.82856	2.294
C	-7.73621	-1.90065	0.2736
C	-8.10041	-1.10045	1.372
C	-7.64851	-1.26955	-0.9792
C	-8.2172	0.28085	1.2495
H	-8.24901	-1.56135	2.345
C	-7.7564	0.11095	-1.0995
H	-7.36921	-1.85285	-1.8518
C	-7.96589	0.92975	0.0252
H	-8.46229	0.86816	2.1302
H	-7.5548	0.56515	-2.0646
C	-7.68508	2.38415	-0.0636
C	-7.77858	3.09085	-1.2791
C	-7.07738	3.04345	1.0267
C	-7.14497	4.31665	-1.445
H	-8.29588	2.64445	-2.1233
C	-6.46377	4.27724	0.8761
H	-6.98508	2.52755	1.9774
C	-6.42667	4.89654	-0.3867
H	-7.13457	4.81095	-2.4122
H	-5.90737	4.72494	1.6924
C	-2.97685	6.83392	-1.2036
C	-3.72875	7.13142	-0.0527
C	-3.13645	7.90872	0.9557
C	-1.80074	8.28361	0.8655
C	-0.99475	7.85951	-0.2109
C	-1.63895	7.18521	-1.2714
H	-3.43246	6.23062	-1.9811
H	-3.72415	8.15772	1.8346
H	-1.05625	6.83401	-2.1166

H	-1.36334	8.86091	1.6744
N	-4.94446	6.48193	0.256
N	-5.50696	5.91314	-0.7251

azo[7]CPP dimer macrocycle

C	-9.59682	2.25301	-14.40079
C	-10.34652	2.42781	-15.51659
C	-10.01993	1.64772	-16.80386
C	-8.38447	1.3072	-14.42729
C	-8.67233	0.11113	-15.35364
C	-9.45176	0.26445	-16.44793
O	-9.04605	2.35418	-17.57066
O	-7.25093	2.03503	-14.90765
C	-8.0785	0.77855	-13.01355
C	-11.29617	1.49799	-17.64918
C	-8.57453	-0.46047	-12.58304
C	-8.19134	-0.96985	-11.33078
C	-7.33452	-0.22545	-10.50299
C	-6.91944	1.05313	-10.90065
C	-7.27874	1.54619	-12.16001
C	-11.51664	2.42781	-18.66881
C	-12.62813	2.30713	-19.5008
C	-13.54998	1.2789	-19.29538
C	-13.36232	0.36455	-18.24371
C	-12.22025	0.46613	-17.42532
C	-14.7581	1.18176	-20.24421
C	-7.78945	-1.87742	-8.62905
C	-8.7885	-1.57874	-7.76788
C	-9.0405	-0.13629	-7.30198
C	-6.8274	-0.79964	-9.16358
C	-6.69466	0.34457	-8.13834
C	-7.71438	0.65729	-7.29202
O	-9.58157	-0.15204	-5.97848
O	-5.54947	-1.40233	-9.38192
C	-10.05683	0.51237	-8.25759
C	-10.9472	-0.31677	-8.94923
C	-11.88849	0.23511	-9.81966
C	-11.95628	1.61993	-9.99075
C	-11.06843	2.45851	-9.29709
C	-10.1056	1.90137	-8.43833
C	-10.81431	-0.8741	-5.97583
C	-5.0684	-1.96515	-8.15891
C	-6.10921	1.17871	-14.96057
C	-8.7615	1.61193	-18.75852
C	-13.01223	2.1952	-10.94884
C	-13.79781	1.31198	-11.70228

C	-14.72293	1.81177	-12.62475
C	-14.87931	3.19286	-12.77932
C	-14.13811	4.07894	-11.98676
C	-13.19369	3.58024	-11.07689
C	-14.79759	2.01643	-21.36712
C	-15.87973	1.95897	-22.24744
C	-16.93875	1.08364	-21.99828
C	-16.90512	0.23967	-20.87506
C	-15.80402	0.27872	-20.00174
N	-18.07772	1.07022	-22.92406
N	-17.96788	1.66417	-23.99864
C	-20.76666	8.46412	-24.34512
C	-19.97485	8.08103	-23.31303
C	-18.97991	6.91216	-23.46395
C	-20.6746	7.76205	-25.7099
C	-20.2913	6.28088	-25.51536
C	-19.52218	5.88778	-24.47198
O	-17.71845	7.4015	-23.93189
O	-19.6865	8.42252	-26.50869
C	-22.03492	7.83149	-26.42211
C	-18.78111	6.23893	-22.09502
C	-22.95186	6.78671	-26.26796
C	-24.17318	6.81953	-26.95243
C	-24.47923	7.90587	-27.78348
C	-23.57912	8.97447	-27.90298
C	-22.35386	8.93414	-27.22549
C	-18.84819	7.01232	-20.93194
C	-18.57297	6.43222	-19.69075
C	-18.24498	5.07448	-19.61364
C	-18.26649	4.27664	-20.76405
C	-18.52452	4.8633	-22.01011
C	-17.84142	4.47162	-18.26083
C	-25.55127	7.31692	-29.96502
C	-25.68369	5.98892	-30.17629
C	-26.10376	5.03923	-29.03873
C	-25.80142	7.92391	-28.57455
C	-26.87075	7.1117	-27.82114
C	-27.01605	5.77986	-28.03978
O	-26.81087	3.93314	-29.60166
O	-26.2619	9.26824	-28.72528
C	-24.85838	4.52641	-28.29438
C	-24.97077	4.14195	-26.95272
C	-23.85278	3.65355	-26.26643
C	-22.61472	3.57171	-26.91501
C	-22.49585	3.97089	-28.25465
C	-23.62053	4.44276	-28.94765

C	-27.98917	4.41417	-30.25701
C	-26.48038	9.83378	-27.43349
C	-19.59909	7.78897	-27.78867
C	-17.1723	8.32222	-22.98034
C	-21.38621	3.04637	-26.15028
C	-21.52816	2.56457	-24.84046
C	-20.40958	2.09314	-24.13992
C	-19.14705	2.12324	-24.74093
C	-19.00294	2.59795	-26.05057
C	-20.12359	3.05176	-26.75998
C	-17.69699	5.31377	-17.15195
C	-17.20793	4.80094	-15.94507
C	-16.88739	3.44172	-15.84521
C	-17.13395	2.57972	-16.9235
C	-17.60192	3.09838	-18.13866
N	-16.27529	2.9209	-14.61807
N	-15.81358	3.70618	-13.78871
H	-9.84076	2.78398	-13.5041
H	-11.16636	3.11408	-15.50577
H	-8.24768	-0.84562	-15.1331
H	-9.66353	-0.57676	-17.07459
H	-9.23708	-1.02045	-13.21047
H	-8.5489	-1.9257	-11.00907
H	-6.31865	1.64966	-10.24582
H	-6.93908	2.51041	-12.47245
H	-10.82539	3.23119	-18.81501
H	-12.77587	3.00571	-20.29734
H	-14.081	-0.40703	-18.06756
H	-12.05864	-0.23956	-16.63709
H	-7.65978	-2.89104	-8.94354
H	-9.41875	-2.36312	-7.40327
H	-5.7829	0.90175	-8.0898
H	-7.59124	1.4662	-6.60115
H	-10.90703	-1.3762	-8.80947
H	-12.56099	-0.40376	-10.35639
H	-11.12341	3.51889	-9.42523
H	-9.41658	2.53517	-7.92063
H	-10.63949	-1.8793	-6.29895
H	-11.5043	-0.39929	-6.64133
H	-11.22156	-0.88326	-4.98511
H	-4.11146	-2.41445	-8.3259
H	-5.75684	-2.70989	-7.81579
H	-4.97792	-1.19554	-7.42076
H	-6.3129	0.35197	-15.60906
H	-5.88936	0.81543	-13.97814
H	-5.27107	1.72832	-15.33449

H -8.02348 2.12949 -19.33477
H -9.65698 1.50628 -19.33608
H -8.3919 0.64226 -18.49274
H -13.68646 0.25375 -11.57594
H -15.31005 1.13828 -13.21237
H -14.28926 5.133 -12.08109
H -12.61309 4.25597 -10.48382
H -13.99482 2.6998 -21.55376
H -15.89961 2.58811 -23.11331
H -17.71527 -0.43299 -20.68727
H -15.76512 -0.37396 -19.15519
H -21.46245 9.26723 -24.21012
H -20.0435 8.59851 -22.37974
H -20.63833 5.55016 -26.21614
H -19.28391 4.85172 -24.3492
H -22.71766 5.96002 -25.63019
H -24.8697 6.01429 -26.84218
H -23.82751 9.81782 -28.51657
H -21.66155 9.74199 -27.32242
H -19.10446 8.04941 -20.99253
H -18.6077 7.02689 -18.80167
H -18.07615 3.22505 -20.69271
H -18.52273 4.26378 -22.89472
H -25.26481 7.95422 -30.77616
H -25.49293 5.59083 -31.15131
H -27.5095 7.60432 -27.11689
H -27.77345 5.23959 -27.51018
H -25.91296 4.22035 -26.4528
H -23.94392 3.34605 -25.24599
H -21.54807 3.91522 -28.74693
H -23.53353 4.73985 -29.97224
H -27.71507 5.1075 -31.02403
H -28.51604 3.59087 -30.69322
H -28.61889 4.90289 -29.54323
H -26.82412 10.84286 -27.53628
H -25.5622 9.82216 -26.88844
H -27.21489 9.25895 -26.90827
H -20.54867 7.84455 -28.28062
H -19.32244 6.76362 -27.66094
H -18.85883 8.2859 -28.38388
H -16.22865 8.68317 -23.33534
H -17.84468 9.14359 -22.85376
H -17.03272 7.8268 -22.0414
H -22.49147 2.55594 -24.37415
H -20.5184 1.71367 -23.14495
H -18.03633 2.61461 -26.51058

H	-20.01263	3.40417	-27.76338
H	-17.95126	6.34949	-17.23128
H	-17.07714	5.44723	-15.10316
H	-16.95568	1.52965	-16.82178
H	-17.76912	2.44786	-18.97213

azo[7]CPP dimer

C	-1.83678	4.44446	1.1523
C	-3.20085	4.68714	1.15797
C	-3.69643	5.93961	0.80211
C	-0.9415	5.45123	0.7993
C	-1.41513	6.73731	0.4764
C	-2.8086	6.9823	0.47244
C	0.54334	5.05641	0.78136
C	-5.22747	6.08664	0.79488
C	1.58994	5.95744	0.50885
C	2.9209	5.47966	0.4535
C	3.17297	4.10964	0.65419
C	2.12705	3.24683	0.9769
C	0.8249	3.71666	1.04646
C	-5.95738	4.96383	1.1824
C	-7.34307	5.00055	1.21119
C	-8.02726	6.16105	0.85166
C	-7.30957	7.30299	0.44316
C	-5.89643	7.26675	0.42143
C	-9.56383	6.10998	0.9383
C	4.61662	2.0836	0.65315
C	5.80975	1.40307	0.46573
C	6.97939	2.09855	0.1661
C	4.56564	3.46999	0.52432
C	5.74514	4.19913	0.27761
C	6.96717	3.50641	0.10536
C	8.23267	1.24356	-0.09716
C	9.51272	1.78296	-0.31953
C	10.59107	0.91726	-0.61567
C	10.36212	-0.46995	-0.70771
C	9.09763	-0.98749	-0.43232
C	8.04468	-0.13856	-0.11975
C	11.45255	-1.47624	-1.12188
C	11.05436	-2.80285	-1.31354
C	11.96219	-3.75116	-1.77915
C	13.28596	-3.38785	-2.03835
C	13.71932	-2.07731	-1.76833
C	12.79507	-1.11077	-1.3205
C	-10.39376	7.18596	0.57794
C	-11.79282	7.07053	0.74378

C	-12.33584	5.88562	1.27836
C	-11.49953	4.80958	1.5807
C	-10.12467	4.92151	1.40857
C	1.52307	-6.0341	-1.49215
C	2.88502	-6.26893	-1.73241
C	3.81916	-6.07386	-0.70548
C	1.09115	-5.64646	-0.21519
C	2.01089	-5.57461	0.8405
C	3.37788	-5.76766	0.591
C	-0.38725	-5.27679	0.02359
C	5.32952	-6.17541	-1.00646
C	-0.87008	-5.07675	1.32628
C	-2.18755	-4.63471	1.52621
C	-3.0028	-4.35084	0.42154
C	-2.54838	-4.63667	-0.87355
C	-1.24756	-5.11863	-1.07079
C	5.77988	-6.68084	-2.23613
C	7.15269	-6.68677	-2.53294
C	8.06735	-6.14858	-1.61622
C	7.62159	-5.70625	-0.36272
C	6.25626	-5.74045	-0.04945
C	9.56059	-6.02455	-1.98254
C	-4.95269	-3.58084	1.90114
C	-6.16327	-2.88686	2.07154
C	-6.78085	-2.28243	0.96593
C	-4.38798	-3.70172	0.62077
C	-5.07683	-3.20969	-0.49391
C	-6.25951	-2.48174	-0.32008
C	-8.01775	-1.3788	1.14978
C	-8.44979	-0.60083	0.06961
C	-9.48824	0.32005	0.23933
C	-10.13375	0.43516	1.477
C	-9.77282	-0.41521	2.53491
C	-8.69918	-1.31114	2.37726
C	-11.22671	1.51012	1.65665
C	-12.05988	1.52376	2.78842
C	-13.02577	2.53691	2.93796
C	-13.12211	3.55487	1.97515
C	-12.29996	3.52627	0.84351
C	-11.37357	2.494	0.67181
C	10.40396	-5.26574	-1.16187
C	11.74193	-5.07177	-1.52028
C	12.25561	-5.67214	-2.67621
C	11.4319	-6.4895	-3.46662
C	10.0763	-6.64826	-3.13056
H	-1.46868	3.47561	1.41898

H	-3.87797	3.90728	1.4344
H	-0.72849	7.5202	0.23274
H	-3.18525	7.9513	0.21917
H	1.37982	6.99316	0.34221
H	3.72766	6.15203	0.2546
H	2.33041	2.21372	1.16822
H	0.02876	3.04486	1.29957
H	-5.44409	4.06747	1.46056
H	-7.88986	4.13173	1.51219
H	-7.82978	8.19175	0.15413
H	-5.33954	8.1299	0.12314
H	3.72691	1.53955	0.8915
H	5.83172	0.33654	0.5489
H	5.71696	5.26627	0.21805
H	7.87282	4.04709	-0.076
H	9.6676	2.84042	-0.26857
H	11.57151	1.31404	-0.77626
H	8.93575	-2.04438	-0.46401
H	7.08027	-0.54656	0.09779
H	10.0436	-3.08909	-1.10893
H	11.64503	-4.75991	-1.94227
H	14.74593	-1.812	-1.91082
H	13.1141	-0.10566	-1.13679
H	-9.96901	8.08621	0.18323
H	-12.43467	7.88166	0.47067
H	-11.91804	3.89622	1.95031
H	-9.49043	4.093	1.64227
H	0.81358	-6.14702	-2.28473
H	3.21211	-6.58436	-2.70078
H	1.67202	-5.36082	1.83271
H	4.08542	-5.67772	1.38976
H	-0.23269	-5.25691	2.16659
H	-2.56393	-4.50199	2.51944
H	-3.19475	-4.48205	-1.71239
H	-0.90788	-5.35275	-2.05823
H	5.07697	-7.05906	-2.94881
H	7.49921	-7.09103	-3.46119
H	8.32479	-5.34056	0.35516
H	5.92074	-5.42387	0.91597
H	-4.45939	-4.0122	2.74647
H	-6.60602	-2.81009	3.0421
H	-4.69168	-3.37849	-1.47792
H	-6.76534	-2.07428	-1.17127
H	-7.977	-0.7034	-0.88468
H	-9.7902	0.93942	-0.57889
H	-10.307	-0.37397	3.46108

H	-8.40034	-1.93799	3.19181
H	-11.96029	0.76492	3.53642
H	-13.67853	2.53539	3.78607
H	-12.38225	4.29722	0.10507
H	-10.7691	2.46162	-0.21091
H	10.02287	-4.82528	-0.26414
H	12.37549	-4.46314	-0.9081
H	11.83258	-6.9841	-4.32668
H	9.43736	-7.24327	-3.75004
N	14.18929	-4.39995	-2.60742
N	13.65824	-5.42421	-3.04478
N	-13.7712	5.72281	1.55502
N	-14.06927	4.67109	2.12536

cis-azo[9]CPP B3LYP

C	0.3928	-4.0184	10.8346
C	0.9052	-5.3381	10.8911
C	1.998	-5.6495	10.041
C	2.5412	-4.6976	9.1734
C	2.0276	-3.3977	9.13
C	0.9649	-3.0578	9.9761
C	1.0168	-7.5834	12.0853
C	0.4399	-8.6416	12.7877
C	-0.9036	-8.6001	13.2236
C	-1.618	-7.3975	12.9819
C	-1.0251	-6.3203	12.2841
C	0.2945	-6.4133	11.7836
C	-2.9864	-9.9815	13.7962
C	-3.6146	-11.2334	13.8881
C	-2.8587	-12.4316	13.9232
C	-1.4589	-12.3045	14.0613
C	-0.8355	-11.0568	13.9686
C	-1.58	-9.8762	13.7372
C	-2.6423	-14.8566	13.1434
C	-3.4734	-13.7569	13.4622
C	-4.8088	-13.8007	13.0053
C	-5.2141	-14.7565	12.0698
C	-4.2979	-15.7037	11.5579
C	-3.0475	-15.8126	12.2074
C	-4.4908	-16.2733	10.1498
C	-3.4048	-16.8743	9.4725
C	-3.3493	-16.8944	8.076
C	-4.3773	-16.3163	7.2969
C	-5.5527	-15.9169	7.9731
C	-5.6091	-15.8967	9.3708
C	-2.81	-15.9933	5.2976

C	-4.0924	-15.8342	5.8717
C	-4.9853	-14.9527	5.2194
C	-4.5554	-14.1332	4.171
C	-3.2137	-14.1577	3.7283
C	-2.3806	-15.1735	4.2493
C	-3.3712	-11.7878	2.7852
C	-2.7517	-10.5569	2.5568
C	-1.3443	-10.4429	2.5227
C	-0.5985	-11.6429	2.5342
C	-1.2177	-12.8756	2.7636
C	-2.6105	-12.9615	2.9905
C	-0.659	-9.0939	2.7354
C	0.7481	-8.9938	2.8617
C	1.351	-7.8389	3.3765
C	0.5764	-6.7407	3.7973
C	-0.8128	-6.7954	3.5737
C	-1.4178	-7.9403	3.0486
C	3.1631	-4.3585	5.3626
C	2.5943	-5.3517	4.5486
C	1.2018	-5.6037	4.578
C	0.4081	-4.8158	5.446
C	0.985	-3.8473	6.2693
C	2.3661	-3.6219	6.2464
N	2.9502	-2.6177	7.0801
N	2.6168	-2.4115	8.2743
H	-0.435	-3.7148	11.4574
H	2.4305	-6.6352	10.0112
H	3.3764	-4.9737	8.5411
H	0.5703	-2.0493	9.9589
H	2.0337	-7.7151	11.7564
H	1.054	-9.5138	12.9088
H	-2.65	-7.2899	13.2749
H	-1.6338	-5.451	12.081
H	-3.6245	-9.1285	13.6391
H	-4.6847	-11.2338	13.7882
H	-0.8045	-13.1562	14.1048
H	0.2396	-11.063	13.9711
H	-1.6169	-14.9181	13.4599
H	-5.5145	-13.0175	13.2134
H	-6.191	-14.6108	11.6474
H	-2.295	-16.515	11.897
H	-2.5115	-17.19	9.9795
H	-2.4214	-17.2279	7.6491
H	-6.3875	-15.4736	7.4616
H	-6.4805	-15.4363	9.7993
H	-2.0656	-16.6412	5.7227

H	-5.9788	-14.7662	5.5835
H	-5.2609	-13.3994	3.8259
H	-1.3467	-15.2681	3.9716
H	-4.4354	-11.7575	2.9287
H	-3.3981	-9.6985	2.5343
H	0.4758	-11.651	2.5014
H	-0.562	-13.7184	2.8859
H	1.4018	-9.8212	2.653
H	2.4186	-7.8622	3.5306
H	-1.4582	-5.9767	3.8525
H	-2.4902	-7.9215	2.9875
H	4.2308	-4.1821	5.3215
H	3.251	-5.9149	3.9034
H	-0.6557	-4.9661	5.5351
H	0.351	-3.2697	6.9297

trans-azo[9]CPP B3LYP

C	-0.7029	-4.6515	11.0158
C	0.1647	-5.7018	11.4145
C	1.3914	-5.8285	10.7107
C	1.6983	-4.993	9.6305
C	0.8022	-3.9953	9.2186
C	-0.3833	-3.8161	9.9355
C	0.6009	-7.7953	12.8338
C	0.14	-8.8795	13.5879
C	-1.2114	-8.9735	13.9949
C	-2.0468	-7.8711	13.7011
C	-1.5835	-6.7853	12.9476
C	-0.2622	-6.7459	12.4471
C	-3.1883	-10.463	14.6514
C	-3.7655	-11.7358	14.6681
C	-2.97	-12.8945	14.5212
C	-1.5675	-12.73	14.5758
C	-0.9929	-11.4586	14.5597
C	-1.7938	-10.2972	14.4912
C	-2.713	-15.2242	13.5177
C	-3.5599	-14.1704	13.927
C	-4.8783	-14.1583	13.4211
C	-5.2413	-14.9898	12.3631
C	-4.2988	-15.8621	11.7756
C	-3.0765	-16.0565	12.4579
C	-4.4285	-16.2431	10.302
C	-3.3169	-16.7648	9.6023
C	-3.2142	-16.638	8.2151
C	-4.2181	-15.9864	7.4637
C	-5.4087	-15.6405	8.1418

C	-5.5131	-15.7672	9.5298
C	-2.6449	-15.6019	5.4767
C	-3.919	-15.4387	6.0674
C	-4.8124	-14.5471	5.4301
C	-4.4072	-13.7633	4.3448
C	-3.0883	-13.8307	3.8408
C	-2.2402	-14.8179	4.3912
C	-3.2941	-11.5844	2.6375
C	-2.6962	-10.4275	2.1356
C	-1.305	-10.3652	1.9031
C	-0.5697	-11.5628	2.0436
C	-1.1691	-12.723	2.5464
C	-2.5303	-12.7365	2.9308
C	-0.6085	-9.0131	1.8221
C	0.7749	-8.9177	2.0925
C	1.3435	-7.7122	2.5003
C	0.5518	-6.5562	2.655
C	-0.7799	-6.6038	2.1913
C	-1.3506	-7.8108	1.7806
C	2.6786	-4.661	5.2019
C	2.3586	-5.3916	4.0499
C	1.0225	-5.4492	3.5793
C	0.0593	-4.638	4.2274
C	0.3857	-3.9241	5.3775
C	1.682	-3.98	5.9068
N	1.9475	-3.549	7.2372
N	0.9964	-3.2719	8.0042
H	-1.6562	-4.4891	11.4864
H	2.0995	-6.6073	10.9282
H	2.6143	-5.1686	9.08
H	-1.0959	-3.0658	9.6166
H	1.6236	-7.8418	12.5057
H	0.847	-9.6702	13.758
H	-3.0895	-7.8584	13.9612
H	-2.3093	-6.0322	12.6986
H	-3.8726	-9.6348	14.6257
H	-4.8398	-11.7671	14.6464
H	-0.883	-13.5512	14.4693
H	0.0764	-11.4279	14.4604
H	-1.7011	-15.3224	13.8677
H	-5.5939	-13.4005	13.6818
H	-6.2004	-14.7892	11.9227
H	-2.3084	-16.7147	12.0948
H	-2.4445	-17.142	10.1031
H	-2.2774	-16.9392	7.7841
H	-6.2276	-15.1482	7.6499

H	-6.3992	-15.3518	9.9734
H	-1.8978	-16.251	5.8949
H	-5.7974	-14.351	5.812
H	-5.1205	-13.0428	3.9884
H	-1.2187	-14.9344	4.0779
H	-4.3326	-11.5001	2.899
H	-3.3293	-9.561	2.0697
H	0.4932	-11.6028	1.88
H	-0.5152	-13.5573	2.7247
H	1.4121	-9.7813	2.1529
H	2.3635	-7.7585	2.8413
H	-1.4368	-5.7521	2.2577
H	-2.4044	-7.7936	1.5639
H	3.6812	-4.7235	5.6063
H	3.1439	-5.9843	3.6099
H	-0.9808	-4.6459	3.9529
H	-0.4065	-3.4144	5.9116

cis-azo[9]CPP M062X

C	-6.19568	2.94218	1.41083
C	-5.31939	2.87088	0.3141
C	-5.61512	2.01933	-0.75655
C	-6.74006	1.19272	-0.7132
C	-7.61174	1.24428	0.37873
C	-7.35383	2.13515	1.43652
C	-3.29902	3.69395	-0.95811
C	-2.03461	4.278	-1.02504
C	-1.45267	4.81776	0.12429
C	-2.2168	4.96042	1.29614
C	-3.51242	4.40066	1.35401
C	-4.01031	3.68848	0.24633
C	0.77828	5.52804	1.20536
C	2.14248	5.48137	1.16404
C	2.78157	5.10379	-0.03073
C	2.0735	5.0966	-1.23111
C	0.68429	5.11897	-1.18582
C	0.04378	5.18402	0.05538
C	4.81333	4.26379	-1.28219
C	4.23527	4.60667	-0.05372
C	4.95241	4.41959	1.13584
C	6.01292	3.50203	1.12743
C	6.29831	2.83323	-0.07122
C	5.87866	3.36432	-1.29076
C	6.97592	1.45901	-0.05829
C	7.22606	0.79301	-1.26545
C	7.26361	-0.60365	-1.24538

C	7.03362	-1.23829	-0.02144
C	7.27194	-0.56181	1.18167
C	7.24868	0.83425	1.16174
C	6.14036	-3.33177	-1.1809
C	6.41341	-2.63874	0.00746
C	6.03038	-3.17271	1.23828
C	4.99819	-4.10899	1.25275
C	4.41783	-4.48479	0.03512
C	5.11472	-4.28862	-1.16555
C	2.27617	-5.00573	1.23797
C	0.88392	-5.06442	1.20884
C	0.22291	-5.18312	-0.01873
C	0.94402	-5.54521	-1.16864
C	2.34951	-5.45747	-1.14462
C	2.98064	-5.02699	0.03357
C	-1.28265	-4.85442	-0.07634
C	-2.05679	-5.05445	-1.23253
C	-3.36572	-4.529	-1.29271
C	-3.87007	-3.79535	-0.20276
C	-3.144	-3.7411	0.99197
C	-1.86381	-4.29086	1.06195
C	-7.27383	-2.38094	-1.40088
C	-6.08732	-3.14637	-1.36791
C	-5.2042	-3.01904	-0.28106
C	-5.51665	-2.1486	0.76918
C	-6.67179	-1.36497	0.71882
C	-7.55442	-1.47626	-0.35988
N	-8.7683	-0.636	-0.36253
N	-8.78931	0.35576	0.3789
H	-5.98544	3.60516	2.2242
H	-4.97072	1.99498	-1.60984
H	-6.93718	0.51938	-1.52133
H	-8.03251	2.19761	2.26127
H	-3.72347	3.2408	-1.8294
H	-1.50197	4.29556	-1.95271
H	-1.81522	5.47839	2.14149
H	-4.10448	4.50462	2.23918
H	0.27458	5.79751	2.10987
H	2.71743	5.70457	2.03825
H	2.58746	5.04402	-2.16786
H	0.11249	5.0652	-2.08899
H	4.42501	4.65792	-2.19795
H	4.67728	4.93418	2.03274
H	6.56516	3.29209	2.01953
H	6.33478	3.06097	-2.20973
H	7.34569	1.3342	-2.18069

H	7.42105	-1.16624	-2.1419
H	7.42821	-1.09685	2.09503
H	7.39313	1.40302	2.05673
H	6.67405	-3.11228	-2.08223
H	6.48808	-2.84411	2.1482
H	4.63528	-4.5063	2.17768
H	4.8488	-4.82484	-2.05263
H	2.79536	-4.91412	2.16914
H	0.32375	-4.99776	2.11808
H	0.43343	-5.85676	-2.05583
H	2.92419	-5.69008	-2.01679
H	-1.6525	-5.59022	-2.06538
H	-3.96442	-4.6749	-2.16738
H	-3.56864	-3.26863	1.85319
H	-1.31908	-4.26358	1.98256
H	-7.95689	-2.48601	-2.21765
H	-5.86059	-3.821	-2.1674
H	-4.86276	-2.07711	1.61262
H	-6.88438	-0.67892	1.51132

trans-azo[9]CPP M062X

C	1.47015	6.69149	1.30538
C	2.10817	6.21444	0.15187
C	1.34749	6.107	-1.025
C	-0.02396	6.29764	-1.01334
C	-0.67119	6.60051	0.1907
C	0.09286	6.86861	1.32933
C	4.25643	5.4004	-0.91763
C	5.24113	4.42093	-0.96093
C	5.43916	3.54914	0.11948
C	4.7353	3.81287	1.30029
C	3.75129	4.79002	1.34325
C	3.43255	5.54544	0.20793
C	6.67071	1.54601	1.05752
C	6.85754	0.16962	1.01722
C	6.4798	-0.57598	-0.10862
C	6.08342	0.13289	-1.24924
C	5.89868	1.50782	-1.20983
C	6.10159	2.22839	-0.02721
C	6.19104	-2.8448	-1.1884
C	6.19053	-2.03153	-0.04589
C	5.61075	-2.55188	1.11751
C	4.89854	-3.74381	1.0906
C	4.73599	-4.45677	-0.10269
C	5.47439	-4.03419	-1.21714
C	3.58353	-5.38501	-0.22315

C	2.75155	-5.247	-1.33997
C	1.44983	-5.72346	-1.32568
C	0.81444	-6.07755	0.05597
C	1.81614	-6.66768	0.84166
C	3.11718	-6.17664	0.83508
C	-1.41179	-6.35037	-1.14763
C	-0.55241	-6.44505	-0.04443
C	-1.13441	-6.31509	1.22396
C	-2.45594	-5.9169	1.37289
C	-3.24372	-5.59228	0.25992
C	-2.72139	-5.91461	-1.00026
C	-4.46563	-3.77708	1.44084
C	-5.26653	-2.64633	1.38902
C	-6.04074	-2.36248	0.25851
C	-6.11937	-3.34706	-0.73531
C	-5.33002	-4.48992	-0.67302
C	-4.41457	-4.68281	0.37301
C	-6.46109	-0.95498	0.0448
C	-6.16803	-0.35451	-1.18475
C	-6.08644	1.02627	-1.30233
C	-6.30513	1.86015	-0.19838
C	-6.78409	1.26302	0.97731
C	-6.85524	-0.11892	1.09873
C	-4.65369	4.98767	-1.49258
C	-5.57617	3.95197	-1.41439
C	-5.74909	3.23739	-0.22031
C	-5.11025	3.72319	0.9335
C	-4.20492	4.76814	0.86829
C	-3.90926	5.35389	-0.36839
N	-2.70289	6.06604	-0.6149
N	-2.05403	6.35416	0.4128
H	2.04463	6.84059	2.21493
H	1.81943	5.73838	-1.93068
H	-0.62261	6.08772	-1.89252
H	-0.42149	7.12286	2.25101
H	4.08416	6.0208	-1.79296
H	5.82186	4.28861	-1.86984
H	4.85973	3.15419	2.15445
H	3.13113	4.8692	2.23067
H	6.90845	2.0899	1.96783
H	7.23937	-0.34221	1.89647
H	5.77912	-0.41168	-2.13786
H	5.45556	2.0037	-2.06829
H	6.69862	-2.5064	-2.08767
H	5.59122	-1.94909	2.02051
H	4.3405	-4.0459	1.97214

H	5.42689	-4.60778	-2.139
H	3.07835	-4.63517	-2.17537
H	0.79828	-5.46412	-2.15313
H	1.56401	-7.4803	1.51704
H	3.65199	-6.07056	1.77534
H	-1.02917	-6.52602	-2.14841
H	-0.51941	-6.41484	2.11299
H	-2.84564	-5.76616	2.37493
H	-3.30512	-5.71693	-1.89388
H	-3.77282	-3.87837	2.26917
H	-5.18036	-1.90264	2.17573
H	-6.76095	-3.18743	-1.59803
H	-5.38114	-5.20871	-1.48574
H	-5.85815	-0.97576	-2.02003
H	-5.71091	1.44952	-2.22867
H	-7.0393	1.88471	1.83098
H	-7.15536	-0.55828	2.04635
H	-4.42923	5.46393	-2.44206
H	-6.10311	3.63865	-2.31082
H	-5.22407	3.18754	1.87074
H	-3.62171	5.05365	1.73637

fullerene C_{60} M062X

C	1.72662	3.12582	-0.93886
C	0.71135	3.62145	0.10758
C	0.87191	3.27871	1.4568
C	2.98762	1.95535	0.94088
C	2.81114	2.33203	-0.54188
C	-0.68818	3.58813	-0.53407
C	-0.35117	2.8687	2.29792
C	3.51647	0.51046	1.00525
C	3.23087	1.11997	-1.39404
C	0.95457	2.78616	-2.2273
C	3.07374	-0.35332	2.01612
C	2.05835	0.14242	3.06257
C	-1.80122	3.21503	0.23129
C	0.08463	1.74298	3.25414
C	-1.62481	2.83838	1.71405
C	3.66679	-0.00586	-0.43786
C	2.52828	0.8108	-2.56652
C	1.33649	1.68316	-3.00276
C	-0.53786	3.07187	-1.97711
C	2.19199	-0.65477	-2.89878
C	0.26365	0.75676	-3.60468
C	-1.51416	2.22892	-2.52492
C	3.36077	-1.33952	-0.74022

C	-2.58867	1.67926	2.02864
C	0.79238	-0.68817	-3.54037
C	-1.09448	1.01677	-3.37701
C	-2.73734	1.81888	-1.68386
C	-3.07363	0.35331	-2.01613
C	-2.52839	-0.81079	2.56654
C	-2.05826	-0.14243	-3.06254
C	-1.57709	-1.45728	-3.00394
C	-2.06363	-2.40642	-1.89313
C	-0.08466	-1.743	-3.25411
C	2.87419	-2.28875	0.37063
C	-3.23095	-1.11993	1.39402
C	2.58858	-1.67925	-2.02867
C	1.62477	-2.83837	-1.71408
C	-3.6668	0.00588	0.4378
C	-1.33657	-1.68318	3.0028
C	-0.95459	-2.78614	2.22733
C	-3.5164	-0.51048	-1.0053
C	-2.98759	-1.95535	-0.94092
C	0.35116	-2.86871	-2.29791
C	-0.87191	-3.27872	-1.4568
C	-2.81117	-2.332	0.54185
C	1.80126	-3.21502	-0.23133
C	0.53789	-3.07186	1.97713
C	-1.72663	-3.12581	0.93887
C	0.68819	-3.58813	0.53408
C	-0.71135	-3.62145	-0.10757
C	-2.1921	0.6548	2.89881
C	-0.79245	0.68819	3.54042
C	-0.26371	-0.75676	3.60476
C	-2.87412	2.28876	-0.37068
C	-3.36078	1.33953	0.74016
C	2.06364	2.40641	1.89313
C	1.57711	1.45725	3.00395
C	1.09456	-1.0168	3.37706
C	2.73745	-1.81892	1.68384
C	1.51424	-2.22897	2.52494

C_{60}@trans-azo[9]CPP M062X

C	2.58207	-6.04082	-2.11364
C	3.18564	-5.69884	-0.89238
C	2.4628	-5.98188	0.28109
C	1.13774	-6.40106	0.23466
C	0.48906	-6.5234	-1.00102
C	1.25036	-6.42563	-2.16918
C	4.59082	-3.94407	-1.94352

C	5.40173	-2.82588	-1.83599
C	6.06591	-2.51278	-0.64231
C	5.97312	-3.4522	0.39616
C	5.15334	-4.5754	0.28804
C	4.38361	-4.81129	-0.86145
C	6.9319	-0.33949	-1.58108
C	6.88721	1.04727	-1.53195
C	6.46036	1.72581	-0.37857
C	6.32194	0.94751	0.78102
C	6.38061	-0.44152	0.73559
C	6.56419	-1.12026	-0.47528
C	5.52074	3.65122	-1.68943
C	5.89065	3.10383	-0.45063
C	5.42143	3.7804	0.68422
C	4.46297	4.78489	0.58762
C	3.94903	5.194	-0.65093
C	4.59179	4.67701	-1.78652
C	2.64013	5.89936	-0.75494
C	2.0158	6.53317	0.33221
C	0.64987	6.80619	0.32968
C	-0.16088	6.46758	-0.76508
C	0.49521	5.98478	-1.90526
C	1.85426	5.7086	-1.89945
C	-2.42612	6.26163	-1.85449
C	-1.6415	6.32465	-0.69181
C	-2.26185	5.9502	0.5076
C	-3.50701	5.32798	0.50998
C	-4.18477	5.05445	-0.68661
C	-3.66781	5.64276	-1.85134
C	-5.9127	3.49947	0.35896
C	-6.51633	2.24515	0.36314
C	-6.426	1.38584	-0.74406
C	-5.84839	1.91567	-1.90471
C	-5.24893	3.16708	-1.91015
C	-5.19332	3.96016	-0.75502
C	-6.6157	-0.08804	-0.6475
C	-6.73212	-0.90299	-1.78557
C	-6.42384	-2.25691	-1.7395
C	-5.99181	-2.86842	-0.55094
C	-6.10339	-2.10164	0.61706
C	-6.39548	-0.74339	0.57016
C	-3.74302	-5.64025	0.70045
C	-4.84769	-4.79801	0.635
C	-5.16844	-4.11268	-0.54926
C	-4.44138	-4.46005	-1.70302
C	-3.35297	-5.31933	-1.65098

C	-2.93958	-5.85039	-0.42421
N	-1.61445	-6.32972	-0.17951
N	-0.91729	-6.45151	-1.2101
C	1.55014	2.38165	2.70889
C	2.0719	2.69169	1.3928
C	1.23828	3.22388	0.42199
C	-0.66097	3.17292	1.98107
C	0.21204	2.61492	2.99635
C	3.03617	1.66866	1.03505
C	1.33018	2.75823	-0.95079
C	-1.96183	2.53821	2.11051
C	-0.54638	1.63736	3.75485
C	2.18978	1.1617	3.1661
C	-2.69913	2.23163	0.97597
C	-2.16941	2.544	-0.34094
C	3.12286	1.22346	-0.27603
C	-0.01198	2.71088	-1.49888
C	2.25302	1.78508	-1.29462
C	-1.89012	1.59141	3.20788
C	0.06583	0.47057	4.19195
C	1.46485	0.22705	3.89062
C	3.10879	0.72334	2.13042
C	-0.63794	-0.79553	4.10414
C	1.62637	-1.18929	3.61563
C	3.2604	-0.63085	1.86637
C	-2.56217	0.38029	3.12249
C	1.87462	0.71421	-2.20111
C	0.32661	-1.82155	3.74841
C	2.5061	-1.60898	2.62738
C	3.34302	-1.09466	0.49549
C	2.645	-2.35913	0.40702
C	-0.115	-0.59739	-2.81741
C	2.12715	-2.67973	1.72344
C	0.88327	-3.28132	1.84826
C	0.10934	-3.58576	0.66203
C	-0.03605	-2.84469	2.88453
C	-3.33598	0.06259	1.93666
C	0.49692	-1.76367	-2.37936
C	-1.92228	-0.83912	3.58101
C	-2.30025	-1.91093	2.67711
C	1.83894	-1.71559	-1.82868
C	-1.51512	-0.3555	-2.51504
C	-2.24193	-1.28842	-1.78936
C	1.9025	-2.65647	-0.72602
C	0.60731	-3.28487	-0.59676
C	-1.37971	-2.89235	2.33764

C	-1.28479	-3.34829	0.96508
C	-0.26304	-2.73903	-1.61876
C	-3.1682	-1.35188	1.66137
C	-3.15982	-0.85014	-0.7517
C	-1.59723	-2.50293	-1.32678
C	-3.07041	-1.78977	0.34941
C	-2.11025	-2.80593	-0.00621
C	0.59014	0.66831	-2.72585
C	-0.3748	1.69231	-2.36706
C	-1.67464	1.06045	-2.23648
C	3.28368	-0.18811	-0.55381
C	2.51282	-0.50525	-1.74174
C	-0.15694	3.46501	0.72162
C	-0.93045	3.14793	-0.46572
C	-2.54857	1.47587	-1.24288
C	-3.40414	0.96817	0.88663
C	-3.30802	0.49993	-0.48477
H	3.13211	-5.92378	-3.04172
H	2.89677	-5.74525	1.24872
H	0.55712	-6.49179	1.14739
H	0.75102	-6.56136	-3.1236
H	3.9986	-4.0536	-2.8458
H	5.41019	-2.11592	-2.65726
H	6.50905	-3.28071	1.32613
H	5.07266	-5.24617	1.13924
H	7.18577	-0.82333	-2.52013
H	7.11757	1.59948	-2.43718
H	6.02893	1.41079	1.71766
H	6.12343	-0.99924	1.63199
H	5.88182	3.20973	-2.6119
H	5.71911	3.45418	1.67615
H	4.02989	5.16666	1.50758
H	4.3069	5.01969	-2.77609
H	2.58994	6.76927	1.22347
H	0.20082	7.2417	1.21836
H	-0.08415	5.68735	-2.77368
H	2.27197	5.20762	-2.76609
H	-2.03089	6.64179	-2.79212
H	-1.70406	5.99874	1.43856
H	-3.87557	4.91435	1.44414
H	-4.21266	5.55564	-2.7869
H	-5.95525	4.10495	1.26031
H	-7.01181	1.90687	1.26901
H	-5.73035	1.28699	-2.78204
H	-4.6917	3.46247	-2.79344
H	-7.00097	-0.46077	-2.74056

H	-6.45855	-2.82989	-2.66144
H	-5.8006	-2.52148	1.5706
H	-6.30904	-0.16774	1.48716
H	-3.42638	-6.06201	1.65002
H	-5.41423	-4.60918	1.54179
H	-4.64574	-3.95086	-2.63967
H	-2.73209	-5.47422	-2.52671

fused azo[11]CPP

C	-5.67711	-4.95885	-0.16877
C	-4.46086	-5.63963	-0.13375
C	-3.33728	-5.09272	0.51026
C	-3.50376	-3.85284	1.15407
C	-4.71468	-3.17606	1.12193
C	-5.82401	-3.69859	0.43606
H	-6.51303	-5.3958	-0.70854
H	-4.38261	-6.60742	-0.62176
H	-2.65703	-3.39019	1.65117
H	-4.8025	-2.22246	1.6343
C	-1.98796	-5.70714	0.45984
C	-1.06797	-5.50431	1.50297
C	-1.52251	-6.38778	-0.67898
C	0.27183	-5.83862	1.35988
H	-1.39714	-5.03676	2.42636
C	-0.18133	-6.73829	-0.81524
H	-2.20302	-6.58265	-1.50338
C	0.76577	-6.41145	0.17289
H	0.95871	-5.57508	2.15749
H	0.13917	-7.23011	-1.72925
C	2.23042	-6.45313	-0.06909
C	2.74806	-6.30144	-1.36877
C	3.15913	-6.41885	0.98751
C	4.078	-5.95827	-1.58364
H	2.08237	-6.3544	-2.22481
C	4.4832	-6.05018	0.77501
H	2.82892	-6.61071	2.00417
C	4.9545	-5.72015	-0.50891
H	4.41702	-5.79569	-2.60263
H	5.13112	-5.91699	1.63639
C	6.18454	-4.90441	-0.67046
C	7.22733	-4.87579	0.27558
C	6.21282	-3.91772	-1.67203
C	8.13211	-3.81706	0.32388
H	7.30004	-5.66242	1.02196
C	7.11405	-2.86405	-1.62463
H	5.43326	-3.8941	-2.42634

C	8.03818	-2.73485	-0.57196
H	8.88425	-3.80465	1.1084
H	7.00153	-2.05776	-2.34183
C	8.73042	0.93314	-1.02354
C	8.61015	1.39109	0.30178
C	8.7429	0.42621	1.3177
C	8.73055	-0.93306	1.02351
C	8.61016	-1.39101	-0.30179
C	8.74278	-0.42613	-1.31772
H	8.68426	1.64293	-1.84436
H	8.74996	0.73632	2.35886
H	8.6845	-1.64286	1.84434
H	8.74974	-0.73625	-2.35889
C	8.03816	2.73491	0.57201
C	7.114	2.86405	1.62465
C	8.1321	3.81716	-0.32378
C	6.21275	3.91771	1.67208
H	7.00146	2.05773	2.34182
C	7.22731	4.87588	-0.27546
H	8.88427	3.80481	-1.10827
C	6.18448	4.90444	0.67055
H	5.43315	3.89403	2.42635
H	7.30002	5.66255	-1.02179
C	4.95443	5.72016	0.50898
C	4.48318	6.05023	-0.77495
C	4.07789	5.95827	1.58369
C	3.15912	6.41889	-0.9875
H	5.13113	5.91706	-1.63631
C	2.74795	6.30143	1.36876
H	4.41687	5.79569	2.60268
C	2.23036	6.45312	0.06907
H	2.82895	6.61076	-2.00417
H	2.08223	6.35438	2.22478
C	-1.988	5.70709	-0.45998
C	-1.5226	6.38785	0.67879
C	-0.18142	6.73836	0.81509
C	0.76572	6.41143	-0.17298
C	0.27182	5.8385	-1.35994
C	-1.06797	5.50418	-1.50306
H	-2.20315	6.5828	1.50314
H	0.13903	7.23026	1.72906
H	0.95873	5.57489	-2.1575
H	-1.3971	5.03655	-2.42643
C	-3.33732	5.09269	-0.51041
C	-3.50377	3.85269	-1.15399
C	-4.46093	5.6397	0.13347

C	-4.71469	3.17592	-1.1218
H	-2.657	3.38994	-1.65093
C	-5.67718	4.95893	0.16854
H	-4.38269	6.60756	0.62134
C	-5.82407	3.69859	-0.4361
H	-4.80248	2.22222	-1.63399
H	-6.51312	5.39597	0.70822
C	-7.0711	2.90226	-0.32692
C	-8.35577	3.50723	-0.37206
C	-6.99156	1.51982	-0.17312
C	-9.49964	2.74228	-0.28202
H	-8.43241	4.58213	-0.50787
C	-8.14373	0.71698	-0.08052
H	-6.01281	1.05874	-0.09814
C	-9.41558	1.33845	-0.13971
H	-10.48897	3.18678	-0.32877
C	-8.14371	-0.71701	0.08061
C	-9.41556	-1.33849	0.13984
C	-9.49959	-2.74232	0.28213
C	-8.35571	-3.50726	0.37212
C	-7.07105	-2.90227	0.32696
C	-6.99154	-1.51983	0.17316
H	-10.48892	-3.18684	0.3289
H	-6.01279	-1.05874	0.09815
H	-8.43233	-4.58217	0.5079
N	-10.61278	0.63965	-0.06518
N	-10.61277	-0.63971	0.06536

fused azo[9]CPP

C	-1.4226	7.2915	-0.134
C	-0.6935	7.3903	-1.3415
C	0.7024	7.3914	-1.3349
C	1.4173	7.2921	-0.1218
C	0.688	7.4456	1.08
C	-0.708	7.4459	1.0733
C	-2.8028	6.6395	-0.1388
C	2.7981	6.6412	-0.0889
C	-3.4276	6.2857	-1.3562
C	-4.3379	5.2269	-1.4081
C	-4.6588	4.4919	-0.2464
C	-4.208	4.9867	0.9913
C	-3.2963	6.0419	1.0466
C	3.2975	6.002	-1.2501
C	4.209	4.9496	-1.1529
C	4.6538	4.4991	0.1037
C	4.3277	5.2751	1.2369

C	3.4177	6.3311	1.1431
C	-5.1436	3.057	-0.3351
C	5.1377	3.0682	0.246
C	-5.5148	2.3102	0.8122
C	-5.53	0.9031	0.7802
C	-5.1489	0.2182	-0.3875
C	-4.9176	0.9628	-1.5562
C	-4.925	2.3501	-1.5365
C	4.9139	2.405	1.4713
C	4.9057	1.0193	1.5408
C	5.1413	0.233	0.4006
C	5.5275	0.8754	-0.7894
C	5.5132	2.2805	-0.8721
C	-4.7624	-1.2333	-0.3373
C	4.7542	-1.2193	0.401
C	-5.3086	-2.1686	0.5724
C	-4.7594	-3.4699	0.6782
C	-3.6211	-3.8205	-0.0773
C	-3.1092	-2.8897	-0.9907
C	-3.673	-1.6376	-1.1312
C	3.6625	-1.595	1.2058
C	3.0987	-2.8512	1.1082
C	3.6126	-3.8138	0.2296
C	4.7531	-3.4904	-0.5348
C	5.3025	-2.1864	-0.4735
C	-2.8911	-5.1165	0.0813
C	2.8828	-5.1147	0.1149
C	-3.543	-6.3472	0.2427
C	-2.7931	-7.5366	0.2841
C	-1.3881	-7.5023	0.2031
C	-0.7156	-6.2691	0.125
C	-1.484	-5.0907	0.0481
C	1.4756	-5.0885	0.1467
C	0.7077	-6.2691	0.1097
C	1.3807	-7.5039	0.0736
C	2.7857	-7.5404	-0.0058
C	3.5351	-6.3501	-0.0044
N	-0.6706	-8.6588	0.2024
N	0.6636	-8.66	0.1135
H	-1.1538	7.2824	-2.3067
H	1.1798	7.2982	-2.2941
H	1.1483	7.3827	2.0492
H	-1.1865	7.3969	2.0355
H	-3.1216	6.6977	-2.3016
H	-4.6661	4.9139	-2.3864
H	-4.3997	4.4667	1.9158

H	-2.873	6.2378	2.0145
H	2.8796	6.1636	-2.2265
H	4.4052	4.3971	-2.0575
H	4.6514	4.9973	2.2272
H	3.1076	6.7757	2.0721
H	-5.687	2.7888	1.7637
H	-5.7005	0.3665	1.7042
H	-4.6345	0.4774	-2.48
H	-4.6117	2.8359	-2.4444
H	4.5972	2.9231	2.3598
H	4.6187	0.5677	2.4804
H	5.7015	0.3059	-1.6928
H	5.6895	2.7244	-1.8394
H	-6.1349	-1.8908	1.2131
H	-5.1724	-4.1661	1.3969
H	-2.2457	-3.127	-1.5996
H	-3.186	-0.9592	-1.8159
H	3.1739	-0.8927	1.8648
H	2.2337	-3.0664	1.723
H	5.1678	-4.2116	-1.2272
H	6.1307	-1.9317	-1.1214
H	-4.6238	-6.394	0.281
H	-3.3065	-8.4868	0.3637
H	-1.0105	-4.1325	-0.0425
H	1.0016	-4.1281	0.2044
H	3.2995	-8.4926	-0.0531
H	4.616	-6.3978	-0.0409

azo[9]CPP macrocycle

C	-3.30594	-5.03131	0.42633
C	-2.54816	-5.29881	-0.8596
C	-1.28777	-5.72783	-0.90507
C	-0.456	-6.02562	0.32588
C	-1.10777	-5.44896	1.56815
C	-2.3614	-4.99838	1.61024
C	-4.13229	-3.74182	0.28298
C	0.98371	-5.49994	0.1891
C	-5.31926	-3.78069	-0.46322
C	-6.10415	-2.64353	-0.62364
C	-5.73742	-1.42662	-0.03212
C	-4.54199	-1.37934	0.69288
C	-3.74751	-2.51983	0.84393
C	1.29884	-4.37382	-0.5784
C	2.62049	-3.93645	-0.70186
C	3.66474	-4.61269	-0.06236
C	3.34149	-5.71677	0.73921

C	2.02537	-6.15089	0.86467
C	-6.61899	-0.18268	-0.24167
C	5.13872	-4.18321	-0.18434
C	-6.54799	0.77394	0.93135
C	-6.35321	2.08805	0.8086
C	-6.12422	2.7947	-0.51134
C	-5.99778	1.80754	-1.65204
C	-6.22314	0.49906	-1.53658
C	5.54836	-3.39579	1.04213
C	6.1849	-2.22736	1.00697
C	6.57841	-1.50696	-0.26545
C	6.03639	-2.22174	-1.48533
C	5.40127	-3.39419	-1.44902
O	5.99025	-5.35444	-0.12255
O	-7.99138	-0.58492	-0.48928
O	-4.20685	-6.16592	0.51582
C	-4.9529	-6.28515	1.71818
O	-0.42578	-7.4484	0.60291
C	-0.08313	-8.29799	-0.48246
C	-4.86248	3.66172	-0.41099
C	6.08193	-0.05101	-0.19092
C	-4.9104	5.05046	-0.56646
C	-3.75234	5.8172	-0.44628
C	-2.51226	5.22644	-0.16003
C	-2.47254	3.82889	-0.01196
C	-3.62595	3.0612	-0.13954
C	4.82439	0.32822	-0.67425
C	4.37474	1.64091	-0.54824
C	5.16752	2.62264	0.06833
C	6.42582	2.23481	0.55759
C	6.87283	0.92285	0.4329
O	-7.20656	3.70552	-0.78927
O	8.02403	-1.53216	-0.23927
C	8.69364	-1.10628	-1.41737
C	5.94102	-6.24064	-1.23097
C	-8.71494	-1.10709	0.61685
C	-8.51394	3.14635	-0.80578
C	-1.28711	6.0474	-0.00968
C	4.69045	4.02018	0.20601
C	-1.03669	7.14903	-0.84637
C	0.10992	7.92069	-0.69869
C	1.06703	7.60112	0.27832
C	0.8098	6.52242	1.14362
C	-0.34383	5.7622	0.9928
C	3.92303	4.62776	-0.80352
C	3.44567	5.92791	-0.66732

C	3.75454	6.64198	0.48802
C	4.54962	6.08821	1.48825
C	4.99528	4.77813	1.35125
N	2.15282	8.49029	0.40863
N	3.33108	8.04528	0.64806
H	-3.11475	-5.15419	-1.77631
H	-0.81948	-5.91641	-1.86852
H	-0.49378	-5.45944	2.46558
H	-2.76458	-4.62532	2.54907
H	-5.63599	-4.72314	-0.89944
H	-7.02425	-2.69488	-1.19688
H	-4.22727	-0.44658	1.15385
H	-2.82293	-2.45154	1.41057
H	0.50899	-3.83561	-1.09594
H	2.83481	-3.06485	-1.31435
H	4.13932	-6.25351	1.24317
H	1.79644	-7.02234	1.46956
H	-6.69409	0.3414	1.91893
H	-6.3578	2.73175	1.68605
H	-5.74986	2.24479	-2.61665
H	-6.16367	-0.15528	-2.40312
H	5.32563	-3.87332	1.99302
H	6.48869	-1.73508	1.92743
H	6.1878	-1.72637	-2.44221
H	5.04904	-3.83719	-2.37827
H	-5.66711	-7.09536	1.54883
H	-4.31466	-6.55128	2.57111
H	-5.50837	-5.36719	1.95671
H	0.86749	-8.01059	-0.95374
H	-0.87116	-8.32162	-1.24635
H	0.02363	-9.29929	-0.05673
H	-5.8611	5.52803	-0.76811
H	-3.8192	6.89753	-0.54325
H	-1.52248	3.33831	0.18237
H	-3.56543	1.98096	-0.03484
H	4.18202	-0.41263	-1.14199
H	3.38318	1.90011	-0.90905
H	7.07486	2.97551	1.01654
H	7.85189	0.64433	0.80865
H	9.75034	-1.02508	-1.14921
H	8.3419	-0.126	-1.76871
H	8.59411	-1.83585	-2.23215
H	6.5072	-7.1267	-0.9317
H	6.41355	-5.80931	-2.12391
H	4.91436	-6.54382	-1.47884
H	-9.64708	-1.50367	0.20551

H	-8.95824	-0.32891	1.35252
H	-8.17643	-1.92093	1.12131
H	-8.85912	2.88546	0.20336
H	-9.16353	3.92378	-1.2163
H	-8.57389	2.24997	-1.43435
H	-1.74376	7.39279	-1.63424
H	0.29219	8.77452	-1.34414
H	1.50032	6.29641	1.94918
H	-0.536	4.94997	1.68825
H	3.71293	4.08223	-1.7183
H	2.85177	6.38115	-1.45287
H	4.80216	6.68236	2.35934
H	5.57431	4.32994	2.15273

azoxy[9]CPP macrocycle

C	-1.8261	7.2757	0.4463
C	-0.9236	6.9752	1.6194
C	0.4135	6.9132	1.5384
C	1.205	7.1101	0.2409
C	0.2729	7.1537	-0.9588
C	-1.0603	7.2291	-0.8731
C	-2.9651	6.2455	0.4204
C	2.2773	6.0267	-0.0021
C	-4.2902	6.6541	0.654
C	-5.3373	5.7465	0.6156
C	-5.1128	4.3832	0.3434
C	-3.7856	3.9549	0.1309
C	-2.7215	4.8781	0.1671
C	2.5433	4.9805	0.9111
C	3.6323	4.1175	0.7117
C	4.4677	4.2646	-0.4156
C	4.1615	5.2699	-1.3488
C	3.0977	6.1407	-1.14
C	-6.2967	3.402	0.317
C	5.7514	3.4435	-0.6299
C	-6.3373	2.5897	-0.9869
C	-6.5468	1.263	-1.0221
C	-6.7241	0.4306	0.2378
C	-6.3575	1.1828	1.5015
C	-6.1629	2.507	1.531
C	5.5408	2.5686	-1.8488
C	5.8348	1.2606	-1.8917
C	6.4328	0.4843	-0.7381
C	6.4614	1.3152	0.5434
C	6.1551	2.6162	0.5896
O	6.8186	4.3271	-0.9777

O	-7.5314	4.0966	0.5247
O	-2.3319	8.5877	0.7234
C	-2.8183	9.2988	-0.4017
O	1.8522	8.3831	0.2535
C	2.693	8.5974	1.3747
C	-5.8038	-0.791	0.1546
C	5.5762	-0.7669	-0.5222
C	-6.32	-2.0861	0.3708
C	-5.493	-3.2032	0.3348
C	-4.123	-3.0774	0.0515
C	-3.6025	-1.7864	-0.1897
C	-4.4299	-0.6559	-0.1201
C	4.2601	-0.6595	-0.0421
C	3.474	-1.8022	0.1501
C	3.9774	-3.0908	-0.1503
C	5.2984	-3.1849	-0.6344
C	6.0811	-2.0478	-0.8121
O	-8.0709	-0.0377	0.335
O	7.7483	0.1377	-1.1825
C	8.6468	-0.2314	-0.1512
C	7.2233	5.1954	0.0665
C	-8.068	4.7124	-0.6349
C	-9.0389	0.9953	0.3769
C	-3.2411	-4.2894	0.0347
C	3.1178	-4.3234	-0.0021
C	-3.5638	-5.423	0.8127
C	-2.7177	-6.5321	0.8444
C	-1.539	-6.5499	0.0982
C	-1.2439	-5.4523	-0.737
C	-2.0699	-4.325	-0.746
C	1.943	-4.308	0.7795
C	1.1168	-5.432	0.8547
C	1.4188	-6.6006	0.1246
C	2.6167	-6.6404	-0.5993
C	3.4509	-5.5253	-0.6682
N	-0.7007	-7.7079	0.1778
N	0.5568	-7.7553	0.1092
O	1.1207	-8.9397	-0.0068
H	-1.3802	6.8818	2.6016
H	0.9616	6.7755	2.466
H	0.7035	7.2012	-1.9536
H	-1.6211	7.3177	-1.7998
H	-4.5326	7.6836	0.8734
H	-6.329	6.1265	0.8122
H	-3.5772	2.9115	-0.0682
H	-1.7107	4.5312	-0.0078

H	1.9494	4.8505	1.8034
H	3.8305	3.3574	1.4546
H	4.7894	5.4177	-2.2188
H	2.9407	6.9382	-1.8542
H	-6.2762	3.1196	-1.9334
H	-6.6417	0.7747	-1.9881
H	-6.3176	0.6332	2.4382
H	-5.9809	2.9736	2.4959
H	5.1767	3.0331	-2.7614
H	5.6893	0.7369	-2.8333
H	6.7795	0.8378	1.4661
H	6.2531	3.122	1.5462
H	-3.4741	10.1165	-0.0383
H	-1.9781	9.7646	-0.9593
H	-3.445	8.6675	-1.0682
H	3.3248	7.7186	1.6247
H	2.0966	8.9227	2.2532
H	3.3955	9.4196	1.1284
H	-7.3667	-2.2456	0.5898
H	-5.9418	-4.1698	0.5122
H	-2.5513	-1.6413	-0.3961
H	-4.0013	0.3244	-0.2862
H	3.8409	0.3139	0.1825
H	2.4656	-1.6585	0.5043
H	5.7498	-4.1331	-0.8744
H	7.0834	-2.1815	-1.1931
H	9.4825	-0.801	-0.6061
H	8.1815	-0.9037	0.6021
H	9.0769	0.6734	0.3288
H	7.7377	6.0658	-0.3895
H	7.9507	4.6853	0.7322
H	6.3739	5.6103	0.6502
H	-8.7706	5.5078	-0.3135
H	-8.6424	3.9756	-1.235
H	-7.2919	5.2105	-1.2563
H	-9.0923	1.5467	-0.5849
H	-10.0328	0.5263	0.5242
H	-8.8895	1.6781	1.239
H	-4.4479	-5.4455	1.4325
H	-2.9728	-7.3784	1.4703
H	-0.3657	-5.4555	-1.3679
H	-1.798	-3.4927	-1.3801
H	1.6492	-3.4347	1.3401
H	0.234	-5.3757	1.4753
H	2.888	-7.5302	-1.1536
H	4.3292	-5.6107	-1.2855

REFERENCES CITED

Chapter I

1. Scott, L. T., Conjugated Belts and Nanorings with Radially Oriented p Orbitals. *Angew Chem, Int Ed* **2003,** *42* (35), 4133-4135.

2. Kawase, T.; Kurata, H., Ball-, Bowl-, and Belt-Shaped Conjugated Systems and Their Complexing Abilities: Exploration of the Concave-Convex π-π Interaction. *Chem Rev* **2006,** *106* (12), 5250-5273.

3. Parekh, V. C.; Guha, P. C., *J. Indian Chem. Soc.* **1934,** *11*, 95–100.

4. Diederich, F.; Rubin, Y.; Knobler, C. B.; Whetten, R. L.; Schriver, K. E.; Houk, K. N.; Li, Y., All-Carbon Molecules: Evidence for the Generation of Cyclo[18]carbon from a Stable Organic Precursor. *Science* **1989,** *245* (4922), 1088-1090.

5. (a) Rubin, Y.; Knobler, C. B.; Diederich, F., Precursors to the cyclo[n]carbons: from 3,4-dialkynyl-3-cyclobutene-1,2-diones and 3,4-dialkynyl-3-cyclobutene-1,2-diols to cyclobutenodehydroannulenes and higher oxides of carbon. *J Am Chem Soc* **1990,** *112* (4), 1607-1617;

(b) Tobe, Y.; Fujii, T.; Matsumoto, H.; Naemura, K.; Achiba, Y.; Wakabayashi, T., A New Entry into Cyclo[n]carbons: [2 + 2] Cycloreversion of Propellane-Annelated Dehydroannulenes. *J Am Chem Soc* **1996,** *118* (11), 2758-2759.

6. Kammermeier, S.; Jones, P. G.; Herges, R., Ring-Expanding Metathesis of Tetradehydro-anthracene—Synthesis and Structure of a Tubelike, Fully Conjugated Hydrocarbon. *Angew Chem, Int Ed* **1996,** *35* (22), 2669-2671.

7. Deichmann, M.; Näther, C.; Herges, R., Pyrolysis of a Tubular Aromatic Compound. *Org Lett* **2003,** *5* (8), 1269-1271.

8. Herges, R.; Deichmann, M.; Wakita, T.; Okamoto, Y., Synthesis of a Chiral Tube. *Angew Chem, Int Ed* **2003,** *42* (10), 1170-1172.

9. Rosenkranz, N.; Thomsen, C., Molecular dynamics simulations of picotube peapods. *Physica Status Solidi (B)* **2009,** *246* (11-12), 2622-2625.

10. (a) Rosenkranz, N.; Machón, M.; Herges, R.; Thomsen, C., Vibrational properties of four consecutive carbon picotubes. *Physica Status Solidi (B)* **2008,** *245* (10), 2145-2148;

(b) Rosenkranz, N.; Machón, M.; Herges, R.; Thomsen, C., Vibrational properties of semitrimer picotubes. *Chem Phys Lett* **2008,** *451* (4-6), 249-251;

(c) Machón, M.; Reich, S.; Maultzsch, J.; Okudera, H.; Simon, A.; Herges, R.; Thomsen, C., Structural, electronic, and vibrational properties of (4,4) picotube crystals. *Physical Review B* **2005,** *72* (15), 155402.

11. Kawase, T.; Darabi, H. R.; Oda, M., Cyclic [6]- and [8]Paraphenylacetylenes. *Angew Chem, Int Ed* **1996,** *35* (22), 2664-2666.

12. Kawase, T.; Ueda, N.; Darabi, H. R.; Oda, M., [2.2.2.2]Metacyclophane-1,9,17,25-tetrayne. *Angew Chem, Int Ed* **1996,** *35* (13-14), 1556-1558.

13. Kawase, T.; Ueda, N.; Tanaka, K.; Seirai, Y.; Oda, M., The newly modified McMurry reaction toward the improved synthesis of cyclic paraphenylacetylenes. *Tetrahedron Lett* **2001,** *42* (32), 5509-5511.

14. Kawase, T.; Seirai, Y.; Darabi, H. R.; Oda, M.; Sarakai, Y.; Tashiro, K., All-Hydrocarbon Inclusion Complexes of Carbon Nanorings: Cyclic [6]- and [8]Paraphenyleneacetylenes. *Angew Chem, Int Ed* **2003,** *42* (14), 1621-1624.

15. Kawase, T.; Tanaka, K.; Fujiwara, N.; Darabi, H. R.; Oda, M., Complexation of a Carbon Nanoring with Fullerenes. *Angew Chem, Int Ed* **2003,** *115* (14), 1662-1666.

16. (a) Atwood, J. L.; Koutsantonis, G. A.; Raston, C. L., Purification of C60 and C70 by selective complexation with calixarenes. *Nature* **1994,** *368* (6468), 229-231;

(b) Suzuki, T.; Nakashima, K.; Shinkai, S., Very Convenient and Efficient Purification Method for Fullerene (C60) with 5,11,17,23,29,35,41,47-Octa-tert-butylcalix[8]arene-49,50,51,52,53,54,55,56-octol. *Chem Lett* **1994,** *23* (4), 699-702.

17. Kawase, T.; Fujiwara, N.; Tsutumi, M.; Oda, M.; Maeda, Y.; Wakahara, T.; Akasaka, T., Supramolecular Dynamics of Cyclic [6]Paraphenyleneacetylene Complexes with [60]- and [70]Fullerene Derivatives: Electronic and Structural Effects on Complexation. *Angew Chem, Int Ed* **2004,** *43* (38), 5060-5062.

18. (a) Kawase, T.; Tanaka, K.; Seirai, Y.; Shiono, N.; Oda, M., Complexation of Carbon Nanorings with Fullerenes: Supramolecular Dynamics and Structural Tuning for a Fullerene Sensor. *Angew Chem, Int Ed* **2003,** *42* (45), 5597-5600;

(b) Kawase, T.; Oda, M., Complexation of carbon nanorings with fullerenes. *Pure Appl Chem* **2006,** *78* (4), 831-839.

19. Kawase, T.; Tanaka, K.; Shiono, N.; Seirai, Y.; Oda, M., Onion-Type Complexation Based on Carbon Nanorings and a Buckminsterfullerene. *Angew Chem, Int Ed* **2004,** *116* (13), 1754-1756.

20. (a) Iijima, S., Helical microtubules of graphitic carbon. *Nature* **1991,** *354* (6348), 56-58;

(b) Ugarte, D., Curling and closure of graphitic networks under electron-beam irradiation. *Nature* **1992,** *359* (6397), 707-709.

21. Armitage, J. B.; Entwistle, N.; Jones, E. R. H.; Whiting, M. C., Researches on acetylenic compounds. Part XLI. The synthesis of diphenylpolyacetylenes. *Journal of the Chemical Society (Resumed)* **1954**, 147-154.

22. (a) Srinivasan, M.; Sankararaman, S.; Hopf, H.; Varghese, B., Synthesis of buta-1,3-diyne-bridged macrocycles with (Z)-1,4-diethynyl1,4-dimethoxycyclohexa-2,5-diene as the building block. *Eur. J. Org. Chem.* **2003,** *2003* (4), 660-665;

(b) Ohkita, M.; Ando, K.; Suzuki, T.; Tsuji, T., Syntheses of Acetylenic Oligophenylene Macrocycles Based on a Novel Dewar Benzene Building Block Approach. *J Org Chem* **2000,** *65* (14), 4385-4390;

(c) Ohkita, M.; Ando, K.; Tsuji, T., Synthesis and characterization of [46]paracyclophanedodecayne derivative. *Chem Commun* **2001,** (24), 2570-2571.

23. Tobe, Y.; Furukawa, R.; Sonoda, M.; Wakabayashi, T., [12.12]Paracyclophanedodecaynes C36H8 and C36Cl8: The Smallest Paracyclophynes and Their Transformation into the Carbon Cluster Ion C36−. *Angew Chem, Int Ed* **2001,** *40* (21), 4072-4074.

24. Jasti, R.; Bhattacharjee, J.; Neaton, J. B.; Bertozzi, C. R., Synthesis, Characterization, and Theory of [9]-, [12]-, and [18]Cycloparaphenylene: Carbon Nanohoop Structures. *J. Am. Chem. Soc.* **2008,** *130* (52), 17646-17647.

25. Ohkita, M.; Ando, K.; Yamamoto, K.-i.; Suzuki, T.; Tsuji, T., First Dewar benzene approach to acetylenic oligophenylene macrocycles: synthesis and structure of a molecular rectangle bearing two spindles. *Chem Commun* **2000,** (1), 83-84.

26. Tobe, Y.; Fujii, T.; Matsumoto, H.; Tsumuraya, K.; Noguchi, D.; Nakagawa, N.; Sonoda, M.; Naemura, K.; Achiba, Y.; Wakabayashi, T., [2 + 2] Cycloreversion of [4.3.2]Propella-1,3,11-trienes: An Approach to Cyclo[n]carbons from Propellane-Annelated Dehydro[n]annulenes. *J Am Chem Soc* **2000,** *122* (8), 1762-1775.

27. (a) Takaba, H.; Omachi, H.; Yamamoto, Y.; Bouffard, J.; Itami, K., Selective Synthesis of [12]Cycloparaphenylene. *Angew Chem, Int Ed* **2009,** *48* (33), 6112-6116;

(b) Omachi, H.; Matsuura, S.; Segawa, Y.; Itami, K., A Modular and Size-Selective Synthesis of [n]Cycloparaphenylenes: A Step toward the Selective Synthesis of [n,n] Single-Walled Carbon Nanotubes. *Angew Chem, Int Ed* **2010,** *49* (52), 10202-10205;

(c) Iwamoto, T.; Watanabe, Y.; Sadahiro, T.; Haino, T.; Yamago, S., Size-Selective Encapsulation of C60 by [10]Cycloparaphenylene: Formation of the Shortest Fullerene-Peapod. *Angew. Chem. Int. Ed.* **2011,** *50* (36), 8342-8344;

(d) Iwamoto, T.; Watanabe, Y.; Sakamoto, Y.; Suzuki, T.; Yamago, S., Selective and Random Syntheses of [n]Cycloparaphenylenes (n = 8-13) and Size Dependence of Their Electronic Properties. *J Am Chem Soc* **2011,** *133* (21), 8354-8361;

(e) Hitosugi, S.; Nakanishi, W.; Yamasaki, T.; Isobe, H., Bottom-up synthesis of finite models of helical (n,m)-single-wall carbon nanotubes. *Nat. Commun.* **2011,** *2*, 492;

(f) Omachi, H.; Segawa, Y.; Itami, K., Synthesis and Racemization Process of Chiral Carbon Nanorings: A Step toward the Chemical Synthesis of Chiral Carbon Nanotubes. *Org Lett* **2011,** *13* (9), 2480-2483;

(g) Segawa, Y.; Miyamoto, S.; Omachi, H.; Matsuura, S.; Šenel, P.; Sasamori, T.; Tokitoh, N.; Itami, K., Concise Synthesis and Crystal Structure of [12]Cycloparaphenylene. *Angew Chem, Int Ed* **2011,** *50* (14), 3244-3248;

(h) Segawa, Y.; Scaron; enel, P.; Matsuura, S.; Omachi, H.; Itami, K., [9]Cycloparaphenylene: Nickel-mediated Synthesis and Crystal Structure. *Chem Lett* **2011,** *40* (4), 423-425;

(i) Sisto, T. J.; Golder, M. R.; Hirst, E. S.; Jasti, R., Selective Synthesis of Strained [7]Cycloparaphenylene: An Orange-Emitting Fluorophore. *J. Am. Chem. Soc.* **2011,** *133* (40), 15800-15802;

(j) Hitosugi, S.; Nakanishi, W.; Isobe, H., Atropisomerism in a Belt-Persistent Nanohoop Molecule: Rotational Restriction Forced by Macrocyclic Ring Strain. *Chemistry – An Asian Journal* **2012**, Early View;

(k) Ishii, Y.; Nakanishi, Y.; Omachi, H.; Matsuura, S.; Matsui, K.; Shinohara, H.; Segawa, Y.; Itami, K., Size-selective synthesis of [9]-[11] and [13]cycloparaphenylenes. *Chemical Science* **2012**, Published Online;

(l) Matsui, K.; Segawa, Y.; Itami, K., Synthesis and Properties of Cycloparaphenylene-2,5-pyridylidene: A Nitrogen-Containing Carbon Nanoring. *Org. Lett.* **2012,** *14* (7), 1888-1891;

(m) Yagi, A.; Segawa, Y.; Itami, K., Synthesis and Properties of [9]Cyclo-1,4-naphthylene: A π-Extended Carbon Nanoring. *J. Am. Chem. Soc.* **2012,** *134* (6), 2962-2965;

(n) Segawa, Y.; Fukazawa, A.; Matsuura, S.; Omachi, H.; Yamaguchi, S.; Irle, S.; Itami, K., Combined experimental and theoretical studies on the photophysical properties of cycloparaphenylenes. *Org. Biomol. Chem.* **2012**;

(o) Xia, J.; Jasti, R., Synthesis, Characterization, and Crystal Structure of [6]Cycloparaphenylene. *Angew. Chem. Int. Ed.* **2012,** *51* (10), 2474-2476;

(p) The Smaller the Redder. *Synfacts* **2011,** *2011* (12), 1309,1309;

(q) Sisto, T. J.; Jasti, R., Overcoming Molecular Strain: Synthesis of [7]Cycloparaphenylene. *Synlett* **2012,** *23* (EFirst), 483-489;

(r) Li, H.-B.; Page, A. J.; Irle, S.; Morokuma, K., Theoretical Insights into Chirality-Controlled SWCNT Growth from a Cycloparaphenylene Template. *ChemPhysChem* **2012,** *13* (6), 1479-1485;

(s) Tian, X.; Jasti, R., Cycloparaphenylenes: The Shortest Possible Segments of Armchair Carbon Nanotubes. In *Fragments of Fullerenes and Carbon Nanotubes*, John Wiley & Sons, Inc.: 2011; pp 291-309;

(t) Bachrach, S. M.; Stück, D., DFT Study of Cycloparaphenylenes and Heteroatom-Substituted Nanohoops. *J Org Chem* **2010,** *75* (19), 6595-6604;

(u) Segawa, Y.; Omachi, H.; Itami, K., Theoretical Studies on the Structures and Strain Energies of Cycloparaphenylenes. *Org Lett* **2010,** *12* (10), 2262-2265;

(v) Jasti, R.; Bertozzi, C. R., Progress and challenges for the bottom-up synthesis of carbon nanotubes with discrete chirality. *Chem Phys Lett* **2010,** *494* (1-3), 1-7;

(w) Sundholm, D.; Taubert, S.; Pichierri, F., Calculation of absorption and emission spectra of [n]cycloparaphenylenes: the reason for the large Stokes shift. *Phys Chem Chem Phys* **2010,** *12* (11), 2751-2757;

(x) Wong, B. M., Optoelectronic Properties of Carbon Nanorings: Excitonic Effects from Time-Dependent Density Functional Theory. *J. Phys. Chem. C* **2009,** *113* (52), 21921-21927.

28. Friederich, R.; Nieger, M.; Vögtle, F., Auf dem Weg zu makrocyclischen para-Phenylenen. *Chemische Berichte* **1993,** *126* (7), 1723-1732.

29. Ellis, K. K.; Wilke, B.; Zhang, Y.; Diver, S. T., A New Method for the Synthesis of Imidazolidinone- and Benzimidazolone-Containing [2.2]Cyclophanes. *Org Lett* **2000,** *2* (24), 3785-3788.

30. Alonso, F.; Yus, M., Easy synthesis of 2,4-dialkyl substituted phenols and anisoles from p-bensoquinone. *Tetrahedron* **1992,** *48* (13), 2709-2714.

31. Nijegorodov, N. I.; Downey, W. S.; Danailov, M. B., Systematic investigation of absorption, fluorescence and laser properties of some p- and m-oligophenylenes. *Spectrochimica Acta Part A: Molecular and Biomolecular Spectroscopy* **2000,** *56* (4), 783-795.

32. Yamago, S.; Watanabe, Y.; Iwamoto, T., Synthesis of [8]Cycloparaphenylene from a Square-Shaped Tetranuclear Platinum Complex. *Angew. Chem. Int. Ed.* **2010,** *49* (4), 757-759.

33. Jagadeesh, M. N.; Makur, A.; Chandrasekhar, J., The Interplay of Angle Strain and Aromaticity: Molecular and Electronic Structures of [0n]Paracyclophanes. *Journal of Molecular Modeling* **2000,** *6* (2), 226-233.

34. (a) Matsuo, Y.; Sato, Y.; Hashiguchi, M.; Matsuo, K.; Nakamura, E., Synthesis, Electrochemical and Photophysical Properties, and Electroluminescent Performance of the Octa- and Deca(aryl)[60]fullerene Derivatives. *Advanced Functional Materials* **2009,** *19* (14), 2224-2229;

(b) Matsuo, Y.; Tahara, K.; Morita, K.; Matsuo, K.; Nakamura, E., Regioselective Eightfold and Tenfold Additions of a Pyridine-Modified Organocopper Reagent to [60]Fullerene. *Angew Chem, Int Ed* **2007,** *46* (16), 2844-2847;

(c) Matsuo, Y.; Tahara, K.; Sawamura, M.; Nakamura, E., Creation of Hoop- and Bowl-Shaped Benzenoid Systems by Selective Detraction of [60]Fullerene Conjugation. [10]Cyclophenacene and Fused Corannulene Derivatives. *J Am Chem Soc* **2004,** *126* (28), 8725-8734;

(d) Nakamura, E.; Tahara, K.; Matsuo, Y.; Sawamura, M., Synthesis, Structure, and Aromaticity of a Hoop-Shaped Cyclic Benzenoid [10]Cyclophenacene. *J. Am. Chem. Soc.* **2003,** *125* (10), 2834-2835.

35. Zhang, X.; Matsuo, Y.; Nakamura, E., Light emission of [10]cyclophenacene through energy transfer from neighboring carbazolylphenyl dendrons. *Org Lett* **2008,** *10* (18), 4145-7.

36. Li, C.-Z.; Matsuo, Y.; Nakamura, E., Luminescent Bow-Tie-Shaped Decaaryl[60]fullerene Mesogens. *J Am Chem Soc* **2009,** *131* (47), 17058-17059.

37. (a) Ashton, P. R.; Brown, G. R.; Isaacs, N. S.; Giuffrida, D.; Kohnke, F. H.; Mathias, J. P.; Slawin, A. M. Z.; Smith, D. R.; Stoddart, J. F.; Williams, D. J., Molecular LEGO. 1. Substrate-directed synthesis via stereoregular Diels-Alder oligomerizations. *J Am Chem Soc* **1992,** *114* (16), 6330-6353;

(b) Cory, R. M.; McPhail, C. L., Transformations of a macrocyclic cyclophane belt into advanced [8]cyclacene and [8]cyclacene triquinone precursors. *Tetrahedron Lett* **1996,** *37* (12), 1987-1990.

38. Godt, A.; Enkelmann, V.; Schlüter, A.-D., Double-Stranded Molecules: A [6] Beltene Derivative and the Corresponding Open-Chain Polymer. *Angew Chem, Int Ed* **1989,** *28* (12), 1680-1682.

39. Esser, B.; Rominger, F.; Gleiter, R., Synthesis of [6.8]3Cyclacene: Conjugated Belt and Model for an Unusual Type of Carbon Nanotube. *J Am Chem Soc* **2008,** *130* (21), 6716-6717.

40. Kintzel, O.; Luger, P.; Weber, M.; Schlüter, A. D., Ring-Chain Equilibrium between an [18]Cyclacene Derivative and a Ladder Oligomer. *Eur J Org Chem* **1998,** *1998* (1), 99-105.

41. (a) Neudorff, W. D.; Lentz, D.; Anibarro, M.; Schlüter, A. D., The Carbon Skeleton of the Belt Region of Fullerene C84 (D2). *Chemistry – A European Journal* **2003,** *9* (12), 2745-2757;

(b) Denekamp, C.; Etinger, A.; Amrein, W.; Stanger, A.; Stuparu, M.; Schlüter, A. D., Towards a Fully Conjugated, Double-Stranded Cycle: A Mass Spectrometric and Theoretical Study. *Chemistry – A European Journal* **2008,** *14* (5), 1628-1637;

(c) Stuparu, M.; Lentz, D.; Rüegger, H.; Schlüter, A. D., Exploring the Chemistry of a Double-Stranded Cycle with the Carbon Skeleton of the Belt Region of the C84 Fullerene. *Eur J Org Chem* **2007,** *2007* (1), 88-100.

Chapter II

1. Eaton, P. E.; Cole, T. W., Cubane. *J. Am. Chem. Soc.* **1964,** *86* (15), 3157-3158.

2. Lawton, R. G.; Barth, W. E., Synthesis of corannulene. *J. Am. Chem. Soc.* **1971,** *93* (7), 1730-1745.

3. Dauben, W. G.; Cargill, R. L., Photochemical transformations,-VIII: The isomerization of Δ2,5-bicyclo[2.2.1]heptadiene to quadricyclo[2.2.1.$0^{2,6}$-$0^{3,5}$]heptane (quadricyclene). *Tetrahedron* **1961,** *15* (1-4), 197-201.

4. Kammermeier, S.; Jones, P. G.; Herges, R., Ring-Expanding Metathesis of Tetradehydro-anthracene—Synthesis and Structure of a Tubelike, Fully Conjugated Hydrocarbon. *Angew. Chem. Int. Ed.* **1996,** *35* (22), 2669-2671.

5. Kane, V. V.; Wolf, A. D.; Jones, M., [6]Paracyclophane. *J. Am. Chem. Soc.* **1974,** *96* (8), 2643-2644.

6. Scott, L. T.; Boorum, M. M.; McMahon, B. J.; Hagen, S.; Mack, J.; Blank, J.; Wegner, H.; de Meijere, A., A Rational Chemical Synthesis of C60. *Science* **2002,** *295* (5559), 1500-1503.

7. (a) Hopf, H., *Classics in Hydrocarbon Chemistry*. Wiley-VCH: Weinheim, 2000; p 560;

(b) Scott, L. T., Conjugated Belts and Nanorings with Radially Oriented p Orbitals. *Angew. Chem. Int. Ed.* **2003,** *42* (35), 4133-4135.

8. Parekh, V. C.; Guha, P. C., Synthesis of p,p-diphenylene disulfide. *J. Indian Chem. Soc.* **1934,** *11*, 95–100.

9. (a) Yamago, S.; Watanabe, Y.; Iwamoto, T., Synthesis of [8]Cycloparaphenylene from a Square-Shaped Tetranuclear Platinum Complex. *Angew. Chem. Int. Ed.* **2010,** *49* (4), 757-759;

(b) Omachi, H.; Matsuura, S.; Segawa, Y.; Itami, K., A Modular and Size-Selective Synthesis of [n]Cycloparaphenylenes: A Step toward the Selective Synthesis of [n,n] Single-Walled Carbon Nanotubes. *Angew. Chem. Int. Ed.* **2010,** *49* (52), 10202-10205;

(c) Jasti, R.; Bhattacharjee, J.; Neaton, J. B.; Bertozzi, C. R., Synthesis, Characterization, and Theory of [9]-, [12]-, and [18]Cycloparaphenylene: Carbon Nanohoop Structures. *J. Am. Chem. Soc.* **2008,** *130* (52), 17646-17647;

(d) Srinivasan, M.; Sankararaman, S.; Hopf, H.; Varghese, B., Synthesis of buta-1,3-diyne-bridged macrocycles with (Z)-1,4-diethynyl1,4-dimethoxycyclohexa-2,5-diene as the building block. *Eur. J. Org. Chem.* **2003,** *2003* (4), 660-665.

10. Xia, J.; Jasti, R., Synthesis, Characterization, and Crystal Structure of [6]Cycloparaphenylene. *Angew. Chem. Int. Ed.* **2012,** *51* (10), 2474-2476.

11. (a) Golder, M. R.; Wong, B. M.; Jasti, R., Photophysical and theoretical investigations of the [8]cycloparaphenylene radical cation and its charge-resonance dimer. *Chem. Sci.* **2013,** *4* (11), 4285-4291;

(b) Zabula, A. V.; Filatov, A. S.; Xia, J.; Jasti, R.; Petrukhina, M. A., Tightening of the Nanobelt upon Multielectron Reduction. *Angew. Chem. Int. Ed.* **2013,** *52* (19), 5033-5036.

12. (a) Iwamoto, T.; Watanabe, Y.; Sadahiro, T.; Haino, T.; Yamago, S., Size-Selective Encapsulation of C60 by [10]Cycloparaphenylene: Formation of the Shortest Fullerene-Peapod. *Angew. Chem. Int. Ed.* **2011,** *50* (36), 8342-8344;

(b) Xia, J.; Bacon, J. W.; Jasti, R., Gram-scale synthesis and crystal structures of [8]- and [10]CPP, and the solid-state structure of C60@[10]CPP. *Chem. Sci.* **2012,** *3* (10), 3018-3021.

13. Hirst, E. S.; Jasti, R., Bending Benzene: Syntheses of [n]Cycloparaphenylenes. *J. Org. Chem.* **2012,** *77* (23), 10473-10478.

14. Omachi, H.; Nakayama, T.; Takahashi, E.; Segawa, Y.; Itami, K., Initiation of carbon nanotube growth by well-defined carbon nanorings. *Nat Chem* **2013,** *5* (7), 572-576.

15. (a) Darzi, E. R.; Sisto, T. J.; Jasti, R., Selective Syntheses of [7]-[12]Cycloparaphenylenes Using Orthogonal Suzuki-Miyaura Cross-Coupling Reactions. *J. Org. Chem.* **2012,** *77* (15), 6624-6628;

(b) Iwamoto, T.; Watanabe, Y.; Sakamoto, Y.; Suzuki, T.; Yamago, S., Selective and Random Syntheses of [n]Cycloparaphenylenes (n = 8-13) and Size Dependence of Their Electronic Properties. *J. Am. Chem. Soc.* **2011,** *133* (21), 8354-8361;

(c) Sisto, T. J.; Golder, M. R.; Hirst, E. S.; Jasti, R., Selective Synthesis of Strained [7]Cycloparaphenylene: An Orange-Emitting Fluorophore. *J. Am. Chem. Soc.* **2011,** *133* (40), 15800-15802;

(d) Kayahara, E.; Iwamoto, T.; Suzuki, T.; Yamago, S., Selective Synthesis of [6]-, [8]-, and [10]Cycloparaphenylenes. *Chem. Lett.* **2013,** *42* (6), 621-623;

(e) Kayahara, E.; Sakamoto, Y.; Suzuki, T.; Yamago, S., Selective Synthesis and Crystal Structure of [10]Cycloparaphenylene. *Org. Lett.* **2012,** *14* (13), 3284-3287;

(f) Sibbel, F.; Matsui, K.; Segawa, Y.; Studer, A.; Itami, K., Selective Synthesis of [7]- and [8]Cycloparaphenylenes. *Chem. Commun.* **2013**;

(g) Segawa, Y.; Scaron; enel, P.; Matsuura, S.; Omachi, H.; Itami, K., [9]Cycloparaphenylene: Nickel-mediated Synthesis and Crystal Structure. *Chem. Lett.* **2011,** *40* (4), 423-425;

(h) Segawa, Y.; Miyamoto, S.; Omachi, H.; Matsuura, S.; Šenel, P.; Sasamori, T.; Tokitoh, N.; Itami, K., Concise Synthesis and Crystal Structure of [12]Cycloparaphenylene. *Angew. Chem. Int. Ed.* **2011,** *50* (14), 3244-3248;

(i) Ishii, Y.; Nakanishi, Y.; Omachi, H.; Matsuura, S.; Matsui, K.; Shinohara, H.; Segawa, Y.; Itami, K., Size-selective synthesis of [9]-[11] and [13]cycloparaphenylenes. *Chem. Sci.* **2012,** *3* (7), 2340-2345.

16. (a) Hitosugi, S.; Nakanishi, W.; Yamasaki, T.; Isobe, H., Bottom-up synthesis of finite models of helical (n,m)-single-wall carbon nanotubes. *Nat. Commun.* **2011,** *2*, 492;

(b) Yagi, A.; Segawa, Y.; Itami, K., Synthesis and Properties of [9]Cyclo-1,4-naphthylene: A π-Extended Carbon Nanoring. *J. Am. Chem. Soc.* **2012,** *134* (6), 2962-2965;

(c) Matsui, K.; Segawa, Y.; Itami, K., Synthesis and Properties of Cycloparaphenylene-2,5-pyridylidene: A Nitrogen-Containing Carbon Nanoring. *Org. Lett.* **2012,** *14* (7), 1888-1891;

(d) Sisto, T. J.; Tian, X.; Jasti, R., Synthesis of tetraphenyl-substituted [12]cycloparaphenylene: toward a rationally designed ultrashort carbon nanotube. *J. Org. Chem.* **2012,** *77* (14), 5857-5860.

17. Wong, B. M., Optoelectronic Properties of Carbon Nanorings: Excitonic Effects from Time-Dependent Density Functional Theory. *J. Phys. Chem. C* **2009,** *113* (52), 21921-21927.

18. Frisch, M. J.; Trucks, G. W.; Schlegel, H. B.; Scuseria, G. E.; Robb, M. A.; Cheeseman, J. R.; Scalmani, G.; Barone, V.; Mennucci, B.; Petersson, G. A.; Nakatsuji, H.; Caricato, M.; Li, X.; Hratchian, H. P.; Izmaylov, A. F.; Bloino, J.; Zheng, G.; Sonnenberg, J. L.; Hada, M.; Ehara, M.; Toyota, K.; Fukuda, R.; Hasegawa, J.; Ishida, M.; Nakajima, T.; Honda, Y.; Kitao, O.; Nakai, H.; Vreven, T.; Montgomery, J. A.; Peralta, J. E.; Ogliaro, F.; Bearpark, M.; Heyd, J. J.; Brothers, E.; Kudin, K. N.; Staroverov, V. N.; Kobayashi, R.; Normand, J.; Raghavachari, K.; Rendell, A.; Burant, J. C.; Iyengar, S. S.; Tomasi, J.; Cossi, M.; Rega, N.; Millam, J. M.; Klene, M.; Knox, J. E.; Cross, J. B.; Bakken, V.; Adamo, C.; Jaramillo, J.; Gomperts, R.; Stratmann, R. E.; Yazyev, O.; Austin, A. J.; Cammi, R.; Pomelli, C.; Ochterski, J. W.; Martin, R. L.; Morokuma, K.; Zakrzewski, V. G.; Voth, G. A.; Salvador, P.; Dannenberg, J. J.; Dapprich, S.; Daniels, A. D.; Farkas; Foresman, J. B.; Ortiz, J. V.; Cioslowski, J.; Fox, D. J., *Gaussian 09, Revision D.01*. Gaussian Inc.: Wallingford CT, 2009.

19. Nakamura, E.; Tahara, K.; Matsuo, Y.; Sawamura, M., Synthesis, Structure, and Aromaticity of a Hoop-Shaped Cyclic Benzenoid [10]Cyclophenacene. *J. Am. Chem. Soc.* **2003,** *125* (10), 2834-2835.

20. Anslyn, E.; Dougherty, D., *Modern Physical Organic Chemistry*. University Science Books: Mill Valley, CA, 2008.

21. (a) Punna, S.; Díaz, D. D.; Finn, M. G., Palladium-Catalyzed Homocoupling of Arylboronic Acids and Esters Using Fluoride in Aqueous Solvents. *Synlett* **2004,** *2004* (13), 2351-2354;

(b) Moreno-Mañas, M.; Pérez, M.; Pleixats, R., Palladium-Catalyzed Suzuki-Type Self-Coupling of Arylboronic Acids. A Mechanistic Study. *J. Org. Chem.* **1996,** *61* (7), 2346-2351.

22. Tobe, Y.; Jimbo, M.; Saiki, S.; Kakiuchi, K.; Naemura, K., Unusual reactivity of [6]paracyclophane toward alkyllithiums. *J. Org. Chem.* **1993,** *58* (22), 5883-5885.

23. Tobe, Y.; Ueda, K.; Kaneda, T.; Kakiuchi, K.; Odaira, Y.; Kai, Y.; Kasai, N., Synthesis and molecular structure of (Z)-[6]Paracycloph-3-enes. *J. Am. Chem. Soc.* **1987,** *109* (4), 1136-1144.

24. Jagadeesh, M. N.; Makur, A.; Chandrasekhar, J., The Interplay of Angle Strain and Aromaticity: Molecular and Electronic Structures of [0n]Paracyclophanes. *Journal of Molecular Modeling* **2000,** *6* (2), 226-233.

25. (a) Allinger, N. L.; Walter, T. J.; Newton, M. G., Synthesis, structure, and properties of the [7]paracyclophane ring system. *J. Am. Chem. Soc.* **1974,** *96* (14), 4588-4597;

(b) Tobe, Y.; Ueda, K.-I.; Kakiuchi, K.; Odaira, Y.; Kai, Y.; Kasai, N., Synthesis, structure and reactivities of [6]paracyclophanes. *Tetrahedron* **1986,** *42* (6), 1851-1858.

26. Baran, P. S.; Burns, N. Z., Total Synthesis of (±)-Haouamine A. *J. Am. Chem. Soc.* **2006,** *128* (12), 3908-3909.

27. Takiguchi, H.; Ohmori, K.; Suzuki, K., Synthesis and determination of the absolute configuration of cavicularin by a symmetrization/asymmetrization approach. *Angew. Chem. Int. Ed.* **2013,** *52* (40), 10472-10476.

28. Nikolaev, A. V.; Dennis, T. J. S.; Prassides, K.; Soper, A. K., Molecular structure of the C70 fullerene. *Chem. Phys. Lett.* **1994,** *223* (3), 143-148.

29. Scott, L. T.; Jackson, E. A.; Zhang, Q.; Steinberg, B. D.; Bancu, M.; Li, B., A Short, Rigid, Structurally Pure Carbon Nanotube by Stepwise Chemical Synthesis. *J. Am. Chem. Soc.* **2011,** *134* (1), 107-110.

30. Fujitsuka, M.; Cho, D. W.; Iwamoto, T.; Yamago, S.; Majima, T., Size-dependent fluorescence properties of [n]cycloparaphenylenes (n = 8-13), hoop-shaped π-conjugated molecules. *Phys. Chem. Chem. Phys.* **2012,** *14* (42), 14585-14588.

31. Kawasumi, K.; Zhang, Q.; Segawa, Y.; Scott, L. T.; Itami, K., A grossly warped nanographene and the consequences of multiple odd-membered-ring defects. *Nat Chem* **2013,** *5* (9), 739-744.

32. Pangborn, A. B.; Giardello, M. A.; Grubbs, R. H.; Rosen, R. K.; Timmers, F. J., Safe and Convenient Procedure for Solvent Purification. *Organometallics* **1996,** *15* (5), 1518-1520.

33. Bruker *APEX2*, Bruker Analytical X-ray Instruments Inc.: Madison, Wisconsin, USA, 2006.

34. Bruker *SAINT*, Bruker Analytical X-ray Instruments Inc.: Madison, Wisconsin, USA, 2006.

35. Sheldrick, G. M. *SHELXL97*, University of Göttingen: Göttingen, Germany, 1997.

36. Dolomanov, O. V.; Bourhis, L. J.; Gildea, R. J.; Howard, J. A. K.; Puschmann, H., OLEX2: a complete structure solution, refinement and analysis program. *Journal of Applied Crystallography* **2009,** *42* (2), 339-341.

37. Sheldrick, G. M. *SADABS*, University of Göttingen: Göttingen, Germany, 1996.

ChapterIII

1. Jasti, R.; Bhattacharjee, J.; Neaton, J. B.; Bertozzi, C. R., Synthesis, Characterization, and Theory of [9]-, [12]-, and [18]Cycloparaphenylene: Carbon Nanohoop Structures. *J Am Chem Soc* **2008,** *130* (52), 17646-17647.

2. (a) Cory, R. M.; McPhail, C. L., Transformations of a macrocyclic cyclophane belt into advanced [8]cyclacene and [8]cyclacene triquinone precursors. *Tetrahedron Lett* **1996,** *37* (12), 1987-1990;

(b) Ashton, P. R.; Isaacs, N. S.; Kohnke, F. H.; Slawin, A. M. Z.; Spencer, C. M.; Stoddart, J. F.; Williams, D. J., Towards the Making of [12]Collarene. *Angewandte Chemie International Edition in English* **1988,** *27* (7), 966-969.

3. Gingras, M., One hundred years of helicene chemistry. Part 3: applications and properties of carbohelicenes. *Chemical Society Reviews* **2013,** *42* (3), 1051-1095.

4. Omachi, H.; Segawa, Y.; Itami, K., Synthesis and Racemization Process of Chiral Carbon Nanorings: A Step toward the Chemical Synthesis of Chiral Carbon Nanotubes. *Org Lett* **2011,** *13* (9), 2480-2483.

5. (a) Hitosugi, S.; Nakanishi, W.; Isobe, H., Atropisomerism in a Belt-Persistent Nanohoop Molecule: Rotational Restriction Forced by Macrocyclic Ring Strain. *Chemistry – An Asian Journal* **2012**, Early View;

(b) Hitosugi, S.; Nakanishi, W.; Yamasaki, T.; Isobe, H., Bottom-up synthesis of finite models of helical (n,m)-single-wall carbon nanotubes. *Nat Commun* **2011,** *2*, 492.

6. Ōki, M., Recent Advances in Atropisomerism. In *Topics in Stereochemistry*, John Wiley & Sons, Inc.: 2007; pp 1-81.

7. Xia, J.; Jasti, R., Synthesis, Characterization, and Crystal Structure of [6]Cycloparaphenylene. *Angew Chem, Int Ed* **2012,** *51* (10), 2474-2476.

8. Xia, J.; Bacon, J. W.; Jasti, R., Gram-scale synthesis and crystal structures of [8]- and [10]CPP, and the solid-state structure of C60@[10]CPP. *Chemical Science* **2012,** *3* (10), 3018-3021.

9. Tam, V. K.; Liu, Q.; Tor, Y., Extended ethidium bromide analogue as a triple helix intercalator: synthesis, photophysical properties and nucleic acids binding. *Chemical Communications* **2006,** (25), 2684-2686.

10. Espino, G.; Kurbangalieva, A.; Brown, J. M., Aryl bromide/triflate selectivities reveal mechanistic divergence in palladium-catalysed couplings; the Suzuki-Miyaura anomaly. *Chemical Communications* **2007,** (17), 1742-1744.

11. Alonso, F.; Yus, M., Easy synthesis of 2,4-dialkyl substituted phenols and anisoles from p-bensoquinone. *Tetrahedron* **1992,** *48* (13), 2709-2714.

12. Correa, A.; León, T.; Martin, R., Ni-Catalyzed Carboxylation of C(sp2)– and C(sp3)–O Bonds with CO2. *Journal of the American Chemical Society* **2014,** *136* (3), 1062-1069.

13. Ramgren, S. D.; Hie, L.; Ye, Y.; Garg, N. K., Nickel-Catalyzed Suzuki–Miyaura Couplings in Green Solvents. *Organic Letters* **2013,** *15* (15), 3950-3953.

14. Pangborn, A. B.; Giardello, M. A.; Grubbs, R. H.; Rosen, R. K.; Timmers, F. J., Safe and Convenient Procedure for Solvent Purification. *Organometallics* **1996,** *15* (5), 1518-1520.

15. Frigoli, M.; Moustrou, C.; Samat, A.; Guglielmetti, R., Synthesis of New Thiophene-Substituted 3,3-Diphenyl-3H-naphtho[2,1-b]pyrans by Cross-Coupling Reactions, Precursors of Photomodulated Materials. *European Journal of Organic Chemistry* **2003,** *2003* (15), 2799-2812.

16. Chen, W.; Shen, Y.; Li, Z.; Zhang, M.; Lu, C.; Shen, Y., Design and synthesis of 2-phenylnaphthalenoids as inhibitors of DNA topoisomeraseIIα and antitumor agents. *European Journal of Medicinal Chemistry* **2014,** *86* (0), 782-796.

17. Frisch, M. J.; Trucks, G. W.; Schlegel, H. B.; Scuseria, G. E.; Robb, M. A.; Cheeseman, J. R.; Scalmani, G.; Barone, V.; Mennucci, B.; Petersson, G. A.; Nakatsuji, H.; Caricato, M.; Li, X.; Hratchian, H. P.; Izmaylov, A. F.; Bloino, J.; Zheng, G.; Sonnenberg, J. L.; Hada, M.; Ehara, M.; Toyota, K.; Fukuda, R.; Hasegawa, J.; Ishida, M.; Nakajima, T.; Honda, Y.; Kitao, O.; Nakai, H.; Vreven, T.; Montgomery, J. A.; Peralta, J. E.; Ogliaro, F.; Bearpark, M.; Heyd, J. J.; Brothers, E.; Kudin, K. N.; Staroverov, V. N.; Kobayashi, R.; Normand, J.; Raghavachari, K.; Rendell, A.; Burant, J. C.; Iyengar, S. S.; Tomasi, J.; Cossi, M.; Rega, N.; Millam, J. M.; Klene, M.; Knox, J. E.; Cross, J. B.; Bakken, V.; Adamo, C.; Jaramillo, J.; Gomperts, R.; Stratmann, R. E.; Yazyev, O.; Austin, A. J.; Cammi, R.; Pomelli, C.; Ochterski, J. W.; Martin, R. L.; Morokuma, K.; Zakrzewski, V. G.; Voth, G. A.; Salvador, P.; Dannenberg, J. J.; Dapprich, S.; Daniels, A. D.; Farkas; Foresman, J. B.; Ortiz, J. V.; Cioslowski, J.; Fox, D. J., *Gaussian 09, Revision D.01*. Gaussian Inc.: Wallingford CT, 2009.

Chapter IV

1. (a) Kawase, T.; Fujiwara, N.; Tsutumi, M.; Oda, M.; Maeda, Y.; Wakahara, T.; Akasaka, T., Supramolecular Dynamics of Cyclic [6]Paraphenyleneacetylene Complexes with [60]- and [70]Fullerene Derivatives: Electronic and Structural Effects on Complexation. *Angew Chem, Int Ed* **2004,** *43* (38), 5060-5062;

(b) Kawase, T.; Kurata, H., Ball-, Bowl-, and Belt-Shaped Conjugated Systems and Their Complexing Abilities: Exploration of the Concave-Convex π-π Interaction. *Chem Rev* **2006,** *106* (12), 5250-5273;

(c) Kawase, T.; Oda, M., Complexation of carbon nanorings with fullerenes. *Pure Appl Chem* **2006,** *78* (4), 831-839;

(d) Kawase, T.; Tanaka, K.; Shiono, N.; Seirai, Y.; Oda, M., Onion-Type Complexation Based on Carbon Nanorings and a Buckminsterfullerene. *Angew Chem, Int Ed* **2004,** *116* (13), 1754-1756.

2. (a) Iwamoto, T.; Watanabe, Y.; Sadahiro, T.; Haino, T.; Yamago, S., Size-Selective Encapsulation of C60 by [10]Cycloparaphenylene: Formation of the Shortest Fullerene-Peapod. *Angew Chem, Int Ed* **2011,** *50* (36), 8342-8344;

(b) Xia, J.; Bacon, J. W.; Jasti, R., Gram-scale synthesis and crystal structures of [8]- and [10]CPP, and the solid-state structure of C60@[10]CPP. *Chemical Science* **2012,** *3* (10), 3018-3021.

3. (a) Nakanishi, Y.; Omachi, H.; Matsuura, S.; Miyata, Y.; Kitaura, R.; Segawa, Y.; Itami, K.; Shinohara, H., Size-Selective Complexation and Extraction of Endohedral Metallofullerenes with Cycloparaphenylene. *Angewandte Chemie International Edition* **2014,** *53* (12), 3102-3106;

(b) Iwamoto, T.; Watanabe, Y.; Takaya, H.; Haino, T.; Yasuda, N.; Yamago, S., Size- and Orientation-Selective Encapsulation of C70 by Cycloparaphenylenes. *Chemistry – A European Journal* **2013,** *19* (42), 14061-14068;

(c) Ueno, H.; Nishihara, T.; Segawa, Y.; Itami, K., Cycloparaphenylene-Based Ionic Donor–Acceptor Supramolecule: Isolation and Characterization of Li+@C60⊂[10]CPP. *Angewandte Chemie International Edition* **2015,** *54* (12), 3707-3711.

4. Matsuno, T.; Sato, S.; Iizuka, R.; Isobe, H., Molecular recognition in curved [small pi]-systems: effects of [small pi]-lengthening of tubular molecules on thermodynamics and structures. *Chemical Science* **2015,** *6* (2), 909-916.

5. Qu, D.-H.; Wang, Q.-C.; Zhang, Q.-W.; Ma, X.; Tian, H., Photoresponsive Host–Guest Functional Systems. *Chemical Reviews* **2015**.

6. Wang, H.; Liu, F.; Helgeson, R. C.; Houk, K. N., Reversible Photochemically Gated Transformation of a Hemicarcerand to a Carcerand. *Angewandte Chemie International Edition* **2013,** *52* (2), 655-659.

7. Ueno, A.; Yoshimura, H.; Saka, R.; Osa, T., Photocontrol of binding ability of capped cyclodextrin. *Journal of the American Chemical Society* **1979,** *101* (10), 2779-2780.

8. Shinkai, S.; Nakaji, T.; Nishida, Y.; Ogawa, T.; Manabe, O., Photoresponsive crown ethers. 1. Cis-trans isomerism of azobenzene as a tool to enforce conformational changes of crown ethers and polymers. *Journal of the American Chemical Society* **1980,** *102* (18), 5860-5865.

9. Puntoriero, F.; Ceroni, P.; Balzani, V.; Bergamini, G.; Vögtle, F., Photoswitchable Dendritic Hosts: A Dendrimer with Peripheral Azobenzene Groups. *Journal of the American Chemical Society* **2007,** *129* (35), 10714-10719.

10. Berryman, O. B.; Sather, A. C.; Rebek Jr, J., A light controlled cavitand wall regulates guest binding. *Chemical Communications* **2011,** *47* (2), 656-658.

11. Liu, M.; Yan, X.; Hu, M.; Chen, X.; Zhang, M.; Zheng, B.; Hu, X.; Shao, S.; Huang, F., Photoresponsive Host−Guest Systems Based on a New Azobenzene-Containing Crytpand. *Organic Letters* **2010,** *12* (11), 2558-2561.

12. Bonvallet, P. A.; Mullen, M. R.; Evans, P. J.; Stoltz, K. L.; Story, E. N., Improved functionality and control in the isomerization of a calix[4]arene-capped azobenzene. *Tetrahedron Letters* **2011,** *52* (10), 1117-1120.

13. Darzi, E. R.; Sisto, T. J.; Jasti, R., Selective Syntheses of [7]-[12]Cycloparaphenylenes Using Orthogonal Suzuki-Miyaura Cross-Coupling Reactions. *The Journal of Organic Chemistry* **2012,** *77* (15), 6624-6628.

14. Zhang, W.; Yoshida, K.; Fujiki, M.; Zhu, X., Unpolarized-Light-Driven Amplified Chiroptical Modulation Between Chiral Aggregation and Achiral Disaggregation of an Azobenzene-alt-Fluorene Copolymer in Limonene. *Macromolecules* **2011,** *44* (13), 5105-5111.

15. Nguyen, T. T. T.; Boussonnière, A.; Banaszak, E.; Castanet, A.-S.; Nguyen, K. P. P.; Mortier, J., Chemoselective Deprotonative Lithiation of Azobenzenes: Reactions and Mechanisms. *The Journal of Organic Chemistry* **2014,** *79* (6), 2775-2780.

16. Busseron, E.; Lux, J.; Degardin, M.; Rebek, J., Synthesis and recognition studies with a ditopic, photoswitchable deep cavitand. *Chemical Communications* **2013,** *49* (42), 4842-4844.

17. Reuter, R.; Wegner, H. A., Synthesis and Isomerization Studies of Cyclotrisazobiphenyl. *Chemistry – A European Journal* **2011,** *17* (10), 2987-2995.

18. Albrecht, M.; Song, Y., Synthesis of Phosphane Oxide Bridged Bis- and Triscatechol Derivatives. *Synthesis* **2006,** *2006* (18), 3037-3042.

19. Biscoe, M. R.; Fors, B. P.; Buchwald, S. L., A New Class of Easily Activated Palladium Precatalysts for Facile C−N Cross-Coupling Reactions and the Low Temperature Oxidative Addition of Aryl Chlorides. *Journal of the American Chemical Society* **2008,** *130* (21), 6686-6687.

20. Kawase, T.; Tanaka, K.; Fujiwara, N.; Darabi, H. R.; Oda, M., Complexation of a Carbon Nanoring with Fullerenes. *Angewandte Chemie International Edition* **2003,** *42* (14), 1624-1628.

21. Siewertsen, R.; Neumann, H.; Buchheim-Stehn, B.; Herges, R.; Näther, C.; Renth, F.; Temps, F., Highly Efficient Reversible Z−E Photoisomerization of a Bridged Azobenzene with Visible Light through Resolved S1(nπ*) Absorption Bands. *Journal of the American Chemical Society* **2009,** *131* (43), 15594-15595.

22. Norikane, Y.; Tamaoki, N., Photochemical and Thermal cis/trans Isomerization of Cyclic and Noncyclic Azobenzene Dimers: Effect of a Cyclic Structure on Isomerization. *European Journal of Organic Chemistry* **2006,** *2006* (5), 1296-1302.

23. Zhao, Y.; Truhlar, D. G., Size-Selective Supramolecular Chemistry in a Hydrocarbon Nanoring. *Journal of the American Chemical Society* **2007,** *129* (27), 8440-8442.

24. Darzi, E. R.; Sisto, T. J.; Li, P.; Golder, M. R.; White, B. M.; Evans, P. J., Unpublished Work. 2015.

25. Takaishi, K.; Kawamoto, M.; Muranaka, A.; Uchiyama, M., Fusion of Photochromic Reaction and Synthetic Reaction: Photoassisted Cyclization to Highly Strained Chiral Azobenzenophanes. *Organic Letters* **2012,** *14* (13), 3252-3255.

26. Fabian, J., TDDFT-calculations of Vis/NIR absorbing compounds. *Dyes and Pigments* **2010,** *84* (1), 36-53.

27. Han, M.; Ishikawa, D.; Muto, E.; Hara, M., Isomerization and fluorescence characteristics of sterically hindered azobenzene derivatives. *Journal of Luminescence* **2009,** *129* (10), 1163-1168.

28. (a) Joshua, C. P.; Pillai, V. N. R., Photochemical cyclodehydrogenation of Lewis acid-conjugates of azobenzenes. *Tetrahedron* **1974,** *30* (18), 3333-3337;

(b) Wimmer, R.; Müller, N., Preparation of 1,10-Dimethyl-benzo[c]cinnolines by Photochemical Cyclodehydrogenation of Azobenzenes. *Monatshefte fuer Chemie* **1998,** *129* (11), 1161-1168.

29. Yoshino, J.; Furuta, A.; Kambe, T.; Itoi, H.; Kano, N.; Kawashima, T.; Ito, Y.; Asashima, M., Intensely Fluorescent Azobenzenes: Synthesis, Crystal Structures, Effects of Substituents, and Application to Fluorescent Vital Stain. *Chemistry – A European Journal* **2010,** *16* (17), 5026-5035.

30. Lu, Y.-C.; Diau, E. W.-G.; Rau, H., Femtosecond Fluorescence Dynamics of Rotation-Restricted Azobenzenophanes: New Evidence on the Mechanism of trans → cis Photoisomerization of Azobenzene. *The Journal of Physical Chemistry A* **2005,** *109* (10), 2090-2099.

31. Pangborn, A. B.; Giardello, M. A.; Grubbs, R. H.; Rosen, R. K.; Timmers, F. J., Safe and Convenient Procedure for Solvent Purification. *Organometallics* **1996,** *15* (5), 1518-1520.

32. Jasti, R.; Bhattacharjee, J.; Neaton, J. B.; Bertozzi, C. R., Synthesis, Characterization, and Theory of [9]-, [12]-, and [18]Cycloparaphenylene: Carbon Nanohoop Structures. *J. Am. Chem. Soc.* **2008,** *130* (Copyright (C) 2013 American Chemical Society (ACS). All Rights Reserved.), 17646-17647.

33. Frisch, M. J.; Trucks, G. W.; Schlegel, H. B.; Scuseria, G. E.; Robb, M. A.; Cheeseman, J. R.; Scalmani, G.; Barone, V.; Mennucci, B.; Petersson, G. A.; Nakatsuji, H.; Caricato, M.; Li, X.; Hratchian, H. P.; Izmaylov, A. F.; Bloino, J.; Zheng, G.; Sonnenberg, J. L.; Hada, M.; Ehara, M.; Toyota, K.; Fukuda, R.; Hasegawa, J.; Ishida, M.; Nakajima, T.; Honda, Y.; Kitao, O.; Nakai, H.; Vreven, T.; Montgomery, J. A.; Peralta, J. E.; Ogliaro, F.; Bearpark, M.; Heyd, J. J.; Brothers, E.; Kudin, K. N.; Staroverov, V. N.; Kobayashi, R.; Normand, J.; Raghavachari, K.; Rendell, A.; Burant, J. C.; Iyengar, S. S.; Tomasi, J.; Cossi, M.; Rega, N.; Millam, J. M.; Klene, M.; Knox, J. E.; Cross, J. B.; Bakken, V.; Adamo, C.; Jaramillo, J.; Gomperts, R.; Stratmann, R. E.; Yazyev, O.; Austin, A. J.; Cammi, R.; Pomelli, C.; Ochterski, J. W.; Martin, R. L.; Morokuma, K.; Zakrzewski, V. G.; Voth, G. A.; Salvador, P.; Dannenberg, J. J.; Dapprich, S.; Daniels, A. D.; Farkas; Foresman, J. B.; Ortiz, J. V.; Cioslowski, J.; Fox, D. J., *Gaussian 09, Revision D.01*. Gaussian Inc.: Wallingford CT, 2009.